

A CLUSTER MODEL OF ${}^6\text{He}$ AND ${}^6\text{Li}$

By

Jeremy Robert Armstrong

AN ABSTRACT OF A DISSERTATION

Submitted to
Michigan State University
in partial fulfillment of the requirements
for the degree of

DOCTOR OF PHILOSOPHY

Department of Physics and Astronomy

2007

Professor Vladimir G. Zelevinsky

ABSTRACT

A CLUSTER MODEL OF ${}^6\text{He}$ AND ${}^6\text{Li}$

By

Jeremy Robert Armstrong

Light nuclei provide an ideal testing ground for few-body theories. Helium-6 is particularly interesting in that it shows an extended neutron system similar to a halo, is loosely-bound, and is a Borromean system. Lithium-6 is also loosely bound, and is a difficult challenge for many theories. An alpha plus two nucleon cluster model using the Brink formalism in secondary quantization was developed for calculating various properties of ${}^6\text{He}$ and ${}^6\text{Li}$. The formalism includes a fully microscopic alpha particle, and allows for the exact treatment of Fermi statistics and the correct construction of eigenstates of angular momentum. Both nuclei were studied as the superposition of two configurations: an alpha plus two nucleon cluster and a nucleon-alpha-nucleon chain, or cigar configuration. The variational principle was used to obtain the binding energies of the nuclei and weights of both configurations. For ${}^6\text{He}$ calculations were made to determine the excitation energy of the 2^+ excited state, the $B(E2)$ for the $0^+ \rightarrow 2^+$ transition and the charge and matter radii. For ${}^6\text{Li}$, the excitation energy of the 2^+ and 3^+ excited states, charge radius, electric quadrupole moment and magnetic dipole moment were calculated. Finally, the lifetime for the ${}^6\text{He}$ Gamov-Teller beta decay was calculated. The results were obtained with the use of three nucleon-nucleon interactions: the Volkov V1 and V2 interactions, and the Minnesota potential. Results were compared with experimental data and the results of other theoretical models. In spite of the deliberate simplicity of the model, it describes the main physical properties of the nuclei on a level comparable with much more sophisticated theories.

A CLUSTER MODEL OF ${}^6\text{He}$ AND ${}^6\text{Li}$

By

Jeremy Robert Armstrong

A DISSERTATION

Submitted to

Michigan State University

in partial fulfillment of the requirements

for the degree of

DOCTOR OF PHILOSOPHY

Department of Physics and Astronomy

2007

ABSTRACT

A CLUSTER MODEL OF ${}^6\text{He}$ AND ${}^6\text{Li}$

By

Jeremy Robert Armstrong

Light nuclei provide an ideal testing ground for few-body theories. Helium-6 is particularly interesting in that it shows an extended neutron system similar to a halo, is loosely-bound, and is a Borromean system. Lithium-6 is also loosely bound, and is a difficult challenge for many theories. An alpha plus two nucleon cluster model using the Brink formalism in secondary quantization was developed for calculating various properties of ${}^6\text{He}$ and ${}^6\text{Li}$. The formalism includes a fully microscopic alpha particle, and allows for the exact treatment of Fermi statistics and the correct construction of eigenstates of angular momentum. Both nuclei were studied as the superposition of two configurations: an alpha plus two nucleon cluster and a nucleon-alpha-nucleon chain, or cigar configuration. The variational principle was used to obtain the binding energies of the nuclei and weights of both configurations. For ${}^6\text{He}$ calculations were made to determine the excitation energy of the 2^+ excited state, the $B(E2)$ for the $0^+ \rightarrow 2^+$ transition and the charge and matter radii. For ${}^6\text{Li}$, the excitation energy of the 2^+ and 3^+ excited states, charge radius, electric quadrupole moment and magnetic dipole moment were calculated. Finally, the lifetime for the ${}^6\text{He}$ Gamov-Teller beta decay was calculated. The results were obtained with the use of three nucleon-nucleon interactions: the Volkov V1 and V2 interactions, and the Minnesota potential. Results were compared with experimental data and the results of other theoretical models. In spite of the deliberate simplicity of the model, it describes the main physical properties of the nuclei on a level comparable with much more sophisticated theories.

ACKNOWLEDGMENTS

I would like first to acknowledge and thank my advisor and friend, Vladimir Zelevinsky. He was patient enough to let me learn as much as I could on my own, without unleashing all his knowledge at once, which would have been too much I am sure. I loved all our discussions no matter what the subject, whether they were on physics, Slavic linguistics, or Soviet film. I hope we will still be able to continue these discussions after I leave.

I would also like to thank the members of my guidance committee: Filomena Nunes, Krzysztof Starosta (Dziękuję), C.P. Yuan, and Carlo Piermarocchi for their suggestions and comments, and even suggesting that I take more classes, because those classes turned out to be some of the most interesting courses I took at MSU.

Next, I would like to thank the cyclotron and physics and astronomy department for providing a great environment to work in and a very good learning environment. I would especially like to mention Shari Conroy, who was able to answer any administrative question and make everything run smoothly. My collaborator, Alexander Sakharuk, also deserves to be mentioned, as he definitely helped to clarify things when the results of the calculations were mystifying, and injected some energy into the project. I should also thank professors Paul Mantica and Dave Morrissey for being very influential in me coming to Michigan State, and helping me through my transition between departments.

There are a lot of thank yous for my fellow graduate students and post-docs. Starting with my chemistry coevals: Bryan Tomlin, Sean Liddick, and Debbie Davies. It was always fun with you guys, and distracting each other enough to make sure the early days of grad school were tolerable. The closest I came to a midnight shift were some of the late night discussions with Bryan, but it didn't feel much like work! From my early days, I would also like to thank Declan Mulhall, who suggested that Vladimir "is a real gas to work for," Heather Zwahlen for getting me running again, Nathan

Frank for organizing the physics soccer team, Michelle Ouellette for always interesting discussions, Michal Mocko for trying to make sure I got at least some work done, Chandana Sumithrarachchi for a great trip to Notre Dame and our many cultural discussions, and Aws Abdo for being a very good mentor. I should of course, mention my office mate of many years now Ivan Brida, for always providing an interesting perspective on everything, our strict lunch schedule, entertainment, and \LaTeX help. For example, when he wanted to demonstrate how to label and then cite an equation, his example equation was labeled “Ivan_is_stupid.” I duly followed his suggestion, and referenced the equation “Ivan_is_stupid” with great enthusiasm. With entertainment and Ivan in mind, I should also acknowledge Wes Hitt, Terrance Strother, Jon Cook, Bryan Tomlin (again), and Andy Rogers for countless moments of levity involving my office-mate. Of the more recent arrivals, I would like to acknowledge Angelo Signoracci (keep the mantra of “she doesn’t care” alive!), Rhiannon Meharchand for making me social again, Phil Voss for the softball, Ania Kwiatkowski for her attempts at making me salsa, my other office-mate Biruk Gebremariam for many interesting talks about soccer and many other subjects, and Arnau Rios, for \LaTeX help and for being a very gracious host for Giuseppe’s coffee breaks. Finally, Francesco would like to say a big “Grazie!” to Giuseppe Lorusso, Stefano Di Chiara, Alfredo Estrade, and Christine Gockel for all the good times, races, and travels.

Last, but certainly not least, I would like to thank my family: my father, James, my mother Claire, and my sister Heather. Their love and support made navigating the vicissitudes of graduate school much easier. Mom and Dad, thanks for everything! Heather, you’re a dork, but you sure make every day more fun with all your messages. Thank you all again for all that you did to help me along my way!

Contents

1	Introduction	1
1.1	Early Attempts	2
1.2	More Advanced Cluster Models	4
1.3	Motivation for the Present Study	6
1.4	Constitution of the present work	7
2	Formalism	9
2.1	Initial Remarks	9
2.2	Non-orthogonal Orbitals	11
2.3	Examples	12
2.4	Angular momentum projection	18
3	Skeletons of the Six-particle Systems	21
3.1	Helium-6	21
3.1.1	Alpha-dineutron configuration	21
3.1.2	Cigar configuration	26
3.1.3	Interference term	30
3.2	Lithium-6	35
3.2.1	Alpha-deuteron configuration	36
3.2.2	Cigar configuration	44
3.2.3	Interference term	47
4	Gaussian Approximation	49
4.1	Helium-6	49
4.1.1	Alpha-dineutron configuration	50
4.1.2	Kinetic energy	54
4.1.3	Interaction	59
4.1.4	Total energy	70
4.1.5	Mean square radius	72
4.2	Cigar configuration	79
4.2.1	Kinetic energy	82
4.2.2	Interaction	84
4.2.3	Total energy	90
4.2.4	Mean square radius	93
4.3	Electromagnetic transitions	95
4.3.1	Background	96

4.3.2	Applied to ${}^6\text{He}$	97
4.4	Interference term	112
4.4.1	Kinetic energy	115
4.4.2	Interaction	116
4.4.3	Mean square radius	119
4.5	Lithium-6	124
4.5.1	Alpha-deuteron configuration	124
4.5.2	Kinetic energy	125
4.5.3	Interaction	126
4.5.4	Total energy	128
4.5.5	Mean square radius	132
4.5.6	Electric quadrupole moment	133
4.6	Cigar configuration	135
4.6.1	Kinetic energy	135
4.6.2	Interaction	136
4.6.3	Total energy	140
4.6.4	Mean square radius	141
4.6.5	Electric quadrupole moment	143
4.7	Magnetic dipole moment	144
4.8	Interference term	147
4.8.1	Interaction	147
4.8.2	Electric quadrupole moment	151
4.9	Beta decay	153
4.9.1	Background	153
4.9.2	Helium-6 beta decay	156
5	Numerical Results	163
5.1	Helium-6	163
5.1.1	Spatial parameters	163
5.1.2	Energy	164
5.1.3	Radii and other observables	167
5.1.4	Asymptotics	169
5.2	Lithium-6	171
5.2.1	Spatial parameters	171
5.2.2	Energy	172
5.2.3	Charge radius and other observables	175
5.3	Beta decay	176
6	Conclusions and outlook	178
6.1	Summary	178
6.2	Conclusions	180
6.3	Future work	181
	<i>Bibliography</i>	183

List of Tables

3.1	Action of spin raising and lowering operator	39
3.2	Table of overlaps for ${}^6\text{Li}$ involving rotated overlaps	41
3.3	The results of the tensor operator acting on all combinations of triplet wave functions	43
5.1	Optimized variational parameters of ${}^6\text{He}$	164
5.2	Energy results for ${}^6\text{He}$	166
5.3	Radii and electromagnetic transition results for ${}^6\text{He}$	169
5.4	Exponential asymptotic calculations in ${}^6\text{He}$	171
5.5	Minimized parameters of ${}^6\text{Li}$	172
5.6	Ground state energies and relative weights of the configurations for ${}^6\text{Li}$	173
5.7	Excited states of ${}^6\text{Li}$	175
5.8	Charge radius, quadrupole moment, and magnetic moment of ${}^6\text{Li}$. .	176
5.9	Beta decay results for ${}^6\text{He}$ β -decay	177

List of Figures

2.1	Diagram of rotated wave function	18
3.1	2-center diagram of helium-6	22
3.2	Cigar configuration diagram	27
3.3	Interference Term Diagram	31
4.1	One-body particle density of the alpha-dineutron configuration of ${}^6\text{He}$	53
4.2	The one-body density of ${}^6\text{He}$ in the alpha-dineutron configuration with ω set larger than ν	54
4.3	The one-body density of ${}^6\text{He}$ in the alpha-dineutron configuration with ν set larger than ω	55
4.4	One-body kinetic energy of the alpha-dineutron configuration of ${}^6\text{He}$.	56
4.5	The total kinetic energy of the alpha-dineutron configuration of ${}^6\text{He}$, with the center-of-mass energy removed	58
4.6	Volkov Potentials (eight different parameter sets)	61
4.7	Expectation value of the Volkov potential as a function of d in the alpha-dineutron configuration of ${}^6\text{He}$	64
4.8	Volkov potential as a function of d in the alpha-dineutron configuration of ${}^6\text{He}$ without Majorana exchange	65
4.9	Volkov V2 potential as a function of d in the alpha-dineutron configuration of ${}^6\text{He}$	65
4.10	Singlet and triplet channels of the Minnesota potential	67
4.11	Expectation value of the Minnesota potential in the alpha-dineutron configuration of ${}^6\text{He}$	69
4.12	Total energy of the alpha-dineutron configuration of ${}^6\text{He}$ calculated with the Volkov V1 potential	71

4.13	Total energy of the alpha-dineutron configuration of ${}^6\text{He}$ calculated with the Minnesota potential	72
4.14	One-particle density of the cigar configuration with equal oscillator lengths	80
4.15	One-particle density of the cigar configuration with $\nu=0.53 \text{ fm}^{-2}$ and $\omega=0.68 \text{ fm}^{-2}$	80
4.16	One particle density of the cigar configuration with $\nu=0.53 \text{ fm}^{-2}$ and $\omega=0.41 \text{ fm}^{-2}$	81
4.17	Total kinetic energy of the cigar configuration of ${}^6\text{He}$	84
4.18	Expectation value of the Volkov V1 potential in the cigar configuration of ${}^6\text{He}$	87
4.19	Expectation value of the Volkov V2 potential in the cigar configuration of ${}^6\text{He}$	87
4.20	Expectation value of the Minnesota Potential in the cigar configuration of ${}^6\text{He}$	90
4.21	The total energy using the Volkov V1 potential of the cigar configuration as a function of d	91
4.22	The total energy using the Volkov V2 potential of the cigar configuration as a function of d	92
4.23	Total energy of the cigar configuration obtained with the Minnesota potential	92
4.24	Overlap of the two configurations as a function of d	114
4.25	Total kinetic energy in the alpha-deuteron configuration of ${}^6\text{Li}$. This has the center-of-mass energy removed	126
4.26	Potential energy of the alpha-deuteron configuration of ${}^6\text{Li}$ using the Volkov V1 potential	129
4.27	Potential energy of the alpha-deuteron configuration of ${}^6\text{Li}$ using the Volkov V2 potential	129
4.28	Potential energy of the alpha-deuteron configuration of ${}^6\text{Li}$ using the Minnesota potential	130
4.29	Spectrum of the alpha-deuteron configuration of ${}^6\text{Li}$ calculated with the Volkov V1 potential	131
4.30	Spectrum of the alpha-deuteron configuration of ${}^6\text{Li}$ calculated with the Volkov V2 potential	131

4.31	Spectrum of the alpha-deuteron configuration of ${}^6\text{Li}$ calculated with the Minnesota potential	132
4.32	Total kinetic energy with the center-of-mass removed of the cigar configuration of ${}^6\text{Li}$	136
4.33	Potential energy calculated with the Volkov V1 potential in the cigar configuration of ${}^6\text{Li}$	138
4.34	Potential energy calculated with the Volkov V2 potential in the cigar configuration of ${}^6\text{Li}$	139
4.35	Potential energy calculated with the Minnesota potential as a function of d in the cigar configuration of ${}^6\text{Li}$	141
4.36	The total energy as a function of d for the cigar configuration of ${}^6\text{Li}$ calculated with the Volkov V1 potential	142
4.37	The total energy as a function of d for the cigar configuration of ${}^6\text{Li}$ calculated with the Volkov V2 potential	142
4.38	Total energy as a function of d for the cigar configuration of ${}^6\text{Li}$ calculated with the Minnesota potential	143

Images in this dissertation are presented in color.

Chapter 1

Introduction

Though the existence of atoms was postulated by the ancient Greek Pre-Socratic philosophers Democritus and Epicurus in the 5th and 4th centuries BC, the modern atomic picture of matter did not begin until the early 19th century. John Dalton published a fledgling atomic model of matter in 1808 [1], and the atomic formulation of matter was furthered along by others such as Avogadro, Guy-Lussac, and Mendeleev. This atomic formulation of matter put chemistry in good stead, but physicists took a little more convincing, and wondered if atoms were indivisible. British physicist J.J. Thomson found that cathode rays were indeed composed of particles, electrons, and that they were sub-atomic particles [2]. This discovery led to theories about how the atom itself was constructed. A defining experiment occurred in 1911, when Rutherford found that the atom consisted of a very small, positively-charged core, and a large amount of empty space [3]. This is one point that can be considered the beginning of nuclear science. Another possible starting point could be Becquerel's discovery of radioactivity in 1896 [4], as this showed a whole new kind of transformation, previously unknown, that is, the transformation of atomic elements. Later, Rutherford and Royds demonstrated the equivalence of alpha particles and helium nuclei, which showed the link between radioactivity and the substructure of the atom [5]. Thus, with the discovery of the nucleus, came questions about the structure of this new object.

Physics had to wait until 1932 before the modern idea that nuclei are made of protons and neutrons could be proposed. English physicist Sir James Chadwick discovered the neutron in 1932 [6], which led Werner Heisenberg to hypothesize that nuclei were made of protons and neutrons [7].

1.1 Early Attempts

After Heisenberg's hypothesis, theories of the structure of the atomic nucleus were developed. Some early models include the uniform model of Wigner [8], the liquid drop model of Bohr [9], the independent particle model, and the alpha-particle model (the modern shell model would not emerge until later). During the 1930s and 40s the models were developed further as more experimental data became available. An excellent discussion of these early models can be found in Chapter VII of [10]. Since the focus of this work is at least inspired by cluster models, we will move to further details in the development of the cluster models.

The basic building block of the first suggested cluster models (and most of the subsequent ones) is the alpha particle. The alpha particle, or ${}^4\text{He}$ nucleus, makes an excellent building block for several reasons. First and foremost, it is exceptionally stable. Its first excited state is not until 20.2 MeV [11], and its binding energy per nucleon of 7.07 MeV/nucleon is not equaled again as one goes through the chart of the nuclides until one gets to ${}^{12}\text{C}$. It is also very compact (a charge radius of 1.673 fm [12]), and has zero for all quantum numbers (spin and isospin), which makes it easy to combine into larger systems. From a modern perspective, it is the first doubly magic nucleus, with the first shell completely full of protons and neutrons, which accounts for its exceptional stability, and thus its use as the basic building block of many nuclear cluster models.

The alpha cluster structure model was first proposed by Wheeler in 1937 [13], with similar models suggested concurrently by Wefelmeier [14], Weizsäcker [15], and

Fano [16]. In this model, the nuclei with $N = Z$ (Z is the number of protons in a nucleus, and N is the number of neutrons) and $A = 4n$ (A is the total number of nucleons in a nucleus and n is an integer) are considered as “molecules” of alpha particles. ${}^8\text{Be}$ would be a dumbbell shape, ${}^{12}\text{C}$ a triangle, ${}^{16}\text{O}$ a tetrahedron, and so forth. Excitations of these nuclei would correspond to vibrations and rotations of the constituent alpha particles, just as in molecules. Allowed states would be only the ones that preserved the Bose statistics of the alpha particles, that is all allowed states had to be symmetric with respect to the interchange of any two alphas. Binding energies would be the sum of the binding energies of the constituent alpha particles (which accounted for over 90% of the total binding energy) and the energy of the “bonds” between alpha particles, which were modeled like the binding between neutral molecules with Coulomb repulsion superimposed. An interesting discovery was that, except for the unbound ${}^8\text{Be}$, the energy of these inter-alpha bonds is relatively constant around 2.40 MeV/bond for ${}^{12}\text{C}$ through ${}^{32}\text{S}$. The model was extended by Hafstad and Teller [17] and Kittel [18] to include the alpha particle nuclei plus or minus an additional nucleon. The analogy with molecules was continued, with the additional nucleon acting as a light electron moving around a heavy, stationary nucleus. The proper quantum numbers were obtained for the ground states of these odd- A nuclei, and tracked the binding energy trends. Magnetic moments were calculated for these nuclei by Bethe [19], Sachs [20], and Inglis [21]. Their values were as good (or as bad) as those obtained in the independent particle model.

Those are some of the successes of the alpha particle model, but it has many limitations. The most obvious shortcoming is that it has no adequate way of treating $4n + 2$ nuclei. One could treat these nuclei as an alpha particle plus two additional particles, or an extra alpha particle with two holes, but these have very different geometries. In 1941, Wheeler analyzed alpha-alpha scattering data, and found that using a potential between two rigid alphas could not even describe the low energy data [22], meaning the alphas do not maintain their separate identities even at low

energies. Also, the agreement in binding energies merely shows that the binding energy per nucleon in the alpha particle is close to that of heavier nuclei (even non-alpha particle nuclei), which seems to indicate a more liquid state. Furthermore, in Wheeler's original paper, he shows spectra of the alpha particle nuclei in terms of rotations of the alpha particles, but the energies of the excited states are far too low. We know now that these excitations are much better thought of as single-particle excitations than the rotation or vibration of an alpha cluster. In addition, the molecular analogy for alpha particle nuclei plus or minus one particle is also questionable. The Born-Oppenheimer [23] approximation works well in atoms, since the electron is 1800 times lighter than the nucleon, but in the case of an additional nucleon outside an alpha particle, it is only 1/4 the mass of the "heavy" core, which is not negligible. For these many reasons, the inert alpha cluster was not seriously pursued much further, but it was the first attempt at a cluster picture of nuclei.

1.2 More Advanced Cluster Models

The next major contributors to the story of cluster models were Wildermuth and Tang [24]. From the early 1960s to the late 1970s, they investigated various clustering phenomena in nuclear physics. Their first improvement was to make the alpha not a structureless boson, but a composite particle made up of four nucleons, represented by Gaussian wave functions (oscillator functions). They showed the equivalence of the oscillator shell model and an oscillator cluster model (i.e., a model where the nucleus consists of separate clusters of oscillator wave functions). They did this by merely relabeling coordinates, instead of having A oscillator functions with one common center, they re-wrote them by referencing clusters of four particles to their own center, and a wave function describing inter-cluster motion. Oscillator quanta of excitation appeared as excitation of this inter-cluster function (since the alpha's first excited state is not until 20 MeV), and they achieved identical results with both formulations.

However, they could not achieve a very good qualitative description of light nuclei with this method, so they developed what they called the generalized cluster formalism. Here their wave function is an anti-symmetrized combination of nucleons in alpha particles and valence particles, described in Jacobi coordinates to remove center of mass motion, an alpha-external cluster relative motion function, and Jastrow factors. Jastrow factors are factors added to a wave function which keep the nucleons from coming too close to one another, as it was Jastrow who first suggested that some factor be added to the wave function to reflect that the nucleon-nucleon force becomes repulsive at very small distances [25]. For the deuteron wave function, they are conscious of the proper asymptotics of a valence cluster, and put an exponential tail onto the wave function after a certain radius. They have many parameters, which are adjusted to fit two nucleon scattering data and the continuity of the wave function and its derivatives. They were able to obtain decent results, depending on the potential used. They were frustrated that their most realistic calculation was limited by the computing abilities at the time. They then applied their structure model to study many low-energy scattering phenomena in light nuclei.

We now turn to two modern cluster-inspired theories of light nuclei: Anti-symmetrized Molecular Dynamics (AMD) and Fermionic Molecular Dynamics (FMD), both nicely reviewed in [26]. Both models were initially inspired by heavy-ion reactions and predicting the products of the reactions, but it was found that they could describe light nuclei as well. Both models are similar in many respects. They both use Gaussian (or superpositions of many Gaussian) wave packets for their single particle wave functions, which contain both position and momentum information. In FMD, they minimize the expectation value of their effective Hamiltonian with respect to the parameters of all their single particle states. The AMD method solves the frictional cooling equation (see, for example, [27]), sometimes with constraints added to fit a particular feature of the system of interest. In addition to applying AMD to its original purpose in fragmentation reactions, several papers have appeared describing helium, lithium, and

beryllium isotope chains, with the occasional calculation on isotopes of boron and carbon as well. A difference between the two methods, though this appears merely to be a choice of the scientist, is that FMD calculations are done with interactions based on nucleon-nucleon scattering, such as CD-Bonn and Argonne V18, whereas the AMD calculations use effective interactions tuned to describe the subject of their study.

1.3 Motivation for the Present Study

The goal of the present study is to use a physically transparent model to describe the structure and some dynamics of loosely bound light nuclei. The model, though simple and straightforward, should be quantum mechanically rigorous and avoid approximations related to the neglect of the Pauli principle. The model should reproduce reasonably the properties of the studied nuclei.

The model will be described in great detail in the following chapter, but some words should be spent on the subject nuclei of our study, ${}^6\text{He}$ and ${}^6\text{Li}$. Helium-6 was first reported in 1936 [28]. Despite its early discovery, it still attracts a large interest today in both theory and experiment. It is a loosely bound (breaks up into $\alpha + 2n$ at an excitation energy of 0.970 MeV) nucleus with an extended neutron structure that some classify as a halo system. It is also a Borromean system, which is a three-body system where none of the two-body subsystems are bound, in this case ${}^5\text{He}$ and the dineutron. This three-body system can be pictured as being, in the two extreme cases, either an alpha particle and dineutron cluster, or a neutron-alpha-neutron chain (“cigar”) configuration. In this work, we calculate the main properties of ${}^6\text{He}$, including the binding energy, charge and matter radius, and beta decay ft value. Additionally, we determine the relative mixture between the two previously mentioned configurations, which is a topic of current interest [29].

Lithium-6 is one of the two beta-stable isotopes of the element lithium, and there-

fore one would expect it to be fairly well studied. Experimentally, this is indeed the case, as work on the excited states of ${}^6\text{Li}$ was already being done in the 1950s [30]. One can find an accumulation of experimental data on both ${}^6\text{He}$ and ${}^6\text{Li}$ in [31]. From a theoretical standpoint, ${}^6\text{Li}$ remains an excellent testing ground for nuclear structure theories. In a simple picture, it exists as an alpha particle plus a deuteron. Since the alpha particle has all quantum numbers equal to zero, it might be expected that ${}^6\text{Li}$ would have many properties similar to the deuteron. It does have a ground state spin of one, like the deuteron, but it also has a curiously small and negative electric quadrupole moment and a magnetic moment that is only slightly different from the deuteron magnetic moment. There are numerous attempts to reproduce these observables, from the models mentioned above to very sophisticated models such as No-Core Shell Model [32] and Variational/Green's Function Monte Carlo [33]. These models have met with varying degrees of success with ${}^6\text{Li}$ and many of this nucleus' unusual features have been ascribed to the effects of three-body forces. At first, our motivation to do calculations for ${}^6\text{Li}$ was in order to calculate the beta decay of ${}^6\text{He}$, but we found that it is an interesting topic of study in its own right

1.4 Constitution of the present work

This dissertation presents the study of ${}^6\text{He}$ and ${}^6\text{Li}$ in a microscopic cluster approach. Chapter Two develops the Brink formalism in secondary quantization and the method of projection into good states of angular momentum. The formalism is first introduced, and then developed through simple examples. Chapter Three applies the formalism to our six-particle systems and obtains the general structure of the matrix elements needed to calculate the various observables, which will be shown in Chapter Four. Chapter Four contains the results in the Gaussian approximation (i.e., the choice of the Gaussian as a single-particle wave function). It contains the results of all calculations outlined in Chapter three and then numerical results. In Chapter Five,

there is a discussion of the results which are then compared with measurements and the results of other models. The dissertation finishes with the conclusions and outlook in Chapter Six.

Chapter 2

Formalism

2.1 Initial Remarks

The basic formalism used in this work was invented by D. M. Brink in 1966 [34]. The specific problems he attacked were alpha-particle nuclei and their different geometries. His model improved upon those of Wheeler [13] and others by treating the alpha particles as composed of four nucleons and those particles obeyed the Pauli principle, and thus there were consequences built into the theory if the alpha particles came to close to each other. We use Brink's model to describe nuclei other than alpha-particle nuclei, and re-cast the model in secondary quantization.

The Brink formalism is extremely flexible. In principle, one can describe a system of as many particles and centers as desired in a rather straight-forward way. Our system is solved variationally, and our trial basis wave function is a product of creation operators operating on the vacuum:

$$\Psi = N \prod_{i=1}^A a_i^\dagger |0\rangle, \quad (2.1)$$

where the a_i^\dagger 's are creation operators for the particles (fermions) of the system, and $|0\rangle$ is the vacuum state. The particles are created into whichever single-particle orbitals

with whatever quantum numbers and at any center required by the problem. The choice of radial dependence of the single-particle wave functions is also completely arbitrary. It should be noted, that once an order of single-particle states is selected in eq.(2.1), one should keep that order for all further calculations. This order is necessary to maintain the phase of the wave function, because we will need a superposition of such functions. These operators are Fermi operators, whose properties will be further elaborated upon shortly, and exchanging them with other fermions can introduce extra minus signs, which can lead to sign errors if the order is not preserved.

To normalize the wave function (i.e., to determine the factor N in eq.(2.1)), one follows the usual recipe:

$$\langle \Psi | \Psi \rangle = |N|^2 \langle 0 | \prod_{i=1}^A a_i \prod_{j=1}^A a_j^\dagger | 0 \rangle. \quad (2.2)$$

This choice of using secondary quantization is not required; it is just more convenient for our purposes. There have been many discussions in the literature of how to represent many-fermion wave functions, often as Slater determinants. Two such works are: [35, 36], and an in-depth treatment can be found in [37]. To evaluate eq.(2.2), one must decide whether the wave function is made of fermions or bosons. Then, one must make eq.(2.2) normal ordered by using either commutation (bosons) or anti-commutation relations (fermions). Since we will be working exclusively with fermions in this work, the rest of the formalism will be developed for fermions. The anti-commutation relations for fermions are:

$$\begin{aligned} \{a_i, a_j\} &= a_i a_j + a_j a_i = 0, \\ \{a_i^\dagger, a_j^\dagger\} &= 0, \\ \{a_i^\dagger, a_j\} &= \theta_{ij}, \end{aligned} \quad (2.3)$$

where θ_{ij} is the overlap of the two orbitals:

$$\theta_{ij} = \langle \phi_i | \phi_j \rangle. \quad (2.4)$$

In the simple case of orthogonal orbitals, then $\theta_{ij} = \delta_{ij}$, the Kronecker symbol. By moving all creation operators to the left (or all destruction operators to the right), one completes all possible Wick contractions [38]. The fact that creation operators anti-commute with themselves (eq.(2.3)), means that switching any two particles in eq.(2.1) induces an overall minus sign in the wave function, which satisfies the Pauli Principle.

2.2 Non-orthogonal Orbitals

In the present work, we will need the orbitals to be non-orthogonal. To demonstrate how these work, we first need a reference set of complete orthogonal orbitals:

$$\begin{aligned} \theta_{12} &= \langle 1|2 \rangle = \delta_{12}, \\ \sum_1 |1\rangle \langle 1| &= 1, \\ \{a_1, a_2^\dagger\} &= \delta_{12}, \\ |\beta\rangle &= \sum_1 \langle 1|\beta\rangle |1\rangle = \sum_1 \theta_{1\beta} |1\rangle, \\ \theta_{\beta 1} &= \theta_{1\beta}^*, \\ \langle \beta|\beta\rangle &= 1. \end{aligned} \quad (2.5)$$

The numbers refer to orthogonal orbitals, whereas Greek labels indicate non-orthogonal orbitals, which in the last line of the above equation we indicated are normalized. Now we have the non-orthogonal orbitals in terms of orthogonal ones. It is then shown how

the general overlap expression, eq.(2.3), is obtained. We define creation and destruction operators of the non-orthogonal orbitals:

$$a_{\beta}^{\dagger} = \sum_1 \theta_{1\beta} a_1^{\dagger} \quad a_{\alpha} = \sum_1 \theta_{\alpha 1} a_1 \quad , \quad (2.6)$$

to obtain the anti-commutation relation:

$$\{a_{\alpha}, a_{\beta}^{\dagger}\} = \sum_{12} \theta_{\alpha 1} \theta_{2\beta} \{a_1, a_2^{\dagger}\} = \sum_1 \theta_{\alpha 1} \theta_{1\beta} = \theta_{\alpha\beta}. \quad (2.7)$$

Thus, we obtained the result shown in eq.(2.4).

2.3 Examples

To demonstrate the machinery of the formalism, we will work with a two-body wave function

$$\Psi_{\alpha\beta} = N a_{\alpha}^{\dagger} a_{\beta}^{\dagger} |0\rangle, \quad (2.8)$$

with the normalization

$$\langle \Psi_{\alpha\beta} | \Psi_{\alpha\beta} \rangle = \langle 0 | a_{\alpha} a_{\beta} a_{\beta}^{\dagger} a_{\alpha}^{\dagger} | 0 \rangle = \theta_{\alpha\alpha} \theta_{\beta\beta} - \theta_{\alpha\beta} \theta_{\beta\alpha}. \quad (2.9)$$

The normalization, written in terms of overlaps in the right-hand side of eq.(2.9), looks like a determinant, which in fact it is. By completing all possible Wick contractions, we generate a determinant of a matrix of overlaps. Generalizing to many-body wave functions:

$$|\Phi_{1,\dots,A}\rangle = N \prod_{i=1}^A a_i^{\dagger} |0\rangle \quad N = [\det(\theta_{ij})]^{-1/2}$$

$$\langle \Phi_{\nu_1, \dots, \nu_A} | \Phi_{\mu_1, \dots, \mu_A} \rangle = [\det(\theta_{\nu_i \nu_j}) \det(\theta_{\mu_i \mu_j})]^{-1/2} \det(\theta_{\nu \mu}). \quad (2.10)$$

It has just been shown how the normalization generalizes to a many-body wave function. Before going further, we would like to include an example on how one can pick the quantum numbers for the created particles. In this two-body wave function example, it is desired to have a pair of particles in a certain spin state $|SM\rangle$. Now our wave function looks like

$$|SM\rangle = N_S \sum_{\sigma_1 \sigma_2} C_{1/2 \sigma_1, 1/2 \sigma_2}^{SM} a_{1\sigma_1}^\dagger a_{2\sigma_2}^\dagger |0\rangle, \quad (2.11)$$

where the subscripts 1 and 2 refer to the spatial wave functions, ψ_1 and ψ_2 , whatever they may be, and $C_{j_1 m_1, j_2 m_2}^{JM}$ is the notation used for Clebsch-Gordan coefficients. The overlap of two such functions is

$$\langle S' M' | SM \rangle = N_{S'}^* N_S \sum_{\sigma_1 \sigma_2 s_1 s_2} C_{1/2 s_1, 1/2 s_2}^{S' M'} C_{1/2 \sigma_1, 1/2 \sigma_2}^{SM} \langle 0 | a_{1s_1} a_{2s_2} a_{2\sigma_2}^\dagger a_{1\sigma_1}^\dagger | 0 \rangle. \quad (2.12)$$

Here, the matrix element is equal to

$$\langle 0 | a_{1s_1} a_{2s_2} a_{2\sigma_2}^\dagger a_{1\sigma_1}^\dagger | 0 \rangle = \delta_{\sigma_1 s_1} \delta_{\sigma_2 s_2} - \delta_{\sigma_1 s_2} \delta_{\sigma_2 s_1} \theta_{12} \theta_{21}, \quad (2.13)$$

as always, the single particle overlap is

$$\theta_{12} = \int \psi_1^*(\mathbf{r}) \psi_2(\mathbf{r}) d^3 \mathbf{r} = \theta_{21}^*. \quad (2.14)$$

To complete the overlap, we must sum up over the spin projections and use the following symmetry property of the Clebsch-Gordan coefficients:

$$C_{s_1 m_1, s_2 m_2}^{SM} = (-)^{s_1 + s_2 - S} C_{s_2 m_2, s_1 m_1}^{SM}. \quad (2.15)$$

Using this property and completing the sum yields

$$\langle S' M' | S M \rangle = \delta_{S S'} \delta_{M M'} |N_S|^2 [1 + (-)^S |\theta_{12}|^2] \quad (2.16)$$

$$|N_S|^2 = \frac{1}{1 + (-)^S |\theta_{12}|^2}. \quad (2.17)$$

One immediately notices the possibility that the denominator of the normalization vanishes for $S = 1$ and $\theta_{12} = 1$. This is because this state is forbidden by Fermi statistics. The triplet spin state means parallel spins (and, to be complete, the symmetric combination of paired spins), and $\theta_{12} = 1$ means the two spatial wave functions are identical, most likely caused by them being at the same point in space. These two things happening simultaneously we know is forbidden by Fermi statistics. This will be further developed after we discuss expectation values.

Now that we have a normalized wave function, we can compute expectation values. Here, we go through the computation of the expectation value of a one-body operator, such as kinetic energy (which is diagonal in spin, which makes the example simpler). The form of our spin-independent one-body operator is:

$$\hat{O}^{(1)} = \int \sum_{\sigma} a_{\sigma}^{\dagger}(\mathbf{r}) O^{(1)} a_{\sigma}(\mathbf{r}) d^3 r, \quad (2.18)$$

where O (sans caret) is the “operational” part of the operator (e.g., for the x position operator, this would be x), whereas $\hat{O}^{(1)}$ is the full second-quantized form of the operator. The the single-particle operators correspond to the localized states so that:

$$\langle 0 | a_{\sigma}(\mathbf{r}) a_{1\sigma_1}^{\dagger} | 0 \rangle = \delta_{\sigma\sigma_1} \int \delta(\mathbf{r} - \mathbf{x}) \psi_1(\mathbf{x}) d^3 x = \delta_{\sigma\sigma_1} \psi_1(\mathbf{r}). \quad (2.19)$$

For our two-body system, eq.(2.11), we have

$$\langle SM|O^{(1)}|SM\rangle = |N_S|^2 \sum_{\sigma\sigma'1\sigma'2s1s2} \int \langle 0|a_{1s1}a_{2s2}a_{\sigma}^{\dagger}O^{(1)}a_{\sigma}a_{2\sigma'2}a_{1\sigma'1}^{\dagger}|0\rangle d^3r. \quad (2.20)$$

After one computes all sums and Wick contractions, one obtains four terms:

$$\begin{aligned} \langle SM|O^{(1)}|SM\rangle &= |N_S|^2 \int \{\psi_1^*(\mathbf{r})O^{(1)}\psi_1(\mathbf{r}) + \psi_2^*(\mathbf{r})O^{(1)}\psi_2(\mathbf{r}) \\ &+ (-)^S[\theta_{12}^*\psi_1^*(\mathbf{r})O^{(1)}\psi_2(\mathbf{r}) + \theta_{12}\psi_2^*(\mathbf{r})O^{(1)}\psi_1(\mathbf{r})]\}d^3r. \end{aligned} \quad (2.21)$$

If $\hat{O}^{(1)}$ had been the kinetic energy operator, the result would have been the kinetic energy of the single particles 1 and 2, plus (or minus) the kinetic energy of the overlap between the two orbitals.

We now turn our attention to two-body operators. The form of a spatial two-body operator is

$$\hat{O}^{(2)} = \frac{1}{2} \iint \sum_{\sigma\sigma'} a_{\sigma}^{\dagger}(\mathbf{r})a_{\sigma'}^{\dagger}(\mathbf{r}')O^{(2)}(\mathbf{r},\mathbf{r}')a_{\sigma'}(\mathbf{r}')a_{\sigma}(\mathbf{r})d^3r d^3r'. \quad (2.22)$$

We find expectation values in the same way as before: we sandwich the operator by the wave function and perform all possible contractions. In this example, there are actually fewer possibilities with the two-body operator, though this is not usually the case in larger systems. There are actually four terms, but symmetry and the factor $\frac{1}{2}$ from eq.(2.22) allows us to write the expectation value as

$$\begin{aligned} \langle SM|O^{(2)}|SM\rangle &= |N_S|^2 \iint [\psi_2^*(\mathbf{r}')\psi_1^*(\mathbf{r})O^{(2)}\psi_1(\mathbf{r})\psi_2(\mathbf{r}')] \\ &+ (-)^S\psi_2^*(\mathbf{r}')\psi_1^*(\mathbf{r})O^{(2)}\psi_2(\mathbf{r})\psi_1(\mathbf{r}')]d^3r d^3r'. \end{aligned} \quad (2.23)$$

The first term is the direct term, and the second the exchange term.

We will now go through another example to demonstrate how the singularity in the denominator of the normalization (eq.(2.16)) is removed. Consider a two particle

system where the particles are identical and have parallel spins (for simplicity, we will work in 1-dimension). The wave function of the second particle, ψ_2 is the same as the first particle, only displaced by some distance d (i.e., $\psi_2 = \psi_1(x - d)$). The normalization is eq.(2.16) with $S = 1$. We take a closer look at the overlap, θ_{12} ,

$$\theta_{12} = \int \psi_1^*(x)\psi_1(x - d)dx = \theta_{12}(d). \quad (2.24)$$

The overlap is a function of the distance d . Expanding the overlap in a Maclaurin series about $d = 0$, we obtain

$$\theta_{12}(d) = \theta_{12}(0) + \theta'_{12}(0)d + \theta''_{12}(0)\frac{d^2}{2} + \dots, \quad (2.25)$$

$$= 1 + \theta''_{12}(0)\frac{d^2}{2} + \dots \quad (2.26)$$

In moving from the first line to the second, we used the fact that θ_{12} is at a maximum at $d = 0$, which allows us to eliminate the term proportional to its first derivative. The normalization is now, to lowest order,

$$|N_S|^2 = \frac{1}{d^2\theta''_{12}(0)}. \quad (2.27)$$

We now would like to find the expectation value of the kinetic energy, T . We know from the general formula, eq.(2.21), that there are four terms. The first two are the diagonal matrix elements of the two particles, and are equal, since the kinetic energy does not depend on translation of the origin:

$$\int \psi_1^*(x)\hat{T}\psi_1(x)dx = \int \psi_1^*(x - d)\hat{T}\psi_1(x - d)dx = T_0. \quad (2.28)$$

The cross terms are also equal to one another:

$$\int \psi_1^*(x)\hat{T}\psi_1(x - d)dx = \int \psi_1^*(x - d)\hat{T}\psi_1(x)dx = t_0(d). \quad (2.29)$$

The result of the cross terms is called $t_0(d)$ because at $d = 0$, $t_0 = T_0$. As with the overlap, we then expand $t_0(d)$:

$$t_0(d) = t_0(0) + t'_0(0)d + t''_0(0)\frac{d^2}{2} \quad (2.30)$$

$$= T_0 + t''_0(0)\frac{d^2}{2}. \quad (2.31)$$

Once again, we have used the fact that $t_0(d)$ has a maximum at $d = 0$ to remove the first derivative term. Plugging in the known terms into eq.(2.21), we have

$$\langle T \rangle = \frac{2T_0 - 2\theta_{12}(d)t_0(d)}{1 - \theta_{12}(d)^2}. \quad (2.32)$$

Plugging in the expansions of $\theta_{12}(d)$ and $t_0(d)$, we have

$$\langle T \rangle = 2 \frac{T_0 - [T_0 + d^2 (T_0\theta''_{12}(0) + t''_0(0)) / 2]}{d^2\theta''_{12}(0)}. \quad (2.33)$$

Simplifying, we find that any dependence on d disappears, and we obtain a finite result:

$$\langle T \rangle = 2 \frac{(T_0\theta''_{12}(0) + t''_0(0)) d^2 / 2}{d^2\theta''_{12}(0)} = T_0 + \frac{t''_0(0)}{\theta''_{12}(0)}. \quad (2.34)$$

Here we see that the kinetic energy is increased when one moves the two particles together. This is expected, as one of the two particles must be promoted to a higher energy level in order to satisfy the Pauli Principle.

Thus, the possibility of having zero in the denominator of a normalization is not a problem of the theory. In fact, it will appear again many times throughout this work; it is just how the theory accounts for Fermi statistics. We now turn to another general part of the formalism, the method of projection into good states of angular momentum.

2.4 Angular momentum projection

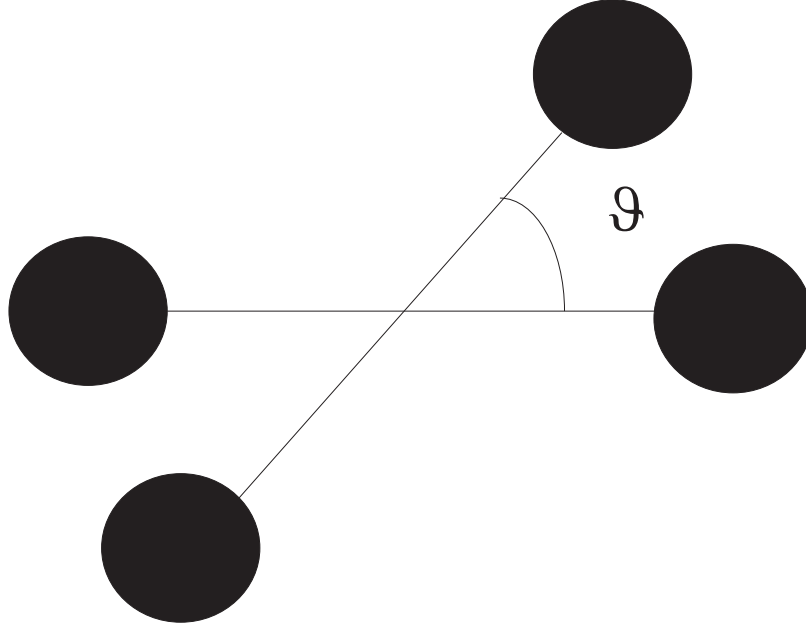


Figure 2.1: Here is a diagram of a two-particle wave function that has been rotated by an angle ϑ . In order to project into a state of good angular momentum, one must find the overlap of these two wave functions and use a projection operator to pick the desired angular momentum quantum numbers.

As our wave function is currently written, it is not in a state of good angular momentum. Here, we will outline the method used to project the wave function into states of good angular momentum. The basic approach is to always calculate overlaps between a wave function and another wave function which has been rotated by some angle and then using a projection technique to pick out the desired quantum numbers (illustrated in Figure 2.1). The general procedure is in many texts, for example [39]. The general formula for axially symmetric systems is:

$$\langle \Psi^{JM} | H | \Psi^{JM} \rangle = \frac{\int d_{KK}^J(\vartheta) \langle \psi | \exp\left(i\vartheta \hat{J}_y\right) H | \psi \rangle d \cos \vartheta}{\int d_{KK}^J(\vartheta) \langle \psi | \exp\left(i\vartheta \hat{J}_y\right) | \psi \rangle d \cos \vartheta}, \quad (2.35)$$

where $e^{i\vartheta \hat{J}_y}$ denotes a rotation about the y -axis, and d_{KK}^J is an element of the reduced rotation matrix that picks out the particular state of interest. It has total spin J and projection $M = K$, K being the projection of angular momentum along the body-

fixed axis. In this convention, the body-symmetry axis is taken to be the z -axis. These matrix elements of finite rotation can be found in any book on angular momentum such as [40].

In the case of ${}^6\text{He}$, the formula simplifies. In the model presented in detail in the next chapter, all spins are coupled to singlets, and thus the only effect of the rotation operator is to rotate the single-particle spatial wave functions, and the projection operator essentially picks an orbital momentum which is then equal to the total angular momentum, and selects the parity of the state [$\pi = (-)^\ell$]. We select the projection of angular momentum equal to zero, which simplifies the rotation matrix elements, $d_{00}^J(\vartheta) = P_J(\cos \vartheta)$, where $P_J(\cos \vartheta)$ is the J th Legendre polynomial. As will be presented in section 3.2, ${}^6\text{Li}$ is more complicated. Lithium-6 has a ground state with $J = 1$, which in our model comes from the spin of the deuteron. There are now two contributions to the total spin, one from orbital angular and the other from spin, so there is no simplification of eq.(2.35) in the case of ${}^6\text{Li}$.

Even though we often work with non-orthogonal orbitals, wave functions of different angular momentum remain orthogonal. We demonstrate this in the following derivation, considering two ${}^6\text{He}$ wave functions with different projections of angular momentum.

$$\langle \Psi_{LM} | \Psi_{L'M'} \rangle = \langle \int D_{M0}^L(\mathfrak{R}) \Psi(\hat{\mathfrak{R}}\mathbf{r}) d\mathfrak{R} | \int D_{M'0}^{L'}(\mathfrak{R}') \Psi(\hat{\mathfrak{R}}'\mathbf{r}) d\mathfrak{R}' \rangle, \quad (2.36)$$

where D_{MK}^J is the Wigner rotation matrix element, and $\hat{\mathfrak{R}}$ is the rotation operator. We can re-write eq.(2.36) into

$$= \iint D_{M0}^{L*}(\mathfrak{R}) D_{M'0}^{L'}(\mathfrak{R}') \langle \Psi(\hat{\mathfrak{R}}\mathbf{r}) | \Psi(\hat{\mathfrak{R}}'\mathbf{r}) \rangle d\mathfrak{R} d\mathfrak{R}'. \quad (2.37)$$

Now we move the rotation operators around in the matrix element by multiplying

through by the inverse rotation, \mathfrak{R}^{-1} :

$$\langle \Psi(\hat{\mathfrak{R}}\mathbf{r}) | \Psi(\hat{\mathfrak{R}}'\mathbf{r}) \rangle = \langle \Psi(\mathbf{r}) | \Psi(\hat{\mathfrak{R}}^{-1}\hat{\mathfrak{R}}'\mathbf{r}) \rangle. \quad (2.38)$$

Let $\mathfrak{R}'' = \mathfrak{R}^{-1}\mathfrak{R}'$, and therefore $\mathfrak{R}' = \mathfrak{R}\mathfrak{R}''$. Returning to the full expression, we have

$$= \iint D_{M_0}^{L*}(\mathfrak{R}) D_{M'_0}^{L'}(\mathfrak{R}\mathfrak{R}'') \langle \Psi(\mathbf{r}) | \Psi(\hat{\mathfrak{R}}''\mathbf{r}) \rangle d\mathfrak{R} d\mathfrak{R}''. \quad (2.39)$$

We rewrite the second D -function

$$D_{M'_0}^{L'}(\mathfrak{R}\mathfrak{R}'') = \sum_{\mu} D_{M'\mu}^{L'}(\mathfrak{R}) D_{\mu 0}^{L'}(\mathfrak{R}''), \quad (2.40)$$

and substitute this result into the full expression, and then integrate over \mathfrak{R} , which generates the required result:

$$= \frac{8\pi^2}{2L+1} \delta_{L'L} \delta_{M'M} \int \langle \Psi(\mathbf{r}) | \Psi(\hat{\mathfrak{R}}''\mathbf{r}) \rangle D_{M_0}^L(\mathfrak{R}'') d\mathfrak{R}''. \quad (2.41)$$

Now it is clear that wave functions of differing angular momenta are orthogonal, and that the projection process comes down to the integration over one rotation (which for axially symmetric systems further simplifies to one angle). More details about the projection process will be shown in chapter 4 with specific single-particle wave functions.

This concludes the chapter on the formalism used in the present work. In the next chapter, we apply the formalism to the two nuclei of interest in a general way. We sketch out the framework of the calculations, starting with the wave functions and going through the calculations of general operators. This sets up the next chapter, where we delve into detailed calculations with a specific choice of single-particle basis functions.

Chapter 3

Skeletons of the Six-particle Systems

3.1 Helium-6

3.1.1 Alpha-dineutron configuration

We apply the formalism now to ${}^6\text{He}$. We will first work with the alpha-dineutron configuration, which is a two-center model (see Figure 3.1).

Since this particular configuration has two centers, there will be some broad similarities with the two-particle example of the previous section. The wave function is

$$|\Psi\rangle = N a_p^\dagger a_{-p}^\dagger a_1^\dagger a_{-1}^\dagger a_2^\dagger a_{-2}^\dagger |0\rangle, \quad (3.1)$$

where the subscript p indicates protons, and the remaining particles are neutrons. The minus signs indicate spin projection, and particles with subscript 1 are the neutrons in the alpha particle, while those with subscript 2 are the dineutron. Next, the wave

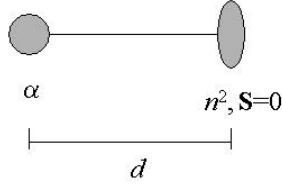


Figure 3.1: Helium-6 as an alpha particle plus dineutron. The dineutron is constructed as a spin singlet, and the parameter d describes the distance between the two centers.

function is normalized:

$$\langle \Psi | \Psi \rangle = \langle 0 | a_{-2} a_2 a_{-1} a_1 a_{-p} a_p a_p^\dagger a_{-p}^\dagger a_1^\dagger a_{-1}^\dagger a_2^\dagger a_{-2}^\dagger | 0 \rangle = \theta_\alpha^2 (\theta_\alpha \theta_d - \theta_{12}^2)^2, \quad (3.2)$$

θ_{12} is defined as in (2.14). θ_α and θ_d are also overlaps, but with particles at the same center, which in many cases is one. We keep the overlap notation, however, because for many of the calculations it is not equal to one, due to the process of projection into states of good angular momentum.

The normalization has now been obtained

$$|N|^2 = \frac{1}{\theta_\alpha^2 (\theta_\alpha \theta_d - \theta_{12}^2)^2}. \quad (3.3)$$

The initial θ_α^2 factor in the denominator comes from the protons, while the remaining expression comes from the neutrons. The neutron part looks like (2.16) with $S = 1$. The triplet spin occurs because the particles at the different centers may have parallel spins (e.g., there is a spin-up neutron in the alpha and in the dineutron), but they are singlets with respect to their own centers, and the triplets are coupled together

to make an overall spin of zero for the ${}^6\text{He}$ nucleus. Another interesting feature of the normalization, is that it could be zero if $\theta_{12}^2 = \theta_\alpha\theta_d$. This would be the case, for example, if the two centers came together, and the single-particle wave functions of the external neutrons were not radically different from those in the alpha particle. Then, as the two centers coincide, the overlaps become the same, and the denominator of the normalization becomes zero (see the discussion in the example following eq.(2.23)). This is because when the two centers are in the same place, four identical spin-1/2 fermions are at the same spatial location, which is forbidden by the Pauli principle. This is a very important feature of the theory, and will be discussed further during the calculation of observables.

One-body operators

Now that the wave function is properly normalized, we can calculate expectation values. We will first go through a one-body operator, of which there are many examples (kinetic energy, mean-square radius, quadrupole moment, etc.). The matrix element we must evaluate is:

$$\langle O^{(1)} \rangle = \int \sum_{\sigma} \langle 0 | a_{-2} a_2 a_{-1} a_1 a_{-p} a_p a_{\sigma}^{\dagger} a_{\sigma} a_{-p}^{\dagger} a_{-p}^{\dagger} a_1^{\dagger} a_{-1}^{\dagger} a_2^{\dagger} a_{-2}^{\dagger} | 0 \rangle d^3r \quad (3.4)$$

As with the 2-particle-example, there are four terms: terms centered at the alpha, terms centered at the dineutron, and two kinds of overlap terms (which for most operators are identical, but we will keep them separate here). The terms are:

$$\begin{aligned} \langle O^{(1)} \rangle_p &= \langle \alpha | O^{(1)} | \alpha \rangle 2\theta_\alpha (\theta_\alpha\theta_d - \theta_{12}^2)^2, \\ \langle O^{(1)} \rangle_n &= \langle \alpha | O^{(1)} | \alpha \rangle 2\theta_\alpha^2 (\theta_\alpha\theta_d^2 - \theta_{12}^2\theta_\alpha\theta_d), \\ \langle O^{(1)} \rangle_\alpha &= \langle \alpha | O^{(1)} | \alpha \rangle 2\theta_\alpha (2\theta_\alpha^2\theta_d^2 + \theta_{12}^4 - 3\theta_\alpha^2\theta_{12}^2\theta_d), \end{aligned} \quad (3.5)$$

where the first two lines in eq.(3.5) are the proton and neutron parts, respectively, of the contribution from the alpha particle. The matrix element in the beginning of each term is the normal expectation value of the operator:

$$\langle \alpha | O^{(1)} | \alpha \rangle = \int \psi_{\alpha}^*(\mathbf{r}) \hat{O}^{(1)} \psi_{\alpha}(\mathbf{r}) d^3r. \quad (3.6)$$

The shorthand used throughout this work for these matrix elements is $|\alpha\rangle$ denotes a wave function centered at the alpha (which assumes that all four particles have the same spatial wave functions), and $|d\rangle$ denotes a wave function centered at the dineutron. The collection of overlaps that follows the matrix element are the remaining parts of the wave function that are not involved in the normalization. Thus, the matrix element from the protons in the alpha particle will be followed by overlaps involving neutrons. Continuing with the rest of the terms,

$$\langle O^{(1)} \rangle_d = \langle d | O^{(1)} | d \rangle 2\theta_{\alpha}^3 (\theta_{\alpha}\theta_d - \theta_{12}^2), \quad (3.7)$$

$$\langle O^{(1)} \rangle_{\alpha d} = \langle \alpha | O^{(1)} | d \rangle 2\theta_{\alpha}^2 (\theta_{12}^3 - \theta_{12}\theta_{\alpha}\theta_d), \quad (3.8)$$

$$\langle O^{(1)} \rangle_{d\alpha} = \langle d | O^{(1)} | \alpha \rangle 2\theta_{\alpha}^2 (\theta_{12}^3 - \theta_{12}\theta_{\alpha}\theta_d). \quad (3.9)$$

These terms are then summed together and multiplied by the normalization. As mentioned before, when the centers come together, the norm develops a singularity in the denominator. If one looks at the one-body terms (eq.(3.5) and following), if the centers coincide, then the overlaps become equal, and each term is zero. Thus, the singularity in the denominator will be removed by the zero in the numerator, generating physical results. More concrete evidence of this will be shown in the next chapter.

Two-body operators

We now turn our attention to two-body operators. As with the one-body operators, we sandwich the operator by the wave function, and perform all Wick contractions to find its expectation value. What will be shown here is the sum of all terms for a given geometric configuration, i.e., unlike in (3.5), only the last line will appear, and there will not be separate entries for proton and neutron contributions. This is not to say that two-body operators cannot distinguish protons and neutrons, but for brevity, only the total contribution from each geometrical matrix element will be given. For operators that are sensitive to isospin, the form of their expectation values will be given in the section that discusses that individual operator. Before listing all the terms, please note the following convention for the order of integration variables in the individual matrix elements:

$$\langle 12|O|34\rangle = \langle \psi_1(\mathbf{x}_1)\psi_2(\mathbf{x}_2)|O|\psi_3(\mathbf{x}_2)\psi_4(\mathbf{x}_1)\rangle. \quad (3.10)$$

Now, the list of the terms resulting from the calculation of the expectation value of a two-body operator:

$$\langle O^{(2)} \rangle_\alpha = \langle \alpha\alpha | O^{(2)} | \alpha\alpha \rangle (6\theta_\alpha^2 \theta_d^2 + \theta_{12}^4 - 6\theta_{12}^2 \theta_\alpha \theta_d), \quad (3.11)$$

$$\langle O^{(2)} \rangle_{\alpha^2 d^2} = \langle d\alpha | O^{(2)} | \alpha d \rangle (8\theta_\alpha^3 \theta_d - 6\theta_\alpha^2 \theta_{12}^2), \quad (3.12)$$

$$\langle O^{(2)} \rangle_{\alpha\alpha\alpha d} = \langle \alpha\alpha | O^{(2)} | \alpha d \rangle 2 (2\theta_{12}^3 \theta_\alpha - 3\theta_\alpha^2 \theta_{12} \theta_d), \quad (3.13)$$

$$\langle O^{(2)} \rangle_{d\alpha\alpha\alpha} = \langle d\alpha | O^{(2)} | \alpha\alpha \rangle 2 (2\theta_{12}^3 \theta_\alpha - 3\theta_\alpha^2 \theta_{12} \theta_d), \quad (3.14)$$

$$\langle O^{(2)} \rangle_{ddd\alpha} = -\langle dd | O^{(2)} | d\alpha \rangle 2\theta_\alpha^3 \theta_{12}, \quad (3.15)$$

$$\langle O^{(2)} \rangle_{\alpha d d d} = -\langle \alpha d | O^{(2)} | dd \rangle 2\theta_\alpha^3 \theta_{12}, \quad (3.16)$$

$$\langle O^{(2)} \rangle_{\alpha d \alpha d} = \langle \alpha\alpha | O^{(2)} | dd \rangle \theta_\alpha^2 \theta_{12}^2, \quad (3.17)$$

$$\langle O^{(2)} \rangle_{d\alpha d\alpha} = \langle dd | O^{(2)} | \alpha\alpha \rangle \theta_\alpha^2 \theta_{12}^2, \quad (3.18)$$

$$\langle O^{(2)} \rangle_{\alpha d d \alpha} = \langle d\alpha | O^{(2)} | d\alpha \rangle 2 (2\theta_\alpha^2 \theta_{12}^2 - \theta_\alpha^3 \theta_d), \quad (3.19)$$

$$\langle O^{(2)} \rangle_d = \langle dd | O^{(2)} | dd \rangle \theta_\alpha^4. \quad (3.20)$$

These are summed together and multiplied by the norm, just as in the case for one-body operators. Once again, a zero divided by zero situation resolves itself amicably, which will be seen in more detail in the next chapter.

This completes the necessary formal calculations for the α -dineutron configuration of ${}^6\text{He}$. All operators here were assumed to be spin-singlet operators. Due to the choice of wave function for ${}^6\text{He}$, no operators that affect spin (e.g., $\mathbf{L} \cdot \mathbf{S}$) have non-zero expectation values.

3.1.2 Cigar configuration

The other extreme in picturing an alpha particle plus two additional valence particles is a particle-alpha-particle chain, colloquially referred to as the cigar configuration (pictured in Figure 3.2). The cigar configuration has a higher degree of symmetry than the alpha dineutron configuration ($D_{\infty h}$ vs. $C_{\infty v}$ in Schoenflies point group

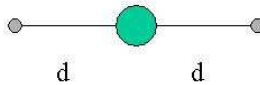


Figure 3.2: Helium-6 pictured in the cigar configuration, which is a neutron-alpha-neutron chain. The external neutrons are constructed as a spin singlet, and the parameter d describes the distance between the central alpha and the external neutrons (they are equidistant from the alpha).

theory parlance), which will have important consequences that shall be seen in the results chapter.

The wave function in the cigar configuration is

$$|\Psi\rangle = N a_p^\dagger a_{-p}^\dagger a_1^\dagger a_{-1}^\dagger \sum_m (-1)^{1/2-m} a_m^\dagger a_{-m}^\dagger |0\rangle. \quad (3.21)$$

The main difference between this wave function and eq.(3.1) is the sum over the spin projections of the external neutrons. Formally, this should have been done in the previous configuration, but since the neutrons in that wave function are located at the same spatial point, the only thing accomplished by summing over the spin projections is the quadrupling of the number of terms. Here, with the neutrons at different locations, the sum introduces important correlations that preserve the higher

symmetry of the cigar configuration. The normalization is

$$\begin{aligned}\langle \Psi | \Psi \rangle &= N^2 \sum_{mm'} \langle 0 | a_{-m'} a_{m'} a_{-1} a_1 a_{-p} a_p a_p^\dagger a_{-p}^\dagger a_1^\dagger a_{-1}^\dagger a_m^\dagger a_{-m}^\dagger | 0 \rangle \\ &= N^2 2\theta_\alpha^2 [\theta_n^2 (\theta_n^2 + \theta_\pm^2) + 2\theta_{12}^4 - 2\theta_{12}^2 \theta_\alpha (\theta_n + \theta_\pm)],\end{aligned}\quad (3.22)$$

$$N^2 = \frac{1}{2\theta_\alpha^2 [\theta_n^2 (\theta_n^2 + \theta_\pm^2) + 2\theta_{12}^4 - 2\theta_{12}^2 \theta_\alpha (\theta_n + \theta_\pm)]}.\quad (3.23)$$

As before, the normalization is a collection of terms involving various overlaps. θ_α remains the overlap inside the alpha particle, θ_n is the overlap of an external neutron with itself, θ_{12} is the overlap between the alpha particle and an external neutron, and θ_\pm is defined below:

$$\theta_\pm = \langle \pm | \mp \rangle = \int \phi_+^*(\mathbf{r}) \phi_-(\mathbf{r}) d^3r.\quad (3.24)$$

$\phi_{+/-}$ is a wave function centered at the right(+) or left(-) side of the alpha particle, so this term is an exchange term introduced by the sum over spin projections in eq.(3.21). Once again, if all of the particles are brought to the same point where all overlaps become equal, the denominator will go to zero, because there will be four s-wave neutrons at the same point (if the alpha and dineutron wave functions are identical).

The calculation of matrix elements proceeds in a similar way to the previous configuration. Here we list the terms for one-body and two-body operators. First, the one-body terms:

$$\langle O^{(1)} \rangle_\alpha = \langle \alpha | O^{(1)} | \alpha \rangle 2\theta_\alpha (2\theta_\alpha^2 (\theta_n^2 + \theta_\pm^2) + 2\theta_{12}^4 - 3\theta_{12}^2 \theta_\alpha (\theta_n + \theta_\pm))\quad (3.25)$$

$$\langle O^{(1)} \rangle_n = \langle \pm | O^{(1)} | \pm \rangle 2\theta_\alpha (\theta_\alpha \theta_n - \theta_{12}^2)\quad (3.26)$$

$$\langle O^{(1)} \rangle_\pm = \langle \pm | O^{(1)} | \mp \rangle 2\theta_\alpha (\theta_\alpha \theta_\pm - \theta_{12}^2)\quad (3.27)$$

$$\langle O^{(1)} \rangle_{\alpha\pm} = \langle \alpha | O^{(1)} | \pm \rangle 2\theta_\alpha^2 (2\theta_{12}^3 - \theta_{12} \theta_\alpha (\theta_n + \theta_\pm))\quad (3.28)$$

$$\langle O^{(1)} \rangle_{\pm\alpha} = \langle \pm | O^{(1)} | \alpha \rangle 2\theta_\alpha^2 (2\theta_{12}^3 - \theta_{12} \theta_\alpha (\theta_n + \theta_\pm)).\quad (3.29)$$

It should be noted that in all of the terms above, \pm can be flipped to \mp in all places in the matrix element without changing the result. If all overlaps become equal, each term becomes equal to zero.

Here is the list of terms involving a general, spin-singlet, two-body operator in the cigar configuration of ${}^6\text{He}$:

$$\langle O^{(2)} \rangle_{\alpha} = \langle \alpha\alpha | O^{(2)} | \alpha\alpha \rangle (6\theta_{\alpha}^2 (\theta_n^2 + \theta_{\pm}^2) + 2\theta_{12}^4 - 6\theta_{12}^2 \theta_{\alpha} (\theta_n + \theta_{\pm})), \quad (3.30)$$

$$\langle O^{(2)} \rangle_{\alpha^2 \pm^2} = \langle \pm\alpha | O^{(2)} | \alpha\pm \rangle 2\theta_{\alpha}^2 (4\theta_{\alpha}\theta_n - 3\theta_{12}^2), \quad (3.31)$$

$$\langle O^{(2)} \rangle_{\alpha^2 \pm\mp} = \langle \pm\alpha | O^{(2)} | \alpha\mp \rangle 2\theta_{\alpha}^2 (4\theta_{\alpha}\theta_{\pm} - 3\theta_{12}^2), \quad (3.32)$$

$$\langle O^{(2)} \rangle_{\alpha\alpha\alpha\pm} = \langle \alpha\alpha | O^{(2)} | \alpha\pm \rangle 2\theta_{\alpha}\theta_{12} (4\theta_{12}^2 - 3\theta_{\alpha} (\theta_n + \theta_{\pm})), \quad (3.33)$$

$$\langle O^{(2)} \rangle_{\pm\alpha\alpha\alpha} = \langle \pm\alpha | O^{(2)} | \alpha\alpha \rangle 2\theta_{\alpha}\theta_{12} (4\theta_{12}^2 - 3\theta_{\alpha} (\theta_n + \theta_{\pm})), \quad (3.34)$$

$$\langle O^{(2)} \rangle_{\pm^2 \mp\alpha} = -\langle \pm\mp | O^{(2)} | \mp\alpha \rangle 2\theta_{\alpha}^3 \theta_{12}, \quad (3.35)$$

$$\langle O^{(2)} \rangle_{\alpha\mp\pm^2} = -\langle \alpha\pm | O^{(2)} | \pm\mp \rangle 2\theta_{\alpha}^3 \theta_{12}, \quad (3.36)$$

$$\langle O^{(2)} \rangle_{\pm\mp\pm\alpha} = -\langle \pm\mp | O^{(2)} | \pm\alpha \rangle 2\theta_{\alpha}^3 \theta_{12}, \quad (3.37)$$

$$\langle O^{(2)} \rangle_{\alpha\pm\pm\mp} = -\langle \alpha\pm | O^{(2)} | \mp\pm \rangle 2\theta_{\alpha}^3 \theta_{12}, \quad (3.38)$$

$$\langle O^{(2)} \rangle_{\alpha\pm\alpha\mp} = \langle \alpha\alpha | O^{(2)} | \pm\mp \rangle 2\theta_{\alpha}^2 \theta_{12}^2, \quad (3.39)$$

$$\langle O^{(2)} \rangle_{\pm\mp\alpha\alpha} = \langle \pm\mp | O^{(2)} | \alpha\alpha \rangle 2\theta_{\alpha}^2 \theta_{12}^2, \quad (3.40)$$

$$\langle O^{(2)} \rangle_{\alpha\pm\pm\alpha} = \langle \alpha\pm | O^{(2)} | \alpha\pm \rangle 2\theta_{\alpha}^2 (2\theta_{12}^2 - \theta_{\alpha}\theta_n), \quad (3.41)$$

$$\langle O^{(2)} \rangle_{\alpha\pm\mp\alpha} = \langle \alpha\pm | O^{(2)} | \alpha\mp \rangle 2\theta_{\alpha}^2 (2\theta_{12}^2 - \theta_{\alpha}\theta_{\pm}), \quad (3.42)$$

$$\langle O^{(2)} \rangle_{+^2 -^2} = \langle + - | O^{(2)} | - + \rangle \theta_{\alpha}^4, \quad (3.43)$$

$$\langle O^{(2)} \rangle_{+---+} = \langle + - | O^{(2)} | + - \rangle \theta_{\alpha}^4. \quad (3.44)$$

As before, when all overlaps are equal, the terms sum to zero. Also, if one takes the limit where the cigar configuration becomes the alpha-dineutron (i.e., $+,- \rightarrow d$ and $\theta_n, \theta_{\pm} \rightarrow \theta_d$), the previous terms become the list of terms for the alpha-dineutron configuration.

With these matrix elements, one can calculate many properties of the cigar configuration of ${}^6\text{He}$. We will now move on to the next section which will discuss the interference of these two configurations.

3.1.3 Interference term

The overall composition of ${}^6\text{He}$ is a mixture of the two previously mentioned non-orthogonal configurations. That is,

$$|\Psi\rangle = c_1|\psi_1\rangle + c_2|\psi_2\rangle, \quad (3.45)$$

where ψ_1 is the alpha-dineutron wave function, ψ_2 is the cigar configuration wave function, and c_1 and c_2 are weighting coefficients. There are many such systems in nature, systems which have a potential with multiple minima, thus allowing a mixture of configurations. One of the simplest example is the ammonia molecule, NH_3 . Its trigonal pyramidal inverts, something which can be measured in the microwave region ([41–43]). Helium-6 is a more complex mixture, and part of our goal is to determine c_1 and c_2 . In order to do this, we must solve the following eigenvalue problem:

$$\begin{pmatrix} \langle\psi_1|H|\psi_1\rangle & \langle\psi_1|H|\psi_2\rangle \\ \langle\psi_2|H|\psi_1\rangle & \langle\psi_2|H|\psi_2\rangle \end{pmatrix} \begin{pmatrix} c_1 \\ c_2 \end{pmatrix} = E \begin{pmatrix} 1 & \langle\psi_1|\psi_2\rangle \\ \langle\psi_2|\psi_1\rangle & 1 \end{pmatrix} \begin{pmatrix} c_1 \\ c_2 \end{pmatrix}. \quad (3.46)$$

The normalization is

$$c_1^2 + c_2^2 + 2c_1c_2\langle\psi_1|\psi_2\rangle = 1. \quad (3.47)$$

In eq.(3.46), \hat{H} is the Hamiltonian operator, E is the energy which will also be determined by solving this equation, $\langle\psi_1|\psi_2\rangle$ is the overlap of the two configurations, and $\langle\psi_1|H|\psi_2\rangle$ is the off-diagonal matrix element of the Hamiltonian between the two configurations. We need to determine two of these quantities: the overlap of the

configurations and the Hamiltonian between the two configurations.

First, we need to represent both systems in the same coordinate system. This is not trivial, as the center-of-mass of the two systems is not at the same point. Figure 3.3 illustrates the two configurations. The center-of-mass of the cigar system is in the alpha particle, whereas in the alpha-dineutron it is between the alpha and dineutron. In calculations such as the mean-square radius, the location of the center-of-mass is very important, and we must make sure that each configuration is properly referenced from the center-of-mass.

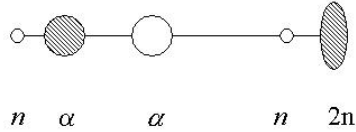


Figure 3.3: The two configurations of Helium-6 pictured together. The alpha-dineutron components are filled with diagonal stripes, the cigar configuration components are open circles and are labeled in italic script. In the figure, the distance between the alpha and the dineutron is the same as the distance across the entire cigar configuration.

Now that we are oriented, we will compute the overlap of the two configurations:

$$\langle \psi_1 | \psi_2 \rangle = N_1 N_2 \langle 0 | a_{-2} a_2 a_{-1} a_1 a_{-p} a_p a_{-p'}^\dagger a_{-p'}^\dagger a_{-1'}^\dagger a_{-1'}^\dagger a_{+1}^\dagger a_{+1}^\dagger | 0 \rangle. \quad (3.48)$$

The primes on the labels of the creation operators indicate that these are particles located at a different location, while the plus and minus labels retain the meaning

from before ((3.24)). It is not necessary to sum over spin projections here, as in (3.21), as the neutrons in the bra are at the same spatial location, so the sum over the projections in the ket does not introduce any new information. After one contracts all the operators in the above equation, one obtains:

$$\langle \psi_1 | \psi_2 \rangle = \frac{\sqrt{2} [\theta_{\alpha\alpha}^4 \theta_{d+} \theta_{d-} + \theta_{d\alpha}^2 \theta_{\alpha+} \theta_{\alpha-} - \theta_{\alpha\alpha}^3 \theta_{d\alpha} (\theta_{d+} \theta_{\alpha-} + \theta_{d-} \theta_{\alpha+})]}{\sqrt{\theta_{\alpha}^2 (\theta_{\alpha} \theta_d - \theta_{12}^2)^2 \theta_{\alpha'}^2 [\theta_{\alpha'}^2 (\theta_n^2 + \theta_{\pm}^2) + 2\theta_{12'}^4 - 2\theta_{12'} \theta_{\alpha'} (\theta_n + \theta_{\pm})]}}. \quad (3.49)$$

The overlaps in the numerator of eq.(3.49) are new overlaps between the two configurations, while the ones in the denominator are the overlaps from the normalizations of the individual configurations, eq.(3.23) and eq.(3.3). The new overlaps are (primes always refer to cigar wave function coordinates):

$$\theta_{\alpha\alpha} = \langle \alpha | \alpha' \rangle, \quad (3.50)$$

$$\theta_{d+} = \langle d | + \rangle, \quad (3.51)$$

$$\theta_{d-} = \langle d | - \rangle, \quad (3.52)$$

$$\theta_{d\alpha} = \langle d | \alpha' \rangle, \quad (3.53)$$

$$\theta_{\alpha+} = \langle \alpha | + \rangle, \quad (3.54)$$

$$\theta_{\alpha-} = \langle \alpha | - \rangle. \quad (3.55)$$

With these overlaps, we can calculate the overlap of the two configurations (eq.(3.49)). They also appear in the terms resulting from the calculation of expectation values, which is shown next.

In order to calculate the expectation value of the Hamiltonian, we need the expectation values of one-body and two-body operators. The procedure is exactly the same

as was shown before, so now we list only the results. First, the one-body operators:

$$\begin{aligned} \langle O^{(1)} \rangle_{\alpha\alpha} &= \langle \alpha | O^{(1)} | \alpha' \rangle \\ &\times (\theta_{\alpha\alpha}^3 \theta_{d+} \theta_{d-} + 2\theta_{\alpha\alpha} \theta_{\alpha+} \theta_{\alpha-} \theta_{d\alpha}^2 - 3\theta_{\alpha\alpha}^2 \theta_{d\alpha} (\theta_{d+} \theta_{\alpha-} + \theta_{d-} \theta_{\alpha+})) \end{aligned} \quad (3.56)$$

$$\langle O^{(1)} \rangle_{d+} = \langle d | O^{(1)} | + \rangle \theta_{\alpha\alpha}^3 (\theta_{\alpha\alpha} \theta_{d-} - \theta_{d\alpha} \theta_{\alpha-}), \quad (3.57)$$

$$\langle O^{(1)} \rangle_{d-} = \langle d | O^{(1)} | - \rangle \theta_{\alpha\alpha}^3 (\theta_{\alpha\alpha} \theta_{d+} - \theta_{d\alpha} \theta_{\alpha+}), \quad (3.58)$$

$$\langle O^{(1)} \rangle_{d\alpha} = \langle d | O^{(1)} | \alpha' \rangle \theta_{\alpha\alpha}^2 (2\theta_{\alpha+} \theta_{\alpha-} \theta_{d\alpha} - \theta_{\alpha\alpha} (\theta_{d+} \theta_{\alpha-} + \theta_{d-} \theta_{\alpha+})), \quad (3.59)$$

$$\langle O^{(1)} \rangle_{\alpha+} = \langle \alpha | O^{(1)} | + \rangle \theta_{\alpha\alpha}^2 \theta_{d\alpha} (\theta_{\alpha-} \theta_{d\alpha} - \theta_{\alpha\alpha} \theta_{d-}), \quad (3.60)$$

$$\langle O^{(1)} \rangle_{\alpha-} = \langle \alpha | O^{(1)} | - \rangle \theta_{\alpha\alpha}^2 \theta_{d\alpha} (\theta_{\alpha+} \theta_{d\alpha} - \theta_{\alpha\alpha} \theta_{d+}). \quad (3.61)$$

As before, these terms are summed together, then divided by a normalization factor, which in this case is the denominator of eq.(3.49). Now, we proceed with the two-body

operators:

$$\begin{aligned} \langle O^{(2)} \rangle_\alpha &= \langle \alpha\alpha | O^{(2)} | \alpha'\alpha' \rangle \\ &= [6\theta_{\alpha\alpha}^2 \theta_{d+} \theta_{d-} + \theta_{d\alpha}^2 \theta_{\alpha+} \theta_{\alpha-} - 3\theta_{\alpha\alpha} \theta_{d\alpha} (\theta_{d+} \theta_{\alpha-} + \theta_{d-} \theta_{\alpha+})], \end{aligned} \quad (3.62)$$

$$\langle O^{(2)} \rangle_{\alpha^2 d+} = \langle \alpha d | O^{(2)} | + \alpha' \rangle \theta_{\alpha\alpha}^2 (4\theta_{\alpha\alpha} \theta_{d-} - 3\theta_{d\alpha} \theta_{\alpha-}), \quad (3.63)$$

$$\langle O^{(2)} \rangle_{\alpha^2 d-} = \langle \alpha d | O^{(2)} | - \alpha' \rangle \theta_{\alpha\alpha}^2 (4\theta_{\alpha\alpha} \theta_{d+} - 3\theta_{d\alpha} \theta_{\alpha+}), \quad (3.64)$$

$$\langle O^{(2)} \rangle_{\alpha\alpha\alpha+} = \langle \alpha\alpha | O^{(2)} | \alpha'+ \rangle (2\theta_{\alpha\alpha} \theta_{\alpha-} \theta_{d\alpha}^2 - 3\theta_{\alpha\alpha}^2 \theta_{d\alpha} \theta_{d-}), \quad (3.65)$$

$$\langle O^{(2)} \rangle_{\alpha\alpha\alpha-} = \langle \alpha\alpha | O^{(2)} | \alpha'- \rangle (2\theta_{\alpha\alpha} \theta_{\alpha+} \theta_{d\alpha}^2 - 3\theta_{\alpha\alpha}^2 \theta_{d\alpha} \theta_{d+}), \quad (3.66)$$

$$\langle O^{(2)} \rangle_{d\alpha\alpha\alpha} = \langle d\alpha' | O^{(2)} | \alpha'\alpha' \rangle \theta_{\alpha\alpha} [4\theta_{d\alpha} \theta_{\alpha-} \theta_{\alpha+} - 3\theta_{\alpha\alpha} (\theta_{\alpha+} \theta_{d-} + \theta_{\alpha-} \theta_{d+})], \quad (3.67)$$

$$\langle O^{(2)} \rangle_{d+d-} = \langle dd | O^{(2)} | + - \rangle \theta_{\alpha\alpha}^4, \quad (3.68)$$

$$\langle O^{(2)} \rangle_{d+d\alpha} = -\langle dd | O^{(2)} | \alpha'+ \rangle \theta_{\alpha\alpha}^3 \theta_{\alpha-}, \quad (3.69)$$

$$\langle O^{(2)} \rangle_{d-d\alpha} = -\langle dd | O^{(2)} | \alpha'- \rangle \theta_{\alpha\alpha}^3 \theta_{\alpha+}, \quad (3.70)$$

$$\langle O^{(2)} \rangle_{d+\alpha-} = -\langle d\alpha | O^{(2)} | - + \rangle \theta_{\alpha\alpha}^3 \theta_{d\alpha}, \quad (3.71)$$

$$\langle O^{(2)} \rangle_{d-\alpha+} = -\langle d\alpha | O^{(2)} | + - \rangle \theta_{\alpha\alpha}^3 \theta_{d\alpha}, \quad (3.72)$$

$$\langle O^{(2)} \rangle_{\alpha+d\alpha} = \langle d\alpha | O^{(2)} | + \alpha' \rangle \theta_{\alpha\alpha}^2 (2\theta_{d\alpha} \theta_{\alpha-} - \theta_{\alpha\alpha} \theta_{d-}), \quad (3.73)$$

$$\langle O^{(2)} \rangle_{\alpha-d\alpha} = \langle d\alpha | O^{(2)} | + \alpha' \rangle \theta_{\alpha\alpha}^2 (2\theta_{d\alpha} \theta_{\alpha+} - \theta_{\alpha\alpha} \theta_{d+}), \quad (3.74)$$

$$\langle O^{(2)} \rangle_{\alpha+\alpha-} = \langle \alpha\alpha | O^{(2)} | + - \rangle \theta_{\alpha\alpha}^2 \theta_{d\alpha}^2, \quad (3.75)$$

$$\langle O^{(2)} \rangle_{d\alpha d\alpha} = \langle dd | O^{(2)} | \alpha'\alpha' \rangle \theta_{\alpha\alpha}^2 \theta_{\alpha+} \theta_{\alpha-}. \quad (3.76)$$

As always, these terms are collected and summed, and divided by the normalization.

With these operators, we can complete the calculation of the expectation value of the Hamiltonian, and thus we can find the minimum energy with eq.(3.46). With the value of E , we can find an expression for c_1 in terms of c_2 :

$$c_1 = -\frac{H_{12} - E \langle \psi_1 | \psi_2 \rangle}{H_{11} - E} c_2, \quad (3.77)$$

where $H_{12} = \langle \psi_1 | H | \psi_2 \rangle$. This value for c_1 is then substituted into eq.(3.47). It should

be noted that when dealing with off-diagonal matrix elements such as $\langle\psi_1|\psi_2\rangle$, the overall sign is arbitrary, so in eq.(3.46), $\langle\psi_1|H|\psi_2\rangle$ and $\langle\psi_1|\psi_2\rangle$ have an arbitrary sign (though once one is chosen for one of these, it determines the sign of the other). How the choice of sign is made is discussed in the next chapter. Once c_1 and c_2 have been determined, the expectation value of any other operator (an observable not in the Hamiltonian) can be computed:

$$\langle O \rangle = c_1^2 \langle \psi_1 | O | \psi_1 \rangle + c_2^2 \langle \psi_2 | O | \psi_2 \rangle + c_1 c_2 (\langle \psi_1 | O | \psi_2 \rangle + \langle \psi_2 | O | \psi_1 \rangle). \quad (3.78)$$

We now have completed the discussion of the basic formalism behind the ${}^6\text{He}$ calculations. The calculation with a specific choice of single-particle wave function will be discussed in the following chapter. We now move on to the discussion of the other nucleus of interest, ${}^6\text{Li}$.

3.2 Lithium-6

The other main subject of this work, ${}^6\text{Li}$, composes 7.5% of natural lithium [44]. As mentioned before, it is well studied experimentally. We study it here because it is the beta-decay product of ${}^6\text{He}$ and is also a difficult test of structure theories. Before going into the two configurations of ${}^6\text{Li}$, we will discuss the projection into good states of angular momentum for ${}^6\text{Li}$, as it is the same for both configurations.

As mentioned in section 2.4, ${}^6\text{Li}$ has a ground state spin equal to one, which, in our model, comes from the deuteron spin. In this case, we must use the full general formula, eq.(2.35). When we rotate the ${}^6\text{Li}$ wave function, we have not only the spatial rotation, as in ${}^6\text{He}$, but also the rotation of the spin part of the wave function. In the case of ${}^6\text{Li}$, this means rotating a spin one object. The d -matrices for spin-one objects can be found in [40]. We can re-write eq.(2.35) to show the effect of the spin-rotation

explicitly:

$$\langle \Psi^{JM} | H | \Psi^{JM} \rangle = \frac{\int d_{KK}^J(\vartheta) \langle \phi | \exp(i\vartheta \hat{J}_y) H | \phi \rangle d_{kk}^1(\vartheta) d \cos \vartheta}{\int d_{KK}^J(\vartheta) \langle \phi | \exp(i\vartheta \hat{J}_y) | \phi \rangle d_{kk}^1(\vartheta) d \cos \vartheta}, \quad (3.79)$$

where ϕ is the spatial wave function, and the d_{kk}^1 is the factor that comes from rotating the spin wave function. Since this projection does not have a definite parity, unlike in ${}^6\text{He}$, we also must project into the desired parity of the state (in ${}^6\text{Li}$'s case, positive).

The parity projection operator is:

$$|\Psi; J^\pi\rangle = \frac{1 \pm \hat{P}^r}{2} |\Psi; J\rangle, \quad (3.80)$$

where \hat{P}^r is the parity operator which inverts the coordinates of Ψ through the origin. The parity can be positive or negative, whichever is desired determines which sign is chosen in eq.(3.80). Now we have the method of choosing specific J^π states in ${}^6\text{Li}$, and can move on to the discussion of the specific configurations.

3.2.1 Alpha-deuteron configuration

The spatial picture of this system is the same as in Figure 3.1. The wave function is

$$|\Psi\rangle = N a_p^\dagger a_{-p}^\dagger a_1^\dagger a_{-1}^\dagger a_{pd}^\dagger a_{nd}^\dagger |0\rangle, \quad (3.81)$$

where the designations for the alpha particle are the same as in eq.(3.3), a_{pd}^\dagger creates the proton in the deuteron, and a_{nd}^\dagger creates the neutron in the external deuteron. The deuteron, and hence ${}^6\text{Li}$, has spin=1. For convenience, we take the spins of the external proton and neutron parallel and in the ‘‘up’’ projection. The normalization expression for ${}^6\text{Li}$ turns out to be the same as in ${}^6\text{He}$, (eq.(3.3)). In fact, the expressions for all the spin- and charge-independent operators are identical to the case of helium, and will not be repeated here. Operators that are sensitive to charge will see a difference,

but for spin- and isospin-independent operators, the results in all configurations of ${}^6\text{Li}$ match the corresponding case in ${}^6\text{He}$. For operators sensitive to isospin, those results will be given in the next chapter in the details about particular operators. We turn now to the case of spin-dependent operators in the alpha-deuteron configuration.

Unfortunately, spin-dependent operators are difficult to treat generally, so we will work with the two specific ones of interest for our calculations, the first one being the spin-orbit operator, $\mathbf{L} \cdot \mathbf{S}$.

The spin-orbit operator is

$$\mathbf{L} \cdot \mathbf{S} = L_x S_x + L_y S_y + L_z S_z = \frac{1}{2} (L_+ S_- + L_- S_+) + L_z S_z, \quad (3.82)$$

where in the term on the far right we re-wrote the expression to be in terms of the spherical generators of the rotation group. L_{\pm} and S_{\pm} are raising and lowering operators for orbital angular momentum and spin angular momentum. They raise (or lower) the projection of the relevant angular momentum on the chosen quantization axis. L_{\pm} has a spatial definition and will be dealt with in the next chapter. All that needs to be mentioned now is that for all of our calculations, $\langle L_- \rangle = -\langle L_+ \rangle$, therefore all expressions in this chapter will be shown in terms of $\langle L_+ \rangle$. This is because the rotation that generates the angular momentum is about the y -axis, thus only L_y is non-vanishing.

The Byzantine inner workings of spin and rotation

Before going into the machinery of the operator, we need to look at the effects of rotation on the spin part of the wave function. Since this operator affects spin, the effect of the angular momentum projection process needs to be taken into account. Protons and neutrons are spin-1/2 particles, and thus obey the following rotation law:

$$\hat{\mathfrak{R}}_y |\frac{1}{2} m\rangle = \sum_{m'} d_{m'm}^{1/2}(\vartheta) |\frac{1}{2} m'\rangle. \quad (3.83)$$

The $d_{m'm}^{1/2}(\vartheta)$ matrix is fairly simple:

$$d_{m'm}^{1/2}(\vartheta) = \begin{pmatrix} \cos \frac{\vartheta}{2} & -\sin \frac{\vartheta}{2} \\ \sin \frac{\vartheta}{2} & \cos \frac{\vartheta}{2} \end{pmatrix}. \quad (3.84)$$

For example, if we rotate a pair of particles with parallel spins pointing “up” (i.e., in the spin state $|SM\rangle = |11\rangle$), we get the following expression:

$$\hat{\mathfrak{R}}a_+^\dagger b_+^\dagger |0\rangle = \left(\cos \frac{\vartheta}{2} a_+^\dagger + \sin \frac{\vartheta}{2} a_-^\dagger \right) \left(\cos \frac{\vartheta}{2} b_+^\dagger + \sin \frac{\vartheta}{2} b_-^\dagger \right) |0\rangle, \quad (3.85)$$

where the + and - denote the spin projection of the particle. Collecting and simplifying, we obtain:

$$= \left(\cos^2 \frac{\vartheta}{2} a_+^\dagger b_+^\dagger + \sin^2 \frac{\vartheta}{2} a_-^\dagger b_-^\dagger + \frac{\sin \vartheta}{2} (a_-^\dagger b_+^\dagger + a_+^\dagger b_-^\dagger) \right) |0\rangle. \quad (3.86)$$

Using the following relation,

$$|+-\rangle = \frac{1}{\sqrt{2}} (|10\rangle + |00\rangle) \quad (3.87)$$

$$|-+\rangle = \frac{1}{\sqrt{2}} (|10\rangle - |00\rangle), \quad (3.88)$$

we can re-write the result in terms of spinors:

$$\hat{\mathfrak{R}}|11\rangle = \cos^2 \frac{\vartheta}{2} |11\rangle + \frac{\sin \vartheta}{\sqrt{2}} |10\rangle + \sin^2 \frac{\vartheta}{2} |1-1\rangle. \quad (3.89)$$

Now that we have these relations, we can move on to the detailed effects of the operator.

The $\mathbf{L} \cdot \mathbf{S}$ operator appears in a two-body potential, so we examine how the operator operates on pairs of particles. We are looking at matrix elements of the kind:

$$\langle V_{LS} \rangle = \frac{1}{2} \langle \alpha\beta; SM | V(\mathbf{r}) (L_- S_+ + L_+ S_-) | \delta\gamma; S'M' \rangle, \quad (3.90)$$

Table 3.1: This table shows the results of the spin raising and lowering operator acting between any combination of spin-1 states in terms of the rotation angle, ϑ , and the potential and orbital angular momentum operators, VL_{\pm} .

	$ 11\rangle$	$ 10\rangle$	$ 1-1\rangle$
$\langle 11 $	$-\sin \vartheta \langle VL_+ \rangle$	$-\cos \vartheta \langle VL_+ \rangle$	$\sin \vartheta \langle VL_+ \rangle$
$\langle 10 $	$\cos \vartheta \langle VL_+ \rangle$	$-\sin \vartheta \langle VL_+ \rangle$	$-\cos \vartheta \langle VL_+ \rangle$
$\langle 1-1 $	$\sin \vartheta \langle VL_+ \rangle$	$\cos \vartheta \langle VL_+ \rangle$	$-\sin \vartheta \langle VL_+ \rangle$

where α, β, γ and δ are spatial wave functions, $V(\mathbf{r})$ is some spatial form-factor of the potential, and $S, S', M,$ and M' are the spin quantum numbers of the pair of particles.

Focusing now on the S_{\pm} operators, they have the following effect:

$$\langle 1M|S_{\pm}|SM'\rangle = \sqrt{2 - M'(M' \pm 1)}\delta_{S,1}\delta_{M,M' \mp 1}. \quad (3.91)$$

We must go through all the matrix elements, couple the bra and ket to good states of spin, then select the non-vanishing terms. By doing derivations like that began in eq.(3.85) and using the definition of the operator in eq.(3.91), we can construct a table containing all combinations for the action of the S_{\pm} operator (Table 3.1).

Spin-orbit continued

With the matrix elements of S_+ and S_- , we now need to multiply them by the correct combinations of overlaps to obtain the complete matrix element. For example, if we are talking about the complete matrix element involving the spin-up proton in the alpha particle and the proton in the deuteron, we need to simplify the following expression:

$$\langle d_p \alpha_{p+} | V_{LS} | \alpha_{p+} dp \rangle \langle 0 | a_{nd} a_{-1} a_1 a_{-p} \tilde{a}_{-p}^{\dagger} \tilde{a}_1^{\dagger} \tilde{a}_{-1}^{\dagger} \tilde{a}_{nd}^{\dagger} | 0 \rangle, \quad (3.92)$$

where the tilde (\tilde{a}) denotes that operator has been rotated with respect to the unmarked operators. The operator matrix element in the beginning of eq.(3.92) is taken care of by using Table 3.1, but we must contend with the rest of the expression, keeping in mind the effects of rotating the operators. In Table 3.2, we collect all the

non-zero combinations for overlaps. There are certain overlaps that are zero, these are of the form

$$\langle 0 | a_\alpha a_{-\alpha} \tilde{a}_\alpha^\dagger \tilde{a}_d^\dagger | 0 \rangle, \quad (3.93)$$

where the a_α operators refer to a particle created or destroyed in the alpha particle. These particles have to be either all protons or all neutrons. Any term with the overlap (3.93) in it is zero, due to the orthogonality of spins. Two particles of the same type in the alpha particle are in a singlet spin state (the annihilation operators in this example), but the created particles have parallel spins, and are thus clearly in the triplet spin state, therefore, the overlap vanishes. This is also true for the transpose of (3.93).

After one combines all the correct matrix elements from Table 3.1 with the appropriate overlap from Table 3.2 and sums together all terms from a certain spatial geometry, we are left with only two terms:

$$\langle V_{LS} \rangle_{\alpha^2 d^2} = -2 \sin \vartheta \langle V_{L+} \rangle_{\alpha^2 d^2} (2\theta_\alpha^3 \theta_n - \theta_\alpha^2 \theta_{12}^2), \quad (3.94)$$

$$\langle V_{LS} \rangle_{\alpha d d \alpha} = 2 \sin \vartheta \langle V_{L+} \rangle_{\alpha d d \alpha} (\theta_\alpha^3 \theta_n - \theta_\alpha^2 \theta_{12}^2). \quad (3.95)$$

These are the two terms which contribute to the spin-orbit interaction for a spin-orbit interaction that does not depend on isospin (heretofore tacitly assumed). They both vanish in the non-rotated picture ($\vartheta = 0$).

Tensor operator

The other spin-dependent operator we will examine is the spherical tensor operator.

The spherical tensor operator, \hat{S}_{12} , is generally written as

$$S_{12} = \frac{3}{r^2} (\boldsymbol{\sigma}_1 \cdot \mathbf{r}) (\boldsymbol{\sigma}_2 \cdot \mathbf{r}) - \boldsymbol{\sigma}_1 \cdot \boldsymbol{\sigma}_2, \quad (3.96)$$

Table 3.2: The overlaps for the ${}^6\text{Li}$ wave function involving rotated operators. The entire list of overlaps is quite extensive. In the interest of brevity, we list only half of the overlaps here, because if one changes every proton into a neutron and vice-versa in each line, the overlap expression is the same. To further reduce the size of the table, each overlap has a certain symmetry with respect to its transpose. It either changes sign or does not. Those that are the same as their transpose are followed by a superscript “+”, and those that change sign are followed by a superscript “-”.

Overlap	Value
$\langle 0 a_{nd}a_{-1}a_1a_{-p}\tilde{a}_{-p}^\dagger\tilde{a}_{-1}^\dagger\tilde{a}_{nd}^\dagger 0\rangle^+$	$\cos^2\frac{\vartheta}{2}(\theta_\alpha^3\theta_n - \theta_\alpha^2\theta_{12}^2)$
$\langle 0 a_{nd}a_{-1}a_1a_p\tilde{a}_{-p}^\dagger\tilde{a}_{-1}^\dagger\tilde{a}_{nd}^\dagger 0\rangle^-$	$-\frac{\sin\vartheta}{2}(\theta_\alpha^3\theta_n - \theta_\alpha^2\theta_{12}^2)$
$\langle 0 a_{nd}a_{-1}a_1a_p\tilde{a}_p^\dagger\tilde{a}_{-1}^\dagger\tilde{a}_{nd}^\dagger 0\rangle^+$	$\cos^2\frac{\vartheta}{2}(\theta_\alpha^3\theta_n - \theta_\alpha^2\theta_{12}^2)$
$\langle 0 a_{nd}a_{-1}a_{-p}a_p\tilde{a}_p^\dagger\tilde{a}_{-p}^\dagger\tilde{a}_{nd}^\dagger 0\rangle^+$	$\cos^2\frac{\vartheta}{2}\theta_\alpha^3\theta_n + \sin^2\frac{\vartheta}{2}\theta_\alpha^2\theta_{12}^2$
$\langle 0 a_{nd}a_1a_{-p}a_p\tilde{a}_p^\dagger\tilde{a}_{-p}^\dagger\tilde{a}_{nd}^\dagger 0\rangle^-$	$-\frac{\sin\vartheta}{2}(\theta_\alpha^3\theta_n - \theta_\alpha^2\theta_{12}^2)$
$\langle 0 a_{nd}a_1a_{-p}a_p\tilde{a}_p^\dagger\tilde{a}_{-p}^\dagger\tilde{a}_{nd}^\dagger 0\rangle^+$	$\cos^2\frac{\vartheta}{2}(\theta_\alpha^3\theta_n - \theta_\alpha^2\theta_{12}^2)$
$\langle 0 a_{nd}a_{pd}a_{-1}a_1\tilde{a}_1^\dagger\tilde{a}_{-1}^\dagger\tilde{a}_{pd}^\dagger\tilde{a}_{nd}^\dagger 0\rangle^+$	$\cos^2\frac{\vartheta}{2}(\theta_\alpha^2\theta_n^2 - \theta_\alpha\theta_{12}^2\theta_n)$
$\langle 0 a_{nd}a_{pd}a_{-1}a_{-p}\tilde{a}_{-p}^\dagger\tilde{a}_{-1}^\dagger\tilde{a}_{pd}^\dagger\tilde{a}_{nd}^\dagger 0\rangle^+$	$(\cos^2\frac{\vartheta}{2}\theta_\alpha\theta_n + \sin^2\frac{\vartheta}{2}\theta_{12}^2)^2$
$\langle 0 a_{nd}a_{pd}a_{-1}a_{-p}\tilde{a}_p^\dagger\tilde{a}_{-1}^\dagger\tilde{a}_{pd}^\dagger\tilde{a}_{nd}^\dagger 0\rangle^-$	$\frac{\sin\vartheta}{2}(\cos^2\frac{\vartheta}{2}\theta_\alpha\theta_n + \sin^2\frac{\vartheta}{2}\theta_{12}^2)(\theta_\alpha\theta_n - \theta_{12}^2)$
$\langle 0 a_{nd}a_{pd}a_{-1}a_{-p}\tilde{a}_{-p}^\dagger\tilde{a}_1^\dagger\tilde{a}_{pd}^\dagger\tilde{a}_{nd}^\dagger 0\rangle^-$	$\frac{\sin\vartheta}{2}(\cos^2\frac{\vartheta}{2}\theta_\alpha\theta_n + \sin^2\frac{\vartheta}{2}\theta_{12}^2)(\theta_\alpha\theta_n - \theta_{12}^2)$
$\langle 0 a_{nd}a_{pd}a_{-1}a_{-p}\tilde{a}_p^\dagger\tilde{a}_1^\dagger\tilde{a}_{pd}^\dagger\tilde{a}_{nd}^\dagger 0\rangle^+$	$\frac{\sin^2\vartheta}{4}(\theta_\alpha\theta_n - \theta_{12}^2)^2$
$\langle 0 a_{nd}a_{pd}a_1a_p\tilde{a}_p^\dagger\tilde{a}_{-1}^\dagger\tilde{a}_{pd}^\dagger\tilde{a}_{nd}^\dagger 0\rangle^-$	$-\frac{\sin\vartheta}{2}\cos^2\frac{\vartheta}{2}(\theta_\alpha\theta_n - \theta_{12}^2)^2$
$\langle 0 a_{nd}a_{pd}a_1a_p\tilde{a}_p^\dagger\tilde{a}_{-1}^\dagger\tilde{a}_{pd}^\dagger\tilde{a}_{nd}^\dagger 0\rangle^-$	$-\frac{\sin\vartheta}{2}\cos^2\frac{\vartheta}{2}(\theta_\alpha\theta_n - \theta_{12}^2)^2$
$\langle 0 a_{nd}a_{pd}a_1a_p\tilde{a}_p^\dagger\tilde{a}_1^\dagger\tilde{a}_{pd}^\dagger\tilde{a}_{nd}^\dagger 0\rangle^+$	$\cos^4\frac{\vartheta}{2}(\theta_\alpha\theta_n - \theta_{12}^2)^2$
$\langle 0 a_{nd}a_{pd}a_{-1}a_1\tilde{a}_p^\dagger\tilde{a}_1^\dagger\tilde{a}_{-1}^\dagger\tilde{a}_{nd}^\dagger 0\rangle^+$	$-\cos^2\frac{\vartheta}{2}(\theta_\alpha^2\theta_n\theta_{12} - \theta_\alpha\theta_{12}^3)$
$\langle 0 a_{nd}a_{pd}a_{-1}a_1\tilde{a}_{-p}^\dagger\tilde{a}_1^\dagger\tilde{a}_{-1}^\dagger\tilde{a}_{nd}^\dagger 0\rangle^-$	$\frac{\sin\vartheta}{2}(\theta_\alpha^2\theta_n\theta_{12} - \theta_\alpha\theta_{12}^3)$
$\langle 0 a_{nd}a_{pd}a_{-1}a_{-p}\tilde{a}_p^\dagger\tilde{a}_{-p}^\dagger\tilde{a}_{-1}^\dagger\tilde{a}_{nd}^\dagger 0\rangle^+$	$-(\cos^2\frac{\vartheta}{2}\theta_\alpha^2\theta_n\theta_{12} + \sin^2\frac{\vartheta}{2}\theta_\alpha\theta_{12}^3)$
$\langle 0 a_{nd}a_{pd}a_{-1}a_{-p}\tilde{a}_p^\dagger\tilde{a}_{-p}^\dagger\tilde{a}_1^\dagger\tilde{a}_{nd}^\dagger 0\rangle^-$	$-\frac{\sin\vartheta}{2}(\theta_\alpha^2\theta_n\theta_{12} - \theta_\alpha\theta_{12}^3)$
$\langle 0 a_{nd}a_{pd}a_1a_{-p}\tilde{a}_p^\dagger\tilde{a}_{-p}^\dagger\tilde{a}_1^\dagger\tilde{a}_{nd}^\dagger 0\rangle^-$	$\frac{\sin\vartheta}{2}(\theta_\alpha^2\theta_n\theta_{12} - \theta_\alpha\theta_{12}^3)$
$\langle 0 a_{nd}a_{pd}a_1a_{-p}\tilde{a}_p^\dagger\tilde{a}_{-p}^\dagger\tilde{a}_1^\dagger\tilde{a}_{nd}^\dagger 0\rangle^+$	$-\cos^2\frac{\vartheta}{2}(\theta_\alpha^2\theta_n\theta_{12} - \theta_\alpha\theta_{12}^3)$
$\langle 0 a_{-1}a_1a_{-p}a_p\tilde{a}_p^\dagger\tilde{a}_{-p}^\dagger\tilde{a}_{-1}^\dagger\tilde{a}_{nd}^\dagger 0\rangle^+$	$-\theta_\alpha^3\theta_{12}$
$\langle 0 a_{nd}a_{pd}a_{-1}a_{-p}\tilde{a}_p^\dagger\tilde{a}_{-p}^\dagger\tilde{a}_1^\dagger\tilde{a}_{-1}^\dagger 0\rangle^+$	$\theta_\alpha^2\theta_{12}^2$
$\langle 0 a_{-1}a_1a_{-p}a_p\tilde{a}_p^\dagger\tilde{a}_{-p}^\dagger\tilde{a}_1^\dagger\tilde{a}_{-1}^\dagger 0\rangle^+$	θ_α^4

where $\boldsymbol{\sigma}_i = 2\mathbf{s}_i$, and $\mathbf{r} = \mathbf{r}_1 - \mathbf{r}_2$. The tensor force is the interaction between particles' spin and relative motion. If one chooses the coordinate system carefully (i.e., placing the z-axis along \mathbf{r}), one can re-write the tensor operator as

$$S_{12} = 2(3S_z^2 - S^2). \quad (3.97)$$

As with the spin-orbit operator, the radial dependence of the force must be added in by hand,

$$\hat{V}_{tensor} = V_t(\mathbf{r}) S_{12}. \quad (3.98)$$

A table similar to Table 3.1 can be constructed for the tensor operator. This table is Table 3.3. The correct combination is picked out for the given term out of this table, then combined with the proper overlap from Table 3.2.

A careful glance at Table 3.3 may reveal something slightly unsettling. Matrix elements that appear to be complex conjugates of each other, $\langle 11|S_{12}\mathcal{R}|10\rangle$ and $\langle 10|S_{12}\mathcal{R}|11\rangle$, differ in the table by a factor of two. The source of this difference is twofold. First, the tensor operator in the form of (3.97) acts differently on the different K states of spin-one systems (projection along the symmetry axis in the body-fixed frame):

$$\hat{S}_{12}|1 \pm 1\rangle = 2|1 \pm 1\rangle, \quad (3.99)$$

$$\hat{S}_{12}|10\rangle = -4|10\rangle. \quad (3.100)$$

Second, and more important, is the location of the quantization axis. In the bra, the quantization axis is a lab frame axis which we have chosen to lie along the symmetry axis of the nucleus. In the ket, we have an axis that rotates with the nucleus, and thus can have any of the three projections in the laboratory frame. As we can see, however, in eq.(3.99), the tensor operator acts differently among the various spin projections in the body-fixed frame, thus when bringing the body-fixed axis back in line with the lab axis, the order of rotation and operation by the tensor operator is important. That is, the tensor operator, in the form of eq.(3.97) does not commute with the rotation operator. Thus, the matrix elements are different, as they are not truly Hermitian conjugates of each other.

Returning back to the tensor operator in ${}^6\text{Li}$, once again, for a given spatial geometry of the matrix element, there are many terms. These are summed over to give the

Table 3.3: Tabulated here are the results from the tensor operator, S_{12} , operates between any pair of triplet wave functions. All results are proportional to the radial dependence of the tensor force, V_t . The angle that appears in the chart is the rotation angle involved in the angular momentum projection process.

	$ 11\rangle$	$ 10\rangle$	$ 1-1\rangle$
$\langle 11 $	$2 \cos^2 \frac{\vartheta}{2}$	$-\sqrt{2} \sin \vartheta$	$2 \sin^2 \frac{\vartheta}{2}$
$\langle 10 $	$-2\sqrt{2} \sin \vartheta$	$-4 \cos \vartheta$	$2\sqrt{2} \sin \vartheta$
$\langle 1-1 $	$2 \sin^2 \frac{\vartheta}{2}$	$\sqrt{2} \sin \vartheta$	$2 \cos^2 \frac{\vartheta}{2}$

total result for the given spatial form-factor integral. These results are listed below:

$$\langle V_t \rangle_\alpha = \langle \alpha\alpha | V_t | \alpha\alpha \rangle \theta_{12}^4 \cos^2 \frac{\vartheta}{2}, \quad (3.101)$$

$$\langle V_t \rangle_{\alpha^2 d^2} = \langle \alpha d | V_t | d\alpha \rangle 2\theta_\alpha^2 \theta_2^2 \cos^2 \frac{\vartheta}{2}, \quad (3.102)$$

$$\langle V_t \rangle_d = \langle dd | V_t | dd \rangle \theta_\alpha^4 \cos^2 \frac{\vartheta}{2}, \quad (3.103)$$

$$\langle V_t \rangle_{\alpha\alpha d} = -\langle \alpha\alpha | V_t | \alpha d \rangle 2\theta_{12}^3 \theta_\alpha \cos^2 \frac{\vartheta}{2}, \quad (3.104)$$

$$\langle V_t \rangle_{d\alpha\alpha} = -\langle d\alpha | V_t | \alpha\alpha \rangle 2\theta_{12}^3 \theta_\alpha \cos^2 \frac{\vartheta}{2}, \quad (3.105)$$

$$\langle V_t \rangle_{ddd} = -\langle dd | V_t | d\alpha \rangle 2\theta_\alpha^3 \theta_{12} \cos^2 \frac{\vartheta}{2}, \quad (3.106)$$

$$\langle V_t \rangle_{\alpha d d} = -\langle \alpha d | V_t | dd \rangle 2\theta_\alpha^3 \theta_{12} \cos^2 \frac{\vartheta}{2}, \quad (3.107)$$

$$\langle V_t \rangle_{\alpha d \alpha d} = \langle \alpha\alpha | V_t | dd \rangle \theta_\alpha^2 \theta_{12}^2 \cos^2 \frac{\vartheta}{2}, \quad (3.108)$$

$$\langle V_t \rangle_{d\alpha d\alpha} = \langle dd | V_t | \alpha\alpha \rangle \theta_\alpha^2 \theta_{12}^2 \cos^2 \frac{\vartheta}{2}, \quad (3.109)$$

$$\langle V_t \rangle_{\alpha d d \alpha} = \langle \alpha d | V_t | \alpha d \rangle 2\theta_\alpha^2 \theta_{12}^2 \cos^2 \frac{\vartheta}{2}. \quad (3.110)$$

As usual, these are summed together and divided by the normalization. It is interesting to note that there is a contribution from the alpha particle (eq.(3.101)). Helium-6 also contains an alpha particle, but the tensor operator vanishes in its case. This is an effect of the overall spin structure of the 6-body wave function. In eq.(3.101), the alpha particle tensor matrix element is proportional to θ_{12}^4 ; in ${}^6\text{He}$, this term comes from the term between the two protons, but the tensor interaction vanishes for spin singlets (like the protons in the alpha particle), and therefore the terms in the alpha

particle vanish in the case of ${}^6\text{He}$. It should also be noted, that for a pure alpha particle with no external particles, the tensor operator vanishes in our model.

This concludes the section on the alpha-deuteron configuration of ${}^6\text{Li}$. We now move on to the cigar configuration.

3.2.2 Cigar configuration

The cigar configuration of ${}^6\text{Li}$ is where the spatial extent of the deuteron is much larger, such that there is a particle on each side of the alpha particle, just as in the diagram for the cigar configuration of ${}^6\text{He}$ (Figure 3.2), only one of the external particles is a proton, and one a neutron. The wave function is

$$|\Psi\rangle = N a_p^\dagger a_{-p}^\dagger a_1^\dagger a_{-1}^\dagger \sum_{\tau} (-)^{1/2-\tau} a_{\tau+}^\dagger a_{-\tau-}^\dagger |0\rangle, \quad (3.111)$$

where + and - indicate the right or left spatial position. As in the alpha-deuteron case, both external particles are created in the “up” spin-projection, but the sum is over isospin. The deuteron is an isosinglet, and we must sum over the projections of isospin in order to preserve the proper quantum numbers. This means, we still have the same cross terms that were in the cigar configuration of ${}^6\text{He}$. In the alpha-deuteron configuration, the normalization and all spin-independent operators had identical results in ${}^6\text{Li}$ as in ${}^6\text{He}$, which is also the case for the cigar configuration. Therefore, we proceed with showing the results of the spin-orbit and tensor operators in the cigar configuration.

The results for the spin-orbit operator follow below. There are additional overlaps to those shown in Table 3.2, but these are easily guessed at. Any term involving the cross term between the right and left side particles substitutes a θ_{\pm} for θ_n which would

appear in Table 3.2. Now, the list of terms of the spin-orbit operator:

$$\langle V_{LS} \rangle_{+^2-^2} = -\sin \vartheta \langle V L_+ \rangle_{+^2-^2} \theta_\alpha^4, \quad (3.112)$$

$$\langle V_{LS} \rangle_{+^{--}+} = -\sin \vartheta \langle V L_+ \rangle_{+^{--}+} \theta_\alpha^4, \quad (3.113)$$

$$\langle V_{LS} \rangle_{\alpha^2\pm^2} = -2 \sin \vartheta \langle V L_+ \rangle_{\alpha^2\pm^2} (2\theta_\alpha^3 \theta_n - \theta_\alpha^2 \theta_{12}^2), \quad (3.114)$$

$$\langle V_{LS} \rangle_{\alpha^2+-} = -2 \sin \vartheta \langle V L_+ \rangle_{\alpha^2+-} (2\theta_\alpha^3 \theta_\pm - \theta_\alpha^2 \theta_{12}^2), \quad (3.115)$$

$$\langle V_{LS} \rangle_{\alpha^{++}\alpha} = 2 \sin \vartheta \langle V L_+ \rangle_{\alpha^{++}\alpha} (\theta_\alpha \theta_n - 2\theta_\alpha \theta_{12}^2), \quad (3.116)$$

$$\langle V_{LS} \rangle_{\alpha^{+-}\alpha} = 2 \sin \vartheta \langle V L_+ \rangle_{\alpha^{+-}\alpha} (\theta_\alpha \theta_\pm - 2\theta_\alpha \theta_{12}^2), \quad (3.117)$$

$$\langle V_{LS} \rangle_{++-\alpha} = 4 \sin \vartheta \langle V L_+ \rangle_{++-\alpha} \theta_{12}^3 \theta_\alpha, \quad (3.118)$$

$$\langle V_{LS} \rangle_{+^{--}\alpha} = 4 \sin \vartheta \langle V L_+ \rangle_{+^{--}\alpha} \theta_{12}^3 \theta_\alpha. \quad (3.119)$$

We now list the results for the tensor operator in the cigar configuration:

$$\langle V_t \rangle_\alpha = \langle \alpha\alpha | V_t | \alpha\alpha \rangle \theta_{12}^4 \cos^2 \frac{\vartheta}{2}, \quad (3.120)$$

$$\langle V_t \rangle_{\alpha^2 \pm^2} = \langle \alpha \pm | V_t | \pm \alpha \rangle 2\theta_\alpha^2 \theta_{12}^2 \cos^2 \frac{\vartheta}{2}, \quad (3.121)$$

$$\langle V_t \rangle_{\alpha^2 + -} = \langle \alpha \pm | V_t | \mp \alpha \rangle 2\theta_\alpha^2 \theta_{12}^2 \cos^2 \frac{\vartheta}{2}, \quad (3.122)$$

$$\langle V_t \rangle_{+^2 -^2} = \langle + - | V_t | - + \rangle \theta_\alpha^4 \cos^2 \frac{\vartheta}{2}, \quad (3.123)$$

$$\langle V_t \rangle_{+ - - +} = \langle + - | V_t | + - \rangle \theta_\alpha^4 \cos^2 \frac{\vartheta}{2}, \quad (3.124)$$

$$\langle V_t \rangle_{\alpha\alpha\alpha\pm} = -\langle \alpha\alpha | V_t | \alpha\pm \rangle 2\theta_\alpha \theta_{12}^3 \cos^2 \frac{\vartheta}{2}, \quad (3.125)$$

$$\langle V_t \rangle_{\pm\alpha\alpha\alpha} = -\langle \pm\alpha | V_t | \alpha\alpha \rangle 2\theta_\alpha \theta_{12}^3 \cos^2 \frac{\vartheta}{2}, \quad (3.126)$$

$$\langle V_t \rangle_{\pm^2 \mp \alpha} = -\langle \pm \mp | V_t | \alpha\pm \rangle 2\theta_\alpha^3 \theta_{12} \cos^2 \frac{\vartheta}{2}, \quad (3.127)$$

$$\langle V_t \rangle_{\alpha\pm\mp^2} = -\langle \alpha \mp | V_t | \mp \pm \rangle 2\theta_\alpha^3 \theta_{12} \cos^2 \frac{\vartheta}{2}, \quad (3.128)$$

$$\langle V_t \rangle_{\pm\mp\mp\alpha} = -\langle \pm \mp | V_t | \alpha\mp \rangle 2\theta_\alpha^3 \theta_{12} \cos^2 \frac{\vartheta}{2}, \quad (3.129)$$

$$\langle V_t \rangle_{\alpha\pm\pm\mp} = -\langle \alpha \pm | V_t | \mp \pm \rangle 2\theta_\alpha^3 \theta_{12} \cos^2 \frac{\vartheta}{2}, \quad (3.130)$$

$$\langle V_t \rangle_{\alpha\pm\pm\alpha} = \langle \alpha \pm | V_t | \alpha\pm \rangle 2\theta_\alpha^2 \theta_{12}^2 \cos^2 \frac{\vartheta}{2}, \quad (3.131)$$

$$\langle V_t \rangle_{\alpha\pm\mp\alpha} = \langle \alpha \mp | V_t | \alpha\pm \rangle 2\theta_\alpha^2 \theta_{12}^2 \cos^2 \frac{\vartheta}{2}, \quad (3.132)$$

$$\langle V_t \rangle_{\alpha+\alpha-} = \langle \alpha\alpha | V_t | + - \rangle \theta_\alpha^2 \theta_{12}^2 \cos^2 \frac{\vartheta}{2}, \quad (3.133)$$

$$\langle V_t \rangle_{+\alpha-\alpha} = \langle + - | V_t | \alpha\alpha \rangle \theta_\alpha^2 \theta_{12}^2 \cos^2 \frac{\vartheta}{2}. \quad (3.134)$$

As before, these are summed together and divided by the normalization to yield a complete expectation value.

This concludes the section on the cigar configuration. Next, we move to the interference term of ${}^6\text{Li}$.

3.2.3 Interference term

As was the case in ${}^6\text{He}$, the overall wave function of ${}^6\text{Li}$ is a combination of the alpha-deuteron configuration and the cigar configuration. The same procedure was followed for ${}^6\text{Li}$ as in ${}^6\text{He}$ (beginning with eq.(3.46)). The one and two-body operators described in the section on the interference term of ${}^6\text{He}$ are the same in ${}^6\text{Li}$. As in the previous two sections, we only need to describe the results for the spin-orbit and tensor operators.

The overlaps for the interference term are not the same as in the alpha-deuteron case which is listed in Table 3.2. It is not necessary, however, to construct a new table. Table 3.2 gives the angular dependence, and one can translate the alpha-deuteron overlaps into interference term overlaps with their definitions in eq.(3.50-3.55). Now, without further ado, the results of the spin-orbit operator in the interference term:

$$\langle V_{LS} \rangle_{\alpha^2 d+} = -\langle V_{L+} \rangle_{\alpha^2 d+} (2\theta_{\alpha\alpha}^3 \theta_{d-} - \theta_{\alpha\alpha}^2 \theta_{d\alpha} \theta_{\alpha-}) \sin \vartheta, \quad (3.135)$$

$$\langle V_{LS} \rangle_{\alpha^2 d-} = -\langle V_{L+} \rangle_{\alpha^2 d-} (2\theta_{\alpha\alpha}^3 \theta_{d+} - \theta_{\alpha\alpha}^2 \theta_{d\alpha} \theta_{\alpha+}) \sin \vartheta, \quad (3.136)$$

$$\langle V_{LS} \rangle_{d\alpha\alpha+} = \langle V_{L+} \rangle_{d\alpha\alpha+} (\theta_{\alpha\alpha}^3 \theta_{d-} - 2\theta_{\alpha\alpha}^2 \theta_{d\alpha} \theta_{\alpha-}) \sin \vartheta, \quad (3.137)$$

$$\langle V_{LS} \rangle_{d\alpha\alpha-} = \langle V_{L+} \rangle_{d\alpha\alpha-} (\theta_{\alpha\alpha}^3 \theta_{d+} - 2\theta_{\alpha\alpha}^2 \theta_{d\alpha} \theta_{\alpha+}) \sin \vartheta, \quad (3.138)$$

$$\langle V_{LS} \rangle_{\alpha+d-} = \langle V_{L+} \rangle_{\alpha+d-} \theta_{\alpha\alpha}^3 \theta_{d\alpha} \sin \vartheta, \quad (3.139)$$

$$\langle V_{LS} \rangle_{\alpha-d+} = \langle V_{L+} \rangle_{\alpha-d+} \theta_{\alpha\alpha}^3 \theta_{d\alpha} \sin \vartheta. \quad (3.140)$$

These are the terms that make up the spin-orbit expectation value for the interference

term. For the tensor operator, the results are:

$$\langle V_t \rangle_\alpha = \langle \alpha\alpha | V_t | \alpha'\alpha' \rangle \theta_{d\alpha}^2 \theta_{\alpha+} \theta_{\alpha-} \cos^2 \frac{\vartheta}{2}, \quad (3.141)$$

$$\langle V_t \rangle_{\alpha^2 d+} = \langle \alpha d | V_t | + \alpha' \rangle \theta_{\alpha\alpha}^2 \theta_{d\alpha} \alpha_- \cos^2 \frac{\vartheta}{2}, \quad (3.142)$$

$$\langle V_t \rangle_{\alpha^2 d-} = \langle \alpha d | V_t | - \alpha' \rangle \theta_{\alpha\alpha}^2 \theta_{d\alpha} \alpha_+ \cos^2 \frac{\vartheta}{2}, \quad (3.143)$$

$$\langle V_t \rangle_{+^2 -^2} = \langle + - | V_t | - + \rangle \theta_{\alpha\alpha}^2 \cos^2 \frac{\vartheta}{2}, \quad (3.144)$$

$$\langle V_t \rangle_{\alpha\alpha\alpha+} = -\langle \alpha\alpha | V_t | \alpha' + \rangle \theta_{d\alpha}^2 \theta_{\alpha+} \theta_{\alpha\alpha} \cos^2 \frac{\vartheta}{2}, \quad (3.145)$$

$$\langle V_t \rangle_{\alpha\alpha\alpha-} = -\langle \alpha\alpha | V_t | \alpha' - \rangle \theta_{d\alpha}^2 \theta_{\alpha-} \theta_{\alpha\alpha} \cos^2 \frac{\vartheta}{2}, \quad (3.146)$$

$$\langle V_t \rangle_{d-\alpha+} = -\langle d\alpha | V_t | + - \rangle \theta_{\alpha\alpha}^3 \theta_{d\alpha} \cos^2 \frac{\vartheta}{2}, \quad (3.147)$$

$$\langle V_t \rangle_{d+d\alpha} = -\langle dd | V_t | + \alpha' \rangle \theta_{\alpha\alpha}^3 \theta_{\alpha-} \cos^2 \frac{\vartheta}{2}, \quad (3.148)$$

$$\langle V_t \rangle_{d-d\alpha} = -\langle dd | V_t | - \alpha' \rangle \theta_{\alpha\alpha}^3 \theta_{\alpha+} \cos^2 \frac{\vartheta}{2}, \quad (3.149)$$

$$\langle V_t \rangle_{\alpha+\alpha-} = \langle \alpha\alpha | V_t | + - \rangle \theta_{\alpha\alpha}^2 \theta_{d\alpha}^2 \cos^2 \frac{\vartheta}{2}, \quad (3.150)$$

$$\langle V_t \rangle_{d\alpha d\alpha} = \langle dd | V_t | \alpha'\alpha' \rangle \theta_{\alpha\alpha}^2 \theta_{\alpha+} \theta_{\alpha-} \cos^2 \frac{\vartheta}{2}, \quad (3.151)$$

$$\langle V_t \rangle_{\alpha+d\alpha} = \langle \alpha d | V_t | \alpha' + \rangle \theta_{\alpha\alpha}^2 \theta_{d\alpha} \theta_{\alpha-} \cos^2 \frac{\vartheta}{2}, \quad (3.152)$$

$$\langle V_t \rangle_{\alpha-d\alpha} = \langle \alpha d | V_t | \alpha' - \rangle \theta_{\alpha\alpha}^2 \theta_{d\alpha} \theta_{\alpha+} \cos^2 \frac{\vartheta}{2}. \quad (3.153)$$

With the spin-orbit and tensor interaction, one can then complete a calculation of the expectation value of the Hamiltonian for the interference term. One can then minimize ${}^6\text{Li}$ in the same way as was done for ${}^6\text{He}$.

Here now ends the chapter on the methods and formalism used in this study. The formalism was introduced through some simple examples, and then we applied the formalism to obtain some formal results in a very general sense for ${}^6\text{He}$ and ${}^6\text{Li}$. The next chapter will go into further detail with specific choices for single-particle wave functions, and inter-particle interactions.

Chapter 4

Gaussian Approximation

In the previous chapters, the general formalism was described. The formalism was then applied to the two nuclei of interest, ${}^6\text{He}$ and ${}^6\text{Li}$. The many expressions for expectation values were left in terms of matrix elements of an operator of a certain type. In this chapter, a specific single-particle basis will be selected, and these matrix elements for all operators will be derived. After the calculation of the matrix elements, numerical results will be given.

4.1 Helium-6

The single particle wave function chosen is the Gaussian wave function. This is a function of the form $f(x) = Ae^{-a(x-x_0)^2}$. This wave function is the ground state wave function of the quantum harmonic oscillator, and thus is a suitable wave function for any system around a potential minimum. Also, Gaussians can be integrated analytically, which greatly simplifies the calculations. Our specific Gaussians are also real, which also reduces the number of terms needed to be calculated, as the forward and reverse matrix elements are nearly always the same. The asymptotic behavior of the Gaussian is not correct, as it falls off too fast. The true asymptotics should be exponential. It will be shown later that for many observables, this is not critical,

however. The Gaussian approximation in the alpha-dineutron configuration will now be discussed.

4.1.1 Alpha-dineutron configuration

The alpha-dineutron configuration is pictured in Figure 3.1. The single-particle wave functions are:

$$\psi_\alpha(\mathbf{r}) = \left(\frac{\nu}{\pi}\right)^{3/4} \exp\left(-\frac{\nu}{2}(\mathbf{r} - \mathbf{d}/3)^2\right), \quad (4.1)$$

$$\phi_d(\mathbf{r}) = \left(\frac{\omega}{\pi}\right)^{3/4} \exp\left(-\frac{\omega}{2}(\mathbf{r} + 2\mathbf{d}/3)^2\right), \quad (4.2)$$

where ψ_α refers to a constituent of the alpha particle and has parameters ν , the oscillator length, and \mathbf{d} , which describes the distance separating the two clusters; ϕ_d refers to a particle in the dineutron, with the same parameter \mathbf{d} as in ψ_α , and ω for its oscillator length. The coefficient of \mathbf{d} is chosen so that the origin of the coordinate system is at the classical center-of-mass of the system. By looking again at the alpha-particle wave function, we can illustrate another nice property of the Gaussian:

$$\psi_\alpha(\mathbf{r}) = N \exp\left(-\frac{\nu}{2}(\mathbf{r} - \mathbf{d}/3)^2\right) = N e^{-\nu(r^2 + d^2/9)/2} \sum_n \frac{1}{n!} (\nu \mathbf{r} \cdot \mathbf{d})^n, \quad (4.3)$$

which shows that every partial wave is wrapped up inside each Gaussian displaced with respect to the center-of-mass. We can select \mathbf{d} to lie along the z -axis, which makes our wave functions (eqs[4.1,4.2]) look like

$$\psi_\alpha(x, y, z) = \left(\frac{\nu}{\pi}\right)^{3/4} \exp\left(-\frac{\nu}{2}(x^2 + y^2 + z^2 + d^2 - 2zd/3)\right) \quad (4.4)$$

$$\phi_d(x, y, z) = \left(\frac{\omega}{\pi}\right)^{3/4} \exp\left(-\frac{\omega}{2}(x^2 + y^2 + z^2 + d^2 + 4zd/3)\right). \quad (4.5)$$

We do not, however, work very often in the body-fixed frame. Instead, we find

the overlaps and matrix elements between a wave function and another wave function that has been rotated with respect to the first wave function, as it was outlined in section 2.4 in the previous chapter. We will rotate the wave functions around the y -axis using the matrix

$$\hat{\mathfrak{R}} = \begin{pmatrix} \cos \vartheta & 0 & -\sin \vartheta \\ 0 & 1 & 0 \\ \sin \vartheta & 0 & \cos \vartheta \end{pmatrix}. \quad (4.6)$$

We now write the rotated wave functions (denoted by the tilde):

$$|\tilde{\alpha}\rangle = \left(\frac{\nu}{\pi}\right)^{3/4} \exp\left(-\frac{\nu}{2}(x^2 + y^2 + z^2 + d^2 - 2d(x \sin \vartheta + z \cos \vartheta)/3)\right) \quad (4.7)$$

$$|\tilde{d}\rangle = \left(\frac{\omega}{\pi}\right)^{3/4} \exp\left(-\frac{\omega}{2}(x^2 + y^2 + z^2 + d^2 + 4d(x \sin \vartheta + z \cos \vartheta)/3)\right). \quad (4.8)$$

With the rotated wave functions, all overlaps and matrix elements can be calculated. We will begin with the overlaps and normalization, and then proceed with the matrix elements. The overlaps are

$$\theta_\alpha \equiv \langle \alpha | \tilde{\alpha} \rangle = \exp\left(\frac{\nu d^2}{18}(\cos \vartheta - 1)\right) \quad (4.9)$$

$$\theta_d \equiv \langle d | \tilde{d} \rangle = \exp\left(\frac{2\omega d^2}{9}(\cos \vartheta - 1)\right) \quad (4.10)$$

$$\theta_{12} \equiv \langle \alpha | \tilde{d} \rangle = \langle d | \tilde{\alpha} \rangle = \left(\frac{2\sqrt{\nu\omega}}{\nu + \omega}\right)^{3/2} \exp\left(-\frac{\nu\omega d^2}{18(\nu + \omega)}(5 + 4\cos \vartheta)\right). \quad (4.11)$$

By taking the body-fixed frame limit ($\cos \vartheta = 1$), one can see that the overlaps make sense. The alpha and dineutron overlaps become one, as the Gaussian wave functions are normalized, and the overlap between the two centers remains, but becomes one if d is zero and the oscillator lengths are equal for each cluster. The only reason the overlaps within the alpha and the dineutron are not one is because we rotate about the center-of-mass which does not coincide with either center. The symbol θ_{12} is used for the overlap between the two centers (centers 1 and 2) first because it is equal to

its transpose, which then gives us more notational options when we come to different overlaps in later sections. The normalization (eq.(3.3)) is reproduced here for easy comparison with the overlaps:

$$N^2 = \frac{1}{\theta_\alpha^2 (\theta_\alpha \theta_d - \theta_{12}^2)^2}.$$

When d goes to zero, all the overlaps tend towards one, which causes the denominator of the normalization to vanish. As mentioned before, this is because of the Pauli principle, and when d is zero, four s -wave neutrons are at the same point in space, which is forbidden by Fermi statistics. Note that this is exactly the case when the oscillator lengths are equal. If the oscillator lengths are different, the wavefunctions of the alpha particle and external neutrons are no longer completely identical. The denominator would still be very small (being one minus the ratio of twice the geometric mean of the two oscillator lengths divided by their sum), but not identically zero.

The first expectation value shown here is the one-body particle density. For the purpose of presentation, this was done in the body-fixed frame with the wave functions in eq.(4.4-4.5). We use the general expression for a one-body operator (eq.(3.5-3.9)). In this case, the operator is just I , the identity matrix, and we integrate over the y -coordinate. The results are shown in Figures 4.1, 4.2, and 4.3. The three figures all show the one-body particle density, but for different values of the parameter ω . In Figure 4.1, they are equal, and the alpha particle (on the right side of the figure) looks bigger than the dineutron cluster. In Figure 4.2, the oscillator length of the dineutron is set to be larger than the alpha particle, which makes the dineutron more sharply peaked, as it is now more focused in space. The last figure, Figure 4.3, shows a more diffuse dineutron. For all three figures, the distance between the two centers was set to be 2.5 fm. There is nothing significant about this distance, it was chosen in order to keep a clear distinction between the two clusters while keeping them close enough so that their densities still overlap somewhat.

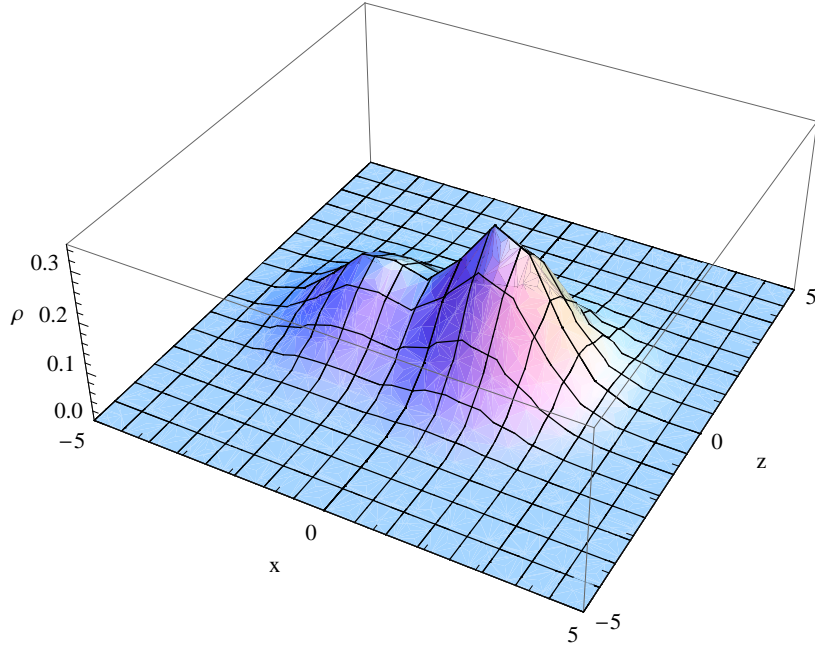


Figure 4.1: The expectation value of the one-body particle density in the intrinsic frame of ${}^6\text{He}$. It is pictured in the xz plane, with the clusters' centers along the z -axis. In this figure, the oscillator lengths are equal in both clusters to 0.53 fm^{-2} and d is set equal to 2.5 fm . The alpha particle is centered in the positive z region, and the dineutron in the negative z region.

This is the only expectation value calculated exclusively in the body-fixed frame. If the body-fixed frame expectation value of any other operator is desired, it can be easily obtained from the projected terms by taking $\cos\vartheta = 1$, and no longer integrating over the angles.

We will begin our tour through the expectation values of various operators with those operators found in the Hamiltonian, which is:

$$\hat{H} = \sum_i T_i - T_{cm} + V_{ij}. \quad (4.12)$$

The first two terms in eq.(4.12) are kinetic energy terms. The first one is the sum of the one-body kinetic energy of the six particles, while the second one removes the energy associated with the motion of the center-of-mass of the particles. The last term is the interaction, the details of which will be covered in the subsections devoted to the potential energy.

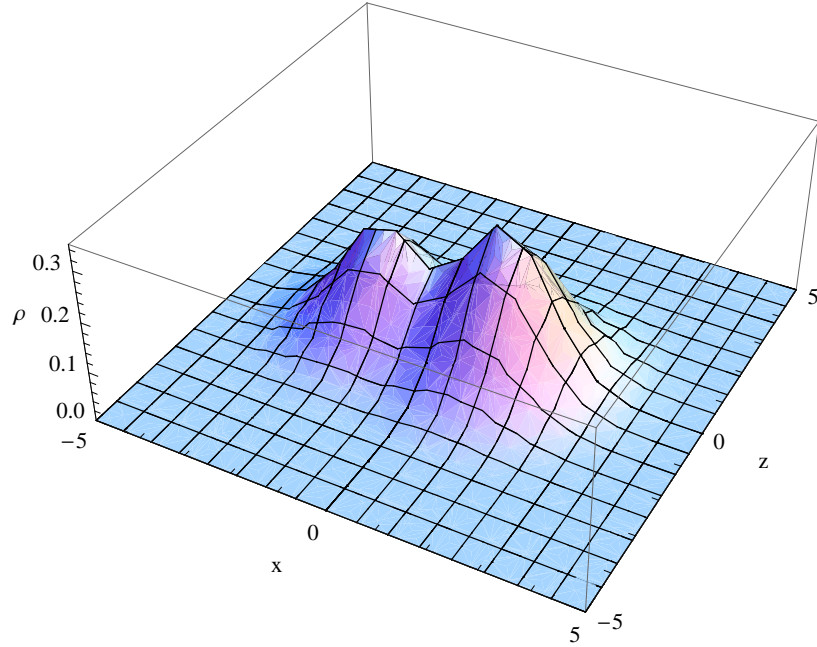


Figure 4.2: The expectation value of the one-body particle density of ${}^6\text{He}$ with $\nu=0.53$ fm^{-2} and $\omega=0.68$ fm^{-2} . The parameter d is set equal to 2.5 fm.

4.1.2 Kinetic energy

The kinetic energy calculation determines the amount of energy due to the motion of the particles present in the system. As just mentioned, there are two parts to this calculation, first the one-body kinetic energy of the six particles in the system, and then a correction to remove spurious motion of the center-of-mass. The one-body kinetic energy operator is:

$$\hat{T} = -\frac{\hbar}{2m}\nabla^2. \quad (4.13)$$

The kinetic energy is diagonal in spin and isospin. For this and all calculations in this work, the nucleons are treated as having the same mass, which for numerical calculations is set equal to 939 MeV. The general form of the expectation value is found in eq.(3.4-3.9). The matrix elements which are summed together in the previously

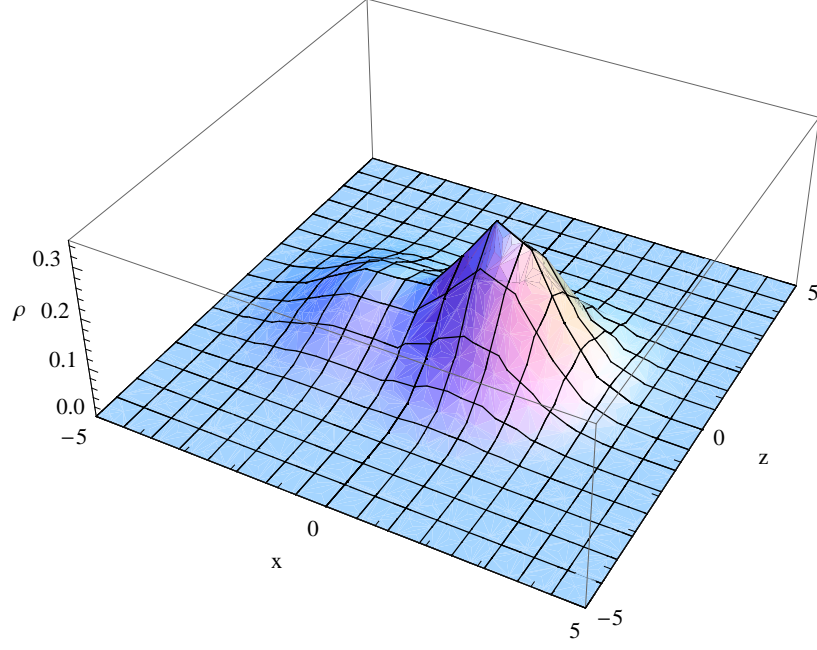


Figure 4.3: The expectation value of the one-body particle density of ${}^6\text{He}$ with $\nu=0.53$ fm^{-2} and $\omega=0.41$ fm^{-2} . The parameter d is set equal to 2.5 fm.

mentioned terms are listed below:

$$\langle \alpha | T | \alpha \rangle = \frac{\nu}{2} \theta_\alpha \left[3 - \frac{\nu d^2 (1-x)}{9} \right], \quad (4.14)$$

$$\langle d | T | \tilde{d} \rangle = \frac{\omega}{2} \theta_d \left[3 - \frac{4\omega d^2 (1-x)}{9} \right], \quad (4.15)$$

$$\langle d | T | \alpha \rangle = \langle \alpha | T | d \rangle = \frac{\nu\omega}{\nu + \omega} \theta_{12} \left[3 - \frac{\nu\omega d^2}{9(\nu + \omega)} (5 + 4x) \right]. \quad (4.16)$$

For these terms, the prefactor, $\hbar^2/2m$, has been suppressed, and $x \equiv \cos \vartheta$. Since the kinetic energy operator does not change the overlaps at all, the matrix elements are written in terms of the overlaps as well. Many operators have this property, and we will use this simplification in writing the matrix elements whenever possible. Most matrix elements also depend on $\cos \vartheta$, but the angular form ($\cos \vartheta$) will be restored if necessary for clarity, or if it is different from $\cos \vartheta$. Additionally, all these matrix elements will now be calculated in the rotated system, so the tilde that was introduced to indicate a rotated wavefunction will now be omitted. All wave functions in the ket should be assumed to have been rotated with respect to the wave functions in the

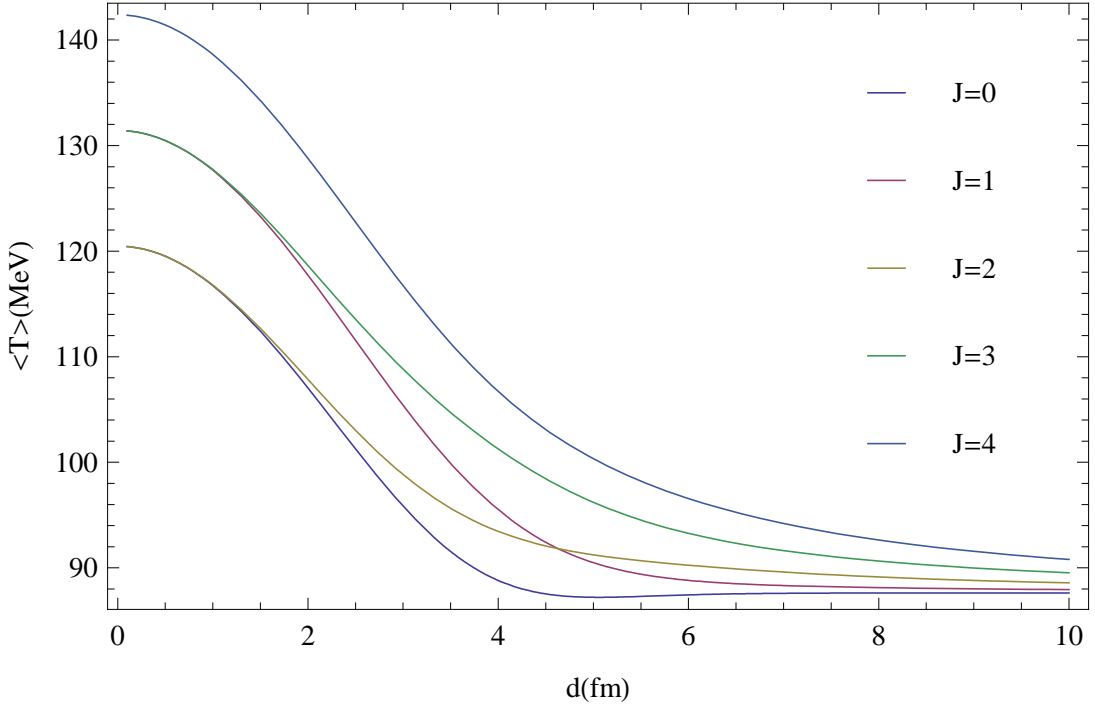


Figure 4.4: The results of the one-body kinetic energy calculation in the alpha-neutron configuration of ${}^6\text{He}$. These results were obtained with $\nu = 0.53 \text{ fm}^{-2}$, the standard value for the alpha particle, and $\omega = \nu$.

bra unless otherwise noted. With these matrix elements, the expectation value of the one-body kinetic energy can be completed.

The one-body kinetic energy as a function of the inter-cluster distance parameter d is shown in Figure 4.4. Curves are seen for the ground state, $J = 0$, up to the $J = 4$ state. At large values of d , the states are in the expected order for rotational states. That is, they go in consecutive numbers of J with spacing $J(J+1)$. Something different is observed at small values of d . Discussion of these features of Figure 4.4 is delayed because first we need to discuss the center-of-mass correction.

We want to remove the energy associated with the motion-of-center of mass of the system:

$$\langle T \rangle_{cm} = \frac{P^2}{2M} = \frac{(\sum_i \mathbf{p}_i)^2}{2Am}, \quad (4.17)$$

where P and M are the momentum of the center-of-mass and the total mass of the system, respectively, which are re-written in terms of the single-particle quantities

on the right-hand side of the equation. Expanding on that, we get a separation into one-body (recoil effect) and two-body terms:

$$\frac{(\sum_i \mathbf{p}_i)^2}{2Am} = \frac{1}{6Am} \left(\frac{1}{2} \sum_i p_i^2 + \sum_{i \neq j} \mathbf{p}_i \cdot \mathbf{p}_j \right). \quad (4.18)$$

The first term is exactly the same as the one-body kinetic energy, while the second term is a two-body term. When we combine this result with the pure one-body calculation, we obtain the following result for the kinetic energy:

$$\langle T \rangle = \frac{1}{A} [(A-1)\langle T^{(1)} \rangle - 2\langle T^{(2)} \rangle], \quad (4.19)$$

where $T^{(1)}$ is the one-body kinetic energy and $T^{(2)}$ is the two-body kinetic energy. We already gave the results for the one-body kinetic energy. Here are given the results of the momentum operator ($\hbar/i\nabla$) in the alpha-dineutron configuration of ${}^6\text{He}$:

$$\langle \alpha | \mathbf{p} | \alpha \rangle = \frac{\nu}{i} \theta_\alpha \frac{d}{6} [\sin \vartheta \hat{\mathbf{x}} + (\cos \vartheta - 1) \hat{\mathbf{z}}] \quad (4.20)$$

$$\langle d | \mathbf{p} | d \rangle = -\frac{\omega}{i} \theta_d \frac{d}{3} [\sin \vartheta \hat{\mathbf{x}} + (\cos \vartheta - 1) \hat{\mathbf{z}}] \quad (4.21)$$

$$\langle \alpha | \mathbf{p} | d \rangle = -\theta_{12} \frac{\nu\omega d}{3i(\nu + \omega)} [2 \sin \vartheta \hat{\mathbf{x}} + (1 + 2 \cos \vartheta) \hat{\mathbf{z}}] \quad (4.22)$$

$$\langle d | \mathbf{p} | \alpha \rangle = \theta_{12} \frac{\nu\omega d}{3i(\nu + \omega)} [\sin \vartheta \hat{\mathbf{x}} + (2 + \cos \vartheta) \hat{\mathbf{z}}]. \quad (4.23)$$

The last two matrix elements are not equal, despite being transposes of each other. This is because the momentum operator is a vector operator (the previous calculation was for the kinetic energy, a scalar). The magnitude of the matrix elements is not changed, but the angular dependence is different. In the absence of rotation ($\vartheta = 0$), the matrix elements are equal. The matrix elements for the two-body terms can be found by taking the scalar products of any of these terms (including with themselves), and multiplying by a prefactor $-\hbar^2/2m$. These matrix elements accompany the overlap expressions in eq.(3.11-3.20), which are summed up in order to find the overall

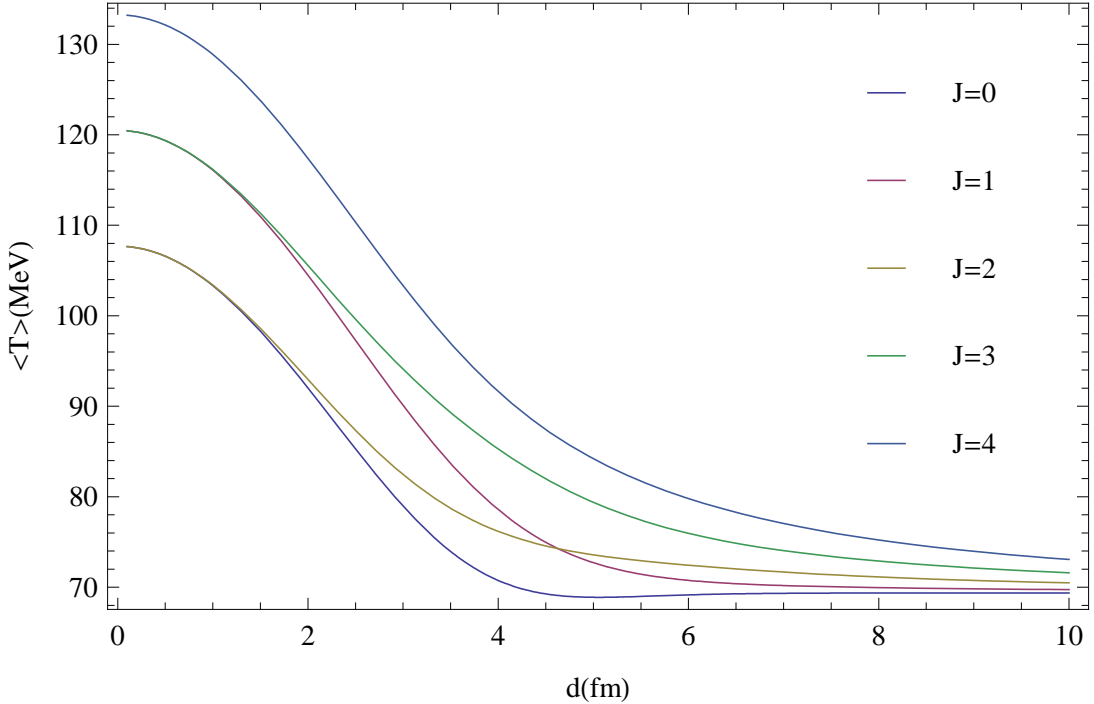


Figure 4.5: The results of the kinetic energy calculation in the alpha-deuteron configuration of ${}^6\text{He}$, with the center-of-mass energy removed. The results were obtained with the oscillator parameters $\nu = \omega = 0.53 \text{ fm}^{-2}$.

expectation value.

The corrected kinetic energy shown in Figure 4.5 is qualitatively similar to the figure showing only the one-body contribution (Figure 4.4), with the energies reduced by around 12 MeV. At large distances, where the order of the states is rotational, the ground state energy corresponds to the sum of the kinetic energy of an alpha particle and dineutron. At small distances, the figure becomes more interesting, with degeneracies appearing. The energy increases because two of the neutrons are forced into higher orbits. When d is large, all four neutrons can remain in s -waves and $J = \ell$, but this is no longer the case when they come close to each other due to the Pauli principle. The lowest state is where $J = 0$ and $J = 2$ are degenerate. This is where both extra neutrons go to the p -shell and couple to $J = 0$ (the two p -orbital particles can couple to both the $\ell = 0$ and the $\ell = 2$ states to produce $J = 0$ at $d = 0$). The next state at small d is where $J = 1$ and $J = 3$ come together. These are negative parity states, and the only way this can be achieved at $d = 0$ is to have one particle

go to the p -shell, and another particle go to the next shell, the sd -shell. Finally, the $J = 4$ state stays high because $\ell = 4$ cannot couple to lower angular momenta. This is where the two particles are pushed into the sd -shell. The states at small d also appear to be equally-spaced, which is characteristic of the quantum harmonic oscillator. This is indeed the cause of the equally spaced levels, as the basis wave functions for the calculation are Gaussians. Because of these basis functions, at $d = 0$, the system is a spherical harmonic oscillator, and thus, has equally spaced levels in the kinetic energy.

The kinetic energy results highlight an interesting feature of the formalism. The system most likely prefers to be at a d -value different from zero (maximum kinetic energy), but not too large, because the nuclear force is short-ranged. The minimum in energy will likely be between the pure s -wave system at large d , and the oscillator limit at $d = 0$, which results in a picture of s -waves and higher orbits. This is automatically handled by the formalism, and is an advantage over theories that would just place the external particles in p -waves, assuming that the s -waves are occupied by the neutrons in the alpha particle. This feature is a strong point of the formalism.

4.1.3 Interaction

Potentials in nuclear physics constitute a large body of work in their own right. For structure studies, one can broadly divide them into two types: mean field potentials, and nucleon-nucleon potentials. The mean field potential averages out the interaction between the nucleons themselves into a one-body potential well, which the nucleons fill. This is an approximation that becomes more valid as the nucleus becomes larger, and since this work deals with light nuclei, we will use interactions that are of the nucleon-nucleon variety.

Volkov interaction

The first interaction we chose to use was the Volkov potential [45]. The Volkov potentials are a set of eight different phenomenological potentials that were designed to

fit features of the alpha particle (binding energy, charge radius). They were chosen here because our systems consist of alpha particles plus a few external particles, and the potentials are Gaussian in form. The framework of the Volkov potentials is

$$V_{ij}(r_{ij}) = \sum_{i < j}^A U(r_{ij}) \left(1 - m + m \hat{P}_{ij}^x\right), \quad (4.24)$$

where m is a parameter, the Majorana exchange parameter, and P_{ij}^x is the Majorana exchange operator. It acts in the following way:

$$\hat{P}_{ij}^x \psi_1(r_1, \sigma_1, \tau_1) \psi_2(r_2, \sigma_2, \tau_2) = \psi_1(r_2, \sigma_1, \tau_1) \psi_2(r_1, \sigma_2, \tau_2). \quad (4.25)$$

It tends to reduce the strength of the potential. The form factor of the potential in eq.(4.24) is

$$U(r_{ij}) = V_a \exp[-(r_{ij}/\alpha)^2] + V_r \exp[-(r_{ij}/\rho)^2], \quad (4.26)$$

where V_a , V_r , α , and ρ are parameters of the potential, which are changed in the eight versions of the potentials. Finally, r_{ij} is the relative distance between the two particles. Figure 4.6 shows a plot of the eight parameter sets. Unless otherwise noted, the plots in this work involving the Volkov potentials are shown with the first set of parameters, Volkov V1.

We now show the matrix elements of the Volkov potentials in the alpha-dineutron configuration. Since the Volkov potentials are Gaussian in nature, there is no simplifying use of the overlaps in this case. One simplification can be made, however. Each matrix element has two terms, one attractive and one repulsive. These two terms are the same, except V_a is replaced with V_r and α is replaced by ρ in going from the attractive to the repulsive term, so only the attractive piece is listed here. Matrix elements with a subscript “+” after them are equal to the transposed term (e.g., $\langle 12|V|34\rangle \rightarrow \langle 43|V|21\rangle$). There is no indicator if this is trivially so (bra and ket are the same). After listing the matrix elements, the effect of the Majorana exchange

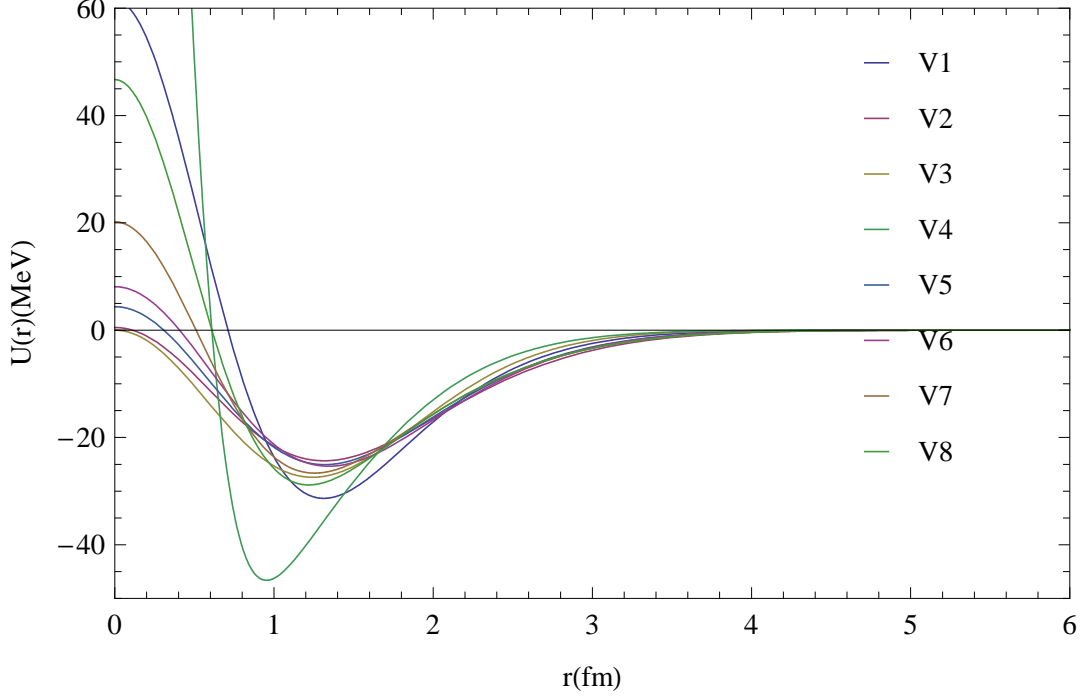


Figure 4.6: Shown here are the eight sets of Volkov potentials as a function of the distance between the two nucleons. The plot that goes off of the graph, V4, is quite repulsive and finally intersects the ordinate at 331.6 MeV.

operator will be addressed.

$$\langle \alpha\alpha | V | \alpha\alpha \rangle = V_a \left(\frac{\nu\alpha^2}{\nu\alpha^2 + 2} \right)^{3/2} \exp [\nu d^2 (x - 1) / 9], \quad (4.27)$$

$$\langle \alpha d | V | d\alpha \rangle = V_a \left(\frac{\nu\omega\alpha^2}{\nu + \omega + \nu\omega\alpha^2} \right)^{3/2} \exp \left[-\frac{(\nu\omega\alpha^2(\nu + 4\omega) + (\nu - 2\omega)^2)(1 - x) + 18\nu\omega}{18(\nu + \omega + \nu\omega\alpha^2)} d^2 \right], \quad (4.28)$$

$$\langle \alpha\alpha | V | \alpha d \rangle_+ = V_a \left(\frac{2\nu\alpha^2\sqrt{\nu\omega}}{D(\nu, \omega)} \right)^{3/2} \exp \left[-\frac{(1-x)(\nu\alpha^2(\nu - 3\omega) + 4\nu - 8\omega) + 9\omega(\nu\alpha^2 + 3)}{18D(\nu, \omega)} \nu d^2 \right], \quad (4.29)$$

$$\langle dd | V | d\alpha \rangle_+ = V_a \left(\frac{2\omega\alpha^2\sqrt{\nu\omega}}{D(\omega, \nu)} \right)^{3/2} \exp \left[-\frac{4(1-x)(\omega^2\alpha^2 - 2\nu + 4\omega) + 9\nu(\omega\alpha^2 + 3)}{18D(\omega, \nu)} \omega d^2 \right], \quad (4.30)$$

where

$$D(x, y) = x\alpha^2(x + y) + 3x + y, \quad (4.31)$$

$$\langle dd|V|dd \rangle = V_a \left(\frac{\omega\alpha^2}{\omega\alpha^2 + 2} \right)^{3/2} \exp [4\omega d^2 (x - 1) / 9], \quad (4.32)$$

$$\langle dd|V|\alpha\alpha \rangle_+ = V_a \left(\frac{4\nu\omega\alpha^2}{(\nu + \omega)\Delta} \right)^{3/2} \exp \left[-\frac{\nu\omega d^2 (5 + 4x)}{9(\nu + \omega)} \right], \quad (4.33)$$

$$\begin{aligned} \langle d\alpha|V|d\alpha \rangle &= V_a \left(\frac{4\nu\omega\alpha^2}{(\nu + \omega)\Delta} \right)^{3/2} \\ &\times \exp \left[-\frac{\nu\omega\Delta (5 + 4x) + 2(1 - x)(\nu + 2\omega)^2}{9(\nu + \omega)\Delta} d^2 \right], \end{aligned} \quad (4.34)$$

where

$$\Delta(p, q) = p\alpha^2 + q\alpha^2 + 4. \quad (4.35)$$

These matrix elements are inserted into the corresponding expression in eqs.(3.11)-(3.20) in order to determine the expectation value of the potential. As listed above, however, these are only for the part of the potential that is proportional to $(1 - m)$ (see eq.(4.24)). The Majorana exchange operator changes things, slightly.

As seen in its definition, eq.(4.25), the Majorana exchange operator switches the spatial locations of a pair of particles, and leaves spin-isospin properties unchanged. One can say then immediately that none of the matrix elements in eq.(4.27)-eq.(4.34) with bra or ket at the same spatial location are affected by the operator. These leaves two of the seven terms, $\langle \alpha d|V|d\alpha \rangle$ and $\langle d\alpha|V|\alpha d \rangle$. These two are changed into each other. Thus, for the term of the potential proportional to $m\hat{P}_{ij}^x$, the same set of overlap terms are used as before, except that $\langle \alpha d|V|d\alpha \rangle$ is switched with $\langle d\alpha|V|\alpha d \rangle$. In other words, instead of eq.(3.12), we have

$$\langle O^{(2)} \rangle_{\alpha^2 d^2} = \langle d\alpha|V|d\alpha \rangle (8\theta_\alpha^3 \theta_d - 6\theta_\alpha^2 \theta_{12}^2), \quad (4.36)$$

and

$$\langle O^{(2)} \rangle_{\alpha d d \alpha} = \langle \alpha d | V | d \alpha \rangle (2\theta_\alpha^2 \theta_{12}^2 - \theta_\alpha^3 \theta_d) \quad (4.37)$$

instead of eq.(3.19). The Majorana exchange operator can also be written as

$$\hat{P}_{ij}^x = -\frac{1}{4} [1 + \boldsymbol{\sigma}_i \cdot \boldsymbol{\sigma}_j + \boldsymbol{\tau}_i \cdot \boldsymbol{\tau}_j + (\boldsymbol{\sigma}_i \cdot \boldsymbol{\sigma}_j) (\boldsymbol{\tau}_i \cdot \boldsymbol{\tau}_j)]. \quad (4.38)$$

This form was used to confirm results obtained with the original formula.

A plot of the potential results is shown in Figure 4.7. At large values of d , where all the curves come together, is the sum of the potential energies of an alpha particle and dineutron. As d becomes smaller, the different levels appear. The lowest levels are once again $J = 0$ and $J = 2$, though the potential breaks the degeneracy. The potential also breaks the degeneracy of $J = 1$ and $J = 3$. Interestingly, $J = 4$ comes in between $J = 1$ and $J = 3$. This is due to the Majorana exchange operator's preference for even waves. When the exchange parameter is set equal to zero (see Figure 4.8), the order of states at d equal zero is $J = 0, 2, 1, 3, 4$, but for Figure 4.7, m is 0.6 (the standard setting for the Volkov potentials), which makes $J = 4$ more attractive compared to the odd waves (however, this may not be the case, see 4.2.2).

Another comparison that can be made is the effect of different sets of Volkov parameters. The plot in Figure 4.7 is with V1, which has a fairly hard core ($V(r) = +60$ MeV at $d = 0$). In Figure 4.9, the expectation value of V2 is shown. Volkov V2 is a soft-core potential, with a value of +0.5 MeV at $d = 0$. As one can see in the figure, qualitatively, there is not a great change by changing the parameter set. Quantitatively, the V2 potential expectation value is deeper by three MeV at $d = 0$. Three MeV can be a lot in these loosely bound nuclei, however, the minimum in binding energy is usually far from $d=0$, and there is less difference between the potentials the higher one goes in d .

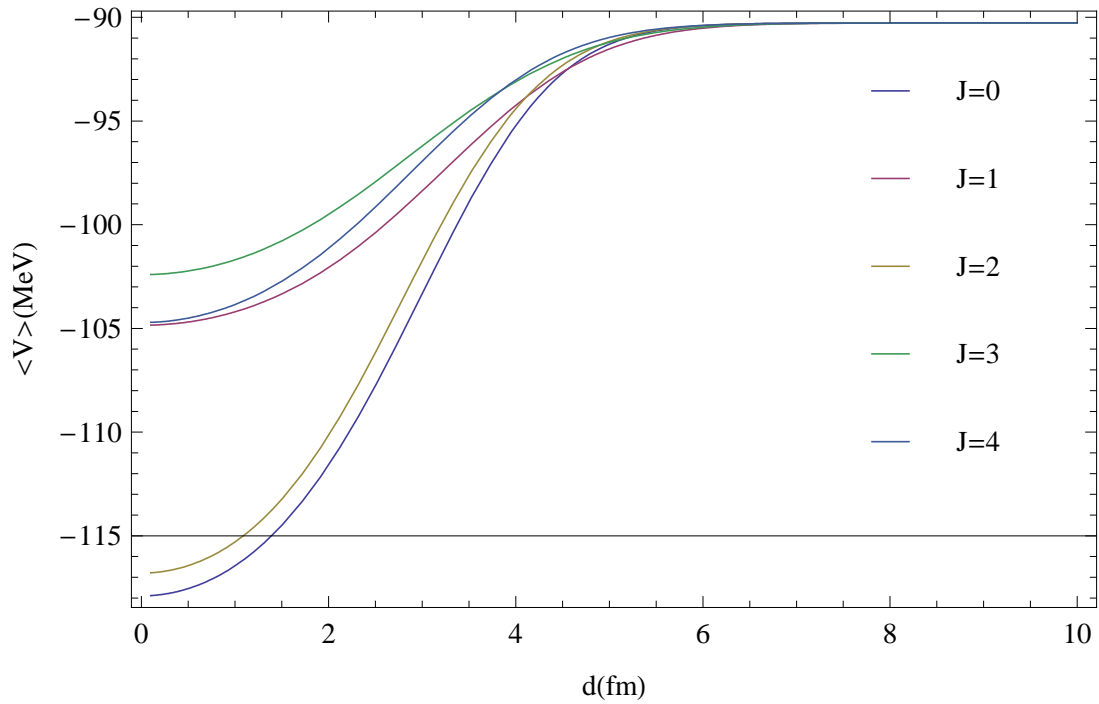


Figure 4.7: The results of the expectation value calculation of the Volkov potentials (V1) in the alpha-dineutron configuration of ${}^6\text{He}$. The results were obtained with both oscillator parameters equal to 0.53 fm^{-2} , and the Majorana exchange operator set to 0.6.

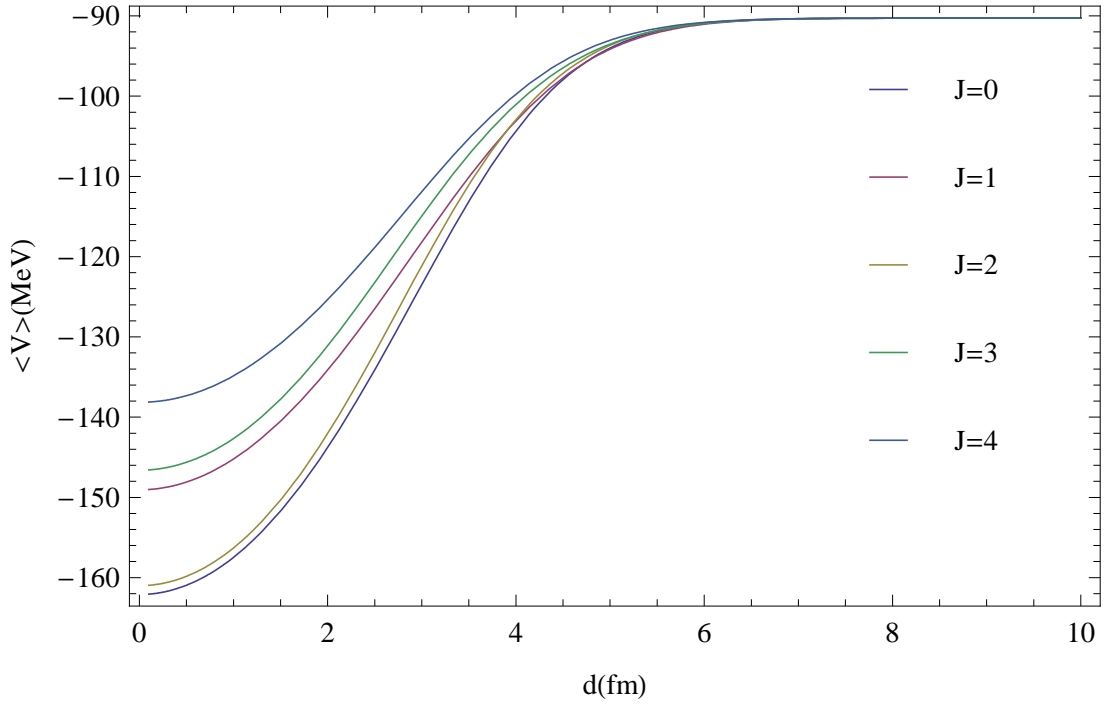


Figure 4.8: The expectation value of the Volkov V1 potential in the alpha-dineutron configuration of ${}^6\text{He}$ as a function of d . In this plot, the Majorana exchange parameter was set equal to zero, but all other parameters are the same as in Figure 4.7.

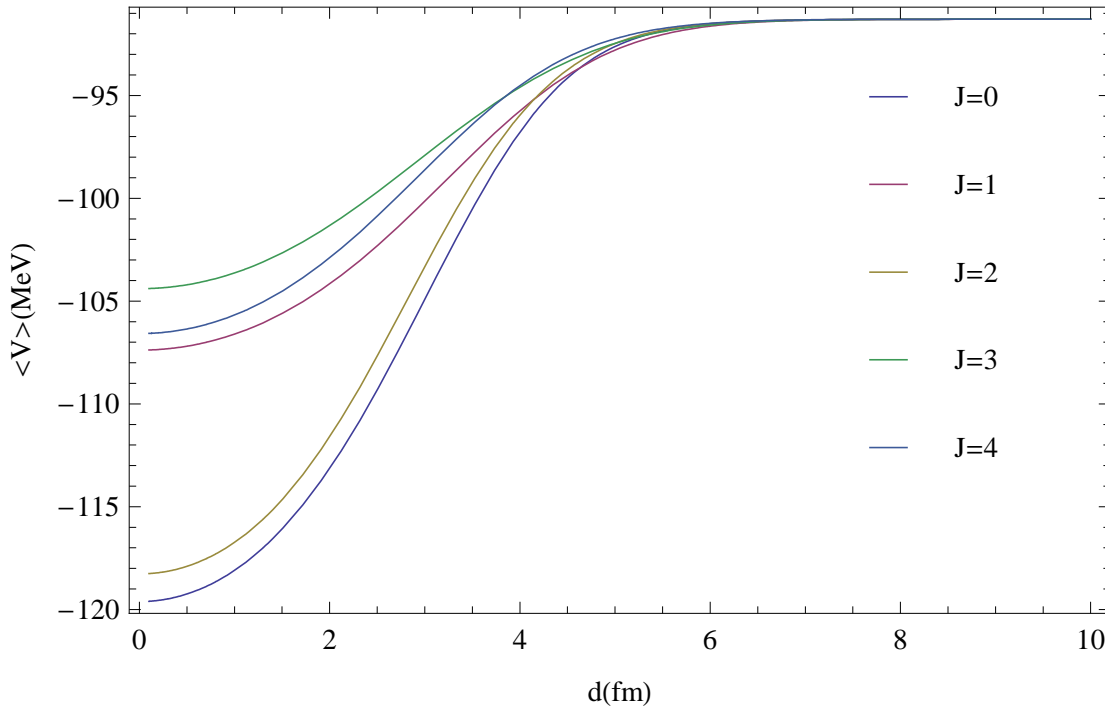


Figure 4.9: The expectation value of the Volkov V2 (soft core) potential in the alpha-dineutron configuration of ${}^6\text{He}$. In this plot, the oscillator parameters are both equal to 0.53 fm^{-2} , and the Majorana exchange parameter is set equal to 0.6.

Minnesota potential

After the Volkov potentials, the next interaction used was the Minnesota potential (first appeared in [46]; the parameters used in present work are borrowed from [47]). In contrast to the Volkov potentials, the Minnesota potential was designed to fit the $n - p$ and $p - p$ s -wave scattering parameters (the scattering length and effective range). They are also expressed as Gaussians, which makes computations simpler. The form of the potential is:

$$V_{ij} = [V_R + 1/2 (1 + P_{ij}^\sigma) V_t + 1/2 (1 - P_{ij}^\sigma) V_s] [u/2 + 1/2 (2 - u) P_{ij}^x], \quad (4.39)$$

where V_R, V_t and V_s are the Gaussian form factors for the repulsive, triplet, and singlet potentials, respectively, P_{ij}^σ is the spin-exchange operator (exchanges the spins of particles i and j , giving +1 in triplet states and -1 in singlet states), P_{ij}^x is the coordinate exchange operator (Majorana exchange operator), and u is the exchange parameter which should be close to one. Figure 4.10 shows the Minnesota potential in the singlet and triplet channel. Clearly, the triplet channel is more attractive, which makes sense as this is the deuteron-like channel, and the deuteron is the only bound two-nucleon system.

Since the form of the Minnesota potential is Gaussian, no new matrix elements need to be listed here. One merely finds the appropriate geometrical term in the list of matrix elements eq.(4.27)-eq.(4.34), and changes the Volkov parameters to Minnesota parameters. However, since the Minnesota potentials explicitly depend on spin, the list of terms in eq.(3.11)-eq.(3.20) need to be re-written in terms of a singlet part and

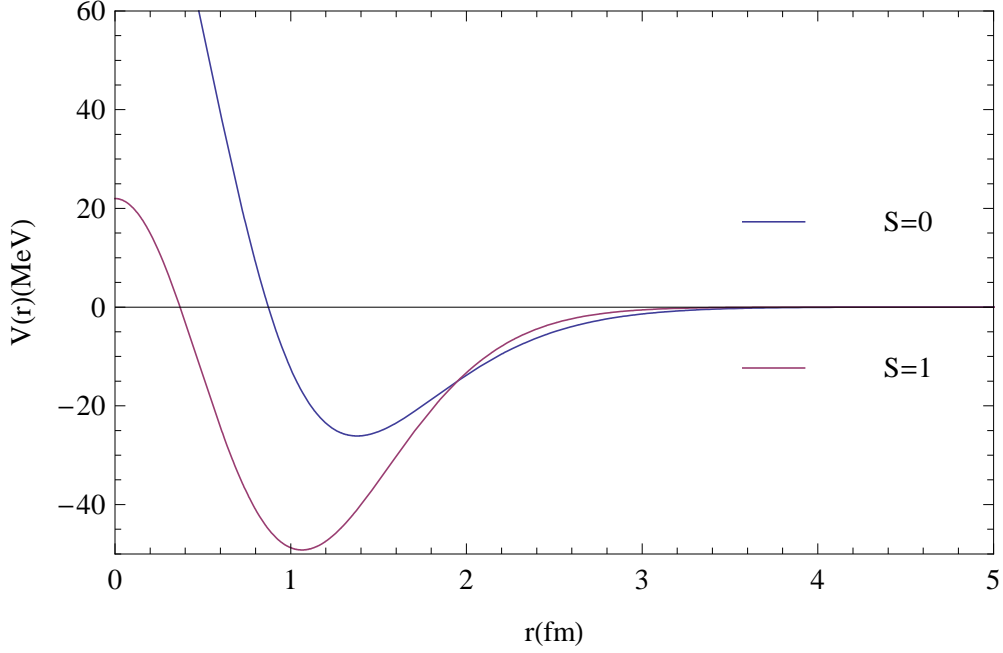


Figure 4.10: This plot shows the singlet ($T=1$) and triplet ($T=0$) channels for the Minnesota potential. The singlet potential has a strong repulsive core, with a value of +109 MeV at $r=0$. The triplet channel has a milder repulsion and a much deeper attraction.

a triplet part. The singlet contribution is

$$\langle V_s \rangle_\alpha = \langle \alpha\alpha | V_s | \alpha\alpha \rangle (3\theta_\alpha^2 \theta_d^2 + \theta_{12}^4 - 3\theta_\alpha \theta_{12}^2 \theta_d), \quad (4.40)$$

$$\langle V_s \rangle_{\alpha^2 d^2} = \langle d\alpha | V_s | \alpha d \rangle (3\theta_\alpha^3 \theta_d - \theta_\alpha^2 \theta_d^2), \quad (4.41)$$

$$\langle V_s \rangle_{\alpha\alpha\alpha d} = \langle V_s \rangle_{d\alpha\alpha\alpha} = \langle \alpha\alpha | V_s | \alpha d \rangle (2\theta_{12}^3 \theta_\alpha - 6\theta_\alpha^2 \theta_{12} \theta_d), \quad (4.42)$$

$$\langle V_s \rangle_{ddd\alpha} = \langle V_s \rangle_{\alpha ddd} = -\langle dd | V_s | d\alpha \rangle 4\theta_\alpha^3 \theta_{12}, \quad (4.43)$$

$$\langle V_s \rangle_{\alpha d\alpha d} = \langle V_s \rangle_{d\alpha d\alpha} = \langle \alpha\alpha | V_s | dd \rangle 2\theta_\alpha^2 \theta_{12}^2, \quad (4.44)$$

$$\langle V_s \rangle_{\alpha d d\alpha} = \langle d\alpha | V_s | d\alpha \rangle 2\theta_\alpha^2 \theta_{12}^2, \quad (4.45)$$

$$\langle V_s \rangle_d = \langle dd | V_s | dd \rangle \theta_\alpha^4. \quad (4.46)$$

The triplet part is

$$\langle V_t \rangle_\alpha = \langle \alpha\alpha | V_t | \alpha\alpha \rangle (3\theta_\alpha^2 \theta_d^2 - 3\theta_\alpha \theta_{12}^2 \theta_d), \quad (4.47)$$

$$\langle V_t \rangle_{\alpha^2 d^2} = \langle d\alpha | V_t | \alpha d \rangle (5\theta_\alpha^3 \theta_d - 5\theta_\alpha^2 \theta_d^2), \quad (4.48)$$

$$\langle V_t \rangle_{\alpha\alpha\alpha d} = \langle V_t \rangle_{d\alpha\alpha\alpha} = \langle \alpha\alpha | V_s | \alpha d \rangle (6\theta_{12}^3 \theta_\alpha - 6\theta_\alpha^2 \theta_{12} \theta_d), \quad (4.49)$$

$$\langle V_t \rangle_{\alpha d d \alpha} = \langle d\alpha | V_t | d\alpha \rangle (2\theta_\alpha^2 \theta_{12}^2 - 2\theta_\alpha^3 \theta_d). \quad (4.50)$$

One can see that if one sums the triplet and singlet terms together for each geometrical term, the list is the same as for the Volkov potentials. The Majorana exchange operator switches the same terms in the Minnesota potential as it did in the Volkov potentials. Terms of the type $\alpha^2 d^2$ are switched with $\alpha d d \alpha$ in both the singlet and triplet cases.

Figure 4.11 shows the expectation value of the Minnesota potential as a function of d . The plot is similar to the plot of the Volkov potentials, but there are some differences. The order of states is the same as in the $m = 0.6$ Volkov plot, but in the case of the Minnesota potential, the $J = 4$ state is around halfway between $J = 1$ and $J = 3$, rather than being very close to $J = 1$ as in the Volkov plot. This could be due to the fact that the exchange term accounts for 50% of the Minnesota potential compared to 60% for the Volkov potential. Another difference is that the magnitude of the potential seems to fall slightly more rapidly in the Minnesota potential than the Volkov potential. The large d limit once again corresponds to the sum of the potential energies of an alpha particle and dineutron.

Gogny interaction

The other interaction examined was the 1970 version of the Gogny interaction [48].

This interaction has four types of contributions:

$$V(r) = V_W(r) + V_T(r)\hat{S}_{12} + V_{LS}(r)\mathbf{L} \cdot \mathbf{S} + V_{LL}(r)\hat{L}_{12}, \quad (4.51)$$

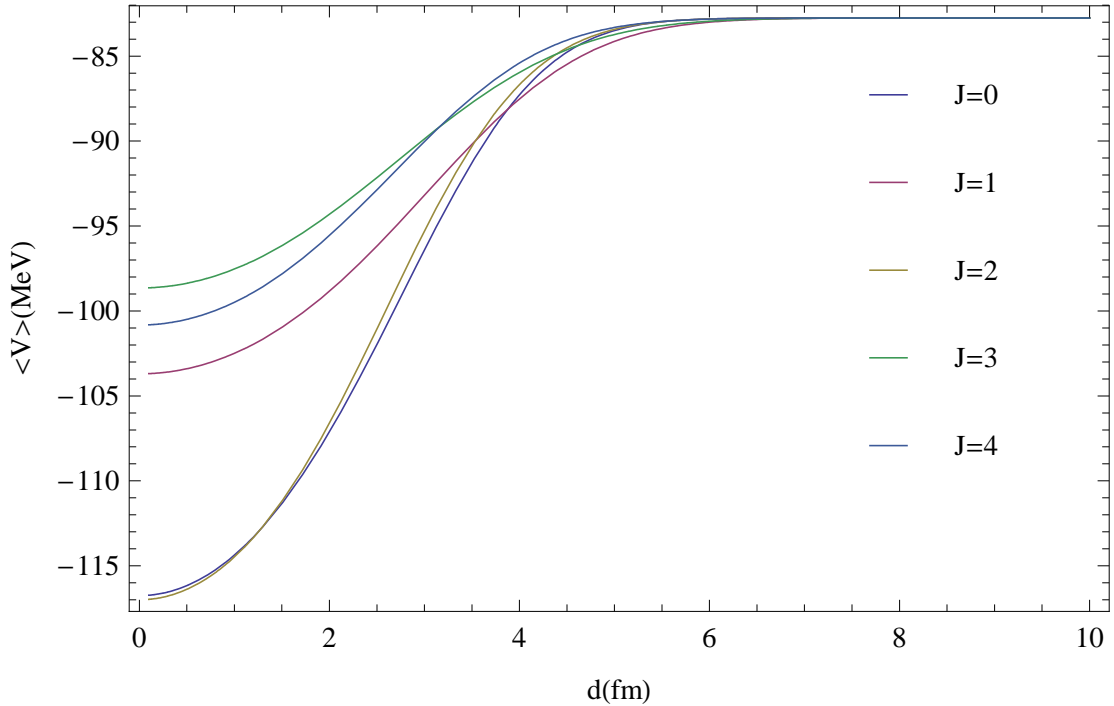


Figure 4.11: Plotted here is the expectation value of the Minnesota potential in the alpha-dineutron configuration of ${}^6\text{He}$. The oscillator parameters are both equal to 0.53 fm^{-2} , and the exchange parameter, u , is set equal to one.

where $V_W(r)$ is the Wigner or central interaction, $V_T(r)$ is the tensor term, $V_{LS}(r)$ is the spin-orbit term, and V_{LL} is a second-order momentum term that we did not consider. The radial dependence was expressed in terms of Gaussian functions, with separate terms for different spin and isospin combinations. This interaction was chosen in order to fit two-nucleon scattering properties and some properties of the deuteron, as well as many properties of heavy spherical nuclei ranging from ${}^{16}\text{O}$ to ${}^{208}\text{Pb}$. We found, however, that this Gogny interaction did not seem suitable for our systems. Its binding energy for our alpha particle was 13 MeV, less than half of the experimental value. This is not too shocking, since the Gogny interaction is essentially an effective interaction for medium and heavy nuclei.

4.1.4 Total energy

While not a new operator per se, the next stop on our tour through ${}^6\text{He}$ is the total energy, which is the sum of the previous two operators. The total energy for the alpha-dineutron configuration calculated with the Volkov V1 potential is shown in Figure 4.12. The large d limit is the sum of the total energy of an alpha particle and a dineutron. Bound behavior is seen only for $J = 0$ and $J = 2$. Also, the level of the minimum of the $J = 2$ curve is nearly equal to its asymptotic energy, which makes it more like a resonance. It's also interesting to note that the minimum in energy occurs around $d = 3.5$ fm. If one looks back at Figure 4.5, one sees that at this value of d , the particles are still mostly in s -waves, with only a small contribution of p -waves. The large increase in kinetic energy caused by accessing higher angular momenta overcomes the increased attraction gained by moving the nucleons closer to each other, causing the external particles to sit further away from the alpha center in this model.

The total energy calculated with the Minnesota potential is pictured in Figure 4.13. Like with the Volkov potential, binding only occurs for $J = 0$ and $J = 2$. The minimum for $J = 2$ is deeper this time, but the overall energy is higher. This is due to the fact that ${}^6\text{He}$ is dominated by singlet spin pairs, which in the Minnesota potentials are much less attractive than triplet pairs. Another similarity with the previous plot is that the minimum in energy is located at a value of d where the external particles are still mostly in s -waves, indicating that also for the Minnesota potentials, avoiding the increase in kinetic energy at small values of d is more advantageous than the increase in binding from the potential.

This ends the discussion on the operators that make up the Hamiltonian for ${}^6\text{He}$. We will now move on to some other calculations performed in the alpha-dineutron configuration of ${}^6\text{He}$.

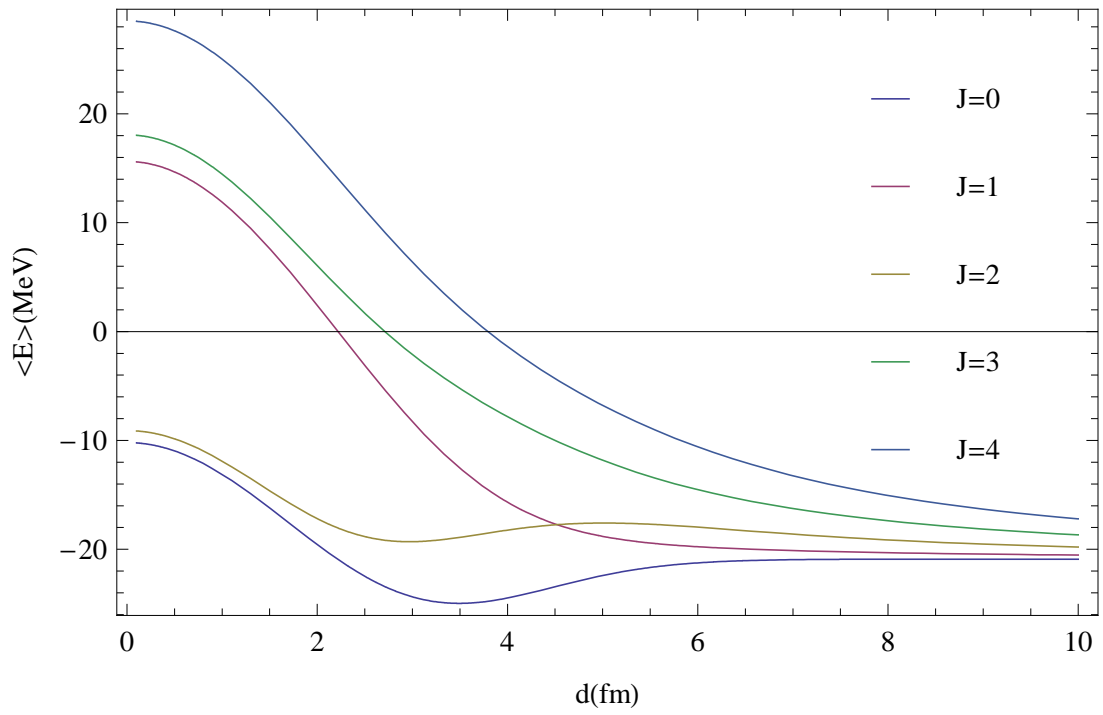


Figure 4.12: This plot shows the total energy of the alpha-dineutron configuration of ${}^6\text{He}$ as a function of d calculated with the Volkov V1 potential. The oscillator parameters are both set equal to 0.53 fm^{-2} and the Majorana exchange parameter is equal to 0.6.

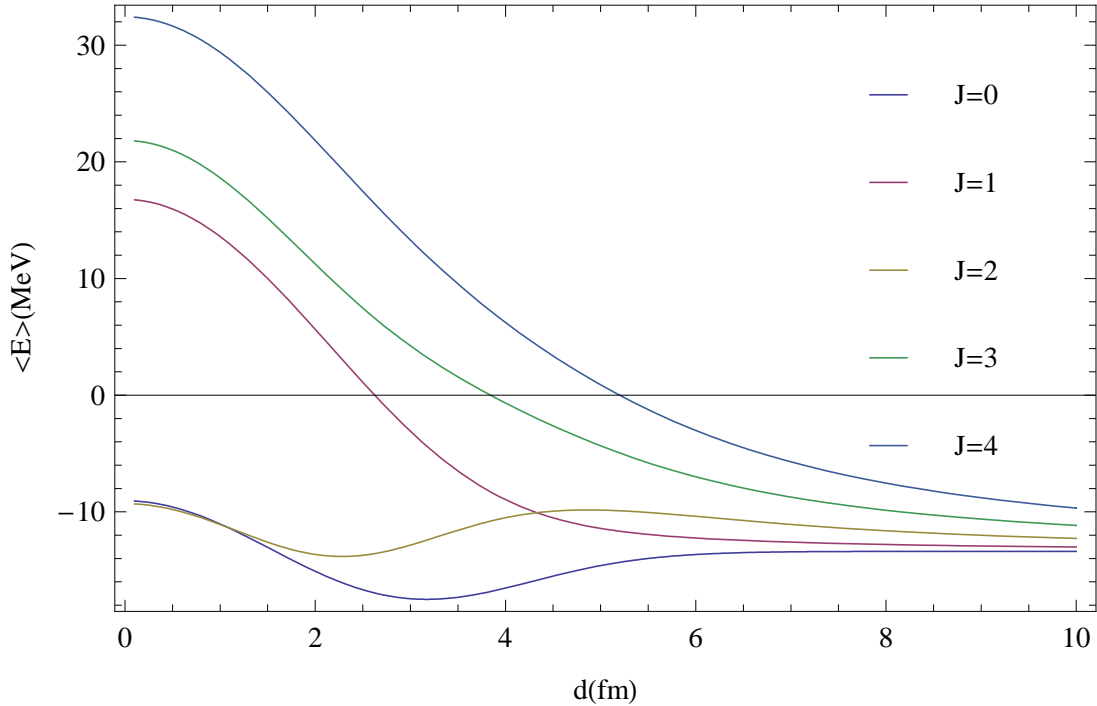


Figure 4.13: This plot displays the total energy of the alpha-dineutron configuration of the ${}^6\text{He}$ calculated with the Minnesota potential. The oscillator parameters are both set equal to $0.53 \text{ fm}^{-2} \text{ fm}$ and the exchange parameter u is set equal to one.

4.1.5 Mean square radius

The mean square radius is a basic property of a nucleus reflecting its spatial extent. Usually, there are two kinds of radius: the charge radius and matter radius. The charge radius reflects the size of the proton distribution in the nucleus, and is the more easily measured of the two, whereas the matter radius is the total size of the nucleus. In some nuclei, these quantities may be the same, or very nearly the same, but in ${}^6\text{He}$ we expect a significant difference between them, because of its extended neutrons.

Since the mean square radius is the size of the system, the location of the origin is very important. The radius must be properly referenced in order to supply a meaningful answer. The single-particle wave functions were all re-written in terms of differences in order to guarantee this. Before going into these details, however, the operator itself has to be properly defined. We start with the matter radius, which is

the radius of all particles in the nucleus, referenced to its center-of-mass:

$$\langle r_m^2 \rangle = \frac{1}{A} \sum_i^A (r_i - R_{cm})^2, \quad (4.52)$$

where R_{cm} is the coordinate of the center of mass, which is defined as

$$\mathbf{R}_{cm} = \frac{1}{M} \sum_i^A m_i \mathbf{r}_i = \frac{1}{A} \sum_i^A \mathbf{r}_i, \quad (4.53)$$

where the far right section is the simplifying case where the mass of all constituent particles is the same. With this definition, we can re-write eq.(4.52) as

$$A \langle r_m^2 \rangle = \sum_i^A r_i^2 - \frac{2}{A} \sum_i^A \mathbf{r}_i \sum_j^A \mathbf{r}_j + \frac{1}{A} \sum_i^A \mathbf{r}_i \sum_j^A \mathbf{r}_j. \quad (4.54)$$

In the later two sums, there are terms where $i = j$, which are like the one-body terms in the first sum, therefore we can simplify this expression into two terms, one-body and two-body:

$$A \langle r_m^2 \rangle = \frac{A-1}{A} \sum_i^A r_i^2 - \frac{2}{A} \sum_{i < j}^A \mathbf{r}_i \cdot \mathbf{r}_j. \quad (4.55)$$

Thus we will need both one-body and two-body matrix elements for the matter radius calculation.

For the charge radius, we will also need both kinds of matrix elements. We proceed in a similar way as in the matter radius, but now we have to be careful and treat protons and neutrons separately. We begin with:

$$\langle r_{ch}^2 \rangle = \frac{1}{Z} \sum_p^Z (r_p - R_{cm})^2, \quad (4.56)$$

where we sum over protons this time (r_p). By using the definition of R_{cm} , we once

again have many sums:

$$Z\langle r_{ch}^2 \rangle = \sum_p^Z r_p^2 - \frac{2}{A} \sum_p^Z \mathbf{r}_p \sum_i^A \mathbf{r}_i + \frac{Z}{A^2} \sum_i^A \mathbf{r}_i \sum_j^A \mathbf{r}_j. \quad (4.57)$$

We now re-group terms. In the second sum, there are three kinds of terms: one-body proton terms ($i = p$), two-body proton terms (i is a proton, but not the same proton as in the first sum), and proton neutron terms (i is a neutron):

$$\frac{2}{A} \sum_p^Z r_p \sum_i^A r_i = \frac{2}{A} \left(\sum_p^Z p^2 + \sum_{p \neq p'}^Z \mathbf{r}_p \mathbf{r}_{p'} + \sum_{pn}^{Z,N} \mathbf{r}_p \mathbf{r}_n \right). \quad (4.58)$$

The third sum in eq.(4.57) contains five terms, the three mentioned previously, plus neutron one-body terms and neutron-neutron two-body terms:

$$\frac{Z}{A^2} \sum_i^A \mathbf{r}_i \cdot \sum_j^A \mathbf{r}_j = \frac{Z}{A^2} \left(\sum_p^Z r_p^2 + \sum_n^N r_n^2 + 2 \sum_{p < p'}^{Z-1, Z} \mathbf{r}_p \cdot \mathbf{r}_{p'} + 2 \sum_{n < n'}^{N-1, N} \mathbf{r}_n \cdot \mathbf{r}_{n'} + 2 \sum_{p, n}^{Z, N} \mathbf{r}_p \cdot \mathbf{r}_n \right). \quad (4.59)$$

When we combine all these terms together, we obtain the following expression:

$$\begin{aligned} Z\langle r_{ch}^2 \rangle &= \frac{A^2 - 2A + Z}{A^2} \sum_p^Z r_p^2 + \frac{Z}{A^2} \sum_n^N r_n^2 + \frac{2Z - 4A}{A^2} \sum_{p < p'}^{Z-1, Z} \mathbf{r}_p \cdot \mathbf{r}_{p'} + \frac{2Z}{A^2} \sum_{n < n'}^{N-1, N} \mathbf{r}_n \cdot \mathbf{r}_{n'} \\ &\quad + \frac{2Z - 2A}{A^2} \sum_{p, n}^{Z, N} \mathbf{r}_p \mathbf{r}_n. \end{aligned} \quad (4.60)$$

Thus, even the charge radius is not independent of the neutrons.

We have the formulas for the expectation values, so we then introduce the new framework in which we calculate radii. Starting in the body-fixed frame, we place two clusters along the z -axis: an alpha cluster at z_1 , and a dineutron at z_2 (z_1 is usually chosen to be 0, and z_2 is moved in order to achieve the same effect as the parameter

d in the previous sections). The single-particle wave functions are:

$$\psi_\alpha(\mathbf{r}) = \left(\frac{\nu}{\pi}\right)^{3/4} \exp[-\nu/2(x^2 + y^2 + (z - z_1))], \quad (4.61)$$

$$\phi_d(\mathbf{r}) = \left(\frac{\omega}{\pi}\right)^{3/4} \exp[-\omega/2(x^2 + y^2 + (z - z_2))]. \quad (4.62)$$

The overlaps in this body-fixed frame are:

$$\theta_\alpha = \theta_d = 1, \quad (4.63)$$

$$\theta_{12} = \left(\frac{2\sqrt{\nu\omega}}{\nu + \omega}\right)^{3/2} \exp\left[-\frac{\nu\omega(z_1 - z_2)^2}{2(\nu + \omega)}\right]. \quad (4.64)$$

We then determine the center of mass of this body-fixed frame system. The form of the operator is given in eq.(4.53). We need only concern ourselves with the z -coordinate, since the x and y center-of-mass coordinates are zero in the body-fixed frame. Therefore, we must find the expectation value of the z -coordinate of the center-of-mass. This is a one-body operator, so we use eq. (3.5)-eq.(3.9) with the following matrix elements:

$$\langle\alpha|Z_{CM}|\alpha\rangle = z_1, \quad (4.65)$$

$$\langle d|Z_{CM}|d\rangle = z_2, \quad (4.66)$$

$$\langle\alpha|Z_{CM}|d\rangle = \langle d|Z_{CM}|\alpha\rangle = \frac{\nu z_1 + \omega z_2}{\nu + \omega} \theta_{12}. \quad (4.67)$$

Thus we see the center-of-mass does not exactly correspond to what one would expect from classical calculations. We would expect the center-of-mass to be located one-third of the way from the alpha-particle to the dineutron cluster, but this is only true for the case where the oscillator lengths are equal. If the lengths are different, the center will move, albeit slightly, weighted by the spatial wave functions.

Now that we have the coordinates of the center-of-mass, $(0,0,Z_{CM})$, we can go to the rotated frame. We rotate about an axis parallel to the y -axis and passing through

the center-of-mass point. The rotated single particle wave functions are:

$$|\tilde{\alpha}\rangle = \left(\frac{\nu}{\pi}\right)^{3/4} \exp\left[-\nu \frac{y^2 + (x - (z_1 - Z_{CM}) \sin \vartheta)^2 + (z - (z_1 - Z_{CM}) \cos \vartheta)^2}{2}\right] \quad (4.68)$$

$$|\tilde{d}\rangle = \left(\frac{\omega}{\pi}\right)^{3/4} \exp\left[-\omega \frac{y^2 + (x - (z_2 - Z_{CM}) \sin \vartheta)^2 + (z - (z_2 - Z_{CM}) \cos \vartheta)^2}{2}\right] \quad (4.69)$$

The rotated overlaps are:

$$\theta_\alpha = \exp\left[\frac{\nu (z_1 - Z_{CM})^2}{2} (x - 1)\right], \quad (4.70)$$

$$\theta_d = \exp\left[\frac{\omega (z_2 - Z_{CM})^2}{2} (x - 1)\right], \quad (4.71)$$

$$\theta_{12} = \left(\frac{2\sqrt{\nu\omega}}{\nu + \omega}\right)^{3/2} \exp\left[-\nu\omega \frac{(z_1 - Z_{CM})^2 + (z_2 - Z_{CM})^2 - 2x (z_1 - Z_{CM}) (z_2 - Z_{CM})}{2(\nu + \omega)}\right]. \quad (4.72)$$

We remind the reader that $x \equiv \cos \vartheta$.

We can now list the one-body matrix elements of the r^2 operator. They are:

$$\langle \alpha | r^2 | \alpha \rangle = \left(\frac{3}{2\nu} + \frac{(z_1 - Z_{CM})^2 (1 + x)}{2} \right) \theta_\alpha, \quad (4.73)$$

$$\langle d | r^2 | d \rangle = \left(\frac{3}{2\omega} + \frac{(z_2 - Z_{CM})^2 (1 + x)}{2} \right) \theta_d, \quad (4.74)$$

$$\begin{aligned} \langle d | r^2 | \alpha \rangle = \langle \alpha | r^2 | d \rangle &= \frac{3}{\nu + \omega} \theta_{12} \\ &+ \frac{\nu^2 (z_1 - Z_{CM})^2 + \omega^2 (z_2 - Z_{CM})^2 + 2\nu\omega (z_1 - Z_{CM}) (z_2 - Z_{CM}) x}{(\nu + \omega)^2} \theta_{12}. \end{aligned} \quad (4.75)$$

The list of terms is now different, as it depends on whether it involves neutrons or protons. The proton term is:

$$\langle r^2 \rangle_\alpha = \langle \alpha | r^2 | \alpha \rangle 2\theta_\alpha (\theta_\alpha \theta_d - \theta_{12}^2)^2. \quad (4.76)$$

The neutron one-body terms are:

$$\langle r^2 \rangle_\alpha = \langle \alpha | r^2 | \alpha \rangle 2\theta_\alpha^2 \theta_d (\theta_\alpha \theta_d - \theta_{12}^2), \quad (4.77)$$

$$\langle r^2 \rangle_d = \langle d | r^2 | d \rangle 2\theta_\alpha^3 (\theta_\alpha \theta_d - \theta_{12}^2), \quad (4.78)$$

$$\langle r^2 \rangle_{12} = \langle \alpha | r^2 | d \rangle 4\theta_\alpha^2 \theta_{12} (\theta_{12}^2 - \theta_\alpha \theta_d), \quad (4.79)$$

where in the last term we have simplified things slightly because the matrix element is equal to its transpose.

The two-body matrix elements are:

$$\langle \alpha\alpha | \mathbf{r}_1 \cdot \mathbf{r}_2 | \alpha\alpha \rangle = \frac{(z_1 - Z_{CM})^2 (1+x)}{2} \theta_\alpha^2, \quad (4.80)$$

$$\langle dd | \mathbf{r}_1 \cdot \mathbf{r}_2 | dd \rangle = \frac{(z_2 - Z_{CM})^2 (1+x)}{2} \theta_d^2, \quad (4.81)$$

$$\langle \alpha d | \mathbf{r}_1 \cdot \mathbf{r}_2 | d\alpha \rangle = \frac{(z_1 - Z_{CM})(z_2 - Z_{CM})(1+x)}{2} \theta_\alpha \theta_d, \quad (4.82)$$

$$\langle \alpha\alpha | \mathbf{r}_1 \cdot \mathbf{r}_2 | \alpha d \rangle = \frac{[\nu(z_1 - Z_{CM})^2 + \omega(z_1 - Z_{CM})(z_2 - Z_{CM})](1+x)}{2(\nu + \omega)} \theta_\alpha \theta_{12}, \quad (4.83)$$

$$\langle dd | \mathbf{r}_1 \cdot \mathbf{r}_2 | dd \rangle = \frac{[\omega(z_2 - Z_{CM})^2 + \nu(z_1 - Z_{CM})(z_2 - Z_{CM})](1+x)}{2(\nu + \omega)} \theta_d \theta_{12}, \quad (4.84)$$

$$\langle \alpha\alpha | \mathbf{r}_1 \cdot \mathbf{r}_2 | dd \rangle = \frac{\nu^2(z_1 - Z_{CM})^2 + \omega^2(z_2 - Z_{CM})^2 + 2\nu\omega(z_1 - Z_{CM})(z_2 - Z_{CM})x}{(\nu + \omega)^2} \theta_{12}^2, \quad (4.85)$$

$$\langle \alpha d | \mathbf{r}_1 \cdot \mathbf{r}_2 | \alpha d \rangle = \frac{2\nu\omega(z_1 - Z_{CM})(z_2 - Z_{CM}) + (\nu^2(z_1 - Z_{CM})^2 + \omega^2(z_2 - Z_{CM})^2)x}{(\nu + \omega)^2} \theta_{12}^2. \quad (4.86)$$

We have three lists of terms to present: proton-proton, neutron-neutron, and neutron-proton. First, we list the proton-proton term:

$$\langle \mathbf{r}_1 \cdot \mathbf{r}_2 \rangle_\alpha = \langle \alpha\alpha | \mathbf{r}_1 \cdot \mathbf{r}_2 | \alpha\alpha \rangle (\theta_\alpha \theta_d - \theta_{12}^2)^2. \quad (4.87)$$

The neutron-neutron terms are:

$$\langle \mathbf{r}_1 \cdot \mathbf{r}_2 \rangle_\alpha = \langle \alpha\alpha | \mathbf{r}_1 \cdot \mathbf{r}_2 | \alpha\alpha \rangle \theta_\alpha^2 \theta_d^2, \quad (4.88)$$

$$\langle \mathbf{r}_1 \cdot \mathbf{r}_2 \rangle_d = \langle dd | \mathbf{r}_1 \cdot \mathbf{r}_2 | dd \rangle \theta_\alpha^4, \quad (4.89)$$

$$\langle \mathbf{r}_1 \cdot \mathbf{r}_2 \rangle_{\alpha\alpha d} = -\langle \alpha\alpha | \mathbf{r}_1 \cdot \mathbf{r}_2 | \alpha d \rangle 4\theta_\alpha^2 \theta_d \theta_{12}, \quad (4.90)$$

$$\langle \mathbf{r}_1 \cdot \mathbf{r}_2 \rangle_{\alpha^2 d^2} = \langle \alpha d | \mathbf{r}_1 \cdot \mathbf{r}_2 | d\alpha \rangle 2\theta_\alpha^2 (2\theta_\alpha \theta_d - \theta_{12}^2), \quad (4.91)$$

$$\langle \mathbf{r}_1 \cdot \mathbf{r}_2 \rangle_{ddd\alpha} = -\langle dd | \mathbf{r}_1 \cdot \mathbf{r}_2 | d\alpha \rangle 4\theta_\alpha^3 \theta_{12}, \quad (4.92)$$

$$\langle \mathbf{r}_1 \cdot \mathbf{r}_2 \rangle_{\alpha d \alpha d} = \langle \alpha\alpha | \mathbf{r}_1 \cdot \mathbf{r}_2 | dd \rangle 2\theta_\alpha^2 \theta_{12}^2, \quad (4.93)$$

$$\langle \mathbf{r}_1 \cdot \mathbf{r}_2 \rangle_{\alpha d d \alpha} = \langle \alpha d | \mathbf{r}_1 \cdot \mathbf{r}_2 | \alpha d \rangle 2\theta_\alpha^2 (2\theta_{12}^2 - \theta_\alpha \theta_d). \quad (4.94)$$

The neutron-proton terms are:

$$\langle \mathbf{r}_1 \cdot \mathbf{r}_2 \rangle_\alpha = \langle \alpha\alpha | \mathbf{r}_1 \cdot \mathbf{r}_2 | \alpha\alpha \rangle 4(\theta_\alpha^2 \theta_d^2 - \theta_{12}^2 \theta_\alpha \theta_d), \quad (4.95)$$

$$\langle \mathbf{r}_1 \cdot \mathbf{r}_2 \rangle_{\alpha\alpha d} = \langle \alpha\alpha | \mathbf{r}_1 \cdot \mathbf{r}_2 | \alpha d \rangle 8\theta_\alpha \theta_{12} (\theta_{12}^2 - \theta_\alpha \theta_d), \quad (4.96)$$

$$\langle \mathbf{r}_1 \cdot \mathbf{r}_2 \rangle_{\alpha^2 d^2} = \langle \alpha d | \mathbf{r}_1 \cdot \mathbf{r}_2 | d\alpha \rangle 4\theta_\alpha^2 (\theta_\alpha \theta_d - \theta_{12}^2). \quad (4.97)$$

All the terms required to calculate the matter radius and charge radius of the alpha-dineutron of ${}^6\text{He}$ have been obtained. We calculate this radius for the set of parameters given by a minimization of the expectation value of the Hamiltonian with respect to the three parameters of the calculation (d, ν, ω), as there is not a minimum principle for the radii. After a number is obtained from the formulae above, there is one last adjustment that needs to be made. The number obtained from the formulae in this section is for point-like nucleons. In order to obtain a number that the fact that the individual nucleons have a finite size, we use the following formula for the charge radius(see, for example [49], but without the Darwin-Foldy contribution):

$$\langle r_{ch}^2 \rangle = \langle r_p^2 \rangle + \langle R_p^2 \rangle + \frac{N}{Z} \langle R_n^2 \rangle, \quad (4.98)$$

where $\langle r_p^2 \rangle$ is the number calculated using the methods presented in this section, $\langle R_p^2 \rangle$ is the proton charge radius which is $\sqrt{R_p^2} = 0.895$ fm [50] and $\langle R_n^2 \rangle$ is the charge radius of the neutron, which is $\langle R_n^2 \rangle = -0.120$ fm² [51]. For the matter radius, we use the same formula, but neglect the negative neutron contribution.

This concludes the section on the various radii calculated for the alpha-dineutron configuration of ⁶He. We move on to the cigar configuration.

4.2 Cigar configuration

The cigar configuration is pictured in Figure 3.2. The single-particle wave functions are:

$$\psi_\alpha(\mathbf{r}) = \left(\frac{\nu}{\pi}\right)^{3/4} \exp(-\nu r^2/2), \quad (4.99)$$

$$\phi_\pm(\mathbf{r}) = \left(\frac{\omega}{\pi}\right)^{3/4} \exp\left[-\frac{\omega}{2}(\mathbf{r} \mp \mathbf{d})^2\right], \quad (4.100)$$

where ψ_α is a constituent of the alpha particle with oscillator parameter ν , and ϕ_\pm is the neutron on the right (+) or left (-) of the alpha particle, with oscillator parameter ω . The parameter d reflects the distance between the alpha particle and the external neutrons. As before, \mathbf{d} is taken to lie along the z -axis. Also as in the previous section, we show one-particle density plots of this configuration. In Figure 4.14, we see the density plot with oscillator parameters equal to each other. Figure 4.15 shows the same quantity but with ω larger than ν , and Figure 4.16 shows the one-particle density with ω smaller than ν . The distance parameter d , was once again set to 2.5 fm. This value was chosen for demonstration purposes only.

All other expectation values, of course, are calculated in the rotated system. The

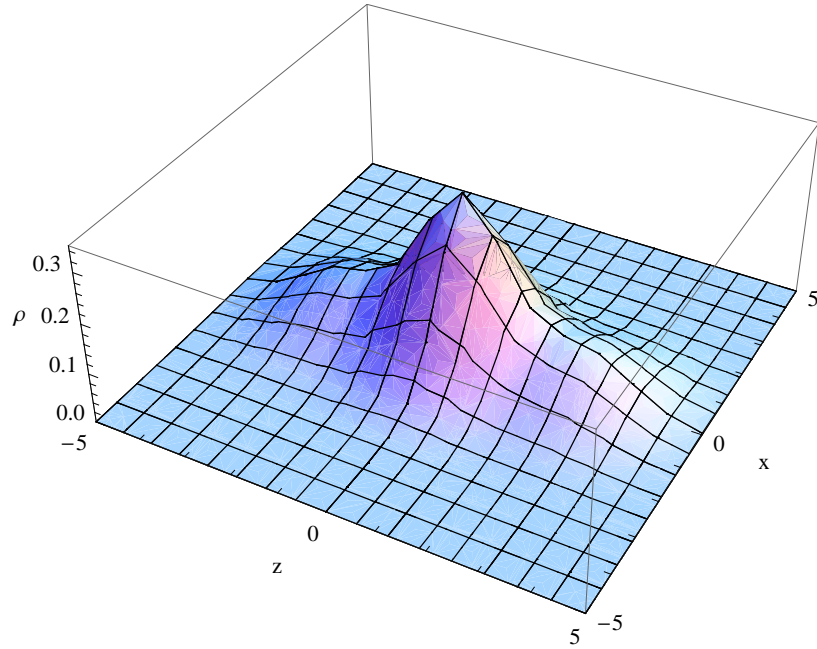


Figure 4.14: Shown here is the one-particle density of the cigar configuration. It is pictured in the xz plane. In this picture, the oscillator lengths are both equal to 0.53 fm^{-2} and d (the distance between the alpha particle and an external particle) is set to 2.5 fm . The alpha particle is located at the origin, and is flanked by both external neutrons.

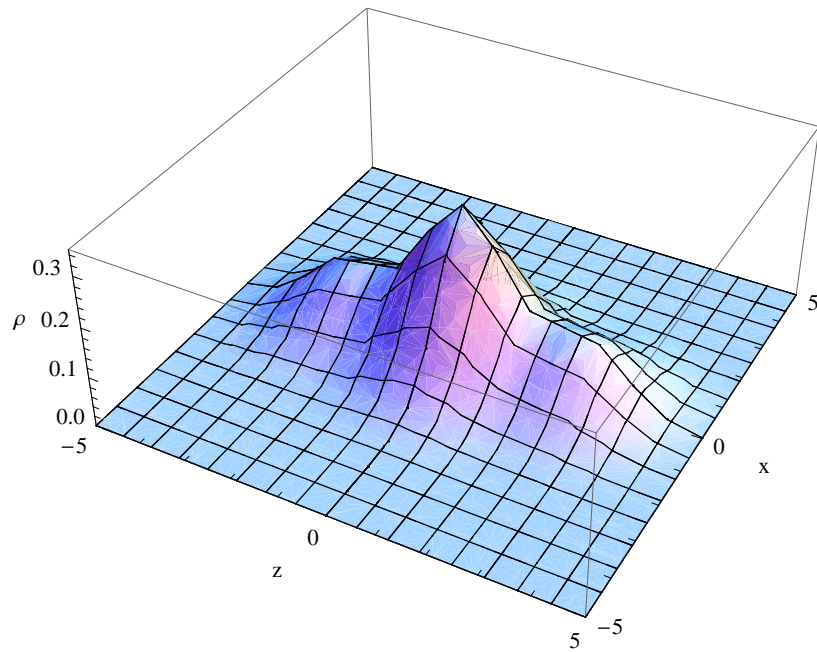


Figure 4.15: The one-particle density of the cigar configuration with unequal oscillator parameters. The alpha oscillator parameter, ν , is set equal to 0.53 fm^{-2} , and the external neutron parameter, ω , is set equal to 0.68 fm^{-2} .

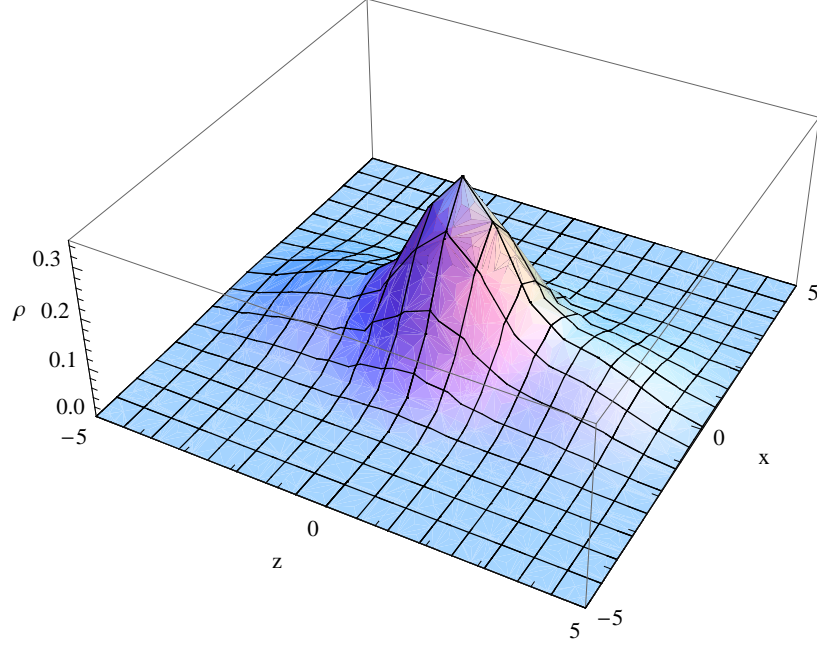


Figure 4.16: The one-particle density of the cigar configuration with $\nu=0.53 \text{ fm}^{-2}$ and $\omega=0.41 \text{ fm}^{-2}$.

rotated single particle wave functions are:

$$\psi_{\alpha}(x, y, z) = \left(\frac{\nu}{\pi}\right)^{3/4} \exp[-\nu(x^2 + y^2 + z^2)/2], \quad (4.101)$$

$$\phi_{\pm}(x, y, z) = \left(\frac{\omega}{\pi}\right)^{3/4} \exp\left[\frac{-\omega}{2}(x^2 \mp 2xd \sin \vartheta + y^2 + z^2 \mp 2zd \cos \vartheta + d^2)\right]. \quad (4.102)$$

The overlaps of the system are:

$$\theta_{\alpha} = \langle \alpha | \tilde{\alpha} \rangle = 1, \quad (4.103)$$

$$\theta_n = \langle \pm | \tilde{\pm} \rangle = \exp[\omega d^2 (x - 1) / 2], \quad (4.104)$$

$$\theta_{\pm} = \langle \pm | \tilde{\mp} \rangle = \exp[-\omega d^2 (x + 1) / 2], \quad (4.105)$$

$$\theta_{12} = \langle \pm | \tilde{\alpha} \rangle = \langle \alpha | \tilde{\pm} \rangle = \left(\frac{2\sqrt{\nu\omega}}{\nu + \omega}\right)^{3/2} \exp\left[-\frac{\nu\omega d^2}{2(\nu + \omega)}\right], \quad (4.106)$$

where $x \equiv \cos \vartheta$. Once again, when d is zero, all the overlaps are equal to one (if $\nu = \omega$). Which causes the norm, eq.(3.23) (reproduced below), to have zero in its

denominator:

$$\frac{1}{2\theta_\alpha^2 [\theta_\alpha^2 (\theta_n^2 + \theta_\pm^2) + 2\theta_{12}^4 - 2\theta_{12}^2 \theta_\alpha (\theta_n + \theta_\pm)]}.$$

As discussed before, this is a consequence of trying to put four identical fermions at the same spatial location.

We move on to calculating the matrix elements between rotated wave functions, beginning with the kinetic energy. As before, tildes in kets will no longer be indicated, as all wave functions in the ket are understood to be rotated with respect to the wave functions in the bra.

4.2.1 Kinetic energy

We start with expectation values of the operators in the Hamiltonian, eq.(4.12). The first of these operators deal with the kinetic energy. The first being the sum of the one-body kinetic energies, and the second correcting for the center-of-mass motion. The matrix elements of the one-body kinetic energy operator (eq.(4.13)) are:

$$\langle \alpha | T | \alpha \rangle = \frac{3\nu}{2}, \quad (4.107)$$

$$\langle \pm | T | \pm \rangle = \omega \theta_n \left[\frac{3}{2} + \frac{(x-1)\omega d^2}{2} \right], \quad (4.108)$$

$$\langle \pm | T | \mp \rangle = \omega \theta_\pm \left[\frac{3}{2} - \frac{(x+1)\omega d^2}{2} \right], \quad (4.109)$$

$$\langle \pm | T | \alpha \rangle = \langle \alpha | T | \pm \rangle = \frac{\nu\omega}{\nu + \omega} \theta_{12} \left(3 - \frac{\nu\omega}{\nu + \omega} d^2 \right). \quad (4.110)$$

As in the previous configuration, the factor $\hbar^2/2m$ has been suppressed. These matrix elements are plugged into eqs.(3.25)-(3.29) to obtain the one-body contribution to the kinetic energy.

The center-of-mass correction to kinetic energy was discussed at length in the section on the alpha-dineutron configuration (following eq.(4.17)). All that remains for us to do here is to enumerate the terms pertaining to the cigar configuration. We

list here the matrix elements of the momentum operator:

$$\langle \alpha | \mathbf{p} | \alpha \rangle = 0, \quad (4.111)$$

$$\langle \pm | \mathbf{p} | \pm \rangle = \pm \frac{\omega}{i} \theta_n \frac{d}{2} [\sin \vartheta \hat{\mathbf{x}} + (\cos \vartheta - 1) \hat{\mathbf{z}}], \quad (4.112)$$

$$\langle \pm | \mathbf{p} | \mp \rangle = \mp \frac{\omega}{i} \theta_{\pm} \frac{d}{2} [\sin \vartheta \hat{\mathbf{x}} + (1 + \cos \vartheta) \hat{\mathbf{z}}], \quad (4.113)$$

$$\langle \pm | \mathbf{p} | \alpha \rangle = \mp \frac{\nu \omega d}{i(\nu + \omega)} \theta_{12} \hat{\mathbf{z}}, \quad (4.114)$$

$$\langle \alpha | \mathbf{p} | \pm \rangle = \pm \frac{\nu \omega d}{i(\nu + \omega)} \theta_{12} (\sin \vartheta \hat{\mathbf{x}} + \cos \vartheta \hat{\mathbf{z}}). \quad (4.115)$$

The scalar product of these terms is taken and then inserted into the correct term in the list of two-body terms found in eqs.(3.30)-(3.44). Since the first matrix element, eq.(4.111), vanishes, many of the terms vanish.

In Figure 4.17, we show the total kinetic energy contribution to the Hamiltonian of the cigar configuration. Like in the result for the alpha-dineutron configuration (Figure 4.5), the small d limit shows an increase in the kinetic energy (because two neutrons are forced into higher orbits) and degeneracy between the $J = 0$ and $J = 2$ levels. The large d limit corresponds to the kinetic energy of the alpha particle and two free neutrons. An interesting difference between Figure 4.17 and Figure 4.5 is that in the cigar configuration, no odd waves appear. This is due to the higher symmetry of the cigar configuration. For example, if one considers only the two external neutrons (which is reasonable since the alpha particle has all angular momentum quantum numbers equal to zero), we must obey the rule for two nucleons, that $(-1)^{L+S+T} = -1$, or that $L+S+T$ must be odd. Since the two particles are neutrons, that means $T = 1$, and by construction, they are in the singlet spin state ($S = 0$), thus the only way to fulfill the condition is to have L be even.

Another check on the calculation, is that at $d = 0$, we have six particles at the same point, and the results should be independent of how they got there. In other words, the values at $d = 0$ should be the same for $d = 0$ for the cigar configuration and

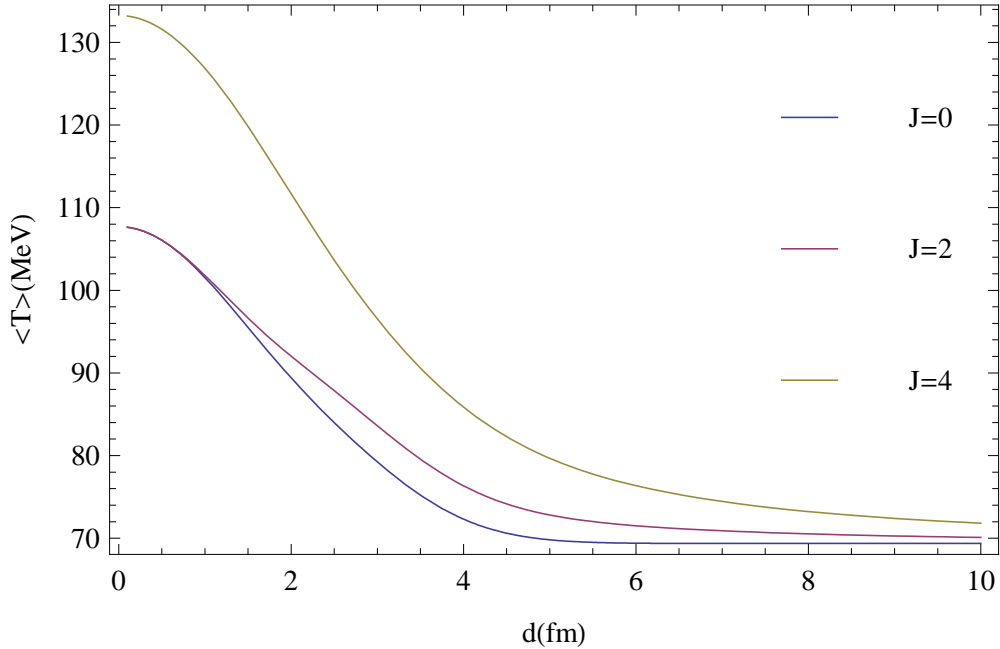


Figure 4.17: The total kinetic energy in the cigar configuration of ${}^6\text{He}$ is shown here. The contribution from the center-of-mass motion has been removed. This plot was obtained with both oscillator parameters equal to 0.53 fm^{-2} .

the alpha-dineutron configuration. Upon examining the figures, one can see that this is true. The $J = 0$ and $J = 2$ degenerate level comes in at just under 108 MeV (107.6 MeV to be precise), and the $J = 4$ level is at 133 MeV in both pictures. One might make the observation, that the $J = 1$ and $J = 3$ levels certainly do not correspond in both configurations, but this is not a problem. In order for the cigar configuration to produce $J = 1$ and $J = 3$ levels at $d = 0$, there would have to be a sudden break in the symmetry at that value of d . Similarly, for the inverse to be the case, those levels would have to disappear for the alpha-dineutron configuration just at $d = 0$, and this sudden creation or destruction of symmetry is not a part of this theory.

4.2.2 Interaction

We turn now to the two-body interactions used in the cigar configuration. The interactions used for ${}^6\text{He}$ were discussed at length in section 4.1.3, so here we can move on directly to the matrix elements. As before, if a matrix element is equal to its

transpose, it will be listed with a subscript- “+” following the matrix element. Also, some matrix elements come in pairs in which the only difference is the sign of the angle term. We will exploit this fact for brevity, and indicate it by the expression $B = A(x \rightarrow -x)$. The matrix elements for the Volkov potentials are:

$$\langle \alpha\alpha | V | \alpha\alpha \rangle = V_a \left(\frac{\nu\alpha^2}{\nu\alpha^2 + 2} \right)^{3/2}, \quad (4.116)$$

$$\langle \alpha \pm | V | \pm \alpha \rangle = V_a \left(\frac{\nu\omega\alpha^2}{\nu\omega\alpha^2 + \nu + \omega} \right)^{3/2} \exp \left[-\frac{\omega(\nu\alpha^2 + 1)(1-x) + 2\nu}{2(\nu\omega\alpha^2 + \nu + \omega)} \omega d^2 \right], \quad (4.117)$$

$$\langle \alpha \pm | V | \mp \alpha \rangle = \langle \alpha \pm | V | \pm \alpha \rangle (x \rightarrow -x), \quad (4.118)$$

$$\langle \alpha\alpha | V | \alpha\pm \rangle_+ = V_a \left(\frac{2\nu\alpha^2\sqrt{\nu\omega}}{D(\nu, \omega)} \right)^{3/2} \exp \left[-\frac{(\nu\alpha^2 + 3)\nu\omega d^2}{2D(\nu, \omega)} \right], \quad (4.119)$$

$$\begin{aligned} \langle \mp \pm | V | \pm \alpha \rangle_+ &= V_a \left(\frac{2\omega\alpha^2\sqrt{\nu\omega}}{D(\omega, \nu)} \right)^{3/2} \\ &\times \exp \left[-\frac{(\omega^2\alpha^2 + \nu\omega\alpha^2)(1-x) + \nu\omega\alpha^2 + 3\nu + 8\omega}{2D(\omega, \nu)} \omega d^2 \right], \end{aligned} \quad (4.120)$$

$$\langle \mp \pm | V | \mp \alpha \rangle_+ = \langle \mp \pm | V | \pm \alpha \rangle_+ (x \rightarrow -x), \quad (4.121)$$

where $D(a, b)$ is defined in eq.(4.31). Continuing:

$$\langle \pm \mp | V | \mp \pm \rangle = V_a \left(\frac{\omega\alpha^2}{\omega\alpha^2 + 2} \right)^{3/2} \exp \left[-\frac{\omega\alpha^2(1-x) + 4}{\omega\alpha^2 + 2} \omega d^2 \right], \quad (4.122)$$

$$\langle \pm \mp | V | \pm \mp \rangle = \langle \pm \mp | V | \mp \pm \rangle (x \rightarrow -x), \quad (4.123)$$

$$\langle \pm \mp | V | \alpha\alpha \rangle_+ = V_a \left(\frac{4\nu\omega\alpha^2}{(\nu + \omega)(\nu\alpha^2 + \omega\alpha^2 + 4)} \right)^{3/2} \exp \left[-\frac{\nu\alpha^2 + 4}{\nu\alpha^2 + \omega\alpha^2 + 4} \omega d^2 \right], \quad (4.124)$$

$$\langle \pm\alpha|V|\pm\alpha\rangle = V_a \left(\frac{4\nu\omega\alpha^2}{(\nu+\omega)(\nu\alpha^2+\omega\alpha^2+4)} \right)^{3/2} \times \exp \left[-\frac{2\omega(1-x)+\nu(\nu\alpha^2+\omega\alpha^2+4)}{(\nu+\omega)(\nu\alpha^2+\omega\alpha^2+4)} \omega d^2 \right], \quad (4.125)$$

$$\langle \pm\alpha|V|\mp\alpha\rangle = \langle \pm\alpha|V|\pm\alpha\rangle(x \rightarrow -x). \quad (4.126)$$

These matrix elements are put alongside the appropriate overlap expression from eq.(3.30)-(3.44) and summed together. This is for the terms proportional to $1 - m$ in the Volkov potential, or to $u/2$ in the Minnesota potential. The Majorana exchange operator shuffles many terms among themselves in the cigar configuration. Eq.(4.117) is switched with eq.(4.125) and eq.(4.118) is switched with eq.(4.126) when one inserts matrix elements into the list starting with eq.(3.30). The Majorana exchange operator also switches eq.(4.122) with eq.(4.123) and eq.(4.120) with eq.(4.121), but the overlap terms that accompany these pairs of matrix elements are the same (eqs.(3.43) with(3.44) and (3.35)-(3.38), respectively), so the Majorana operator has no net effect in these instances.

The expectation value of the Volkov potential is shown in Figure 4.18 for V1 and in Figure 4.19 for V2. They are similar to the pictures for the alpha-dineutron configuration, save for the absence of odd waves. The $J = 4$ level is bound much more weakly, and $J = 0$ and $J = 2$ are bound much more tightly, with a very small separation between the two of them. The potential energy of the cigar configuration seems to fall off faster than in the alpha-dineutron configuration, because as d increases, not only are the external neutrons moving away from the alpha particle, they are also moving away from each other, which is not the case in the other configuration. The large d limit here contains only the potential energy within the alpha particle, as the two neutrons do not attract each other at large distances. As before, there is not much difference between V1 and V2, except near $d = 0$.

As with the kinetic energy, we can compare the potentials in both configurations at $d = 0$. The first two levels look to be at the same value, and they are to many

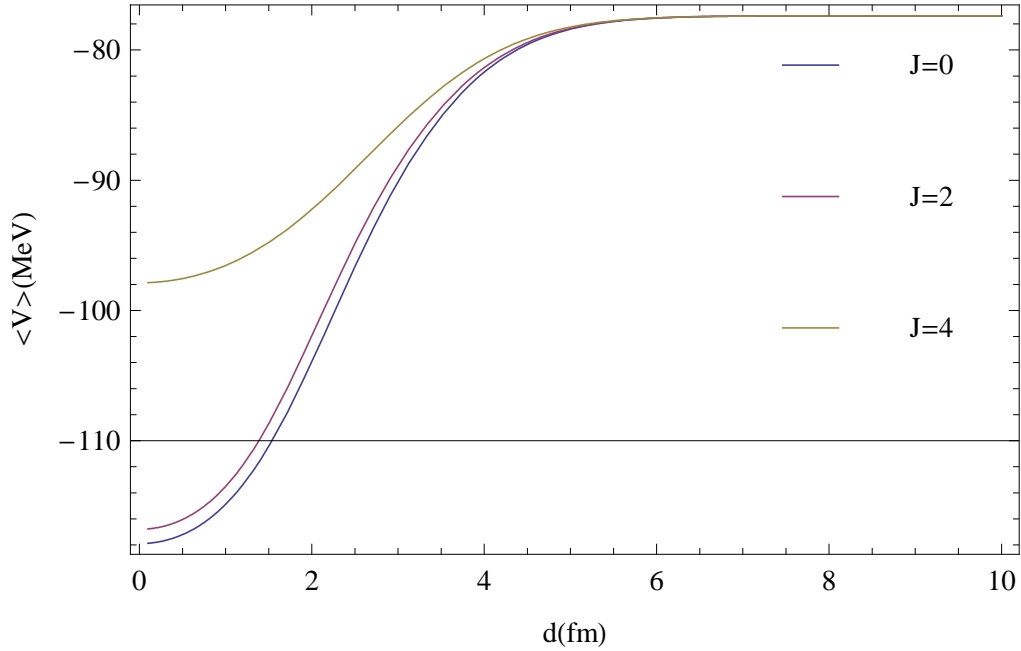


Figure 4.18: Plotted here is the expectation value as a function of d of the Volkov V1 interaction in the cigar configuration of ${}^6\text{He}$. In this plot, the oscillator lengths were both set equal to 0.53 fm^{-2} , and the Majorana exchange parameter was set equal to 0.6.

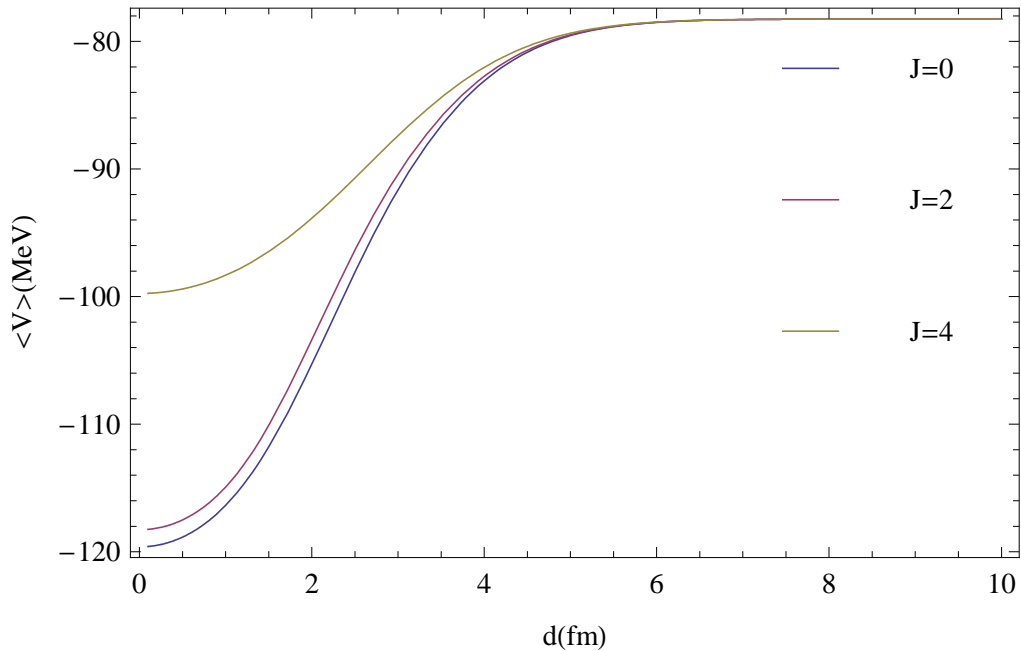


Figure 4.19: Displayed here is the expectation value of the Volkov V2 potential for three different levels of the cigar configuration of ${}^6\text{He}$. These results were produced with both oscillator parameters equal to 0.53 fm^{-2} and the Majorana exchange parameter equal to 0.6.

digits (-117.9 and -116.78 MeV, respectively, for the V1 expectation value), but the $J = 4$ levels don't appear to agree (-104.7 MeV for the alpha-dineutron configuration and -97.8 MeV for the cigar). They agree better with the Majorana part of the interaction turned off (-138.1 MeV for the alpha-dineutron case and -139.4 for the cigar configuration), but the lack of agreement is puzzling. Many checks were performed, including calculating the Majorana effects with the operator in its alternate form, eq.(4.38), but this did not change the results. This behavior of the highly excited state is not yet fully understood.

We now turn to the Minnesota potential. The general form of the potential was written in eq.(4.39). The form factors are all Gaussian:

$$V_k(r_{ij}) = V_k \exp(-\kappa_i r_{ij}^2). \quad (4.127)$$

One can use the matrix elements listed in eq.(4.116)-eq.(4.126) with the substitution $\kappa_i = 1/\alpha^2$ and the appropriate magnitude instead of V_a . We do, however, have to re-write the general cigar two-body matrix elements (eqs.(3.30)-(3.44)) in terms of singlet and triplet spin terms. The terms listed in eqs.(3.30)-(3.44) can be used for

the repulsive term in the Minnesota potential. The singlet terms are:

$$\begin{aligned}\langle V_s \rangle_\alpha &= \langle \alpha\alpha | V_s | \alpha\alpha \rangle \\ &= [2\theta_\alpha^2 (\theta_n^2 + \theta_\pm) + 2\theta_{12}^4 - 2\theta_{12}^2 \theta_\alpha (\theta_n + \theta_\pm)],\end{aligned}\quad (4.128)$$

$$\langle V_s \rangle_{\alpha^2 n^2} = \langle \alpha \pm | V_s | \pm \alpha \rangle (3\theta_\alpha^3 \theta_n - \theta_\alpha^2 \theta_{12}^2), \quad (4.129)$$

$$\langle V_s \rangle_{\alpha^2 \pm^2} = \langle \alpha \pm | V_s | \mp \alpha \rangle (3\theta_\alpha^3 \theta_\pm - \theta_\alpha^2 \theta_{12}^2), \quad (4.130)$$

$$\langle V_s \rangle_{\alpha\alpha n} = \langle V_s \rangle_{n\alpha\alpha} = \langle \alpha\alpha | V_s | \alpha\pm \rangle [2\theta_{12}^3 \theta_\alpha - 3\theta_\alpha^2 \theta_{12} (\theta_n + \theta_\pm)], \quad (4.131)$$

$$\langle V_s \rangle_{\pm^2 \mp \alpha} = \langle V_s \rangle_{\alpha \mp \pm^2} = -2\langle \mp \pm | V_s | \pm \alpha \rangle \theta_\alpha^3 \theta_{12}, \quad (4.132)$$

$$\langle V_s \rangle_{\alpha \mp \mp \pm} = -2\langle V_s \rangle_{\alpha \mp \pm^2} = \langle \mp \pm | V_s | \mp \alpha \rangle \theta_\alpha^3 \theta_{12}, \quad (4.133)$$

$$\langle V_s \rangle_{\alpha+\alpha-} = \langle V_s \rangle_{+\alpha-\alpha} = \langle \alpha\alpha | V_s | + - \rangle 2\theta_\alpha^2 \theta_{12}^2, \quad (4.134)$$

$$\langle V_s \rangle_{\alpha\pm\pm\alpha} = \langle \alpha \pm | V_s | \alpha\pm \rangle 2\theta_\alpha \theta_{12}, \quad (4.135)$$

$$\langle V_s \rangle_{\alpha\pm\mp\alpha} = \langle \alpha \mp | V_s | \alpha\pm \rangle 2\theta_\alpha \theta_{12}, \quad (4.136)$$

$$\langle V_s \rangle_n = \langle \pm \mp | V_s | \mp \pm \rangle \theta_\alpha^4, \quad (4.137)$$

$$\langle V_s \rangle_\pm = \langle \pm \mp | V_s | \pm \mp \rangle \theta_\alpha^4. \quad (4.138)$$

There triplet terms are:

$$\langle V_t \rangle_\alpha = \langle \alpha\alpha | V_t | \alpha\alpha \rangle [2\theta_\alpha^2 (\theta_n^2 + \theta_\pm) - 2\theta_{12}^2 \theta_\alpha (\theta_n + \theta_\pm)],\quad (4.139)$$

$$\langle V_t \rangle_{\alpha^2 n^2} = \langle \alpha \pm | V_t | \pm \alpha \rangle (5\theta_\alpha^3 \theta_n - 5\theta_\alpha^2 \theta_{12}^2), \quad (4.140)$$

$$\langle V_t \rangle_{\alpha^2 \pm^2} = \langle \alpha \pm | V_t | \mp \alpha \rangle (5\theta_\alpha^3 \theta_\pm - 5\theta_\alpha^2 \theta_{12}^2), \quad (4.141)$$

$$\langle V_t \rangle_{\alpha\alpha n} = \langle V_t \rangle_{n\alpha\alpha} = \langle \alpha\alpha | V_t | \alpha\pm \rangle [6\theta_{12}^3 \theta_\alpha - 3\theta_\alpha^2 \theta_{12} (\theta_n + \theta_\pm)], \quad (4.142)$$

$$\langle V_t \rangle_{\alpha\pm\pm\alpha} = \langle \alpha \pm | V_t | \alpha\pm \rangle (2\theta_\alpha \theta_{12} - 2\theta_\alpha^3 \theta_n), \quad (4.143)$$

$$\langle V_t \rangle_{\alpha\pm\mp\alpha} = \langle \alpha \mp | V_t | \alpha\pm \rangle (2\theta_\alpha \theta_{12} - 2\theta_\alpha^3 \theta_\pm). \quad (4.144)$$

The exchange operator in eq.(4.39) switches the same terms as in the Volkov potentials.

The expectation value of the Minnesota potential as a function of d is shown

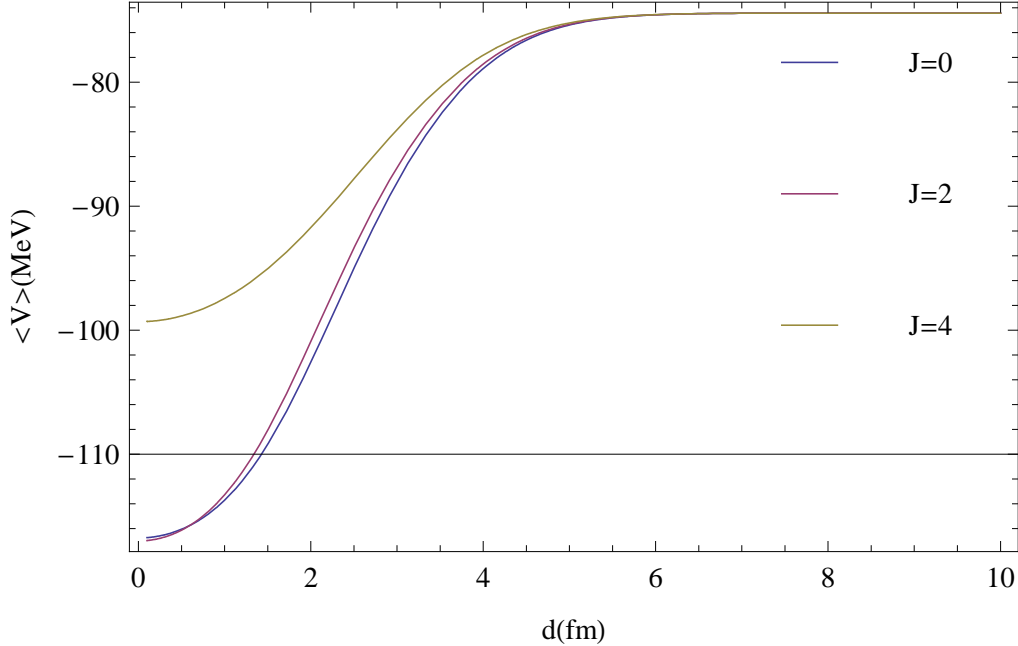


Figure 4.20: Plotted here is the expectation value of the Minnesota potential in the cigar configuration of ${}^6\text{He}$. These results were obtained with the oscillator lengths both equal to 0.53 fm^{-2} , and the exchange parameter, u , equal to one.

in Figure 4.20. The plot is similar to the plot in the alpha-dineutron configuration (Figure 4.11), except that the odd levels are missing. The first two levels, $J = 0$ and $J = 2$, are very close together, and $J = 4$ is much less bound than the first two levels. At $d = 0$, as before we see agreement with the alpha-dineutron configuration in the values of the potential for the first two levels (-116.7 MeV and -117.0 MeV), but the $J = 4$ levels do not coincide (-100.8 MeV in the alpha-dineutron configuration and -99.3 MeV for the cigar configuration), but they are closer than with the Volkov potential.

4.2.3 Total energy

We now turn to the sum of the results of the kinetic energy and potential energy, which is the total energy of the cigar configuration. In Figure 4.21, we show the total energy as a function of d obtained with the Volkov V1 potential. Here we see again bound behavior for only $J = 0$ and $J = 2$, but at a much higher energy than for the alpha-

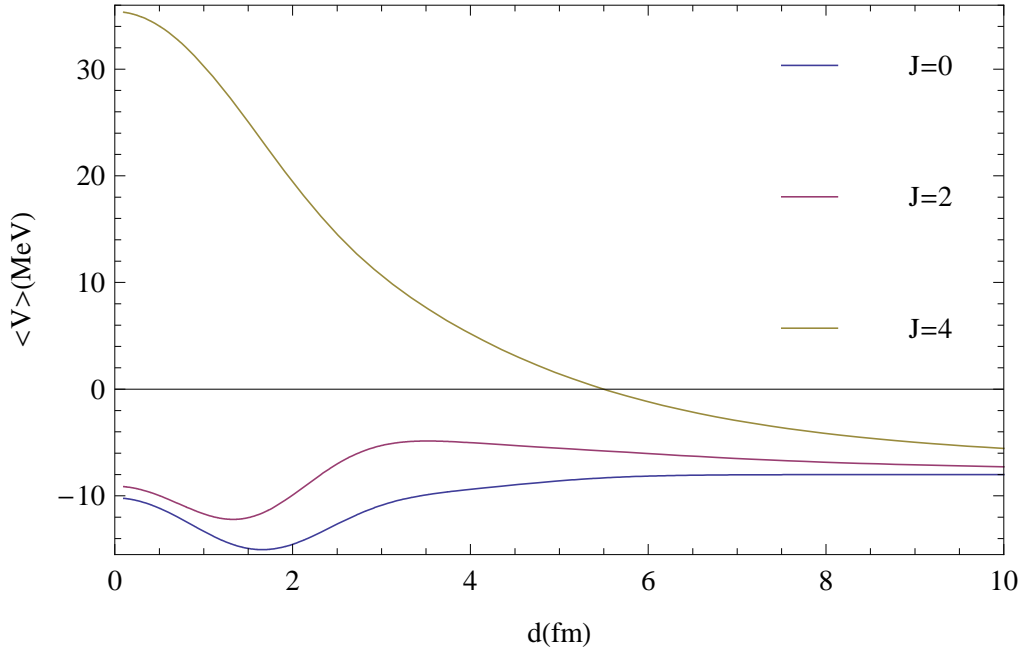


Figure 4.21: Shown here is the total energy of the cigar configuration, with the Volkov V1 potential used as the interaction. For this plot, the oscillator parameters were both equal to 0.53 fm^{-2} , and the Majorana exchange parameter is 0.6.

dineutron configuration (Figure 4.12). The $J = 2$ excited state appears to be a bound excited state rather than a resonance, which was the case in the other configuration. The large d energy corresponds to the total energy of an alpha particle and two free neutrons, which is why it is different than the large d limit of the alpha-dineutron configuration. At small d , the first two levels correspond in both configurations, but $J = 4$ does not, for reasons noted in the section on the potential. Figure 4.22 shows the total energy calculated with the Volkov V2 interaction. The picture is very similar to the previous plot, except the energies are slightly lower.

Figure 4.23 shows the same quantity calculated with the Minnesota potential. This spectrum is similar to the other two. It is perhaps the highest in energy, and the first two states are closer to each other than with the Volkov potentials. It also has the same $d = 0$ behavior as the Volkov potentials: agreement for $J = 0, 2$ and a mismatch for $J = 4$.

This concludes the discussion of the operators that make up the Hamiltonian. We

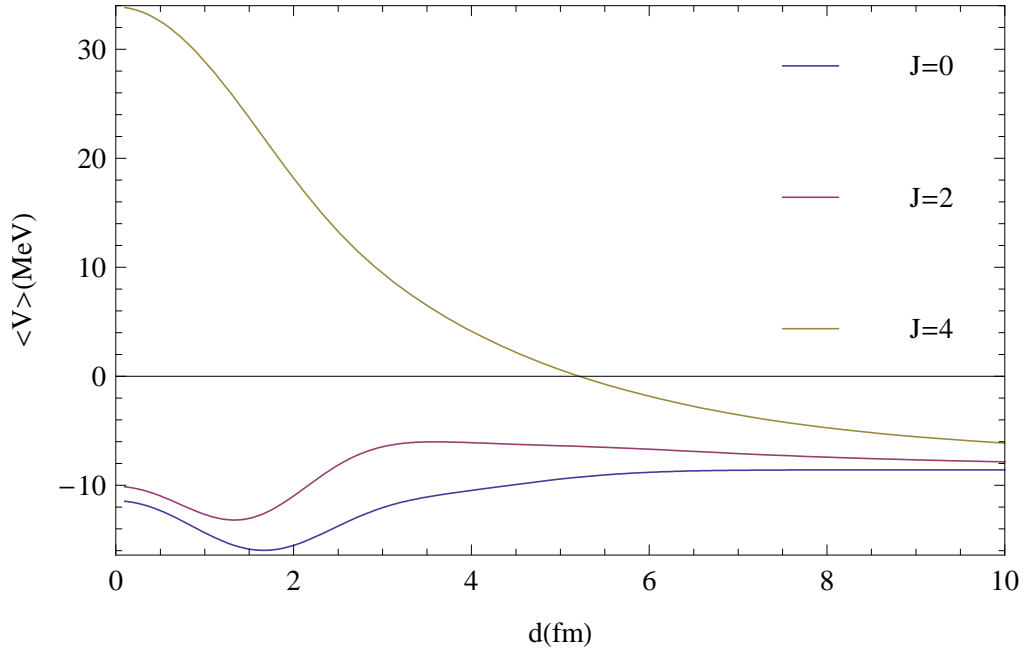


Figure 4.22: Plotted here is the total energy of the cigar configuration, with the Volkov V2 potential used as the interaction. For this plot, the oscillator parameters were both equal to 0.53 fm^{-2} , and the Majorana exchange parameter is 0.6.

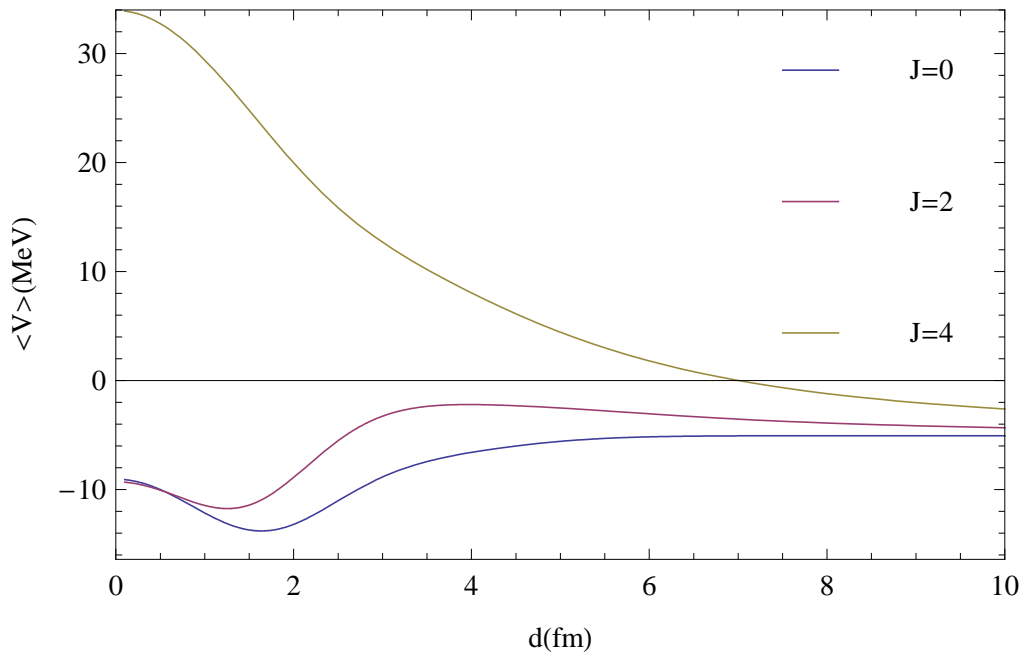


Figure 4.23: This plot shows the total energy spectrum of the cigar configuration obtained with the Minnesota potential. In this plot, the oscillator parameters are both equal to 0.53 fm^{-2} , and the exchange parameter, u , is equal to one.

now move on to the discussion of other calculations in the cigar configuration.

4.2.4 Mean square radius

In the previous configuration, we had to re-write the coordinates in order to carefully determine the center-of-mass. In the cigar configuration, this is not necessary. Due to its high symmetry, the single-particle wave functions (eqs.(4.101)-(4.102)) do not have to be re-written. The alpha particle is always at the center-of-mass. The form of the operators for the matter radius and charge radius remain the same (eqs.(4.55) and (4.60), respectively).

We begin, then, with the one-body matrix elements:

$$\langle \alpha | r^2 | \alpha \rangle = \frac{3}{2\nu}, \quad (4.145)$$

$$\langle \pm | r^2 | \pm \rangle = \theta_n \left[\frac{3}{2\omega} + \frac{d^2(1+x)}{2} \right], \quad (4.146)$$

$$\langle \pm | r^2 | \mp \rangle = \theta_{\pm} \left[\frac{3}{2\omega} + \frac{d^2(1-x)}{2} \right], \quad (4.147)$$

$$\langle \pm | r^2 | \alpha \rangle = \langle \alpha | r^2 | \pm \rangle = \theta_{12} \left[\frac{3}{\nu + \omega} + \frac{\omega^2}{(\nu + \omega)^2} d^2 \right]. \quad (4.148)$$

We must separate the one-body terms into proton and neutron terms. The proton term is:

$$\langle r^2 \rangle_p = \langle \alpha | r^2 | \alpha \rangle \theta_{\alpha} \left[\theta_{\alpha}^2 (\theta_n^2 + \theta_{\pm}^2) + 2\theta_{12}^4 - 2\theta_{12}^2 \theta_{\alpha} (\theta_n + \theta_{12}) \right] \quad (4.149)$$

The neutron terms are:

$$\langle r^2 \rangle_\alpha = \langle \alpha | r^2 | \alpha \rangle \theta_\alpha^2 [\theta_\alpha (\theta_n^2 + \theta_\pm^2) - \theta_{12}^2 (\theta_n + \theta_\pm)], \quad (4.150)$$

$$\langle r^2 \rangle_n = \langle \pm | r^2 | \pm \rangle \theta_\alpha^3 (\theta_\alpha \theta_n - \theta_{12}^2), \quad (4.151)$$

$$\langle r^2 \rangle_\pm = \langle \pm | r^2 | \mp \rangle \theta_\alpha^3 (\theta_\alpha \theta_\pm - \theta_{12}^2), \quad (4.152)$$

$$\langle r^2 \rangle_{\alpha\pm} = \langle \alpha | r^2 | \pm \rangle 2\theta_\alpha^2 \theta_{12} [2\theta_{12}^2 - \theta_\alpha (\theta_n + \theta_\pm)], \quad (4.153)$$

$$\langle r^2 \rangle_{\pm\alpha} = \langle \pm | r^2 | \alpha \rangle 2\theta_\alpha^2 \theta_{12} [2\theta_{12}^2 - \theta_\alpha (\theta_n + \theta_\pm)]. \quad (4.154)$$

Those are summed together with the proper coefficients shown eqs.(4.55) and (4.60).

The two-body matrix elements are formed from the scalar products of the one-body matrix elements $\langle \mathbf{r}_1 \rangle \cdot \langle \mathbf{r}_2 \rangle$. They are:

$$\langle \pm | \mathbf{r} | \pm \rangle \cdot \langle \mp | \mathbf{r} | \mp \rangle = -\theta_n^2 (1+x) d^2 / 2, \quad (4.155)$$

$$\langle \pm | \mathbf{r} | \mp \rangle \cdot \langle \mp | \mathbf{r} | \pm \rangle = \theta_\pm^2 (x-1) d^2 / 2, \quad (4.156)$$

$$\langle \pm | \mathbf{r} | \pm \rangle \cdot \langle \mp | \mathbf{r} | \alpha \rangle = -\theta_n \theta_{12} \frac{\omega d^2}{2(\nu + \omega)} (1+x), \quad (4.157)$$

$$\langle \pm | \mathbf{r} | \pm \rangle \cdot \langle \alpha | \mathbf{r} | \mp \rangle = -\theta_n \theta_{12} \frac{\omega d^2}{2(\nu + \omega)} (1+x), \quad (4.158)$$

$$\langle \pm | \mathbf{r} | \mp \rangle \cdot \langle \mp | \mathbf{r} | \alpha \rangle = \theta_\pm \theta_{12} \frac{\omega d^2}{2(\nu + \omega)} (x-1), \quad (4.159)$$

$$\langle \pm | \mathbf{r} | \mp \rangle \cdot \langle \alpha | \mathbf{r} | \pm \rangle = \theta_\pm \theta_{12} \frac{\omega d^2}{2(\nu + \omega)} (x-1), \quad (4.160)$$

$$\langle \alpha | \mathbf{r} | \pm \rangle \cdot \langle \alpha | \mathbf{r} | \mp \rangle = -\theta_{12}^2 \frac{\omega^2 d^2}{(\nu + \omega)^2}, \quad (4.161)$$

$$\langle \pm | \mathbf{r} | \alpha \rangle \cdot \langle \mp | \mathbf{r} | \alpha \rangle = -\theta_{12}^2 \frac{\omega^2 d^2}{(\nu + \omega)^2}, \quad (4.162)$$

$$\langle \alpha | \mathbf{r} | \pm \rangle \cdot \langle \pm | \mathbf{r} | \alpha \rangle = \theta_{12}^2 \frac{\omega^2 d^2}{(\nu + \omega)^2} x, \quad (4.163)$$

$$\langle \alpha | \mathbf{r} | \mp \rangle \cdot \langle \pm | \mathbf{r} | \alpha \rangle = -\theta_{12}^2 \frac{\omega^2 d^2}{(\nu + \omega)^2} x. \quad (4.164)$$

There are no terms involving the direct alpha terms ($\langle \alpha | \mathbf{r} | \alpha \rangle$), because the alpha is at the origin and this matrix element is zero. Because of this fact, the only two-body

terms are neutron-neutron terms. They are:

$$\langle \mathbf{r}_1 \cdot \mathbf{r}_2 \rangle_n = \langle \pm | \mathbf{r} | \pm \rangle \cdot \langle \mp | \mathbf{r} | \mp \rangle \theta_\alpha^4, \quad (4.165)$$

$$\langle \mathbf{r}_1 \cdot \mathbf{r}_2 \rangle_\pm = \langle \pm | \mathbf{r} | \mp \rangle \cdot \langle \mp | \mathbf{r} | \pm \rangle \theta_\alpha^4, \quad (4.166)$$

$$\langle \mathbf{r}_1 \cdot \mathbf{r}_2 \rangle_{\pm^2 \mp \alpha} = -\langle \pm | \mathbf{r} | \pm \rangle \cdot \langle \mp | \mathbf{r} | \alpha \rangle 2\theta_\alpha^3 \theta_{12}, \quad (4.167)$$

$$\langle \mathbf{r}_1 \cdot \mathbf{r}_2 \rangle_{\pm^2 \alpha \mp} = -\langle \pm | \mathbf{r} | \pm \rangle \cdot \langle \alpha | \mathbf{r} | \mp \rangle 2\theta_\alpha^3 \theta_{12}, \quad (4.168)$$

$$\langle \mathbf{r}_1 \cdot \mathbf{r}_2 \rangle_{\pm \mp \mp \alpha} = -\langle \pm | \mathbf{r} | \mp \rangle \cdot \langle \mp | \mathbf{r} | \alpha \rangle 2\theta_\alpha^3 \theta_{12}, \quad (4.169)$$

$$\langle \mathbf{r}_1 \cdot \mathbf{r}_2 \rangle_{\pm \mp \alpha \pm} = -\langle \pm | \mathbf{r} | \mp \rangle \cdot \langle \alpha | \mathbf{r} | \pm \rangle 2\theta_\alpha^3 \theta_{12}, \quad (4.170)$$

$$\langle \mathbf{r}_1 \cdot \mathbf{r}_2 \rangle_{\alpha \pm \alpha \mp} = \langle \alpha | \mathbf{r} | \pm \rangle \cdot \langle \alpha | \mathbf{r} | \mp \rangle 2\theta_\alpha^2 \theta_{12}^2, \quad (4.171)$$

$$\langle \mathbf{r}_1 \cdot \mathbf{r}_2 \rangle_{\pm \alpha \mp \alpha} = \langle \pm | \mathbf{r} | \alpha \rangle \cdot \langle \mp | \mathbf{r} | \alpha \rangle 2\theta_\alpha^2 \theta_{12}^2, \quad (4.172)$$

$$\langle \mathbf{r}_1 \cdot \mathbf{r}_2 \rangle_{\alpha \pm \alpha \mp} = \langle \alpha | \mathbf{r} | \pm \rangle \cdot \langle \alpha | \mathbf{r} | \mp \rangle 2\theta_\alpha^2 \theta_{12}^2, \quad (4.173)$$

$$\langle \mathbf{r}_1 \cdot \mathbf{r}_2 \rangle_{\alpha \pm \pm \alpha} = \langle \alpha | \mathbf{r} | \pm \rangle \cdot \langle \pm | \mathbf{r} | \alpha \rangle 2 (2\theta_\alpha^2 \theta_{12}^2 - \theta_\alpha^3 \theta_n), \quad (4.174)$$

$$\langle \mathbf{r}_1 \cdot \mathbf{r}_2 \rangle_{\alpha \pm \mp \alpha} = \langle \alpha | \mathbf{r} | \pm \rangle \cdot \langle \mp | \mathbf{r} | \alpha \rangle 2 (2\theta_\alpha^2 \theta_{12}^2 - \theta_\alpha^3 \theta_\pm). \quad (4.175)$$

These terms are summed together and divided by the normalization in order to obtain the matter or charge radius in the cigar configuration.

4.3 Electromagnetic transitions

Electromagnetic processes connect the various states of a nucleus. When an excited state decays to the ground state, or when a nucleus is excited into one of its higher levels, the nucleus emits or absorbs an electromagnetic wave. This process has been studied in great length and all details can be found in any text on nuclear physics, such as [10] or [52]. We will just give a brief summary of the theory here.

4.3.1 Background

We are interested in the transition probability, T_{fi} , between an initial and final state (which is the reciprocal of the lifetime for transition from an excited state to a lower state):

$$T_{fi} = \frac{8\pi}{\hbar} \frac{\lambda + 1}{\lambda [(2\lambda + 1)!!]^2} k^{2\lambda+1} |\langle f | O_{\lambda\mu} | i \rangle|^2, \quad (4.176)$$

where k is the wave vector of the emitted or absorbed gamma ray, and O_{LM} is the operator, electric or magnetic, which connects the initial and final states. We now separate O_{LM} into magnetic and electric components:

$$O_{\lambda\mu} = E_{\lambda\mu} + \mathcal{M}_{\lambda\mu}, \quad (4.177)$$

where

$$E_{\lambda\mu} = \sum_{j=1}^A e_j r_j^\lambda Y_{\lambda\mu}(\Omega), \quad (4.178)$$

and

$$\mathcal{M}_{\lambda\mu} = \mu_N \sum_{j=1}^A \left[\frac{2}{\lambda + 1} g_\ell^{(j)} \boldsymbol{\ell}_j + g_s^{(j)} \mathbf{s}_j \right] \cdot \nabla [r_j^\lambda Y_{\lambda\mu}(\Omega)], \quad (4.179)$$

where e_j is the charge of the particle, μ_N is the nuclear magneton, $\mu_N = e\hbar/2m_p c$, g_ℓ and g_s are the orbital and spin gyromagnetic ratios, respectively, $\boldsymbol{\ell}$ is the orbital angular momentum of the particle and \mathbf{s} is the spin angular momentum of the particle. The two operators have different selection rules with respect to the parity of the transition. For electric transitions, $\pi_f \pi_i = (-1)^\lambda$, and for magnetic transitions, $\pi_f \pi_i = (-1)^{\lambda-1}$. Thus, for each pair of initial and final states and given λ , only one type is allowed.

Now that we have the operators divided into electric and magnetic multipoles, we would like to separate out the phase space and kinematic factors in eq.(4.176). We

can sum over μ and the final state angular momentum projections to obtain:

$$T_{fi} = \frac{8\pi}{\hbar} \frac{\lambda + 1}{\lambda [(2\lambda + 1)!!]^2} k^{2\lambda+1} B(O\lambda\mu), \quad (4.180)$$

where

$$B(O\lambda\mu) = \sum_{\mu M_f} |\langle f; J_f M_f | O(\lambda\mu) | i; J_i M_i \rangle|^2. \quad (4.181)$$

We call $B(O\lambda\mu)$ the reduced transition probability, and it is the quantity that we will calculate here.

4.3.2 Applied to ${}^6\text{He}$

In the case of ${}^6\text{He}$, we are talking about the transition between the $J = 0$ ground state and the $J = 2$ excited state. Since the parity of both of these states is positive, the lowest multipolarity that can connect the states is an $E2$, electric quadrupole. Thus, we want to calculate the $B(E2)$ for this transition. First, we must see how a tensor operator works in our rotated system.

We begin with the tensor operator, O_{kq} , an irreducible tensor of rank k , and we want to find the matrix element:

$$\langle \psi_{L'M'}(\mathfrak{R}') | O_{kq} | \psi_{LM}(\mathfrak{R}) \rangle = \iint D_{M'0}^{L'*}(\mathfrak{R}') D_{M0}^L(\mathfrak{R}) \langle \hat{\mathfrak{R}}' \psi | O_{kq} | \hat{\mathfrak{R}} \psi \rangle d\mathfrak{R}' d\mathfrak{R}. \quad (4.182)$$

Remember that in ${}^6\text{He}$, the L -value of the projection is the same as the J -value for the state, since the only angular momentum in that system is orbital angular momentum.

We then rewrite the matrix element as:

$$\langle \hat{\mathfrak{R}}' \psi | O_{kq} | \hat{\mathfrak{R}} \psi \rangle = \langle \psi | \hat{\mathfrak{R}}'^{-1} O_{kq} \hat{\mathfrak{R}} | \psi \rangle. \quad (4.183)$$

Since O_{kq} is a tensor operator, we know that

$$\hat{\mathfrak{R}}'^{-1}O_{kq}\hat{\mathfrak{R}}' = \sum_{q''} O_{kq''}D_{q''q}^k(\mathfrak{R}'^{-1}). \quad (4.184)$$

We then insert $\hat{\mathfrak{R}}'\hat{\mathfrak{R}}'^{-1}$ into the matrix element in order to use this relation:

$$\langle \psi | \hat{\mathfrak{R}}'^{-1}O_{kq}\hat{\mathfrak{R}}' | \hat{\mathfrak{R}}'^{-1}\hat{\mathfrak{R}}'\psi \rangle = \sum_{q''} D_{qq''}^{k*}(\mathfrak{R}') \langle \psi | O_{kq''} | \hat{\mathfrak{R}}'^{-1}\hat{\mathfrak{R}}'\psi \rangle. \quad (4.185)$$

We then use the definition $\hat{\mathfrak{R}}'^{-1}\hat{\mathfrak{R}}' \equiv \hat{\mathfrak{R}}''$ and rewrite the full equation (RHS of eq.(4.182)) as

$$\langle \psi_{L'M'}(\mathfrak{R}') | O_{kq} | \psi_{LM}(\mathfrak{R}) \rangle = \iint \sum_{q''} D_{M'0}^{L'*}(\mathfrak{R}') D_{qq''}^{k*}(\mathfrak{R}') D_{M0}^L(\mathfrak{R}'\mathfrak{R}'') \langle \psi | O_{kq''} | \hat{\mathfrak{R}}''\psi \rangle d\mathfrak{R}' d\mathfrak{R}''. \quad (4.186)$$

By using the same relation as in eq.(2.40), we work on performing the first integration (over \mathfrak{R}'):

$$\begin{aligned} \int D_{M'0}^{L'*}(\mathfrak{R}') D_{qq''}^{k*}(\mathfrak{R}') D_{M0}^L(\mathfrak{R}') d\mathfrak{R}' &= \\ &= (-1)^{q''-q} \frac{8\pi^2}{2L'+1} C_{LMk-q}^{L'M'} C_{LM''k-q''}^{L'0}. \end{aligned} \quad (4.187)$$

We can now write the final general formula for the expectation value of tensor operators in our rotated coordinate system:

$$\begin{aligned} \langle \psi_{L'M'}(\mathfrak{R}') | O_{kq} | \psi_{LM}(\mathfrak{R}) \rangle &= \frac{8\pi^2}{2L'+1} \sum_{q''M''} (-1)^{q''-q} C_{LMk-q}^{L'M'} C_{LM''k-q''}^{L'0} \\ &\times \int D_{M''0}^L(\mathfrak{R}'') \langle \psi | O_{kq''} | \mathfrak{R}''\psi \rangle d\mathfrak{R}''. \end{aligned} \quad (4.188)$$

We then look at eq.(4.188) for an $E2$ transition between initial state $J = 0$ and

final state $J = 2$. For this transition, eq.(4.188) becomes

$$\begin{aligned} \langle \psi_{2M'}(\mathfrak{R}') | \sum_i e_i r_i^2 Y_{20} | \psi_{00}(\mathfrak{R}) \rangle &= \frac{8\pi^2}{5} \sum_{q'' M''} (-1)^{q''} C_{00,20}^{2M'} C_{0M'',2-q''}^{20} \\ &\times \int D_{M''0}^0(\mathfrak{R}'') \langle \psi | \sum_i e_i r_i^2 Y_{20} | \hat{\mathfrak{R}}'' \psi \rangle d\mathfrak{R}''. \end{aligned} \quad (4.189)$$

Here, we chose to only do the calculation with Y_{20} , because of the powerful Wigner-Eckart theorem [53, 54], which states:

$$\langle njm | T_{kq} | n' j' m' \rangle = C_{kq, j' m'}^{jm} \langle nj || T_k || n' j' \rangle, \quad (4.190)$$

where T_k is a tensor operator of rank k , and n stands for all other quantum numbers. Once a calculation has been made for one particular T_{kq} , all others in the multiplet can be obtained with Clebsch-Gordan coefficients. This is especially easy in our specific case since all the Clebsch-Gordan coefficients are equal to one.

Resuming, we perform the sums over q'' and M'' and obtain:

$$= \frac{8\pi^2}{5} \int D_{00}^0(\mathfrak{R}'') \delta_{0M'} \langle \psi | \sum_i e_i r_i^2 Y_{20} | \hat{\mathfrak{R}}'' \psi \rangle d\mathfrak{R}''. \quad (4.191)$$

We then integrate over the Euler angles α and γ , which leads us to the final result:

$$= \frac{32\pi^4}{5} \int \langle \psi | \sum_i e_i r_i^2 Y_{20} | \hat{\mathfrak{R}}'' \psi \rangle d(\cos \vartheta). \quad (4.192)$$

Everything is now in terms of the $er^2 Y_{20}$ matrix elements. The form of the operator is (in the lab frame):

$$er^2 Y_{20}(x, y, z) = e \sqrt{\frac{5}{16\pi}} (2z^2 - x^2 - y^2). \quad (4.193)$$

This operator requires that the distances be taken from the center-of-mass of the system. Though the sum is over charge, the neutrons contribute through the recoil of

the center-of-mass. Thus, we have the same collection of terms as was derived in the discussion of the charge radius (eq.(4.60)).

The expectation value of the operator in eq.(4.193) must be calculated for all possible transitions, that is, alpha-dineutron to alpha-dineutron, cigar to cigar, and both cross terms. We start first with the alpha-dineutron to alpha-dineutron transition.

Alpha-dineutron to alpha-dineutron

The notation for the parameters is the following: all parameters will have a subscript indicating the state in which they belong, zero for the ground state, and 2 for the excited state. Greek letters indicate the alpha-dineutron configuration, and Latin letters indicate the cigar configuration. We will also use the notation introduced in the radii section in the alpha-dineutron section for referring to particle locations (eq.(4.61)). For the coordinates themselves, z_1 and z_2 refer to the ground state, and primed coordinates refer to the excited state. The center-of-mass is also different in the excited state, but we need a common reference point in order to properly perform the calculations. Thus, we need the location of the alpha particle and dineutron, z'_1 and z'_2 , respectively, in terms of the center-of-mass of the ground state, Z , and the distance between the alpha and dineutron, d' . In order to obtain expressions for z'_1 and z'_2 , we use the definition of the center-of-mass, eq.(4.53), and the simple relation $d' = z'_2 - z'_1$. From these two equations, we obtain the relation for z'_1 and z'_2 :

$$z'_2 = \frac{d'(\nu_2 + \omega_2)[2 - (\theta'_{12})^2] - 2\nu_2(\theta'_{12})^2 + 3Z(\nu_2 + \omega_2)[1 - (\theta'_{12})^2]}{3(\nu_2 + \omega_2)[1 - (\theta'_{12})^2]}, \quad (4.194)$$

$$z'_1 = \frac{2\omega_2 z'_2 (\theta'_{12})^2 + (\nu_2 + \omega_2)[3Z(1 - (\theta'_{12})^2) - z'_2]}{(\nu_2 + \omega_2)[2 - (\theta'_{12})^2] - 2\nu_2(\theta'_{12})^2}, \quad (4.195)$$

where θ'_{12} is the overlap between the two centers in the excited state. The definition for z'_1 is recursive, but we keep it this way for the sake of brevity.

Before listing the matrix elements, we need to list the overlaps for the transitions.

The overlaps are:

$$\langle \alpha_2 | \alpha_0 \rangle = \left(\frac{2\sqrt{\nu_0\nu_2}}{\nu_0 + \nu_2} \right)^{3/2} \exp[-F(\nu_0, \nu_2, z_1, z'_1)], \quad (4.196)$$

where

$$F(a, b, z_i, z'_i) = \frac{ab[(z_i - Z)^2 + (z'_i - Z)^2 - 2x(z_i - Z)(z'_i - Z)]}{2(a + b)}. \quad (4.197)$$

Continuing:

$$\langle d_2 | d_0 \rangle = \left(\frac{2\sqrt{\omega_0\omega_2}}{\omega_0 + \omega_2} \right)^{3/2} \exp[-F(\omega_0, \omega_2, z_2, z'_2)], \quad (4.198)$$

$$\langle d_2 | \alpha_0 \rangle = \left(\frac{2\sqrt{\nu_0\omega_2}}{\nu_0 + \omega_2} \right)^{3/2} \exp[-F(\nu_0, \omega_2, z_1, z'_2)], \quad (4.199)$$

$$\langle \alpha_2 | d_0 \rangle = \left(\frac{2\sqrt{\omega_0\nu_2}}{\nu_2 + \omega_0} \right)^{3/2} \exp[-F(\omega_0, \nu_2, z_2, z'_1)]. \quad (4.200)$$

We can proceed now with the matrix elements. All terms should be multiplied by the prefactor $e\sqrt{\frac{5}{16\pi}}$, that will not be written in the following expressions. The one-body terms are:

$$\langle \alpha_2 | er^2 Y_{20} | \alpha_0 \rangle = \theta_{\alpha\alpha} f(\nu_0, \nu_2, z_1, z'_1), \quad (4.201)$$

where

$$f(a, b, z_i, z'_i) = \frac{a^2(z_i - Z)^2(3x^2 - 1) + 2b^2(z'_i - Z) + 4abx(z_i - Z)(z'_i - Z)}{(a + b)^2} \quad (4.202)$$

Resuming:

$$\langle d_2 | er^2 Y_{20} | d_0 \rangle = \theta_{dd} f(\omega_0, \omega_2, z_2, z'_2), \quad (4.203)$$

$$\langle d_2 | er^2 Y_{20} | \alpha_0 \rangle = \theta_{d\alpha} f(\nu_0, \omega_2, z_1, z'_2), \quad (4.204)$$

$$\langle \alpha_2 | er^2 Y_{20} | d_0 \rangle = \theta_{\alpha d} f(\omega_0, \nu_2, z_2, z'_1). \quad (4.205)$$

These matrix elements are put into the terms listed in eqs.(4.76)-(4.79) in order to calculate the proton and neutron one-body contributions.

The two-body form of the operator is $2\mathbf{z}_1 \cdot \mathbf{z}_2 - \mathbf{x}_1 \cdot \mathbf{x}_2 - \mathbf{y}_1 \cdot \mathbf{y}_2$. The two-body terms are:

$$\langle \alpha_2 \alpha_2 | er^2 Y_{20} | \alpha_0 \alpha_0 \rangle = \theta_{\alpha\alpha}^2 G(\nu_0, \nu_0, \nu_2, \nu_2, z_1, z_1, z'_1, z'_1), \quad (4.206)$$

where

$$\begin{aligned} G(a, b, u, v, z_i, z_k, z'_i, z'_k) = & \frac{1}{(a+u)(b+v)} \{ z_i z_k (z_i - Z)(z_k - Z)(3x^2 - 1) \\ & + 2uv(z'_i - Z)(z'_k - Z) \\ & + 2x[av(z_i - Z)(z'_k - Z) + bu(z_k - Z)(z'_i - Z)] \}. \end{aligned} \quad (4.207)$$

Resuming:

$$\langle \alpha_2 d_2 | er^2 Y_{20} | d_0 \alpha_0 \rangle = \theta_{\alpha\alpha} \theta_{dd} G(\nu_0, \omega_0, \nu_2, \omega_2, z_1, z_2, z'_1, z'_2), \quad (4.208)$$

$$\langle \alpha_2 \alpha_2 | er^2 Y_{20} | \alpha_0 d_0 \rangle = \theta_{\alpha\alpha} \theta_{\alpha d} G(\nu_0, \omega_0, \nu_2, \nu_2, z_1, z_2, z'_1, z'_1), \quad (4.209)$$

$$\langle \alpha_2 d_2 | er^2 Y_{20} | \alpha_0 \alpha_0 \rangle = \theta_{\alpha\alpha} \theta_{d\alpha} G(\nu_0, \nu_0, \nu_2, \omega_2, z_1, z_1, z'_1, z'_2), \quad (4.210)$$

$$\langle d_2 \alpha_2 | er^2 Y_{20} | d_0 d_0 \rangle = \theta_{dd} \theta_{\alpha d} G(\omega_0, \omega_0, \nu_2, \omega_2, z_2, z_2, z'_1, z'_2), \quad (4.211)$$

$$\langle d_2 d_2 | er^2 Y_{20} | d_0 \alpha_0 \rangle = \theta_{dd} \theta_{d\alpha} G(\nu_0, \omega_0, \omega_2, \omega_2, z_1, z_2, z'_2, z'_2), \quad (4.212)$$

$$\langle d_2 d_2 | er^2 Y_{20} | \alpha_0 \alpha_0 \rangle = \theta_{d\alpha}^2 G(\nu_0, \nu_0, \omega_2, \omega_2, z_1, z_1, z'_2, z'_2), \quad (4.213)$$

$$\langle \alpha_2 \alpha_2 | er^2 Y_{20} | d_0 d_0 \rangle = \theta_{\alpha d}^2 G(\omega_0, \omega_0, \nu_2, \nu_2, z_2, z_2, z'_1, z'_1), \quad (4.214)$$

$$\langle \alpha_2 d_2 | er^2 Y_{20} | \alpha_0 d_0 \rangle = \theta_{d\alpha} \theta_{\alpha d} G(\nu_0, \omega_0, \omega_2, \nu_2, z_1, z_2, z'_2, z'_1), \quad (4.215)$$

$$\langle d_2 d_2 | er^2 Y_{20} | d_0 d_0 \rangle = \theta_{dd}^2 G(\omega_0, \omega_0, \omega_2, \omega_2, z_2, z_2, z'_2, z_2). \quad (4.216)$$

These matrix elements are inserted into the proper two-body term from eqs.(4.80)-(4.97). This is then squared and divided by the square of the norms of both states, and this completes the contribution of the alpha-dineutron to alpha-dineutron part of the transition.

Cigar to cigar

In the cigar to cigar transition, the only contribution is from the recoil of the neutrons. This is because our spherical alpha particle is located at the origin, which means the proton charge contribution to the transition is zero. The only terms that contribute then are the pure neutron one-body terms (eqs.(4.150)-(4.154)) and the neutron-neutron two-body terms (eqs.(4.165)-(4.175)). The proper coefficient for each term is found in the charge radius section, in equation (4.60), except that the entire equation is not divided by the total charge of the nucleus as it is for the charge radius.

Proceeding to the actual calculation, we first need the overlaps. The overlaps are:

$$\langle \alpha_2 | \alpha_0 \rangle \equiv \theta_{00} = \left(\frac{2\sqrt{n_2 n_0}}{n_0 + n_2} \right)^{3/2}, \quad (4.217)$$

$$\langle \pm_2 | \pm_0 \rangle \equiv \theta_{nn} = \left(\frac{2\sqrt{w_2 w_0}}{w_0 + w_2} \right)^{3/2} \exp \left[-\frac{w_0 w_2 (d_0^2 + d_2^2 - 2x d_0 d_2)}{2(w_0 + w_2)} \right], \quad (4.218)$$

$$\langle \pm_2 | \mp_0 \rangle \equiv \theta_{ri} = \left(\frac{2\sqrt{w_2 w_0}}{w_0 + w_2} \right)^{3/2} \exp \left[-\frac{w_0 w_2 (d_0^2 + d_2^2 + 2x d_0 d_2)}{2(w_0 + w_2)} \right], \quad (4.219)$$

$$\langle \pm_2 | \alpha_0 \rangle \equiv \theta_{n\alpha} = \left(\frac{2\sqrt{w_2 n_0}}{n_0 + w_2} \right)^{3/2} \exp \left[-\frac{w_0 w_2 d_2^2}{2(n_0 + w_2)} \right], \quad (4.220)$$

$$\langle \alpha_2 | \pm_0 \rangle \equiv \theta_{\alpha n} = \left(\frac{2\sqrt{w_0 n_2}}{w_0 + n_2} \right)^{3/2} \exp \left[-\frac{w_0 n_2 d_0^2}{2(w_0 + n_2)} \right]. \quad (4.221)$$

To remind the reader, the oscillator parameters are written with Latin letters because we are referring to the cigar configuration here (n replaces ν , and w replaces ω).

We proceed with the matrix elements. We will only list the non-zero elements (those diagonal in the alpha particle will be zero). First, the one-body matrix elements:

$$\langle \pm_2 | er^2 Y_{20} | \pm_0 \rangle = \frac{\theta_{nn}}{(w_0 + w_2)^2} [w_0^2 d_0^2 (3x^2 - 1) + 2w_2^2 d_2^2 + 4w_0 w_2 x d_0 d_2], \quad (4.222)$$

$$\langle \pm_2 | er^2 Y_{20} | \pm_0 \rangle = \frac{\theta_{rl}}{(w_0 + w_2)^2} [w_0^2 d_0^2 (3x^2 - 1) + 2w_2^2 d_2^2 - 4w_0 w_2 x d_0 d_2], \quad (4.223)$$

$$\langle \pm_2 | er^2 Y_{20} | \alpha_0 \rangle = \theta_{n\alpha} \frac{2w_2 d_2^2}{(n_0 + w_2)^2}, \quad (4.224)$$

$$\langle \alpha_2 | er^2 Y_{20} | \pm_0 \rangle = \theta_{\alpha n} \frac{2w_0 d_0^2}{(w_0 + n_2)^2}. \quad (4.225)$$

The non-vanishing two-body matrix elements are:

$$\langle +_2 -_2 | er^2 Y_{20} | -_0 +_0 \rangle = - \frac{\theta_{nn}^2}{(w_0 + w_2)^2} [w_0^2 d_0^2 (3x^2 - 1) + 2w_2^2 d_2^2 + 4w_0 w_2 x d_0 d_2], \quad (4.226)$$

$$\langle \pm_2 \mp_2 | er^2 Y_{20} | \pm_0 \mp_0 \rangle = - \frac{\theta_{rl}^2}{(w_0 + w_2)^2} [w_0^2 d_0^2 (3x^2 - 1) + 2w_2^2 d_2^2 - 4w_0 w_2 x d_0 d_2], \quad (4.227)$$

$$\langle \pm_2 \alpha_2 | er^2 Y_{20} | \mp_0 \pm_0 \rangle = - \theta_{nn} \theta_{\alpha n} \frac{w_0^2 d_0^2 (3x^2 - 1) + 2w_0 w_2 x d_0 d_2}{(w_0 + w_2)(w_0 + n_2)}, \quad (4.228)$$

$$\langle \pm_2 \mp_2 | er^2 Y_{20} | \alpha_0 \pm_0 \rangle = - \theta_{nn} \theta_{n\alpha} \frac{2w_2^2 d_2^2 + 2w_0 w_2 x d_0 d_2}{(w_0 + w_2)(n_0 + w_2)}, \quad (4.229)$$

$$\langle \pm_2 \alpha_2 | er^2 Y_{20} | \pm_0 \mp_0 \rangle = - \theta_{rl} \theta_{\alpha n} \frac{w_0^2 d_0^2 (3x^2 - 1) - 2w_0 w_2 x d_0 d_2}{(w_0 + w_2)(w_0 + n_2)}, \quad (4.230)$$

$$\langle \pm_2 \mp_2 | er^2 Y_{20} | \alpha_0 \mp_0 \rangle = - \theta_{rl} \theta_{n\alpha} \frac{2w_2^2 d_2^2 - 2w_0 w_2 x d_0 d_2}{(w_0 + w_2)(n_0 + w_2)}, \quad (4.231)$$

$$\langle +_2 -_2 | er^2 Y_{20} | \alpha_0 \alpha_0 \rangle = -\theta_{n\alpha}^2 \frac{2w_2^2 d_2^2}{(n_0 + w_2)^2}, \quad (4.232)$$

$$\langle \alpha_2 \alpha_2 | er^2 Y_{20} | +_0 -_0 \rangle = -\theta_{\alpha n}^2 \frac{w_0^2 d_0^2 (3x^2 - 1)}{(w_0 + n_2)^2}, \quad (4.233)$$

$$\langle \alpha_2 \pm_2 | er^2 Y_{20} | \alpha_0 \pm \rangle = \theta_{n\alpha} \theta_{\alpha n} \frac{2w_0 w_2 d_0 d_2 x}{(w_0 + n_2)(n_0 + w_2)}, \quad (4.234)$$

$$\langle \alpha_2 \pm_2 | er^2 Y_{20} | \alpha_0 \mp \rangle = -\theta_{n\alpha} \theta_{\alpha n} \frac{2w_0 w_2 d_0 d_2 x}{(w_0 + n_2)(n_0 + w_2)}. \quad (4.235)$$

This finishes off the cigar to cigar contribution to the reduced transition rate. Next is the first of the cross terms, the alpha-dineutron to cigar transition.

Alpha-dineutron to cigar

The alpha-dineutron to cigar transition is the first of the two cross terms in the calculation of the $B(E2)$. We would expect its contribution to be less than the direct terms, but could perhaps still be important. The overlap structure is similar to the one- and two-body terms found in the discussion of the interference term in the previous chapter, but it is not the same. We will start with the overlaps, then the list of overlap terms, and finally the matrix elements. Before starting with the overlaps, we will clarify the notations used in this section. For the oscillator parameters, Greek letters will be the alpha-dineutron parameters (still subscripted for absolute clarity), and Latin letters will refer to the cigar configuration. For the distances, z_1 and z_2 are the locations of the alpha particle and the dineutron, respectively, in the alpha-dineutron configuration. The center-of-mass will be referred to be Z , and the distance parameter in the cigar configuration will be $\zeta' \equiv d_2 + Z$, where d_2 is the normal alpha-external neutron distance used in previous calculations. The introduction of ζ' allows us to keep everything in terms of a difference between a coordinate and the center-of-mass.

We then continue with the overlaps for this transition:

$$\langle \alpha_2 | \alpha_0 \rangle \equiv \theta_{\alpha\alpha} = \left(\frac{2\sqrt{\nu_0 n_2}}{\nu_0 + n_2} \right)^{3/2} \exp \left[-\frac{\nu_0 n_2 (z_1 - Z)^2}{2(\nu_0 + n_2)} \right], \quad (4.236)$$

$$\langle \alpha_2 | d_0 \rangle \equiv \theta_{\alpha d} = \left(\frac{2\sqrt{\omega_0 n_2}}{\omega_0 + n_2} \right)^{3/2} \exp \left[-\frac{\omega_0 n_2 (z_2 - Z)^2}{2(\omega_0 + n_2)} \right], \quad (4.237)$$

$$\langle +_2 | \alpha_0 \rangle \equiv \theta_{+\alpha} = \left(\frac{2\sqrt{\nu_0 w_2}}{\nu_0 + w_2} \right)^{3/2} \exp[-F(\nu_0, w_2, z_1, \zeta')], \quad (4.238)$$

where F was defined in eq.(4.197). Continuing:

$$\langle -_2 | \alpha_0 \rangle \equiv \theta_{-\alpha} = \left(\frac{2\sqrt{\nu_0 w_2}}{\nu_0 + w_2} \right)^{3/2} \exp[-F(\nu_0, w_2, z_1, \zeta')](x \rightarrow -x), \quad (4.239)$$

$$\langle +_2 | d_0 \rangle \equiv \theta_{+d} = \left(\frac{2\sqrt{\omega_0 w_2}}{\omega_0 + w_2} \right)^{3/2} \exp[-F(\omega_0, w_2, z_2, \zeta')], \quad (4.240)$$

$$\langle -_2 | d_0 \rangle \equiv \theta_{-d} = \left(\frac{2\sqrt{\omega_0 w_2}}{\omega_0 + w_2} \right)^{3/2} \exp[-F(\omega_0, w_2, z_2, \zeta')](x \rightarrow -x). \quad (4.241)$$

We will now list the overlap expressions. The pattern follows the charge radius calculation, and thus we have five terms as in eq.(4.60). The proton one-body term is:

$$\langle B(E2) \rangle_p = \langle \alpha_2 | er^2 Y_{20} | \alpha_0 \rangle \theta_{\alpha\alpha} [\theta_{\alpha\alpha}^2 \theta_{+d} \theta_{-d} + \theta_{\alpha d}^2 \theta_{+\alpha} \theta_{-\alpha} - \theta_{\alpha\alpha} \theta_{\alpha d} (\theta_{+\alpha} \theta_{-d} + \theta_{-\alpha} \theta_{+d})]. \quad (4.242)$$

The neutron one-body terms are:

$$\langle B(E2) \rangle_\alpha = \langle \alpha_2 | er^2 Y_{20} | \alpha_0 \rangle \theta_{\alpha\alpha}^2 [2\theta_{\alpha\alpha} \theta_{+d} \theta_{-d} - \theta_{\alpha d} (\theta_{+\alpha} \theta_{-d} + \theta_{-\alpha} \theta_{+d})], \quad (4.243)$$

$$\langle B(E2) \rangle_{+d} = \langle +_2 | er^2 Y_{20} | d_0 \rangle \theta_{\alpha\alpha}^3 (\theta_{\alpha\alpha} \theta_{-d} - \theta_{\alpha d} \theta_{-\alpha}), \quad (4.244)$$

$$\langle B(E2) \rangle_{-d} = \langle -_2 | er^2 Y_{20} | d_0 \rangle \theta_{\alpha\alpha}^3 (\theta_{\alpha\alpha} \theta_{+d} - \theta_{\alpha d} \theta_{+\alpha}), \quad (4.245)$$

$$\langle B(E2) \rangle_{\alpha d} = \langle \alpha_2 | er^2 Y_{20} | d_0 \rangle \theta_{\alpha\alpha}^2 [2\theta_{\alpha d} \theta_{+\alpha} \theta_{-\alpha} - \theta_{\alpha\alpha} (\theta_{+\alpha} \theta_{-d} + \theta_{-\alpha} \theta_{+d})], \quad (4.246)$$

$$\langle B(E2) \rangle_{+\alpha} = \langle +_2 | er^2 Y_{20} | \alpha_0 \rangle \theta_{\alpha\alpha}^2 \theta_{\alpha d} (\theta_{-\alpha} \theta_{\alpha d} - \theta_{\alpha\alpha} \theta_{-d}), \quad (4.247)$$

$$\langle B(E2) \rangle_{-\alpha} = \langle -_2 | er^2 Y_{20} | \alpha_0 \rangle \theta_{\alpha\alpha}^2 \theta_{\alpha d} (\theta_{+\alpha} \theta_{\alpha d} - \theta_{\alpha\alpha} \theta_{+d}). \quad (4.248)$$

This finishes the one-body terms. We start the two-body terms with the proton-proton term:

$$\begin{aligned} \langle B(E2)^{(2)} \rangle_p &= \langle \alpha_2 \alpha_2 | er^2 Y_{20} | \alpha_0 \alpha_0 \rangle \\ &\times [\theta_{\alpha\alpha}^2 \theta_{+d} \theta_{-d} + \theta_{\alpha d}^2 \theta_{+\alpha} \theta_{-\alpha} - \theta_{\alpha\alpha} \theta_{d\alpha} (\theta_{+\alpha} \theta_{-d} + \theta_{-\alpha} \theta_{+d})]. \end{aligned} \quad (4.249)$$

The neutron-neutron terms are:

$$\langle B(E2)^{(2)} \rangle_\alpha = \langle \alpha_2 \alpha_2 | er^2 Y_{20} | \alpha_0 \alpha_0 \rangle \theta_{\alpha\alpha}^2 \theta_{+d} \theta_{-d}, \quad (4.250)$$

$$\langle B(E2)^{(2)} \rangle_{rdd} = \langle +_2 -_2 | er^2 Y_{20} | d_0 d_0 \rangle \theta_{\alpha\alpha}^4, \quad (4.251)$$

$$\langle B(E2)^{(2)} \rangle_{\alpha\alpha d} = - \langle \alpha_2 \alpha_2 | er^2 Y_{20} | \alpha_0 d_0 \rangle \theta_{\alpha\alpha}^2 (\theta_{+\alpha} \theta_{-d} + \theta_{-\alpha} \theta_{+d}), \quad (4.252)$$

$$\langle B(E2)^{(2)} \rangle_{\alpha\alpha r\alpha} = - \langle +_2 \alpha_2 | er^2 Y_{20} | \alpha_0 \alpha_0 \rangle \theta_{\alpha\alpha}^2 \theta_{\alpha d} \theta_{-d}, \quad (4.253)$$

$$\langle B(E2)^{(2)} \rangle_{\alpha\alpha l\alpha} = - \langle -_2 \alpha_2 | er^2 Y_{20} | \alpha_0 \alpha_0 \rangle \theta_{\alpha\alpha}^2 \theta_{\alpha d} \theta_{+d}, \quad (4.254)$$

$$\langle B(E2)^{(2)} \rangle_{\alpha\alpha r d} = \langle +_2 \alpha_2 | er^2 Y_{20} | \alpha_0 d_0 \rangle \theta_{\alpha\alpha}^2 (2\theta_{\alpha\alpha} \theta_{-d} - \theta_{-\alpha} \theta_{\alpha d}), \quad (4.255)$$

$$\langle B(E2)^{(2)} \rangle_{\alpha\alpha l d} = \langle -_2 \alpha_2 | er^2 Y_{20} | \alpha_0 d_0 \rangle \theta_{\alpha\alpha}^2 (2\theta_{\alpha\alpha} \theta_{+d} - \theta_{+\alpha} \theta_{\alpha d}), \quad (4.256)$$

$$\langle B(E2)^{(2)} \rangle_{r d l\alpha} = \langle +_2 -_2 | er^2 Y_{20} | \alpha_0 d_0 \rangle \theta_{\alpha\alpha}^3 \theta_{\alpha d}, \quad (4.257)$$

$$\langle B(E2)^{(2)} \rangle_{l d r\alpha} = \langle -_2 +_2 | er^2 Y_{20} | \alpha_0 d_0 \rangle \theta_{\alpha\alpha}^3 \theta_{\alpha d}, \quad (4.258)$$

$$\langle B(E2)^{(2)} \rangle_{r d \alpha d} = \langle +_2 \alpha_2 | er^2 Y_{20} | d_0 d_0 \rangle \theta_{\alpha\alpha}^3 \theta_{-\alpha}, \quad (4.259)$$

$$\langle B(E2)^{(2)} \rangle_{l d \alpha d} = \langle -_2 \alpha_2 | er^2 Y_{20} | d_0 d_0 \rangle \theta_{\alpha\alpha}^3 \theta_{+\alpha}, \quad (4.260)$$

$$\langle B(E2)^{(2)} \rangle_{r \alpha l\alpha} = \langle +_2 -_2 | er^2 Y_{20} | \alpha_0 \alpha_0 \rangle \theta_{\alpha\alpha}^2 \theta_{\alpha d}^2, \quad (4.261)$$

$$\langle B(E2)^{(2)} \rangle_{\alpha d \alpha d} = \langle \alpha_2 \alpha_2 | er^2 Y_{20} | d_0 d_0 \rangle \theta_{\alpha\alpha}^2 \theta_{+\alpha} \theta_{-\alpha}, \quad (4.262)$$

$$\langle B(E2)^{(2)} \rangle_{r \alpha \alpha d} = \langle +_2 \alpha_2 | er^2 Y_{20} | d_0 \alpha_0 \rangle \theta_{\alpha\alpha}^2 (2\theta_{\alpha d} \theta_{-\alpha} - \theta_{\alpha\alpha} \theta_{-d}), \quad (4.263)$$

$$\langle B(E2)^{(2)} \rangle_{l \alpha \alpha d} = \langle -_2 \alpha_2 | er^2 Y_{20} | d_0 \alpha_0 \rangle \theta_{\alpha\alpha}^2 (2\theta_{\alpha d} \theta_{+\alpha} - \theta_{\alpha\alpha} \theta_{+d}). \quad (4.264)$$

In the above list, r has been substituted for “+” and l for “-” in the term labels. We

now list the final group of terms, the proton-neutron two-body terms:

$$\langle B(E2)^{(2)} \rangle_{pn} = \langle \alpha_2 \alpha_2 | er^2 Y_{20} | \alpha_0 \alpha_0 \rangle 2\theta_{\alpha\alpha} [2\theta_{\alpha\alpha} \theta_{+d} \theta_{-d} - \theta_{\alpha d} (\theta_{+\alpha} \theta_{-d} + \theta_{-\alpha} \theta_{+d})], \quad (4.265)$$

$$\langle B(E2)^{(2)} \rangle_{\alpha\alpha\alpha d} = \langle \alpha_2 \alpha_2 | er^2 Y_{20} | \alpha_0 d_0 \rangle 2\theta_{\alpha\alpha} [2\theta_{\alpha d} \theta_{+\alpha} \theta_{-\alpha} - \theta_{\alpha\alpha} (\theta_{+\alpha} \theta_{-d} + \theta_{-\alpha} \theta_{+d})], \quad (4.266)$$

$$\langle B(E2)^{(2)} \rangle_{\alpha\alpha r\alpha} = \langle \alpha_2 +_2 | er^2 Y_{20} | \alpha_0 \alpha_0 \rangle 2\theta_{\alpha\alpha} \theta_{\alpha d} (\theta_{\alpha d} \theta_{-\alpha} - \theta_{\alpha\alpha} \theta_{-d}), \quad (4.267)$$

$$\langle B(E2)^{(2)} \rangle_{\alpha\alpha l\alpha} = \langle \alpha_2 -_2 | er^2 Y_{20} | \alpha_0 \alpha_0 \rangle 2\theta_{\alpha\alpha} \theta_{\alpha d} (\theta_{\alpha d} \theta_{+\alpha} - \theta_{\alpha\alpha} \theta_{+d}), \quad (4.268)$$

$$\langle B(E2)^{(2)} \rangle_{\alpha\alpha r d} = \langle \alpha_2 +_2 | er^2 Y_{20} | d\alpha_0 \rangle 2\theta_{\alpha\alpha}^2 (\theta_{\alpha\alpha} \theta_{-d} - \theta_{\alpha d} \theta_{-\alpha}), \quad (4.269)$$

$$\langle B(E2)^{(2)} \rangle_{\alpha\alpha l d} = \langle \alpha_2 +_2 | er^2 Y_{20} | d\alpha_0 \rangle 2\theta_{\alpha\alpha}^2 (\theta_{\alpha\alpha} \theta_{-d} - \theta_{\alpha d} \theta_{-\alpha}). \quad (4.270)$$

The list of terms is now complete. We already have the definitions of the overlaps, so we now move to the matrix elements.

The one-body matrix elements are:

$$\langle \alpha_2 | er^2 Y_{20} | \alpha_0 \rangle = \theta_{\alpha\alpha} \frac{\nu_0^2 (z_1 - Z)^2 (3x^2 - 1)}{(\nu_0 + n_2)^2}, \quad (4.271)$$

$$\langle +_2 | er^2 Y_{20} | d_0 \rangle = \theta_{+d} f(\omega_0, w_2, z_2, \zeta'), \quad (4.272)$$

where the function f was defined in eq.(4.202). Resuming:

$$\langle -_2 | er^2 Y_{20} | d_0 \rangle = \theta_{-d} f(\omega_0, w_2, z_2, \zeta') (x \rightarrow -x), \quad (4.273)$$

$$\langle +_2 | er^2 Y_{20} | \alpha_0 \rangle = \theta_{+\alpha} f(\nu_0, w_2, z_1, \zeta'), \quad (4.274)$$

$$\langle -_2 | er^2 Y_{20} | \alpha_0 \rangle = \theta_{-\alpha} f(\nu_0, w_2, z_1, \zeta') (x \rightarrow -x), \quad (4.275)$$

$$\langle \alpha_2 | er^2 | d_0 \rangle = \theta_{\alpha d} \frac{\omega_0^2 (z_2 - Z)^2 (3x^2 - 1)}{(\omega_0 + n_2)^2}. \quad (4.276)$$

The two-body matrix elements are:

$$\langle \alpha_2 \alpha_2 | er^2 Y_{20} | \alpha_0 \alpha_0 \rangle = \theta_{\alpha\alpha}^2 \frac{\nu_0^2 (z_1 - Z)^2 (3x^2 - 1)}{(\nu_0 + n_2)^2}, \quad (4.277)$$

$$\langle +_2 \alpha_2 | er^2 Y_{20} | \alpha_0 \alpha_0 \rangle = \theta_{\alpha\alpha} \theta_{+\alpha} g(\nu_0, \nu_0, w_2, n_2, z_1, z_1, \zeta'), \quad (4.278)$$

where

$$g(a, b, u, v, z_1, z_1, \zeta) = \frac{a(z_i - Z) [b(z_k - Z)(3x^2 - 1) + 2ux(\zeta - Z)]}{(a + v)(b + u)}. \quad (4.279)$$

Resuming:

$$\langle -_2 \alpha_2 | er^2 Y_{20} | \alpha_0 \alpha_0 \rangle = \theta_{\alpha\alpha} \theta_{-\alpha} g(\nu_0, \nu_0, w_2, n_2, z_1, z_1, \zeta') (x \rightarrow -x), \quad (4.280)$$

$$\langle \alpha_2 \alpha_2 | er^2 Y_{20} | \alpha_0 d_0 \rangle = \theta_{\alpha\alpha} \theta_{\alpha d} \frac{\nu_0 \omega_0 (z_1 - Z)(z_2 - Z)(3x^2 - 1)}{(\nu_0 + n_2)(\omega_0 + n_2)}, \quad (4.281)$$

$$\langle \alpha_2 +_2 | er^2 Y_{20} | d_0 \alpha_0 \rangle = \theta_{\alpha\alpha} \theta_{+d} g(\nu_0, \omega_0, w_2, n_2, z_1, z_2, \zeta'), \quad (4.282)$$

$$\langle \alpha_2 -_2 | er^2 Y_{20} | d_0 \alpha_0 \rangle = \theta_{\alpha\alpha} \theta_{-d} g(\nu_0, \omega_0, w_2, n_2, z_1, z_2, \zeta') (x \rightarrow -x), \quad (4.283)$$

$$\langle \alpha_2 +_2 | er^2 Y_{20} | \alpha_0 d_0 \rangle = \theta_{\alpha d} \theta_{+\alpha} g(\omega_0, \nu_0, w_2, n_2, z_2, z_1, \zeta'), \quad (4.284)$$

$$\langle \alpha_2 -_2 | er^2 Y_{20} | \alpha_0 d_0 \rangle = \theta_{\alpha d} \theta_{-\alpha} g(\omega_0, \nu_0, w_2, n_2, z_2, z_1, \zeta') (x \rightarrow -x), \quad (4.285)$$

$$\langle \alpha_2 +_2 | er^2 Y_{20} | d_0 d_0 \rangle = \theta_{+d} \theta_{\alpha d} g(\omega_0, \omega_0, w_2, n_2, z_2, z_2, \zeta'), \quad (4.286)$$

$$\langle \alpha_2 -_2 | er^2 Y_{20} | d_0 d_0 \rangle = \theta_{-d} \theta_{\alpha d} g(\omega_0, \omega_0, w_2, n_2, z_2, z_2, \zeta') (x \rightarrow -x), \quad (4.287)$$

$$\langle \alpha_2 \alpha_2 | er^2 Y_{20} | d_0 d_0 \rangle = \theta_{\alpha d}^2 \frac{\omega_0^2 (z_2 - Z)^2 (3x^2 - 1)}{(\omega_0 + w_2)^2}, \quad (4.288)$$

$$\langle +_2 -_2 | er^2 Y_{20} | \alpha_0 \alpha_0 \rangle = \theta_{+\alpha} \theta_{-\alpha} \frac{\nu_0^2 (z_1 - Z)^2 (3x^2 - 1) - 2w_2^2 (\zeta' - Z)^2}{(\nu_0 + w_2)^2}, \quad (4.289)$$

$$\langle +_2 -_2 | er^2 Y_{20} | d_0 d_0 \rangle = \theta_{+d} \theta_{-d} \frac{\omega_0^2 (z_2 - Z)^2 (3x^2 - 1) - 2w_2^2 (\zeta' - Z)^2}{(\omega_0 + w_2)^2}, \quad (4.290)$$

$$\langle +_2 -_2 | er^2 Y_{20} | \alpha_0 d_0 \rangle = \theta_{+d} \theta_{-\alpha} G'(\nu_0, \omega_0, w_2, w_2, z_1, z_2, \zeta', \zeta'), \quad (4.291)$$

$$\langle -_2 +_2 | er^2 Y_{20} | \alpha_0 d_0 \rangle = \theta_{-d} \theta_{+\alpha} G'(\nu_0, \omega_0, w_2, w_2, z_1, z_2, \zeta', \zeta') (x \rightarrow -x), \quad (4.292)$$

where the G' function is very similar to the function defined in eq.(4.207), but with

a few sign changes:

$$\begin{aligned}
G'(a, b, u, v, z_i, z_k, z'_i, z'_k) &= \frac{1}{(a+u)(b+v)} \left\{ z_i z_k (z_i - Z)(z_k - Z)(3x^2 - 1) \right. \\
&\quad - 2uv(z'_i - Z)(z'_k - Z) \\
&\quad \left. + 2x[av(z_i - Z)(z'_k - Z) - bu(z_k - Z)(z'_i - Z)] \right\}. \quad (4.293)
\end{aligned}$$

With these matrix elements, the alpha-dineutron to cigar part of the transition is complete.

Cigar to alpha-dineutron

The final section of the $B(E2)$ calculation is the other cross term, which takes the cigar configuration to the alpha-dineutron. Most of the terms and matrix elements in this section are analogues to one from the previous section, with a transformation between them. We will exploit this whenever possible. The first transformation is among the oscillator parameters. The cigar parameters are now subscripted with 0 instead of 2, and the reverse for the alpha-dineutron. The primed coordinates are now z_1 and z_2 , while ζ becomes unprimed. This is the case with the overlaps, which remain the same, save the above mentioned changes, and the positions become transposed, but not the state. We illustrate below with one overlap:

$$\begin{aligned}
\theta_{+d} \rightarrow \langle d|+\rangle \equiv \theta_{d+} &= \left(\frac{2\sqrt{\omega_2 w_0}}{\omega_2 + w_0} \right)^{3/2} \\
&\quad \times \exp \left[-\frac{\omega_2 w_0 [(z'_2 - Z)^2 + (\zeta - Z)^2 + 2x(z'_2 - Z)(\zeta - Z)]}{2(\omega_2 + w_0)} \right]. \quad (4.294)
\end{aligned}$$

When one compares the above equation with eq.(4.240), one can see the transformation rules clearly. The overlap terms also look the same when one properly switches the names of the overlaps and matrix elements. The matrix elements themselves, however, are not quite as straight forward. The angular terms change because now it is the cigar term that is rotated. The effect is that any term in a matrix element that

was multiplied with $3x^2 - 1$ is now multiplied with 2, and the $3x^2 - 1$ is now multiplying the term that had just a 2 in front of it before (and no angular dependence). Terms linear in x remain unchanged. This transformation is demonstrated below:

$$\begin{aligned} \langle +_2 | er^2 Y_{20} | d_0 \rangle \rightarrow \langle d_2 | er^2 Y_{20} | +_0 \rangle = \frac{\theta_{d+}}{(\omega_2 + w_0)^2} [2\omega_2(z'_2 - Z)^2 + w_0^2(\zeta - Z)^2 \\ + 4\omega_2 w_0(z'_2 - Z)(\zeta - Z)]. \end{aligned} \quad (4.295)$$

Compare with eq.(4.272) to see how the angle changes. The two-body matrix elements transform in the same way. With these transformation rules, we can somewhat quickly obtain everything needed to calculate the final piece of the reduced transition rate.

The final $B(E2)$ is a weighted sum of all the contributions. First, the result of each individual piece is obtained by adding together all the different parts together (i.e., proton one-body, neutron one-body, etc), squaring the result, and dividing by the norms of the initial and final states. That is, the expression looks like:

$$B(E2)_{0 \rightarrow 2} = \beta \frac{|\langle er^2 Y_{20} \rangle|^2}{N_f^2 N_i^2}, \quad (4.296)$$

where β is a numerical factor taken from eq.(4.192),(4.193), and the normalization factors of the initial and final states (eq.(2.41)). Beta is $e^2/4\pi$ for this transition. The weighted sum for the final expectation value is:

$$B(E2; 0 \rightarrow 2)_{total} = c_1 \chi_1 B(E2)_{11} + c_2 \chi_2 B(E2)_{22} + c_1 \chi_2 B(E2)_{12} + c_2 \chi_1 B(E2)_{21}, \quad (4.297)$$

where the c 's are the weighting coefficients of the given configurations in the ground state, which will be obtained in the next section. The χ 's are the weights in the excited state which are determined in the same way, and the various $B(E2)$'s have been calculated in this section.

This concludes the discussion of electromagnetic transitions and the application to the transition to the first excited state in ${}^6\text{He}$. We then proceed with the discussion of the interference term in the Gaussian approximation.

4.4 Interference term

The interference term comes from the overlap of the two separate configurations, which arises because they are not orthogonal. We need to calculate the expectation value of the Hamiltonian in order to minimize the energy of the overall ${}^6\text{He}$ system as outlined in section 3.1.3.

Figure 3.3 shows the picture of the interference term, with the two configurations on the same coordinate frame. We will now go through the matrix elements calculated with the Gaussian approximation. The single-particle wave functions are nearly unchanged. The only change that was made was to the cigar configuration, where $d \rightarrow d/2$, in order for the distances to properly correspond. There is a change in notation, in order to keep the configurations straight. All the parameters of the alpha-dineutron configuration will be written in Greek letters— ν, ω, δ , where δ is the distance parameter. For the cigar configuration, we will use Latin letters— n, w, d , where n is the alpha particle oscillator parameter, w is the oscillator parameter for the external neutrons, and d is the previously mentioned distance parameter. We list

the overlaps:

$$\theta_{\alpha\alpha} \equiv \langle \alpha | \alpha' \rangle = \left(\frac{2\sqrt{\nu n}}{\nu + n} \right)^{3/2} \exp \left[-\frac{\nu n \delta^2}{18(\nu + n)} \right], \quad (4.298)$$

$$\theta_{\alpha+} \equiv \langle \alpha | + \rangle = \left(\frac{2\sqrt{\nu w}}{\nu + w} \right)^{3/2} \exp \left[-\frac{\nu w (9d^2 + 4\delta^2 + 12d\delta x)}{72(\nu + w)} \right], \quad (4.299)$$

$$\theta_{\alpha-} \equiv \langle \alpha | - \rangle = \left(\frac{2\sqrt{\nu w}}{\nu + w} \right)^{3/2} \exp \left[-\frac{\nu w (9d^2 + 4\delta^2 - 12d\delta x)}{72(\nu + w)} \right], \quad (4.300)$$

$$\theta_{d\alpha} \equiv \langle d | \alpha' \rangle = \left(\frac{2\sqrt{\omega n}}{\omega + n} \right)^{3/2} \exp \left[-\frac{2\omega n \delta^2}{9(\omega + n)} \right], \quad (4.301)$$

$$\theta_{d+} \equiv \langle d | + \rangle = \left(\frac{2\sqrt{\omega w}}{\omega + w} \right)^{3/2} \exp \left[-\frac{\omega w (9d^2 + 16\delta^2 - 24d\delta x)}{72(\omega + w)} \right], \quad (4.302)$$

$$\theta_{d-} \equiv \langle d | - \rangle = \left(\frac{2\sqrt{\omega w}}{\omega + w} \right)^{3/2} \exp \left[-\frac{\omega w (9d^2 + 16\delta^2 + 24d\delta x)}{72(\omega + w)} \right]. \quad (4.303)$$

Since the wave functions are real, the transpose of the overlaps and all matrix elements is the same, thus we will only write these matrix elements with the alpha-dineutron wave function in the bra and the cigar wave function in the ket. The first quantity we calculated was the overlap of the two configurations:

$$\frac{\sqrt{2} \langle \psi_1 | \psi_2 \rangle}{\sqrt{\langle \psi_1 | \psi_1 \rangle \langle \psi_2 | \psi_2 \rangle}} = \frac{\theta_{\alpha\alpha}^2 [\theta_{\alpha\alpha}^2 \theta_{d+} \theta_{d-} + \theta_{d\alpha}^2 \theta_{\alpha+} \theta_{\alpha-} - \theta_{\alpha\alpha} \theta_{d\alpha} (\theta_{d+} \theta_{\alpha-} + \theta_{d-} \theta_{\alpha+})]}{\sqrt{\langle \psi_1 | \psi_1 \rangle \langle \psi_2 | \psi_2 \rangle}}. \quad (4.304)$$

This quantity as a function of the distance parameters (left equal to each other) is shown in Figure 4.24. For this plot, all four oscillator parameters are equal, so we would expect the overlap to be one at $d, \delta = 0$. We see in the plot that is in fact minus one. This is because the sign between off-diagonal matrix elements is random. So we then add by hand an extra minus sign to make the overlap positive, which defines the overall sign for the matrix elements (i.e., makes the expectation value of the Hamiltonian negative). When the distance is large, the overlap goes to zero, because at large distances, the two configurations are orthogonal.

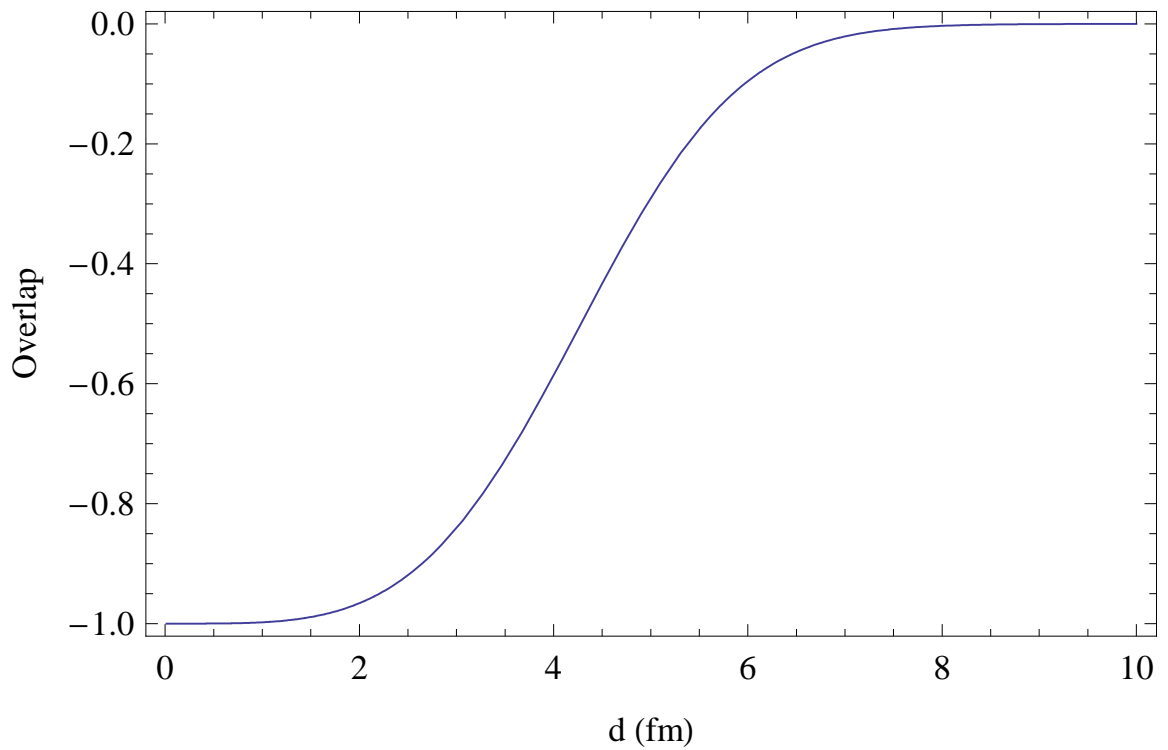


Figure 4.24: Plotted here is the overlap of the two configurations. They were plotted under the conditions where they should be identical at the origin, so all four oscillator parameters and both distance parameters are equal to each other.

4.4.1 Kinetic energy

We need to find the matrix element of the Hamiltonian between the two configurations. The first step is the kinetic energy. As before, this will have a one-body and two-body component. The one-body matrix elements are:

$$\langle \alpha|T|\alpha' \rangle = \theta_{\alpha\alpha} \frac{\nu n}{2(\nu+n)} \left(3 - \frac{\nu n \delta^2}{2(\nu+n)} \right), \quad (4.305)$$

$$\langle \alpha|T|+ \rangle = \theta_{\alpha+} \frac{\nu w}{2(\nu+w)} \left(3 - \frac{\nu w (9d^2 + 4\delta^2 + 12d\delta x)}{36(\nu+w)} \right), \quad (4.306)$$

$$\langle \alpha|T|- \rangle = \theta_{\alpha-} \frac{\nu w}{2(\nu+w)} \left(3 - \frac{\nu w (9d^2 + 4\delta^2 - 12d\delta x)}{36(\nu+w)} \right), \quad (4.307)$$

$$\langle d|T|+ \rangle = \theta_{d+} \frac{\omega w}{2(\omega+w)} \left(3 - \frac{\omega w (9d^2 + 16\delta^2 - 24d\delta x)}{36(\omega+w)} \right), \quad (4.308)$$

$$\langle d|T|- \rangle = \theta_{d+} \frac{\omega w}{2(\omega+w)} \left(3 - \frac{\omega w (9d^2 + 16\delta^2 + 24d\delta x)}{36(\omega+w)} \right), \quad (4.309)$$

$$\langle d|T|\alpha' \rangle = \theta_{d\alpha} \frac{\omega n}{2(\omega+n)} \left(3 - \frac{4\omega n \delta^2}{9(\omega+n)} \right). \quad (4.310)$$

Once again, the factor that gives the dimensions of energy, $\hbar^2/2m$, has been suppressed. These matrix elements are inserted into eqs.(3.56)-(3.61) and divided by the normalization.

For the center-of-mass correction, we need the expectation values of the momentum operator. They are:

$$\langle \alpha|\mathbf{p}|\alpha' \rangle = \theta_{\alpha\alpha} \frac{\nu n \delta}{3\iota(\nu+n)} \hat{\mathbf{z}}, \quad (4.311)$$

$$\langle \alpha|\mathbf{p}|+ \rangle = \theta_{\alpha+} \frac{\nu w}{2\iota(\nu+w)} \left[d \sin \vartheta \hat{\mathbf{x}} + \frac{2\delta + 3d \cos \vartheta}{3} \hat{\mathbf{z}} \right], \quad (4.312)$$

$$\langle \alpha|\mathbf{p}|- \rangle = \theta_{\alpha-} \frac{\nu w}{2\iota(\nu+w)} \left[d \sin \vartheta \hat{\mathbf{x}} + \frac{3d \cos \vartheta - 2\delta}{3} \hat{\mathbf{z}} \right], \quad (4.313)$$

$$\langle d|\mathbf{p}|+ \rangle = \theta_{d+} \frac{\omega w}{2\iota(\omega+w)} \left[d \sin \vartheta \hat{\mathbf{x}} + \frac{3d \cos \vartheta - 4\delta}{3} \hat{\mathbf{z}} \right], \quad (4.314)$$

$$\langle d|\mathbf{p}|- \rangle = \theta_{d+} \frac{\omega w}{2\iota(\omega+w)} \left[d \sin \vartheta \hat{\mathbf{x}} + \frac{3d \cos \vartheta + 4\delta}{3} \hat{\mathbf{z}} \right], \quad (4.315)$$

$$\langle d|\mathbf{p}|\alpha' \rangle = -\theta_{d\alpha} \frac{2\omega n \delta}{3\iota(\omega+n)} \hat{\mathbf{z}}. \quad (4.316)$$

In these matrix elements, the dimensional factor \hbar has been suppressed. All possible scalar products are taken between these matrix elements, and they are inserted into eqs.(3.62)-(3.76). The proper weighting of each term is discussed in section 4.1.2.

4.4.2 Interaction

We now move on to the two-body interaction. As mentioned for the two configurations, we used interactions of the Gaussian type. We will list the matrix elements using the Volkov parameters V_a and α , which are defined in eq.(4.24). These matrix elements are mostly rather lengthy, and we will try to use intermediate notations in order to make things clearer. We will also make use of the $x \rightarrow -x$ property of many of the matrix elements that was used before in the cigar configuration. The matrix elements are:

$$\langle \alpha\alpha|V|\alpha'\alpha'\rangle = V_a \left(\frac{4\nu n\alpha^2}{(\nu+n)\Delta(\nu,n)} \right)^{3/2} \exp \left[-\frac{\nu n\delta^2}{9(\nu+n)} \right], \quad (4.317)$$

$$\langle \alpha\alpha|V\alpha'+\rangle = V_a \left(\frac{4\nu\alpha^2\sqrt{nw}}{D'(\nu,n,\nu,w)} \right)^{3/2} \exp \left[-\frac{N}{72D'(\nu,n,\nu,w)} \right], \quad (4.318)$$

$$\langle \alpha\alpha|V\alpha'-\rangle = \langle \alpha\alpha|V\alpha'+\rangle(x \rightarrow -x), \quad (4.319)$$

where $\Delta(p,q)$ is defined in eq.(4.35), and

$$D'(a,b,c,d) = \alpha^2(a+b)(c+d) + 2(a+b+c+d), \quad (4.320)$$

and

$$N = 4\nu\delta^2[\nu\alpha^2(n+w) + 2nw\alpha^2 + 4n + 4w] + 9wd^2[\nu\alpha^2(\nu+n) + 4\nu + 2n] \quad (4.321)$$

$$+ 12\nu w\delta dx\Delta(\nu,n).$$

Resuming:

$$\begin{aligned} \langle d\alpha|V|\alpha'\alpha'\rangle &= \left(\frac{4n\alpha^2\sqrt{\nu\omega}}{D'(\nu, n, n, \omega)} \right)^{3/2} & (4.322) \\ &\times \exp \left[-\frac{\delta^2 (n\alpha^2 (\nu n + 4\omega n + 5\nu\omega) + 4\nu n + 16\omega n + 18\nu\omega)}{18D'(\nu, n, n, \omega)} \right], \end{aligned}$$

$$\langle d\alpha|V|\alpha+\rangle = V_a \left(\frac{4\alpha^2\sqrt{\nu\omega n w}}{D'(\nu, n, \omega, w)} \right)^{3/2} \exp \left[-\frac{\mathcal{N}}{72D'(\nu, n, \omega, w)} \right] \quad (4.323)$$

$$\langle d\alpha|V|\alpha-\rangle = \langle d\alpha|V|\alpha+\rangle(x \rightarrow -x), \quad (4.324)$$

where

$$\begin{aligned} \mathcal{N} &= 4\delta^2 (\alpha^2 (\nu n(\omega + w) + 4\omega w(\nu + n)) + 2(\nu + 4\omega)(n + w) + 18\nu\omega) & (4.325) \\ &+ 9wd^2[\omega\alpha^2(\nu + n) + 2(\nu + \omega + n)] + 24wd\delta x (\omega\alpha^2(\nu + n) - \nu + 2\omega). \end{aligned}$$

Resuming:

$$\langle dd|V|+-\rangle = V_a \left(\frac{4\omega w\alpha^2}{(\omega + w)\Delta(\omega, w)} \right)^{3/2} \quad (4.326)$$

$$\times \exp \left[-\frac{16\omega\delta^2\Delta(\omega, w) + 9wd^2(\omega\alpha^2(\omega + w) + 4\omega + 4w)}{36(\omega + w)\Delta(\omega, w)} \right], \quad (4.327)$$

$$\langle dd|V|\alpha'+\rangle = V_a \left(\frac{4\omega\alpha^2\sqrt{n w}}{D'(\omega, n, \omega, w)} \right)^{3/2} \exp \left[-\frac{N'}{72D'(\omega, n, \omega, w)} \right], \quad (4.328)$$

$$\langle dd|V|\alpha'-\rangle = \langle dd|V|\alpha'+\rangle(x \rightarrow -x), \quad (4.329)$$

where

$$N' = 16\omega\delta^2[\omega\alpha^2(n + w) + 2nw\alpha^2 + 4n + 4w] \quad (4.330)$$

$$+ 9wd^2[\omega\alpha^2(n + w) + 2n + 4w] - 24w\omega\delta dx\Delta(n, \omega).$$

Resuming:

$$\langle d\alpha|V|+-\rangle = V_a \left(\frac{4w\alpha^2\sqrt{\nu\omega}}{D'(\nu, w, \omega, w)} \right)^{3/2} \exp \left[-\frac{\mathbf{N}}{72D'(\nu, w, \omega, w)} \right], \quad (4.331)$$

$$\langle d\alpha|V|-+\rangle = \langle d\alpha|V|+-\rangle(x \rightarrow -x), \quad (4.332)$$

where

$$\begin{aligned} \mathbf{N} = & 4\delta^2[w\alpha^2(\nu w + \omega w + \nu\omega) + 4\nu w + 16\omega w + 18\nu\omega] \quad (4.333) \\ & + 9wd^2[\alpha^2(\nu w + \omega w + \nu\omega) + 4\omega + 8w] + 12w\alpha^2 d\delta x(\nu w + 2\omega w + 3\nu\omega). \end{aligned}$$

Resuming:

$$\langle \alpha d|V|\alpha'+\rangle = V_a \left(\frac{4\alpha^2\sqrt{\nu\omega n w}}{D'(\nu, w, n, \omega)} \right)^{3/2} \exp \left[-\frac{\mathcal{N}'}{72D'(\nu, w, n, \omega)} \right], \quad (4.334)$$

$$\langle \alpha d|V|\alpha'-\rangle = \langle \alpha d|V|\alpha'+\rangle(x \rightarrow -x), \quad (4.335)$$

where

$$\begin{aligned} \mathcal{N}' = & 4\delta^2[\nu w\alpha^2(n + \omega) + 4\omega n\alpha^2(\nu + w) + 2(\nu + 4\omega)(n + w)] \quad (4.336) \\ & + 9wd^2[\nu\alpha^2(n + \omega) + 2(\nu + \omega + n)] + 12w\delta dx[\nu\alpha^2(n + \omega) + 2\nu - 4\omega]. \end{aligned}$$

Resuming:

$$\begin{aligned} \langle \alpha\alpha|V|+-\rangle = & V_a \left(\frac{4\nu w\alpha^2}{(\nu + w)\Delta(\nu, w)} \right)^{3/2} \quad (4.337) \\ & \times \exp \left[-\frac{4\nu w\delta^2\Delta(\nu, w) + 9wd^2(\nu\alpha^2 + 4)(\nu + w)}{36(\nu + w)\Delta(\nu, w)} \right], \end{aligned}$$

$$\langle dd|V|\alpha'\alpha'\rangle = V_a \left(\frac{4\omega n\alpha^2}{(\omega + n)\Delta(\omega, n)} \right)^{3/2} \exp \left[-\frac{4\omega n\delta^2}{9(\omega + n)} \right]. \quad (4.338)$$

These matrix elements are then inserted into eqs.(3.62)-(3.76) and divided by the normalization to obtain the potential energy in the interference term.

All the operators in the Hamiltonian have now been accounted for and we can then follow the minimization procedure discussed in eq.(3.46) and following. This will determine the minimum energy as well as the weights of each configuration, which will be necessary in calculating observables (see eq.(3.78)).

4.4.3 Mean square radius

In order to calculate mean radii, we need to also take into account the interference term, as was just mentioned. In the individual configurations, we needed to re-write the alpha-dineutron configuration to pay special attention to the center-of-mass, whereas we could leave the cigar configuration as it was first written. For the interference term, we will have to re-label particle locations. The alpha particle in the alpha-dineutron term (configuration one) is located at (in the body-fixed frame) z_1 , and the dineutron (or deuteron, anticipating the problem for lithium) is placed at z_2 . The alpha particle in the cigar configuration (configuration two), is placed at Z , which is the center-of-mass of the system. The coordinate ζ is assigned the value $Z + d$, and one of the cigar particles is placed there. The other particle is placed at $2Z - \zeta$. In practice, we always work with differences ($\pm(\zeta - Z)$), so it is only the physical distance d that is important.

With these labels, the overlaps are (very similar to the ones used for the electro-

magnetic transitions):

$$\theta_{\alpha\alpha} = \left(\frac{2\sqrt{\nu n}}{\nu + n} \right)^{3/2} \exp \left(-\frac{\nu n (z_1 - Z)^2}{2(\nu + n)} \right), \quad (4.339)$$

$$\theta_{\alpha+} = \left(\frac{2\sqrt{\nu w}}{\nu + w} \right)^{3/2} \exp[-F(\nu, w, z_1, \zeta)], \quad (4.340)$$

$$\theta_{\alpha-} = \left(\frac{2\sqrt{\nu w}}{\nu + w} \right)^{3/2} \exp[-F(\nu, w, z_1, \zeta)](x \rightarrow -x), \quad (4.341)$$

$$\theta_{d+} = \left(\frac{2\sqrt{\omega w}}{\omega + w} \right)^{3/2} \exp[-F(\omega, w, z_2, \zeta)], \quad (4.342)$$

$$\theta_{d-} = \left(\frac{2\sqrt{\omega w}}{\omega + w} \right)^{3/2} \exp[-F(\omega, w, z_2, \zeta)](x \rightarrow -x), \quad (4.343)$$

$$\theta_{d\alpha} = \left(\frac{2\sqrt{\omega n}}{\omega + n} \right)^{3/2} \exp \left(-\frac{\omega n (z_2 - Z)^2}{2(\omega + n)} \right), \quad (4.344)$$

where the F function was defined in eq.(4.197).

With these overlaps, we can continue with the one-body matrix elements:

$$\langle \alpha | r^2 | \alpha' \rangle = \theta_{\alpha\alpha} \left(\frac{3}{\nu + n} + \frac{\nu (z_1 - Z)^2}{(\nu + n)^2} \right), \quad (4.345)$$

$$\langle \alpha | r^2 | + \rangle = \theta_{\alpha+} R(\nu, w, z_1, \zeta), \quad (4.346)$$

$$\langle \alpha | r^2 | - \rangle = \theta_{\alpha-} R(\nu, w, z_1, \zeta)(x \rightarrow -x), \quad (4.347)$$

$$\langle d | r^2 | + \rangle = \theta_{d+} R(\omega, w, z_2, \zeta), \quad (4.348)$$

$$\langle d | r^2 | - \rangle = \theta_{d-} R(\omega, w, z_2, \zeta)(x \rightarrow -x), \quad (4.349)$$

$$\langle d | r^2 | \alpha' \rangle = \theta_{d\alpha} \left(\frac{3}{\omega + n} + \frac{\omega^2 (z_2 - Z)^2}{(\omega + n)^2} \right), \quad (4.350)$$

where

$$R(a, b, z_i, z'_i) = \frac{3}{a + b} + \frac{a^2(z_i - Z)^2 + b^2(z'_i - Z)^2 + 2abx(z_i - Z)(z'_i - Z)}{(a + b)^2}. \quad (4.351)$$

These one-body matrix elements are inserted into the following terms, the first being

the proton-proton term:

$$\langle r^2 \rangle_p = \langle \alpha | r^2 | \alpha' \rangle 2\theta_{\alpha\alpha} \left[\theta_{\alpha\alpha}^2 \theta_{d+} \theta_{d-} + \theta_{d\alpha}^2 \theta_{\alpha+} \theta_{\alpha-} - \theta_{\alpha\alpha} \theta_{d\alpha} (\theta_{\alpha+} \theta_{d-} + \theta_{\alpha-} \theta_{d+}) \right]. \quad (4.352)$$

The neutron one-body terms are:

$$\langle r^2 \rangle_{\alpha} = \langle \alpha | r^2 | \alpha' \rangle \theta_{\alpha\alpha}^2 [2\theta_{\alpha\alpha} \theta_{d+} \theta_{d-} - \theta_{d\alpha} (\theta_{\alpha+} \theta_{d-} + \theta_{\alpha-} \theta_{d+})], \quad (4.353)$$

$$\langle r^2 \rangle_{\alpha+} = \langle \alpha | r^2 | + \rangle \theta_{\alpha}^2 \theta_{d\alpha} (\theta_{\alpha-} \theta_{d\alpha} - \theta_{\alpha\alpha} \theta_{d-}), \quad (4.354)$$

$$\langle r^2 \rangle_{\alpha-} = \langle \alpha | r^2 | - \rangle \theta_{\alpha}^2 \theta_{d\alpha} (\theta_{\alpha+} \theta_{d\alpha} - \theta_{\alpha\alpha} \theta_{d+}), \quad (4.355)$$

$$\langle r^2 \rangle_{d+} = \langle d | r^2 | + \rangle \theta_{\alpha\alpha}^3 (\theta_{\alpha\alpha'} \theta_{d-} - \theta_{\alpha-} \theta_{d\alpha}), \quad (4.356)$$

$$\langle r^2 \rangle_{d-} = \langle d | r^2 | - \rangle \theta_{\alpha\alpha}^3 (\theta_{\alpha\alpha'} \theta_{d+} - \theta_{\alpha+} \theta_{d\alpha}), \quad (4.357)$$

$$\langle r^2 \rangle_{d\alpha} = \langle d | r^2 | \alpha' \rangle \theta_{\alpha\alpha}^2 [2\theta_{\alpha+} \theta_{\alpha-} \theta_{d\alpha}^2 - \theta_{\alpha} (\theta_{\alpha+} \theta_{d-} + \theta_{\alpha-} \theta_{d+})]. \quad (4.358)$$

These are the terms added together with the proper weighting coefficients in eq.(4.60) in order to obtain the one-body contribution to the charge radius calculation. For the matter radius, eq.(4.55) is used along with the general one-body operator expression for the interference term (eqs.(3.56)-(3.61)).

Turning to the two-body section of the aforementioned equations, we begin with the two-body matrix elements:

$$\langle \alpha\alpha | r^2 | \alpha'\alpha \rangle = \theta_{\alpha\alpha}^2 \left(\frac{\nu(z_1 - Z)}{\nu + n} \right)^2, \quad (4.359)$$

$$\langle \alpha\alpha | r^2 | \alpha' + \rangle = \theta_{\alpha\alpha} \theta_{\alpha+} R'(\nu, \nu, w, n, z_1, z_1, \zeta, x), \quad (4.360)$$

$$(4.361)$$

where

$$R'(a, b, u, v, z_i, z_k, z', x) = \frac{ab(z_i - Z)(z_k - Z) + avx(z_i - Z)(z' - Z)}{(a + v)(b + u)}. \quad (4.362)$$

Resuming:

$$\langle \alpha\alpha|r^2|\alpha'-\rangle = \theta_{\alpha\alpha}\theta_{\alpha-}R'(\nu, \nu, w, n, z_1, z_1, \zeta, -x), \quad (4.363)$$

$$\langle \alpha d|r^2|\alpha'\alpha'\rangle = \theta_{\alpha\alpha}\theta_{d\alpha} \frac{\nu\omega(z_1 - Z)(z_2 - Z)}{(\nu + n)(\omega + n)}, \quad (4.364)$$

$$\langle \alpha d|r^2|+\alpha'\rangle = \theta_{\alpha\alpha}\theta_{d+}R'(\nu, \omega, w, n, z_1, z_2, \zeta, x), \quad (4.365)$$

$$\langle \alpha d|r^2|-\alpha'\rangle = \theta_{\alpha\alpha}\theta_{d-}, R'(\nu, \omega, w, n, z_1, z_2, \zeta, -x) \quad (4.366)$$

$$\langle dd|r^2|\alpha'+\rangle = \theta_{d+}\theta_{d\alpha}R'(\omega, \omega, w, n, z_2, z_2, \zeta, x), \quad (4.367)$$

$$\langle dd|r^2|\alpha'-\rangle = \theta_{d-}\theta_{d\alpha}R'(\omega, \omega, w, n, z_2, z_2, \zeta, -x), \quad (4.368)$$

$$\begin{aligned} \langle \alpha d|r^2|+-\rangle &= \frac{\theta_{\alpha-}\theta_{d+}}{(\omega + w)(\nu + w)} \{ \nu\omega(z_2 - Z)(z_1 - Z) - w^2(\zeta - Z)^2 \\ &\quad + wx(\zeta - Z)[\nu(z_1 - Z) - \omega(z_2 - Z)] \}, \end{aligned} \quad (4.369)$$

$$\begin{aligned} \langle \alpha d|r^2|-+\rangle &= \frac{\theta_{\alpha+}\theta_{d-}}{(\omega + w)(\nu + w)} \{ \nu\omega(z_2 - Z)(z_1 - Z) - w^2(\zeta - Z)^2 \\ &\quad - wx(\zeta - Z)[\nu(z_1 - Z) - \omega(z_2 - Z)] \}, \end{aligned} \quad (4.370)$$

$$\langle dd|r^2|+-\rangle = \theta_{d+}\theta_{d-} \frac{\omega^2(z_2 - Z) - w^2(\zeta - Z)^2}{(\omega + w)^2}, \quad (4.371)$$

$$\langle \alpha d|r^2|\alpha'+\rangle = \theta_{d\alpha}\theta_{\alpha+}R'(\omega, \nu, w, n, z_2, z_1, \zeta, x), \quad (4.372)$$

$$\langle \alpha d|r^2|\alpha'-\rangle = \theta_{d\alpha}\theta_{\alpha-}R'(\omega, \nu, w, n, z_2, z_1, \zeta, -x), \quad (4.373)$$

$$\langle dd|r^2|\alpha'\alpha'\rangle = \theta_{d\alpha}^2 \left(\frac{\omega(z_2 - Z)}{(\omega + n)} \right)^2, \quad (4.374)$$

$$\langle \alpha\alpha|r^2|+-\rangle = \theta_{\alpha+}\theta_{\alpha-} \frac{\nu^2(z_1 - Z)^2 - w^2(\zeta - Z)^2}{(\nu + w)^2}. \quad (4.375)$$

For the matter radius, all we need are these matrix elements, then they can be inserted into the general form for two-body operators in the interference term (eqs.(3.62)-(3.76)), with the coefficients in eq.(4.55). For the charge radius, we need to separate the terms into proton-proton, neutron-neutron, and proton-neutron. The proton-proton term is:

$$\langle r^2 \rangle_p = \langle \alpha\alpha|r^2|\alpha'\alpha'\rangle [\theta_{\alpha\alpha}^2\theta_{d+}\theta_{d-} + \theta_{d\alpha}^2\theta_{\alpha+}\theta_{\alpha-} - \theta_{\alpha\alpha}\theta_{d\alpha}(\theta_{\alpha+}\theta_{d-} + \theta_{\alpha-}\theta_{d+})]. \quad (4.376)$$

The neutron-neutron terms are:

$$\langle r^2 \rangle_\alpha = \langle \alpha\alpha | r^2 | \alpha'\alpha' \rangle \theta_{\alpha\alpha}^2 \theta_{d+} \theta_{d-}, \quad (4.377)$$

$$\langle r^2 \rangle_{\alpha\alpha d+} = \langle d\alpha | r^2 | + \alpha' \rangle \theta_{\alpha\alpha}^2 [2\theta_{\alpha\alpha} \theta_{d-} - \theta_{\alpha-} \theta_{d\alpha}], \quad (4.378)$$

$$\langle r^2 \rangle_{\alpha\alpha d-} = \langle d\alpha | r^2 | - \alpha' \rangle \theta_{\alpha\alpha}^2 [2\theta_{\alpha\alpha} \theta_{d+} - \theta_{\alpha+} \theta_{d\alpha}], \quad (4.379)$$

$$\langle r^2 \rangle_{\alpha\alpha\alpha+} = \langle \alpha\alpha | r^2 | \alpha'+ \rangle \theta_{\alpha\alpha}^2 \theta_{d\alpha} \theta_{d-}, \quad (4.380)$$

$$\langle r^2 \rangle_{\alpha\alpha\alpha-} = \langle \alpha\alpha | r^2 | \alpha'- \rangle \theta_{\alpha\alpha}^2 \theta_{d\alpha} \theta_{d+}, \quad (4.381)$$

$$\langle r^2 \rangle_{d\alpha\alpha\alpha} = -\langle d\alpha | r^2 | \alpha'\alpha' \rangle \theta_{\alpha\alpha}^2 (\theta_{\alpha+} \theta_{d-} + \theta_{\alpha-} \theta_{d+}), \quad (4.382)$$

$$\langle r^2 \rangle_{\alpha+d-} = -\langle d\alpha | r^2 | + - \rangle \theta_{\alpha\alpha}^3 \theta_{d\alpha}, \quad (4.383)$$

$$\langle r^2 \rangle_{\alpha-d+} = -\langle d\alpha | r^2 | - + \rangle \theta_{\alpha\alpha}^3 \theta_{d\alpha}, \quad (4.384)$$

$$\langle r^2 \rangle_{d\alpha d+} = -\langle dd | r^2 | + \alpha' \rangle \theta_{\alpha\alpha}^3 \theta_{\alpha-}, \quad (4.385)$$

$$\langle r^2 \rangle_{d\alpha d-} = -\langle dd | r^2 | - \alpha' \rangle \theta_{\alpha\alpha}^3 \theta_{\alpha+}, \quad (4.386)$$

$$\langle r^2 \rangle_{d+d-} = \langle dd | r^2 | + - \rangle \theta_{\alpha\alpha}^4, \quad (4.387)$$

$$\langle r^2 \rangle_{d\alpha\alpha+} = \langle d\alpha | r^2 | + \alpha' \rangle \theta_{\alpha\alpha}^2 (2\theta_{d\alpha} \theta_{\alpha-} - \theta_{\alpha\alpha} \theta_{d-}), \quad (4.388)$$

$$\langle r^2 \rangle_{d\alpha\alpha-} = \langle d\alpha | r^2 | - \alpha' \rangle \theta_{\alpha\alpha}^2 (2\theta_{d\alpha} \theta_{\alpha+} - \theta_{\alpha\alpha} \theta_{d+}), \quad (4.389)$$

$$\langle r^2 \rangle_{d\alpha d\alpha} = \langle dd | r^2 | \alpha'\alpha' \rangle \theta_{\alpha\alpha}^2 \theta_{\alpha+} \theta_{\alpha-}, \quad (4.390)$$

$$\langle r^2 \rangle_{\alpha+\alpha-} = \langle \alpha\alpha | r^2 | + - \rangle \theta_{\alpha\alpha}^2 \theta_{d\alpha}^2. \quad (4.391)$$

The proton-neutron terms are:

$$\langle r^2 \rangle_\alpha = \langle \alpha\alpha | r^2 | \alpha'\alpha' \rangle \theta_{\alpha\alpha} [4\theta_{\alpha\alpha} \theta_{d+} \theta_{d-} - 2\theta_{d\alpha} (\theta_{\alpha+} \theta_{d-} + \theta_{\alpha-} \theta_{d+})], \quad (4.392)$$

$$\langle r^2 \rangle_{\alpha\alpha\alpha+} = \langle \alpha\alpha | r^2 | \alpha'+ \rangle 2\theta_{\alpha\alpha} (\theta_{d\alpha}^2 \theta_{\alpha-} - \theta_{\alpha\alpha} \theta_{d\alpha} \theta_{d-}), \quad (4.393)$$

$$\langle r^2 \rangle_{\alpha\alpha\alpha-} = \langle \alpha\alpha | r^2 | \alpha'- \rangle 2\theta_{\alpha\alpha} (\theta_{d\alpha}^2 \theta_{\alpha+} - \theta_{\alpha\alpha} \theta_{d\alpha} \theta_{d+}), \quad (4.394)$$

$$\langle r^2 \rangle_{d\alpha\alpha\alpha} = \langle d\alpha | r^2 | \alpha'\alpha' \rangle \theta_{\alpha\alpha} [4\theta_{d\alpha} \theta_{\alpha+} \theta_{\alpha-} - 2\theta_{\alpha\alpha} (\theta_{\alpha+} \theta_{d-} + \theta_{\alpha-} \theta_{d+})], \quad (4.395)$$

$$\langle r^2 \rangle_{\alpha^2 d+} = \langle \alpha d | r^2 | + \alpha' \rangle 2\theta_{\alpha\alpha}^2 (\theta_{\alpha\alpha} \theta_{d-} - \theta_{d\alpha} \theta_{\alpha-}), \quad (4.396)$$

$$\langle r^2 \rangle_{\alpha^2 d-} = \langle \alpha d | r^2 | - \alpha' \rangle 2\theta_{\alpha\alpha}^2 (\theta_{\alpha\alpha} \theta_{d+} - \theta_{d\alpha} \theta_{\alpha+}). \quad (4.397)$$

This completes the discussion of the mean-square radii in the interference term of ${}^6\text{He}$ and the discussion of the Gaussian approximation for ${}^6\text{He}$. We will then move on to the second nucleus of interest, ${}^6\text{Li}$.

4.5 Lithium-6

The treatment of ${}^6\text{Li}$ in the Gaussian approximation has many similarities with the previous section on ${}^6\text{He}$. This will allow us to be briefer, and focus on the differences and additions to the calculations outlined in great detail in the preceding pages. The kinetic energies are identical, save for the different projection process, as is the central and Majorana interactions. There are some additional words to say about the spin-orbit and tensor interactions, and then we will discuss the mean-square radius, as that differs slightly because the charge radius depends on proton and neutron number, which is of course different in the case of ${}^6\text{Li}$. We then will move on to the additional calculation of the quadrupole moment of the ground state of ${}^6\text{Li}$. This general sequence of discussion will be carried through both configurations and the interference term, with a discussion of the magnetic moment coming just before the before the interference term, and then finally finishing the chapter with a discussion of both nuclei and all configurations in a section on beta decay.

4.5.1 Alpha-deuteron configuration

The general set-up of the alpha-deuteron configuration of ${}^6\text{Li}$ was discussed in section 3.2. The single-particle wave functions are the same as in the case of ${}^6\text{He}$. The one-particle densities look the same as in the previous configuration. The kinetic and central potential energy calculations are also the same, save for the angular momentum projection, which is different (see eq.(3.79)). There is another difference, however, that effects all calculations, and that is the parity projection.

The parity projection operator, eq.(3.80), ensures that we are in a good state

of parity. This is necessary for lithium, since it has more contributions to the total angular momentum than just the orbital angular momentum as seen in the case of ${}^6\text{He}$. All the states in ${}^6\text{Li}$ have positive parity, so we will always use the upper sign of eq.(3.80). Because of this operator, all calculations now have two main terms, one where everything is unchanged, and the other where the parity operator has been applied. The effect of the parity operator is to change the sign of any term proportional to the rotation angle. No new matrix elements need to be calculated because of this simple rule, but we should note that the norm now consists of two terms, one just as in the case of ${}^6\text{He}$, plus an additional term affected by the parity operator:

$$\langle \Psi ({}^6\text{Li}) | \frac{1 + \hat{P}^r}{2} | \Psi ({}^6\text{Li}) \rangle = \frac{1}{2} \left[\theta_\alpha^2 (\theta_\alpha \theta_d - \theta_{12}^2)^2 + \bar{\theta}_\alpha^2 (\bar{\theta}_\alpha \bar{\theta}_d - \bar{\theta}_{12}^2) \right], \quad (4.398)$$

where a bar over an overlap means that the sign of the angle has been changed from the normal overlap, e.g.:

$$\bar{\theta}_\alpha = \exp \left[-\frac{(x+1)}{18} \nu d^2 \right]. \quad (4.399)$$

By looking at eq.(4.9), one can see the only thing that has been affected by the parity operator is the sign of the angle term. This is the same for all alpha-deuteron ${}^6\text{Li}$ calculations. There are always two terms, and the second (the one where the parity operator acts) has all signs changed from what was shown in the alpha-dineutron section of ${}^6\text{He}$.

4.5.2 Kinetic energy

Since we do not need to show any new calculations here, we can go straight to the plots of the results. Figure 4.25 shows the kinetic energy of the system as a function of d . In this plot, the center-of-mass motion has been removed. There are three levels here, $J = 1, 2$ and 3 . There is very little differentiation between them in the kinetic energy. The large d kinetic energy corresponds to the kinetic energy of a deuteron and the kinetic energy of an alpha particle summed together. At small d , we see all three

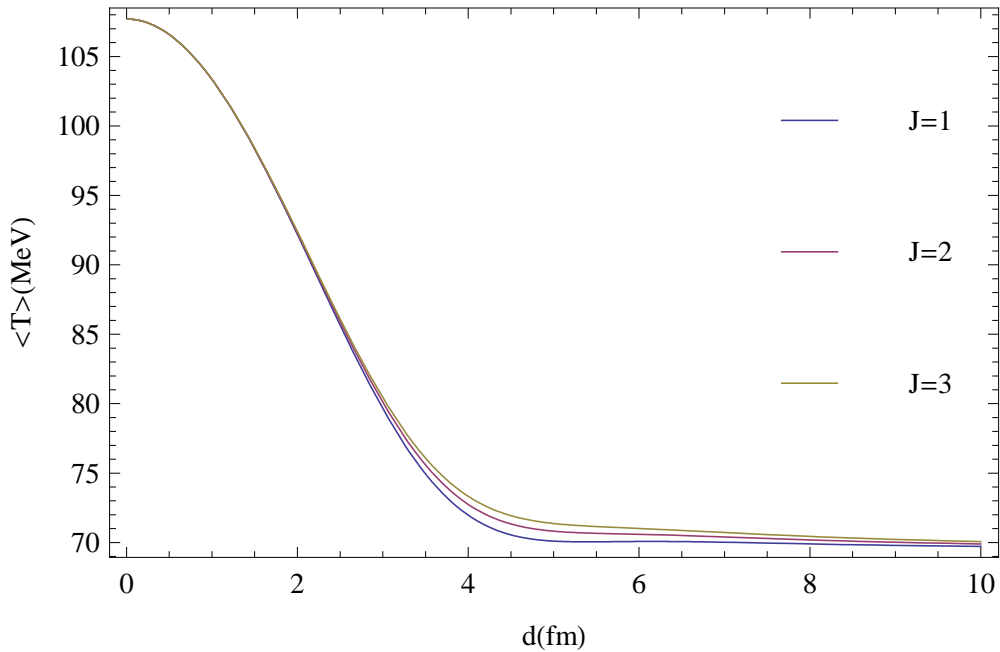


Figure 4.25: This plot shows the kinetic energy of the alpha-deuteron configuration of ${}^6\text{Li}$ as a function of d . For this plot, both oscillator parameters were set equal to 0.53 fm^{-2} .

levels come together. At small d , a proton and a neutron are forced into the next shell, the p -shell. All states are of even parity, by projection, and there are only minimal contributions from any orbital momenta higher than $\ell = 2$, so both the particles can sit comfortably in the p -shell.

4.5.3 Interaction

For lithium, the same interactions (Volkov and Minnesota) as in the case of helium were used, but there were more kinds of forces (tensor and spin-orbit in addition to central). The central and Majorana exchange are done exactly in the same manner as in helium, with the only difference coming once again from the projection process. The Minnesota potential, however, has some difference as the spin structure of ${}^6\text{Li}$ is different than in ${}^6\text{He}$. We must re-write the two-body terms into a singlet part and a

triplet part. The singlet part is:

$$\langle V_s \rangle_\alpha = \langle \alpha\alpha | V_s | \alpha\alpha \rangle 2\theta_\alpha\theta_d (\theta_\alpha\theta_d - \theta_{12}^2), \quad (4.400)$$

$$\langle V_s \rangle_{\alpha^2 d^2} = \langle \alpha d | V_s | d\alpha \rangle 3\theta_\alpha^2 (\theta_\alpha\theta_d - \theta_{12}^2), \quad (4.401)$$

$$\langle V_s \rangle_{\alpha\alpha d} = \langle \alpha\alpha | V_s | \alpha d \rangle 6\theta_\alpha\theta_{12} (\theta_{12}^2 - \theta_\alpha\theta_d). \quad (4.402)$$

The triplet part is:

$$\langle V_t \rangle_\alpha = \langle \alpha\alpha | V_t | \alpha\alpha \rangle (3\theta_\alpha^2\theta_d^2 + \theta_{12}^4 - 3\theta_\alpha\theta_d\theta_{12}^2), \quad (4.403)$$

$$\langle V_t \rangle_{\alpha^2 d^2} = \langle \alpha d | V_t | d\alpha \rangle \theta_\alpha^2 (5\theta_\alpha\theta_d - 3\theta_{12}^2), \quad (4.404)$$

$$\langle V_t \rangle_{\alpha\alpha d} = \langle \alpha\alpha | V_t | \alpha d \rangle \theta_\alpha\theta_{12} (2\theta_{12}^2 - 6\theta_\alpha\theta_d), \quad (4.405)$$

$$\langle V_t \rangle_{ddd\alpha} = -\langle dd | V_t | d\alpha \rangle 4\theta_\alpha^3\theta_{12}, \quad (4.406)$$

$$\langle V_t \rangle_d = \langle dd | V_t | dd \rangle \theta_\alpha^4, \quad (4.407)$$

$$\langle V_t \rangle_{\alpha dd\alpha} = \langle \alpha d | V_t | \alpha d \rangle 2\theta_\alpha^2 (2\theta_{12}^2 - \theta_\alpha\theta_d), \quad (4.408)$$

$$\langle V_t \rangle_{\alpha d\alpha d} = \langle \alpha\alpha | V_t | dd \rangle \theta_\alpha^2\theta_{12}^2. \quad (4.409)$$

We turn now to the discussions of the new operators in the potential. The tensor interaction was discussed before in section 3.2.1. There is not much more to add here, except that the radial form factor that was used was the Volkov potentials. For the Minnesota potential, the tensor interaction was not used.

The spin-orbit potential form is

$$\hat{V}_{LS} = V_{so} r_0^2 \frac{1}{r} \frac{d}{dr} \exp(-\gamma r_{ij}^2) \mathbf{L} \cdot \mathbf{S} = -2\gamma r_0^2 V_{so} \exp(-\gamma r_{ij}^2) \mathbf{L} \cdot \mathbf{S}. \quad (4.410)$$

In our calculations, V_{so} was set equal to 20 MeV, γ was equal to 0.5 fm^{-2} , and r_0 , the nuclear radius, was set equal to 1.2 fm. The inner workings of the $\mathbf{L} \cdot \mathbf{S}$ were discussed in detail in section 3.2.1. Here, we only need to provide the two non-vanishing matrix

elements of the \hat{V}_{LS} operator:

$$\begin{aligned} \langle \alpha d | V_{LS} | d \alpha \rangle &= \left(\frac{\nu \omega}{\nu \omega + \gamma(\nu + \omega)} \right)^{3/2} \frac{\nu \omega d^2 (\nu + 2\omega)}{12 [\nu \omega + \gamma(\nu + \omega)]} \sin \vartheta \\ &\times \exp \left[- \frac{(1-x) [\gamma(\nu - 4\omega)^2 + \nu \omega(\nu + 4\omega)] + 18\gamma\nu\omega}{18 [\nu \omega + \gamma(\nu + \omega)]} d^2 \right], \end{aligned} \quad (4.411)$$

$$\begin{aligned} \langle \alpha d | V_{LS} | \alpha d \rangle &= - \left(\frac{4\nu\omega}{(\nu + \omega)(\nu + \omega + 4\gamma)} \right)^{3/2} \frac{\nu \omega d^2 (\nu + 2\omega)}{3(\nu + \omega)(\nu + \omega + 4\gamma)} \sin \vartheta \\ &\times \exp \left[- \frac{(1-x) [2\gamma(\nu - 2\omega)^2 - 4\nu\omega(\nu + \omega)] + 36\gamma\nu\omega + 9\nu\omega(\nu + \omega)}{9(\nu + \omega)(\nu + \omega + 4\gamma)} d^2 \right]. \end{aligned} \quad (4.412)$$

The factor $-2\gamma r_0^2 V_{so}$ has been suppressed because it is the same in both terms. These two matrix elements are plugged into eqs.(3.94) and (3.95) and divided by the norm to obtain the spin-orbit contribution to the interactions.

The results of all the interactions with the Volkov potentials are shown in Figure 4.26 (V1) and Figure 4.27 (V2). There is little difference qualitatively between the two sets of parameters. Quantitatively, the V2 potential is about 3 MeV deeper than the V1 potential. These potentials do not distinguish the three states very much, similar to the kinetic energy results. We would then expect in the total energy plots to see the three levels very close together.

The results of the Minnesota potential are showed in Figure 4.28. The Minnesota potential seems to show more differentiation between the states of ${}^6\text{Li}$ compared to the Volkov potentials. The magnitude of the interaction at small d is comparable to the Volkov V1 potential, though at large d it is smaller. This is due to the lack of a tensor interaction which is an important part of the overall interaction in the deuteron.

4.5.4 Total energy

In this subsection, we show the spectra of the alpha-deuteron configuration of ${}^6\text{Li}$ with the three previously mentioned potentials. First, we examine the spectrum calculated with the Volkov V1 interaction (Figure 4.29). As anticipated, the spread in energies

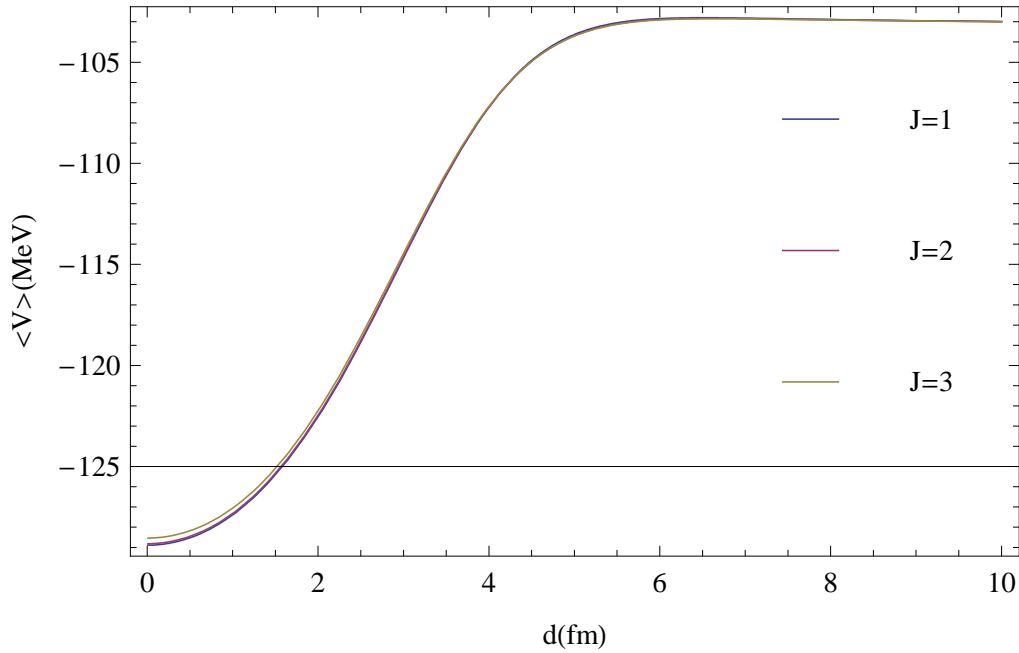


Figure 4.26: The expectation value of the Volkov V1 potential as a function of d in the alpha-deuteron configuration of ${}^6\text{Li}$. The oscillator parameters were both equal to 0.53 fm^{-2} , the Majorana exchange parameter was 0.6, and the parameters of the spin-orbit potential were $V_{so}=20 \text{ MeV}$ and $\gamma=0.5 \text{ fm}^{-2}$.

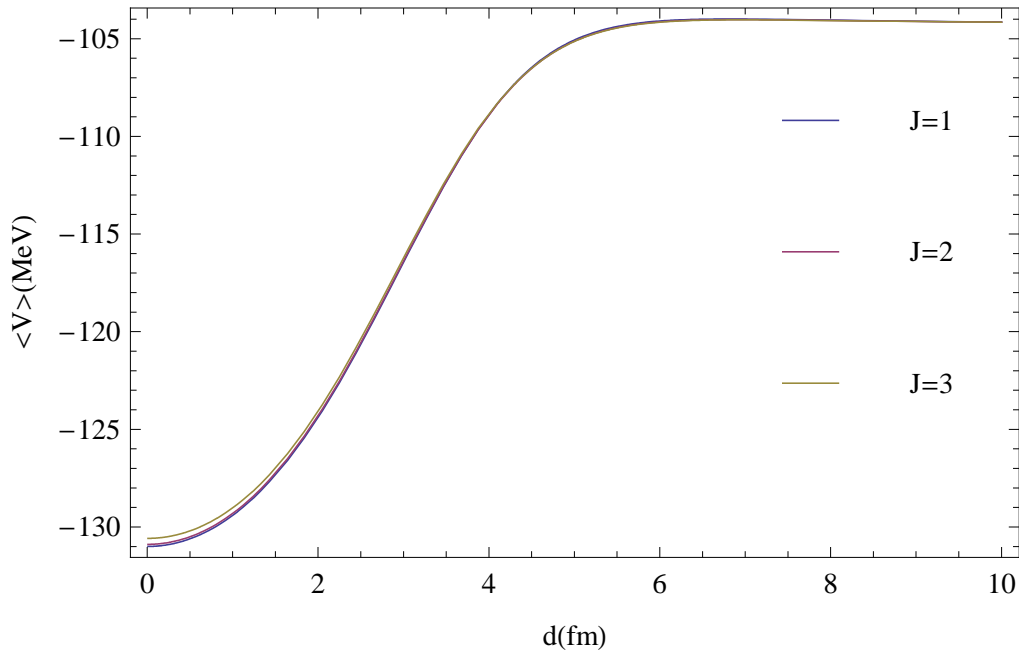


Figure 4.27: The expectation value of the Volkov V2 potential as a function of d in the alpha-deuteron configuration of ${}^6\text{Li}$. The oscillator parameters were both equal to 0.53 fm^{-2} , the Majorana exchange parameter was 0.6, and the parameters of the spin-orbit potential were $V_{so}=20 \text{ MeV}$ and $\gamma=0.5 \text{ fm}^{-2}$.

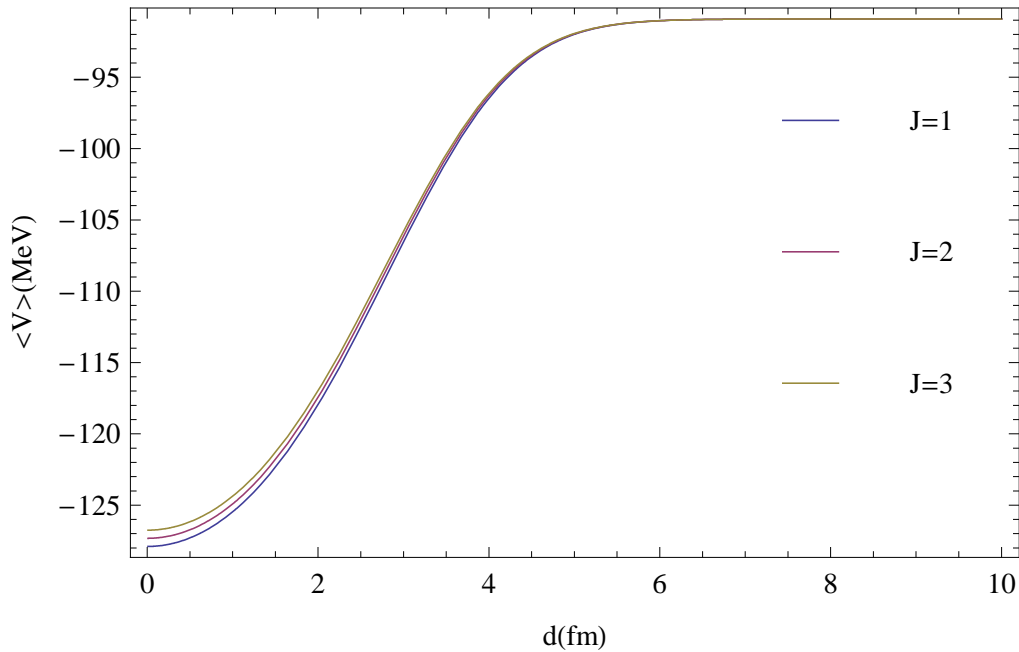


Figure 4.28: The expectation value of the Minnesota potential as a function of d in the alpha-deuteron configuration of ${}^6\text{Li}$. The oscillator parameters are both equal to 0.53 fm^{-2} , the exchange parameter u is equal to one, and the parameters of the spin-orbit potential were the same as in previous plots. There is no tensor interaction in this plot.

of the three levels is small. Perhaps 1 MeV separate the $J = 1$ ground state from the $J = 3$ excited state. At values of d smaller than about 2 fm, what separation there was almost disappears. All three of these states are bound since they are lower than their asymptotic energies. The minima also occur around 3.5 fm, where the external particles are still mostly in s -waves. The picture is essentially the same for the Volkov V2 interaction (Figure 4.30), except that the curves are shifted around 2 MeV to more negative energies.

Figure 4.31 shows the energy spectrum calculated with the Minnesota potential. This spectrum shows differences from the spectra calculated with the Volkov potentials. First of all, the three levels are clearly separate for all values of d . The bound states appear in a much deeper well compared to their asymptotic energies than in the Volkov potential, and they occur at less than 3 fm, making the overall nucleus much smaller. The sequence of states remains the same, and the higher energy can

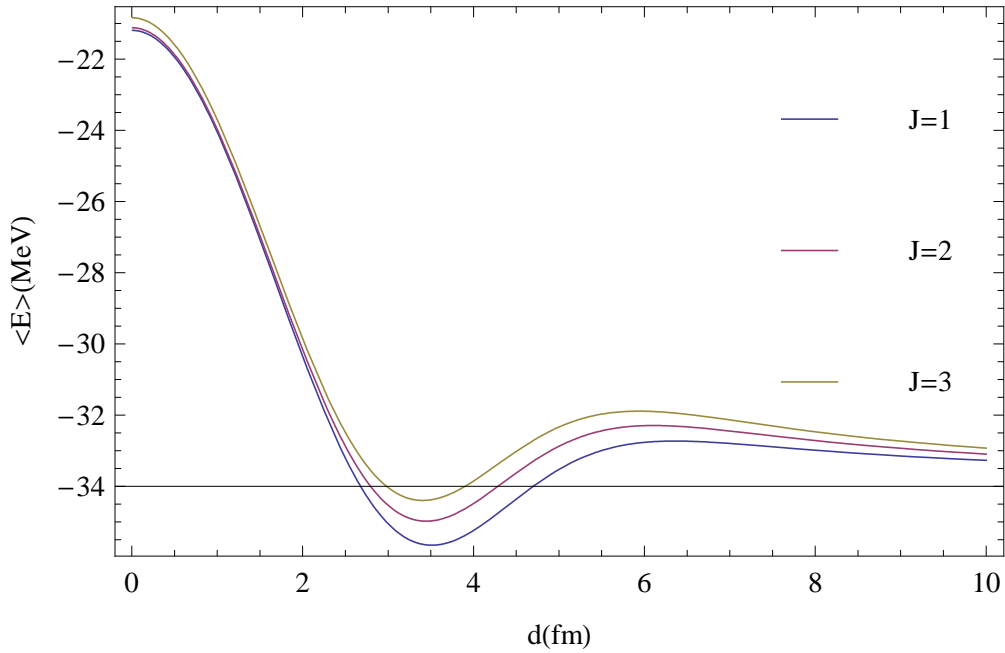


Figure 4.29: The spectrum of the alpha-deuteron configuration of ${}^6\text{Li}$ calculated with the Volkov V1 interaction. The oscillator parameters are both equal to 0.53 fm^{-2} , the Majorana exchange parameter is equal to 0.6, and the parameters of the spin-orbit potential are the same as in previous plots.

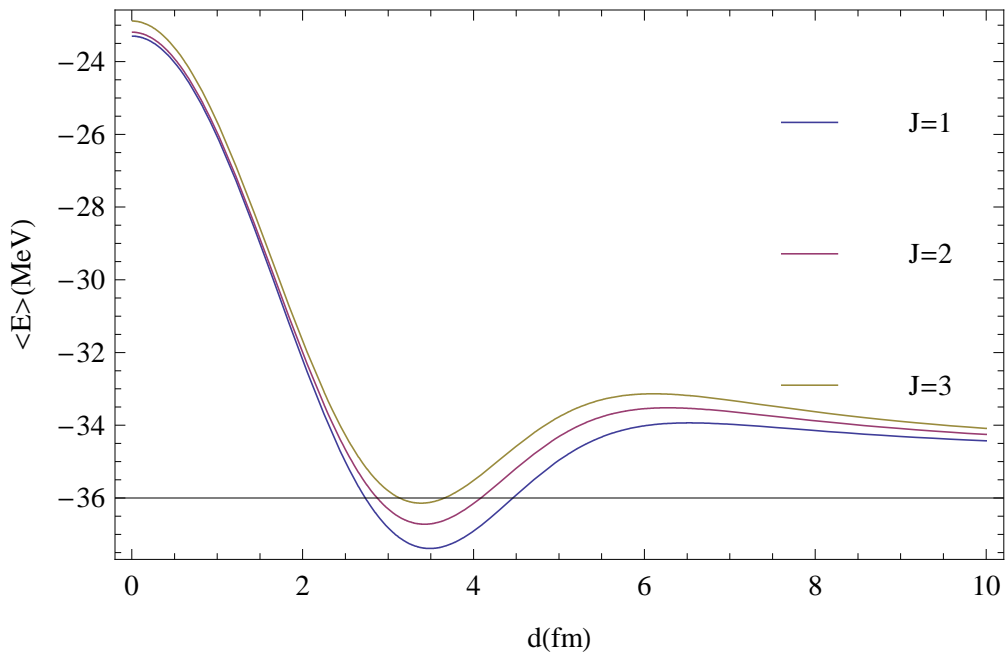


Figure 4.30: The spectrum of the alpha-deuteron configuration of ${}^6\text{Li}$ calculated with the Volkov V2 interaction. The oscillator parameters are both equal to 0.53 fm^{-2} , the Majorana exchange parameter is equal to 0.6, and the parameters of the spin-orbit potential are the same as in previous plots.

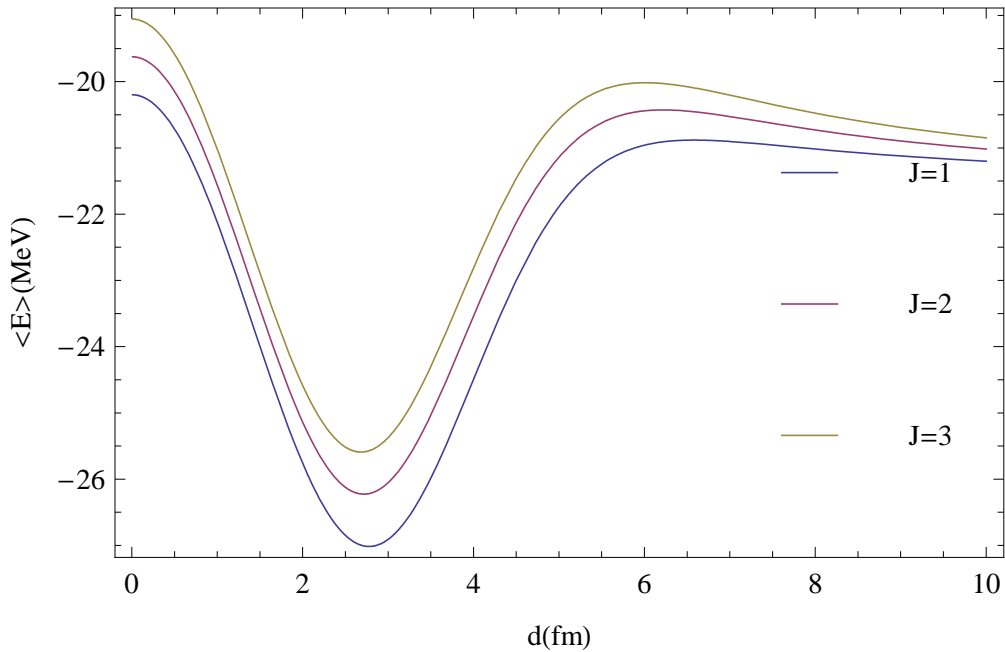


Figure 4.31: The spectrum of the alpha-deuteron configuration of ${}^6\text{Li}$ calculated with the Minnesota potential. The oscillator parameters are both equal to 0.53 fm^{-2} , the exchange parameter, u , is equal to one, and the values of the spin-orbit parameters are unchanged from previous plots.

be attributed to the lack of a tensor interaction.

This concludes the discussion on the operators of the Hamiltonian of ${}^6\text{Li}$. We will now move on to the calculation of other observables.

4.5.5 Mean square radius

The calculation of the mean square radius of the alpha-deuteron configuration proceeds in the same manner as has been discussed in section 4.1.5, except that the angular momentum projection is different. Also, one will have to do the parity projection, which has also been discussed previously (see eq.(3.80) and following plus the last paragraph of section 4.5.1). The distinction between charge and matter radius is lost in the case of ${}^6\text{Li}$, as now there is a proton in the external cluster. One just needs to follow the procedure outlined in the previously mentioned section on the matter radius, and that will give the charge and matter radius for ${}^6\text{Li}$.

4.5.6 Electric quadrupole moment

The quadrupole moment is an indication of the shape of a nucleus. The quadrupole moment operator is:

$$\hat{Q}_0 = \sqrt{\frac{16\pi}{5}} r^2 Y_{20}(\Omega) = 2z^2 - x^2 - y^2, \quad (4.413)$$

and one sums over all particles for a matter quadrupole moment or just over protons for the electric quadrupole moment. As one can see from the form of the operator, the expectation value in spherical nuclei should be zero. If it is positive, then the nucleons are more concentrated along the symmetry axis of the nucleus and is said to be prolate. If it is negative, then the nucleons accumulate around the equator of the nucleus, and the nucleus is said to be oblate. By convention, the quadrupole moment is tabulated in the state of maximum angular momentum projection, $|J, M = J\rangle$. This does not mean any change for us, since all our calculations for the ground state of ${}^6\text{Li}$ are in the $|11\rangle$ state. The operator in eq.(4.413) is in the body-fixed frame. In our laboratory frame, the expectation of the quadrupole moment is:

$$\langle JJ|Q_{JK}|JJ\rangle = \frac{3K^2 - J(J+1)}{(J+1)(2J+3)} Q_0, \quad (4.414)$$

where K is the projection of angular momentum on the body-fixed axis.

Before calculating the matrix elements, we must make sure the quadrupole moment has no contamination from the center-of-mass. This is essentially the same procedure as in the mean-square radius calculation (starting with eq.(4.52)). The result is essentially the same as eq.(4.55):

$$\langle Q \rangle = \frac{A-1}{A} Q_I - \frac{2}{A} Q_{II}, \quad (4.415)$$

where Q_I is the one-body expectation value and Q_{II} is the two-body expectation value. For the charge quadrupole moment, we can use this formula and divide the

answer by two, since half of the particles are protons.

We can now give the matrix elements. Note that we must use the same style of coordinates as in the center-of-mass calculations (see eqs.(4.61)-(4.72)). The one-body matrix elements of the Q_0 operator (eq.(4.413)) are:

$$\langle \alpha | Q_0 | \alpha \rangle = \theta_\alpha \frac{(z_1 - Z)^2 (1 + 3x)(1 + x)}{4}, \quad (4.416)$$

$$\langle d | Q_0 | d \alpha \rangle = \theta_d \frac{(z_2 - Z)^2 (1 + 3x)(1 + x)}{4}, \quad (4.417)$$

$$\langle \alpha | Q_0 | d \rangle = \theta_{12} \frac{2\nu^2 (z_1 - Z)^2 + \omega^2 (z_2 - Z)^2 (3x^2 - 1) + 4\nu\omega x (z_1 - Z)(z_2 - Z)}{(\nu + \omega)^2}, \quad (4.418)$$

$$\langle d | Q_0 | \alpha \rangle = \theta_{12} \frac{2\omega^2 (z_2 - Z)^2 + \nu^2 (z_1 - Z)^2 (3x^2 - 1) + 4\nu\omega x (z_1 - Z)(z_2 - Z)}{(\nu + \omega)^2}, \quad (4.419)$$

where Z is the location of the center-of-mass (replaces Z_{CM} from the previous calculations). We have all the ingredients to calculate the one-body expectation value of the quadrupole moment. We then need the two-body terms:

$$\langle \alpha \alpha | Q_0 | \alpha \alpha \rangle = \theta_\alpha^2 \frac{(z_1 - Z)^2 (1 + 3x)(1 + x)}{4}, \quad (4.420)$$

$$\langle \alpha d | Q_0 | d \alpha \rangle = \theta_\alpha \theta_d \frac{(z_1 - Z)(z_2 - Z)(1 + 3x)(1 + x)}{4}, \quad (4.421)$$

$$\langle \alpha \alpha | Q_0 | \alpha d \rangle = \theta_\alpha \theta_{12} \frac{(z_1 - Z)(1 + x)[\omega(z_2 - Z)(3x - 1) + 2\nu(z_1 - Z)]}{2(\nu + \omega)}, \quad (4.422)$$

$$\langle d \alpha | Q_0 | \alpha \alpha \rangle = \theta_\alpha \theta_{12} \frac{(z_1 - Z)(1 + x)[\nu(z_1 - Z)(3x - 1) + 2\omega(z_2 - Z)]}{2(\nu + \omega)}, \quad (4.423)$$

$$\langle dd | Q_0 | d \alpha \rangle = \theta_d \theta_{12} \frac{(z_2 - Z)(1 + x)[\nu(z_1 - Z)(3x - 1) + 2\omega(z_2 - Z)]}{2(\nu + \omega)}, \quad (4.424)$$

$$\langle \alpha d | Q_0 | dd \rangle = \theta_d \theta_{12} \frac{(z_2 - Z)(1 + x)[\omega(z_2 - Z)(3x - 1) + 2\nu(z_1 - Z)]}{2(\nu + \omega)}, \quad (4.425)$$

$$\langle dd|Q_0|dd\rangle = \theta_d^2 \frac{(z_2 - Z)^2 (1 + 3x)(1 + x)}{4}, \quad (4.426)$$

$$\langle d\alpha|Q_0|d\alpha\rangle = \theta_{12}^2 \frac{\nu\omega (z_2 - Z) (z_1 - Z) (3x^2 + 1) + 2x [\omega^2 (z_2 - Z)^2 + \nu^2 (z_1 - Z)^2]}{(\nu + \omega)^2}, \quad (4.427)$$

$$\langle dd|Q_0|\alpha\alpha\rangle = \theta_{12}^2 \frac{\nu^2 (z_1 - Z)^2 (3x^2 - 1) + 2\omega^2 (z_2 - Z)^2 + 4\nu\omega x (z_1 - Z) (z_2 - Z)}{(\nu + \omega)^2}, \quad (4.428)$$

$$\langle \alpha\alpha|Q_0|dd\rangle = \theta_{12}^2 \frac{2\nu^2 (z_1 - Z)^2 + \omega^2 (z_2 - Z)^2 (3x^2 - 1) + 4\nu\omega x (z_1 - Z) (z_2 - Z)}{(\nu + \omega)^2}. \quad (4.429)$$

These matrix elements are inserted into the proper term from eqs.(3.11)-(3.20). This is all that is needed to calculate the quadrupole moment.

This concludes the section on the alpha-deuteron configuration of ${}^6\text{Li}$. We now go to the cigar configuration.

4.6 Cigar configuration

The cigar configuration of ${}^6\text{Li}$ was introduced already in section 3.2.2, and also has many similarities with the ${}^6\text{He}$ cigar configuration (section 4.2). We just need to add here the things that are different for lithium, and show the various energy plots.

We should note that the parity projection is not necessary in this configuration. The symmetrization procedure (outlined starting with eq.(3.21)) of the external spins takes care of parity of the state.

4.6.1 Kinetic energy

The kinetic energy calculation in the cigar configuration proceeds just as in the case of ${}^6\text{He}$, save for the different angular momentum projection factor. We then examine the plot that shows the total kinetic energy of the system (center-of-mass energy removed), which is shown in Figure 4.32. The picture is remarkably similar to the

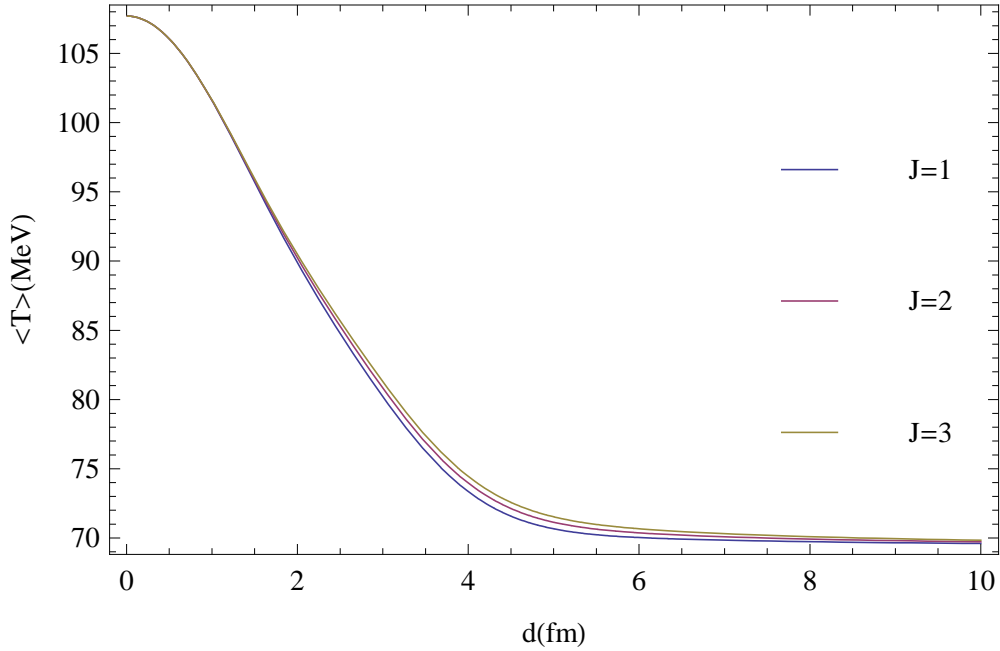


Figure 4.32: The kinetic energy of the cigar configuration of ${}^6\text{Li}$ as a function of d . The spurious center-of-mass motion has been removed. The oscillator parameters were both set equal to 0.53 fm^{-2} .

alpha-deuteron result (Figure 4.25). The $d = 0$ value is 108 MeV in both plots, which is what we expect. There is also very little separation between the three levels in both plots. The cigar plot falls perhaps slightly faster than the alpha-deuteron case.

4.6.2 Interaction

The details of much of the two-body interaction calculation have been covered before, especially in the case of the Volkov potentials. These are calculated in exactly the same way as for the cigar configuration of ${}^6\text{He}$, save for projecting into different states. There are the additional tensor and spin-orbit interactions, however. The tensor interaction uses the Volkov form factors, and its relevant terms are eqs.(3.120)-(3.134). The spin-

orbit operator introduces new matrix elements. They are:

$$\begin{aligned} \langle \alpha \pm |V_{LS}| \pm \alpha \rangle &= \left(\frac{\nu\omega}{\nu\omega + \gamma(\nu + \omega)} \right)^{3/2} \frac{\nu\omega^2 d^2}{4[\nu\omega + \gamma(\nu + \omega)]} \sin \vartheta \\ &\times \exp \left(-\frac{(1-x)\omega(\gamma + \nu) + \gamma\nu}{2[\nu\omega + \gamma(\nu + \omega)]} \omega d^2 \right), \end{aligned} \quad (4.430)$$

$$\langle \alpha \pm |V_{LS}| \mp \alpha \rangle = -\langle \alpha \pm |V_{LS}| \pm \alpha \rangle (x \rightarrow -x) \quad (4.431)$$

$$\begin{aligned} \langle \alpha \pm |V_{LS}| \alpha \pm \rangle &= -\left(\frac{4\nu\omega}{(\nu + \omega)\Delta_\gamma(\nu, \omega)} \right)^{3/2} \frac{\nu\omega^2 d^2}{(\nu + \omega)\Delta_\gamma(\nu, \omega)} \sin \vartheta \\ &\times \exp \left[-\frac{\nu^2 + \nu\omega + 2\gamma[2\nu + \omega(1+x)]}{(\nu + \omega)\Delta_\gamma(\nu, \omega)} \right], \end{aligned} \quad (4.432)$$

$$\langle \alpha \pm |V_{LS}| \alpha \mp \rangle = \langle \alpha \pm |V_{LS}| \alpha \pm \rangle (x \rightarrow -x), \quad (4.433)$$

where

$$\Delta_\gamma(a, b) = a + b + 4\gamma,$$

continuing:

$$\begin{aligned} \langle \pm \mp |V_{LS}| \mp \alpha \rangle &= \left(\frac{2\omega\sqrt{\nu\omega}}{D_\gamma(\omega, \nu)} \right)^{3/2} \frac{(\nu + \omega)\omega^2 d^2}{2D_\gamma(\omega, \nu)} \sin \vartheta \\ &\times \exp \left[-\frac{(1-x)(\omega^2 + \nu\omega) + 2\nu\omega + \gamma(3\nu + 8\omega)}{2D_\gamma(\omega, \nu)} \omega d^2 \right], \end{aligned} \quad (4.434)$$

$$\langle \pm \mp |V_{LS}| \pm \alpha \rangle = -\langle \pm \mp |V_{LS}| \mp \alpha \rangle (x \rightarrow -x), \quad (4.435)$$

where

$$D_\gamma(a, b) = a(a + b) + \gamma(3a + b),$$

$$\begin{aligned} \langle - + |V_{LS}| + - \rangle &= \left(\frac{\omega}{\omega + 2\gamma} \right)^{3/2} \frac{\omega^2 d^2}{\omega + 2\gamma} \\ &\times \exp \left(-\frac{\omega(1-x) + 4\gamma}{\omega + 2\gamma} \omega d^2 \right), \end{aligned} \quad (4.436)$$

$$\langle - + |V_{LS}| - + \rangle = -\langle - + |V_{LS}| + - \rangle (x \rightarrow -x). \quad (4.437)$$

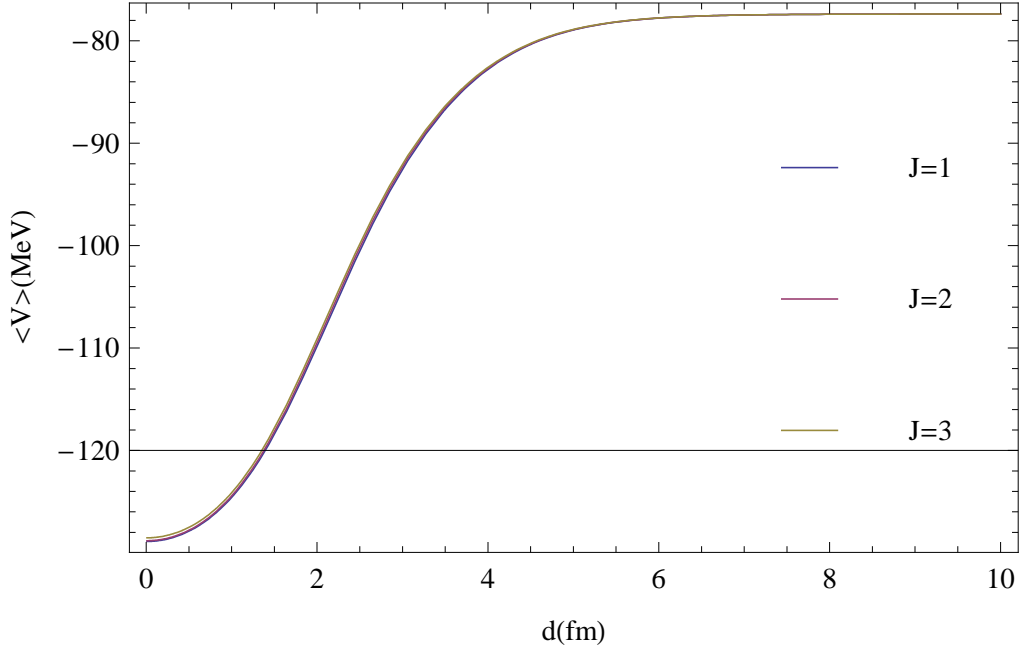


Figure 4.33: The potential energy as a function of d in the cigar configuration of ${}^6\text{Li}$, calculated with the Volkov V1 interaction. In this plot, the oscillator parameters are both equal to 0.53 fm^{-2} , the Majorana exchange parameter is equal to 0.6, and the spin-orbit parameters are $V_{so}=20 \text{ MeV}$, and $\gamma=0.5 \text{ fm}^{-2}$.

In the listed matrix elements above, the prefactor $-2\gamma r_0^2 V_{so}$ has been suppressed since it appears in all of them. These matrix elements are then plugged into the terms listed in eqs.(3.112)-(3.119) and divided by the norm.

We show plots of the Volkov V1 and V2 results in Figures 4.33 and 4.34. These plots include the tensor and spin-orbit interactions. These plots are qualitatively the same, with the only difference being that the V2 plot is shifted two or three MeV lower in energy. At $d = 0$, the plots correspond with the values found in the alpha-deuteron configuration (Figures 4.26 and 4.27).

For the Minnesota potential, we must separate the terms into singlet and triplet

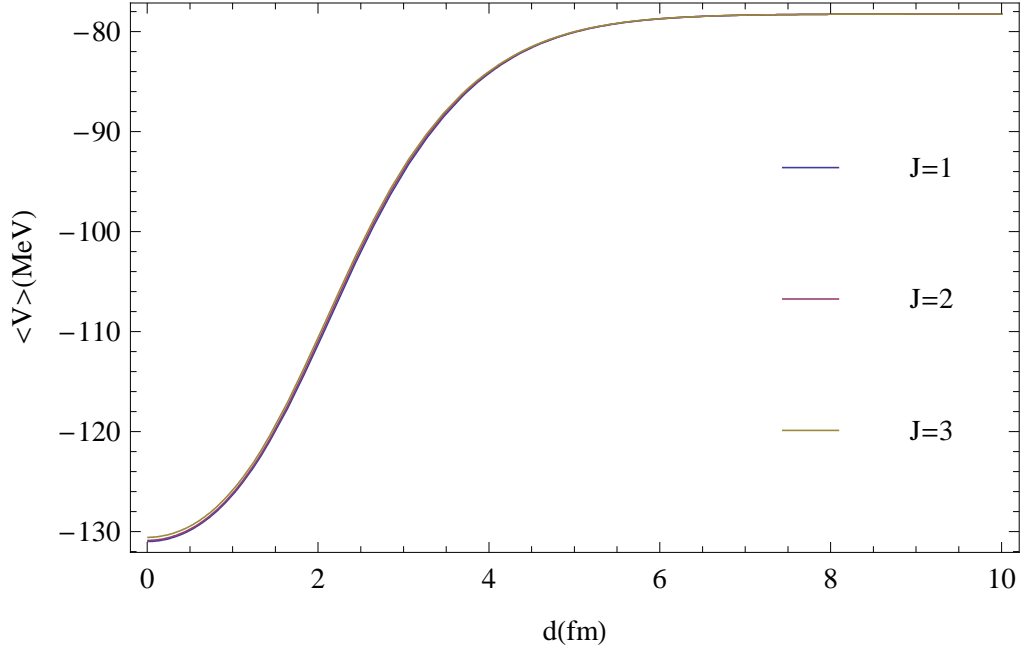


Figure 4.34: The potential energy as a function of d in the cigar configuration of ${}^6\text{Li}$, calculated with the Volkov V2 interaction. In this plot, the oscillator parameters are both equal to 0.53 fm^{-2} , the Majorana exchange parameter is equal to 0.6, and the spin-orbit parameters are unchanged from the previous plot.

terms, which is different in lithium than in helium. The singlet terms are:

$$\langle V_s \rangle_\alpha = \langle \alpha\alpha | V_s | \alpha\alpha \rangle \theta_\alpha [3\theta_\alpha (\theta_n^2 + \theta_\pm^2) - 3\theta_{12}^2 (\theta_n + \theta_\pm)], \quad (4.438)$$

$$\langle V_s \rangle_{\alpha^2 n^2} = \langle \alpha \pm | V_s | \pm \alpha \rangle 2\theta_\alpha^2 (2\theta_\alpha \theta_n - \theta_{12}^2), \quad (4.439)$$

$$\langle V_s \rangle_{\alpha^2 \pm^2} = \langle \alpha \pm | V_s | \mp \alpha \rangle 2\theta_\alpha^2 (2\theta_\alpha \theta_p m - \theta_{12}^2), \quad (4.440)$$

$$\langle V_s \rangle_{\alpha\alpha\alpha\pm} = \langle \alpha\alpha | V_s | \alpha\pm \rangle 6\theta_\alpha \theta_{12} [2\theta_{12}^2 - \theta_\alpha (\theta_n + \theta_\pm)]. \quad (4.441)$$

The triplet terms are:

$$\langle V_t \rangle_\alpha = \langle \alpha\alpha | V_t | \alpha\alpha \rangle [3\theta_\alpha^2 (\theta_n^2 + \theta_\pm^2) + 2\theta_{12}^4 - 3\theta_{12}^2 \theta_\alpha (\theta_n + \theta_\pm)], \quad (4.442)$$

$$\langle V_t \rangle_{\alpha^2 n^2} = \langle \alpha \pm | V_t | \pm \alpha \rangle \theta_\alpha^2 (5\theta_\alpha \theta_n - 3\theta_{12}^2), \quad (4.443)$$

$$\langle V_t \rangle_{\alpha^2 \pm^2} = \langle \alpha \pm | V_t | \mp \alpha \rangle \theta_\alpha^2 (5\theta_\alpha \theta_\pm - 3\theta_{12}^2), \quad (4.444)$$

$$\langle V_t \rangle_{\alpha\alpha\alpha\pm} = \langle \alpha\alpha | V_t | \alpha\pm \rangle 2\theta_\alpha \theta_{12} [2\theta_{12}^2 - 3\theta_\alpha (\theta_n + \theta_\pm)], \quad (4.445)$$

$$\langle V_t \rangle_{\pm^2 \mp \alpha} = -\langle \mp \pm | V_t | \pm \alpha \rangle 4\theta_\alpha^3 \theta_{12}, \quad (4.446)$$

$$\langle V_t \rangle_{\pm \mp \mp \alpha} = -\langle \pm \mp | V_t | \pm \alpha \rangle 4\theta_\alpha^3 \theta_{12}, \quad (4.447)$$

$$\langle V_t \rangle_{+^2 -^2} = \langle \pm \mp | V_t | \mp \pm \rangle \theta_\alpha^4, \quad (4.448)$$

$$\langle V_t \rangle_{\pm \mp \mp \pm} = \langle \pm \mp | V_t | \pm \mp \rangle \theta_\alpha^4, \quad (4.449)$$

$$\langle V_t \rangle_{\alpha\pm\pm\alpha} = \langle \alpha \pm | V_t | \alpha\pm \rangle 2\theta_\alpha (2\theta_{12} - \theta_\alpha \theta_n), \quad (4.450)$$

$$\langle V_t \rangle_{\alpha\pm\mp\alpha} = \langle \alpha \mp | V_t | \alpha\pm \rangle 2\theta_\alpha (2\theta_{12} - \theta_\alpha \theta_p m), \quad (4.451)$$

$$\langle V_t \rangle_{\alpha+\alpha-} = \langle \alpha\alpha | V_t | + - \rangle 4\theta_\alpha^2 \theta_{12}^2. \quad (4.452)$$

Figure 4.35 shows the expectation value of the Minnesota potential as a function of d . As with the other plots, there is little differentiation of the three levels, though there is more here than in the case of the Volkov interactions. The $d=0$ limit correspond with the alpha-deuteron case (Figure 4.28), with the lowest state coming in at around -128 MeV.

4.6.3 Total energy

The energy spectra of the cigar configuration calculated with the Volkov V1 and V2 potentials are shown in Figures 4.36 and 4.37. Once again, all three levels are very close together, even more so, the first two levels. Since the asymptotic state is an alpha particle and two free nucleons, the well is much deeper (in contrast with the other configuration which asymptotically is an alpha particle and bound deuteron). Finally, they are consistent with the alpha-deuteron configuration at $d=0$, where they

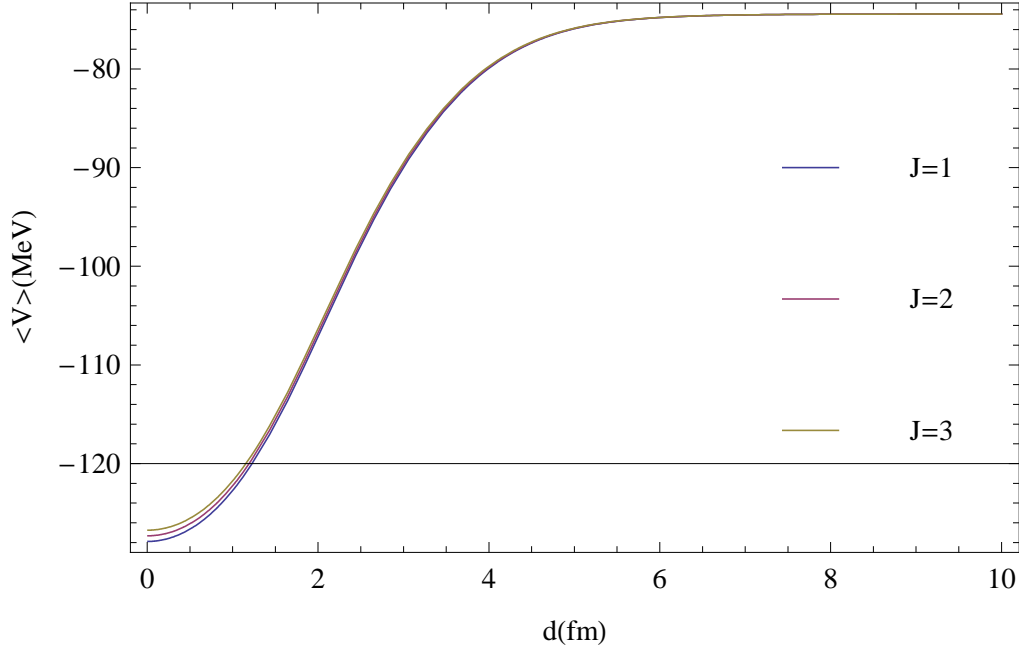


Figure 4.35: The expectation value of the Minnesota potential as a function of d calculated in the cigar configuration of ${}^6\text{Li}$. For this plot, the oscillator parameters are both equal to 0.53 fm^{-2} , the exchange parameter, u , is equal to one, and the spin-orbit parameters remain unchanged from previous calculations. There is no tensor interaction in this calculation.

both have a value of -21.2 MeV (V1) and -23.3 MeV (V2).

The story is similar with the Minnesota potential, which is shown in Figure 4.38. There is a more clear separation of states, though they are still very close together. The minimum still occurs close to 1 fm , and the well is still quite deep. As in the previous case, the value of the energy at $d=0$ (-20.2 MeV) is the same in both configurations.

4.6.4 Mean square radius

The mean square radius calculation in the cigar configuration has been discussed before in the ${}^6\text{He}$ cigar configuration section (section 4.2.4). For lithium, the calculation is the same except for the projection process. Also, the charge and matter radius are the same for lithium, so only one calculation is necessary.

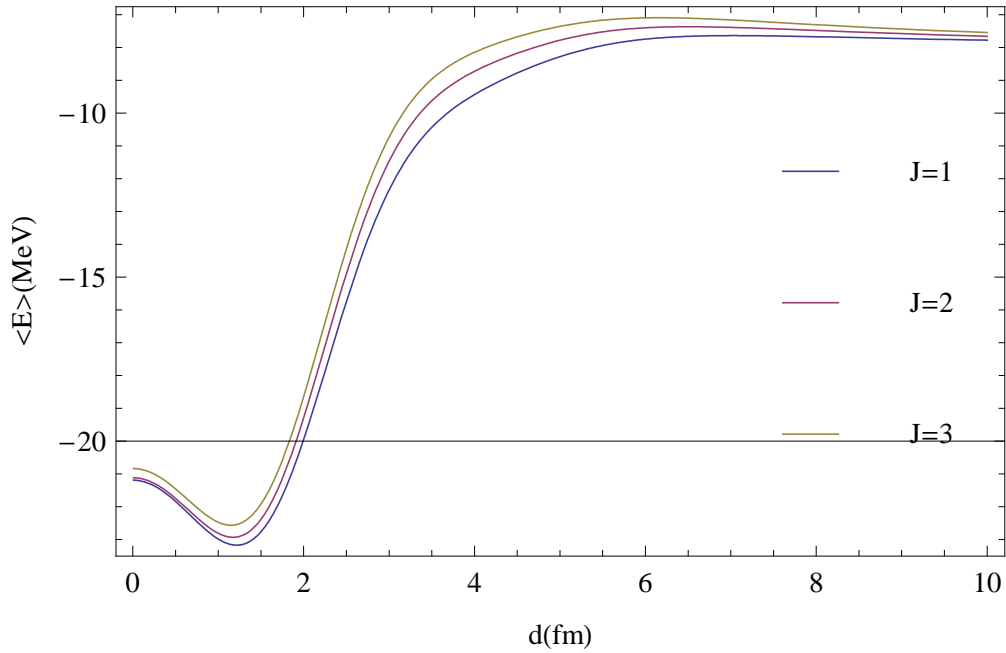


Figure 4.36: The energy spectrum of the cigar configuration of ${}^6\text{Li}$ calculated with the Volkov V1 potential. The oscillator parameters are both equal to 0.53 fm^{-2} , the Majorana exchange parameter is equal to 0.6, and the spin-orbit parameters were not changed from the previous graphs.

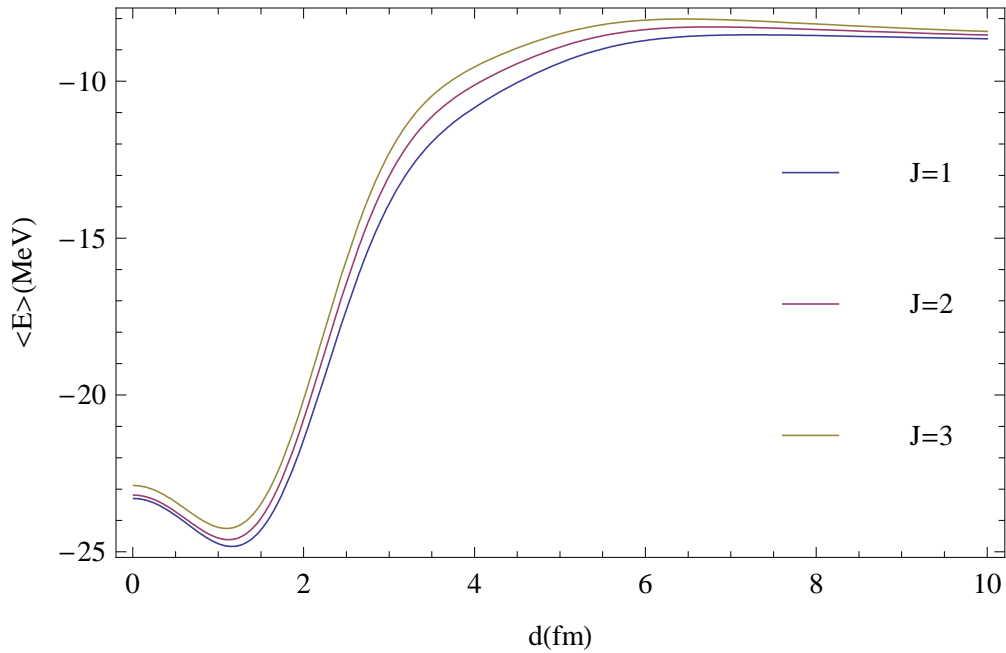


Figure 4.37: The energy spectrum of the cigar configuration of ${}^6\text{Li}$ calculated with the Volkov V2 potential. The oscillator parameters are both equal to 0.53 fm^{-2} , the Majorana exchange parameter is equal to 0.6, and the spin-orbit parameters were not changed from the previous graphs.

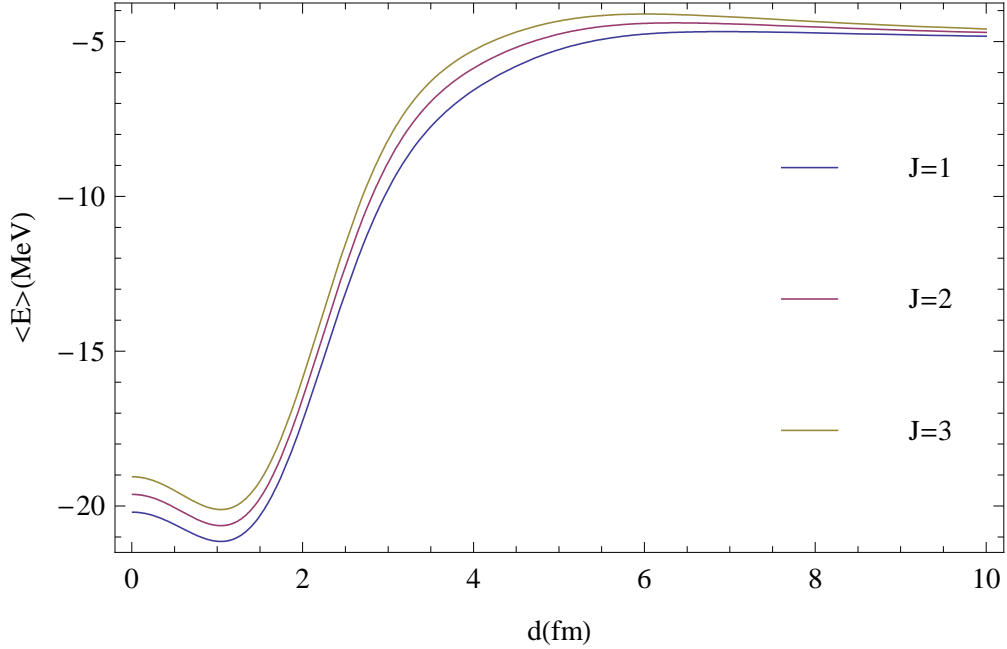


Figure 4.38: The energy spectrum of the cigar configuration of ${}^6\text{Li}$ calculated with the Minnesota potential. The oscillator parameters are both equal to 0.53 fm^{-2} , the exchange parameter, u , is equal to one, and all spin-orbit parameters are the same as in the previous plots. There is no tensor interaction in this plot.

4.6.5 Electric quadrupole moment

The quadrupole moment operator was defined in eq.(4.414). We also must be concerned with the center-of-mass contamination, so we must use eq.(4.415) in order to remove the center-of-mass terms. In that equation, there are one-body and two-body terms. The one-body matrix elements are:

$$\langle \alpha | Q_0 | \alpha \rangle = 0, \quad (4.453)$$

$$\langle \pm | Q_0 | \pm \rangle = \theta_n \frac{d^2}{4} (1 + 3x)(1 + x), \quad (4.454)$$

$$\langle \pm | Q_0 | \mp \rangle = \theta_{\pm} \frac{d^2}{4} (1 - 3x)(1 - x), \quad (4.455)$$

$$\langle \pm | Q_0 | \alpha \rangle = \theta_{12} \frac{\omega^2 d^2}{(\nu + \omega)^2} (3x^2 - 1), \quad (4.456)$$

$$\langle \alpha | Q_0 | \pm \rangle = \theta_{12} \frac{2\omega^2 d^2}{(\nu + \omega)^2}. \quad (4.457)$$

The alpha term vanishes because the alpha is spherically symmetric and is located at the origin. Similarly, all two-body matrix elements which involve a diagonal alpha term vanish, and will not be included in the list. The non-vanishing two-body matrix elements are:

$$\langle + - | Q_0 | - + \rangle = -\theta_n^2 \frac{d^2}{4} (1 + 3x)(1 + x), \quad (4.458)$$

$$\langle + - | Q_0 | + - \rangle = -\theta_{\pm}^2 \frac{d^2}{4} (1 - 3x)(1 - x), \quad (4.459)$$

$$\langle + - | Q_0 | \alpha + \rangle = -\theta_n \theta_{12} \frac{\omega d^2}{2(\nu + \omega)} (3x - 1)(1 + x), \quad (4.460)$$

$$\langle + \alpha | Q_0 | - + \rangle = -\theta_n \theta_{12} \frac{\omega d^2}{\nu + \omega} (1 + x), \quad (4.461)$$

$$\langle + - | Q_0 | \alpha - \rangle = -\theta_{\pm} \theta_{12} \frac{\omega d^2}{\nu + \omega} (1 - x), \quad (4.462)$$

$$\langle + \alpha | Q_0 | + - \rangle = -\theta_{\pm} \theta_{12} \frac{\omega d^2}{2(\nu + \omega)} (x - 1)(3x + 1), \quad (4.463)$$

$$\langle + \alpha | Q_0 | + \alpha \rangle = \theta_{12}^2 \frac{2\omega^2 d^2}{(\nu + \omega)^2} x, \quad (4.464)$$

$$\langle + \alpha | Q_0 | - \alpha \rangle = -\theta_{12}^2 \frac{2\omega^2 d^2}{(\nu + \omega)^2} x, \quad (4.465)$$

$$\langle + - | Q_0 | \alpha \alpha \rangle = -\theta_{12}^2 \frac{2\omega^2 d^2}{(\nu + \omega)^2}, \quad (4.466)$$

$$\langle \alpha \alpha | Q_0 | + - \rangle = -\theta_{12}^2 \frac{\omega^2 d^2}{(\nu + \omega)^2} (3x^2 - 1). \quad (4.467)$$

The one-body matrix elements are plugged into eqs.(3.25)-(3.29), then divided by the norm. For the two body matrix elements, the relevant equations are eqs.(3.30)-(3.44). This then completes the quadrupole moment calculations.-

4.7 Magnetic dipole moment

In addition to electric quadrupole moments, nuclei with non-zero angular momentum have magnetic moments as well, which is a measure of the asymmetry in the “magnetic charge” of the nucleus. These magnetic charges come from the intrinsic magnetic moments of the protons and neutrons, and the orbital motion of the protons (neutrons,

being uncharged, do not produce any additional magnetic field with their motion). The magnetic dipole moment operator is

$$\hat{\boldsymbol{\mu}}_m = \mu_N \sum_i^A [g_\ell(i) \boldsymbol{\ell}_m(i) + g_s(i) \mathbf{s}_m(i)], \quad (4.468)$$

where μ_N is the nuclear magneton ($= e\hbar/2M_p c$), g_ℓ and g_s are the orbital and spin g -factors of the i -th nucleon, and m is the projection of the operator, since the magnetic dipole moment is a vector operator. The g -factors are equal to:

$$g_\ell = \begin{cases} 1 & \text{for a proton} \\ 0 & \text{for a neutron} \end{cases} \quad g_s = \begin{cases} 5.586 & \text{for a proton} \\ -3.826 & \text{for a neutron} \end{cases}. \quad (4.469)$$

As was the case in the quadrupole moment, we calculate the expectation value of the magnetic moment in the state of maximum projection. We actually calculate the projection of the magnetic moment along the nuclear spin:

$$\langle JJ | \mu_0 | JJ \rangle = \frac{1}{J+1} \langle JJ | (\boldsymbol{\mu} \cdot \mathbf{J}) | JJ \rangle. \quad (4.470)$$

For our ${}^6\text{Li}$ system, we can make a few simplifications. The alpha particle is spinless, and the orbital g -factor of the neutrons is zero, so we can re-write eq.(4.468) as:

$$\hat{\boldsymbol{\mu}}_0 = \mu_N \left[g_s(n) \mathbf{s}(n) + g_s(p) \mathbf{s}(p) + \sum_p^Z \boldsymbol{\ell}(p) \right], \quad (4.471)$$

where the first two terms are from the spins of the external proton and neutron, and the sum runs only over protons. We can simplify the operator further by working with the total spin of the external particles, $\mathbf{S} = \mathbf{s}(n) + \mathbf{s}(p)$, and the total angular momentum, \mathbf{L} . Making this substitution, the operator becomes:

$$\hat{\boldsymbol{\mu}}_0/\mu_n = \frac{1}{2} [(g_s(n) + g_s(p)) \mathbf{S} + (g_s(p) - g_s(n))(\mathbf{s}(p) - \mathbf{s}(n)) + \mathbf{L}], \quad (4.472)$$

where the factor $1/2$ appears before \mathbf{L} because ${}^6\text{Li}$ is an $N = Z$ nucleus, and we can consider half of the orbital angular momentum to come from the protons. The operator $\mathbf{s}(p) - \mathbf{s}(n)$ plays no role in our calculation as our system is completely symmetric with respect to protons and neutrons. We then take the scalar product of this operator with the total angular momentum, \mathbf{J} :

$$(\boldsymbol{\mu} \cdot \mathbf{J}) \mathbf{J} / \mu_N = g_S \frac{\mathbf{S} \cdot \mathbf{J}}{J(J+1)} \mathbf{J} + \frac{\mathbf{L} \cdot \mathbf{J}}{2J(J+1)} \mathbf{J}, \quad (4.473)$$

where g_S is $(g_s(n) + g_s(p))/2$ or the sum of the magnetic moments of the free proton and free neutron. Since we are working the state of maximum projection, $S = S_z = 1$ and $J = J_z = 1$. We can simplify the first term by using the relation similar to that used for the spin orbit operator:

$$\mathbf{S} \cdot \mathbf{J} = \frac{1}{2} (S_+ J_- + S_- J_+) + S_z J_z. \quad (4.474)$$

The terms with raising and lowering operators vanish in the state of maximum projection, and we are left with $S_z J_z = J^2$. For the second term in eq.(4.473), we use the relation $\mathbf{L} = \mathbf{J} - \mathbf{S}$. The resulting expression for the magnetic moment is:

$$\mu_0 / \mu_N = g_S \frac{J^2}{J+1} + \frac{J(J+1) - J^2}{2(J+1)}, \quad (4.475)$$

where J^2 is just a number, not the operator. This is our final expression, which depends only on quantum numbers. It is independent of the spatial configuration. The numerical result will be given in the next chapter and discussed.

4.8 Interference term

As with the two separate configurations of ${}^6\text{Li}$, there is a lot of repetition with the helium calculations. In the interest of brevity, we will only add the new material here. Thus, there will be no sections on the kinetic energy or mean-square radius, as they are exactly the same as the helium case save for the angular momentum projection. Projecting onto parity is not necessary in the interference term, as all matrix elements already have a partner which is identical save for an angle-dependent term which has the opposite sign. We will then skip the kinetic energy, and move straight to the interaction.

4.8.1 Interaction

The Volkov central interaction is unchanged from the ${}^6\text{He}$ interference term. The tensor term has the Volkov matrix elements plugged into eqs.(3.141)-(3.153). For the spin-orbit interaction, we do have new matrix elements. The matrix elements of the spin orbit operator (eq.(4.410)) with the prefactor $-2\gamma r_0^2 V_{so}$ suppressed are:

$$\begin{aligned} \langle \alpha d | V_{LS} | + \alpha' \rangle &= \left(\frac{4\sqrt{\nu\omega n w}}{D'_\gamma(\nu, n, \omega, w)} \right)^{3/2} \frac{wd\delta[3\nu\omega + n(\nu + 2\omega)]}{12D'_\gamma(\nu, n, \omega, w)} \sin \vartheta \quad (4.476) \\ &\times \exp \left[-\frac{N}{72D'_\gamma(\nu, n, \omega, w)} \right], \end{aligned}$$

$$\langle \alpha d | V_{LS} | - \alpha' \rangle = - \langle \alpha d | V_{LS} | + \alpha' \rangle (x \rightarrow -x), \quad (4.477)$$

where

$$D'_\gamma(a, b, c, d) = (a + b)(c + d) + 2\gamma(a + b + c + d),$$

and

$$\begin{aligned} N &= 4\delta^2 \{ \nu n(\omega + w) + 4\omega w(\nu + n) + 8\gamma[(\nu + 4\omega)(n + w) + 9\nu\omega] \} \\ &+ 9wd^2 [(\nu + n)(\omega + 2\gamma) + 2\gamma\omega] - 24wd\delta x [\omega(\nu + n) + \gamma(2\omega - \nu)]. \end{aligned}$$

Resuming, we have:

$$\begin{aligned} \langle \alpha d | V_{LS} | \alpha' + \rangle &= - \left(\frac{4\sqrt{\nu\omega n w}}{D'_\gamma(\nu, n, \omega, w)} \right)^{3/2} \frac{wd\delta[3\nu\omega + n(\nu + 2\omega)]}{12D'_\gamma(\nu, n, \omega, w)} \sin \vartheta \\ &\times \exp \left[-\frac{N'}{72D'_\gamma(\nu, n, \omega, w)} \right], \end{aligned} \quad (4.478)$$

$$\langle \alpha d | V_{LS} | \alpha' - \rangle = - \langle \alpha d | V_{LS} | \alpha' + \rangle (x \rightarrow -x), \quad (4.479)$$

where

$$\begin{aligned} N' &= 4\delta^2 [(\nu + 4\omega)(nw + 2\gamma(n + w)) + \nu\omega(4n + w) + 18\gamma\nu\omega] \\ &+ 9wd^2[\nu(n + \omega) + 2\gamma(n + \nu + \omega)] + 12wd\delta x[\nu(\omega + n) + 2\gamma(\nu - 2\omega)]. \end{aligned}$$

Continuing:

$$\begin{aligned} \langle \alpha d | V_{LS} | + - \rangle &= \left(\frac{4w\sqrt{\nu\omega}}{D'_\gamma(\nu, w, \omega, w)} \right)^{3/2} \frac{wd\delta[3\nu\omega + w(\nu + 2\omega)]}{6D'_\gamma(\nu, w, \omega, w)} \sin \vartheta \\ &\times \exp \left[-\frac{T}{72D'_\gamma(\nu, w, \omega, w)} \right] \end{aligned} \quad (4.480)$$

$$\langle \alpha d | V_{LS} | - + \rangle = - \langle \alpha d | V_{LS} | + - \rangle (x \rightarrow -x). \quad (4.481)$$

where

$$\begin{aligned} T &= 4\delta^2 [w(\nu w + 4\omega w + 5\nu\omega) + 2\gamma(2\nu w + 8\omega w + 9\nu\omega)] \\ &+ 9wd^2[w(\nu + \omega) + 2\nu\omega + 4\gamma(\nu + \omega + 2w)] - 12wd\delta x(\nu w + 2\omega w + 3\nu\omega). \end{aligned}$$

These matrix elements are plugged into eqs.(3.135)-(3.140). We remind the reader that in the interference term, Greek letters refer to parameters of the alpha-deuteron configuration, while Latin letters are used for the parameters of the cigar configuration.

We have now addressed the tensor and spin-orbit interactions. What is left is the

Minnesota potential in the interference term of ${}^6\text{Li}$. As was mentioned before, the Minnesota potential has spin-dependent forces, and one must separate the terms into singlet and triplet terms, and this separation is not the same in the two studied nuclei.

In the interference term, the singlet part is:

$$\langle V_s \rangle_\alpha = \langle \alpha\alpha | V_s | \alpha'\alpha' \rangle \theta_{\alpha\alpha} \left[3\theta_{\alpha\alpha}\theta_{d+}\theta_{d-} - \frac{3}{2}\theta_{d\alpha}(\theta_{\alpha+}\theta_{d-} + \theta_{\alpha-}\theta_{d+}) \right], \quad (4.482)$$

$$\langle V_s \rangle_{\alpha^2 d+} = \langle \alpha d | V_s | +\alpha' \rangle \frac{3}{2}\theta_{\alpha\alpha}^2 (\theta_{\alpha\alpha}\theta_{d-} - \theta_{d\alpha}\theta_{\alpha-}), \quad (4.483)$$

$$\langle V_s \rangle_{\alpha^2 d-} = \langle \alpha d | V_s | -\alpha' \rangle \frac{3}{2}\theta_{\alpha\alpha}^2 (\theta_{\alpha\alpha}\theta_{d+} - \theta_{d\alpha}\theta_{\alpha+}), \quad (4.484)$$

$$\langle V_s \rangle_{\alpha\alpha\alpha+} = \langle \alpha\alpha | V_s | \alpha'+ \rangle \frac{3}{2}\theta_{\alpha\alpha}\theta_{d\alpha} (\theta_{\alpha-}\theta_{d\alpha} - \theta_{\alpha\alpha}\theta_{d-}), \quad (4.485)$$

$$\langle V_s \rangle_{\alpha\alpha\alpha-} = \langle \alpha\alpha | V_s | \alpha'- \rangle \frac{3}{2}\theta_{\alpha\alpha}\theta_{d\alpha} (\theta_{\alpha+}\theta_{d\alpha} - \theta_{\alpha\alpha}\theta_{d+}), \quad (4.486)$$

$$\langle V_s \rangle_{d\alpha\alpha\alpha} = \langle d\alpha | V_s | \alpha'\alpha' \rangle \theta_{\alpha\alpha} \left[3\theta_{d\alpha}\theta_{\alpha+}\theta_{\alpha-} - \frac{3}{2}\theta_{\alpha\alpha}(\theta_{\alpha+}\theta_{d-} + \theta_{\alpha-}\theta_{d+}) \right]. \quad (4.487)$$

The triplet component is:

$$\langle V_t \rangle_\alpha = \langle \alpha\alpha | V_t | \alpha'\alpha' \rangle \quad (4.488)$$

$$\times \left[3\theta_{\alpha\alpha}^2 \theta_{d+} \theta_{d-} + \theta_{d\alpha}^2 \theta_{\alpha+} \theta_{\alpha-} - \frac{3}{2} \theta_{\alpha\alpha} \theta_{d\alpha} (\theta_{\alpha+} \theta_{d-} + \theta_{\alpha-} \theta_{d+}) \right],$$

$$\langle V_t \rangle_{\alpha^2 d+} = \langle \alpha d | V_t | + \alpha' \rangle \frac{1}{2} \theta_{\alpha\alpha}^2 (5\theta_{\alpha\alpha} \theta_{d-} - 3\theta_{d\alpha} \theta_{\alpha-}), \quad (4.489)$$

$$\langle V_t \rangle_{\alpha^2 d-} = \langle \alpha d | V_t | - \alpha' \rangle \frac{1}{2} \theta_{\alpha\alpha}^2 (5\theta_{\alpha\alpha} \theta_{d+} - 3\theta_{d\alpha} \theta_{\alpha+}), \quad (4.490)$$

$$\langle V_t \rangle_{\alpha\alpha\alpha+} = \langle \alpha\alpha | V_t | \alpha'+ \rangle \frac{1}{2} \theta_{\alpha\alpha} \theta_{d\alpha} (\theta_{d\alpha} \theta_{\alpha-} - 3\theta_{\alpha\alpha} \theta_{d-}), \quad (4.491)$$

$$\langle V_t \rangle_{\alpha\alpha\alpha-} = \langle \alpha\alpha | V_t | \alpha'- \rangle \frac{1}{2} \theta_{\alpha\alpha} \theta_{d\alpha} (\theta_{d\alpha} \theta_{\alpha+} - 3\theta_{\alpha\alpha} \theta_{d+}), \quad (4.492)$$

$$\langle V_t \rangle_{d\alpha\alpha\alpha} = \langle d\alpha | V_t | \alpha'\alpha' \rangle \theta_{\alpha\alpha} \left[\theta_{d\alpha} \theta_{\alpha+} \theta_{\alpha-} - \frac{3}{2} \theta_{\alpha\alpha} (\theta_{\alpha+} \theta_{d-} + \theta_{\alpha-} \theta_{d+}) \right], \quad (4.493)$$

$$\langle V_t \rangle_{\alpha-d+} = -\langle \alpha d | V_t | + - \rangle \theta_{\alpha\alpha}^3 \theta_{d\alpha}, \quad (4.494)$$

$$\langle V_t \rangle_{\alpha+d-} = -\langle \alpha d | V_t | - + \rangle \theta_{\alpha\alpha}^3 \theta_{d\alpha}, \quad (4.495)$$

$$\langle V_t \rangle_{d\alpha d+} = -\langle dd | V_t | \alpha+ \rangle \theta_{\alpha\alpha}^3 \theta_{\alpha-}, \quad (4.496)$$

$$\langle V_t \rangle_{d\alpha d-} = -\langle dd | V_t | \alpha- \rangle \theta_{\alpha\alpha}^3 \theta_{\alpha+}, \quad (4.497)$$

$$\langle V_t \rangle_{d+d-} = \langle dd | V_t | + - \rangle \theta_{\alpha\alpha}^4, \quad (4.498)$$

$$\langle V_t \rangle_{\alpha+d\alpha} = \langle d\alpha | V_t | + \alpha' \rangle \theta_{\alpha\alpha}^2 (2\theta_{d\alpha} \theta_{\alpha-} - \theta_{\alpha\alpha} \theta_{d-}), \quad (4.499)$$

$$\langle V_t \rangle_{\alpha-d\alpha} = \langle d\alpha | V_t | - \alpha' \rangle \theta_{\alpha\alpha}^2 (2\theta_{d\alpha} \theta_{\alpha+} - \theta_{\alpha\alpha} \theta_{d+}), \quad (4.500)$$

$$\langle V_t \rangle_{\alpha+\alpha-} = \langle \alpha\alpha | V_t | \alpha'\alpha' \rangle \theta_{\alpha\alpha}^2 \theta_{d\alpha}^2, \quad (4.501)$$

$$\langle V_t \rangle_{d\alpha d\alpha} = \langle dd | V_t | \alpha'\alpha' \rangle \theta_{\alpha\alpha}^2 \theta_{\alpha+} \theta_{\alpha-}. \quad (4.502)$$

The matrix elements for these terms are the same as the Volkov matrix elements. These are plugged into the terms above, and summed together in order to calculate the expectation value of the Minnesota potential.

This completes our discussion of interactions in the interference term of ${}^6\text{Li}$. Next, we look at the electric quadrupole moment.

4.8.2 Electric quadrupole moment

In order to complete the calculation of the expectation value of the electric quadrupole moment, we need the contribution from the interference term. The quadrupole moment has been introduced in the previous sections on the subject, so here we just include the matrix elements of the operator in the interference term. As shown in eq.(4.415), there are one-body and two-body terms. The one-body terms are:

$$\langle \alpha | Q_0 | \alpha' \rangle = \theta_{\alpha\alpha} \frac{2\nu^2 (z_2 - Z)^2}{(\nu + n)^2}, \quad (4.503)$$

$$\langle \alpha | Q_0 | + \rangle = \theta_{\alpha+} f(w, \nu, \zeta, z_1), \quad (4.504)$$

$$\langle \alpha | Q_0 | - \rangle = \theta_{\alpha-} f(w, \nu, \zeta, z_2) (x \rightarrow -x), \quad (4.505)$$

$$\langle d | Q_0 | + \rangle = \theta_{d+} f(w, \omega, \zeta, z_2), \quad (4.506)$$

$$\langle d | Q_0 | - \rangle = \theta_{d-} f(w, \omega, \zeta, z_2) (x \rightarrow -x), \quad (4.507)$$

$$\langle d | Q_0 | \alpha' \rangle = \theta_{d\alpha} \frac{2\omega^2 (z_2 - Z)^2}{(\omega + n)^2}, \quad (4.508)$$

where f was defined in eq.(4.202).

The two-body terms are:

$$\langle \alpha\alpha | Q_0 | \alpha'\alpha' \rangle = \theta_{\alpha\alpha}^2 \frac{2\nu^2 (z_1 - Z)^2}{(\nu + n)^2}, \quad (4.509)$$

$$\langle \alpha d | Q_0 | + \alpha' \rangle = \theta_{\alpha\alpha} \theta_{d+} \frac{2\nu (z_1 - Z) [\omega(z_2 - Z) + wx(\zeta - Z)]}{(\nu + n)(\omega + w)}, \quad (4.510)$$

$$\langle \alpha d | Q_0 | - \alpha' \rangle = \theta_{\alpha\alpha} \theta_{d-} \frac{2\nu (z_1 - Z) [\omega(z_2 - Z) - wx(\zeta - Z)]}{(\nu + n)(\omega + w)}, \quad (4.511)$$

$$\langle \alpha\alpha|Q_0|\alpha'+\rangle = \theta_{\alpha\alpha}\theta_{\alpha+} \frac{2\nu(z_1 - Z) [\nu(z_1 - Z) + wx(\zeta - Z)]}{(\nu + n)(\nu + w)}, \quad (4.512)$$

$$\langle \alpha\alpha|Q_0|\alpha'-\rangle = \theta_{\alpha\alpha}\theta_{\alpha-} \frac{2\nu(z_1 - Z) [\nu(z_1 - Z) - wx(\zeta - Z)]}{(\nu + n)(\nu + w)}, \quad (4.513)$$

$$\langle \alpha d|Q_0|\alpha'\alpha'\rangle = \theta_{\alpha\alpha}\theta_{d\alpha} \frac{2\nu\omega(z_1 - Z)(z_2 - Z)}{(\nu + n)(\omega + n)}, \quad (4.514)$$

$$\langle dd|Q_0|\alpha'+\rangle = \theta_{d+}\theta_{d\alpha} \frac{2\omega(z_2 - Z) [\omega(z_2 - Z) + wx(\zeta - Z)]}{(\omega + n)(\omega + w)}, \quad (4.515)$$

$$\langle dd|Q_0|\alpha'-\rangle = \theta_{d-}\theta_{d\alpha} \frac{2\omega(z_2 - Z) [\omega(z_2 - Z) + wx(\zeta - Z)]}{(\omega + n)(\omega + w)}, \quad (4.516)$$

$$\begin{aligned} \langle d\alpha|Q_0|-\rangle = & \frac{\theta_{d+}\theta_{\alpha-}}{(\nu + w)(\omega + w)} [2\nu\omega(z_2 - Z)(z_1 - Z) \\ & + 2wx(\zeta - Z) [\nu(z_1 - Z) - \omega(z_2 - Z)] - w^2(\zeta - Z)^2(3x^2 - 1)], \end{aligned} \quad (4.517)$$

$$\begin{aligned} \langle d\alpha|Q_0|+\rangle = & \frac{\theta_{d-}\theta_{\alpha+}}{(\nu + w)(\omega + w)} [2\nu\omega(z_2 - Z)(z_1 - Z) \\ & - 2wx(\zeta - Z) [\nu(z_1 - Z) - \omega(z_2 - Z)] - w^2(\zeta - Z)^2(3x^2 - 1)], \end{aligned} \quad (4.518)$$

$$\langle dd|Q_0|+\rangle = \theta_{d+}\theta_{d-} \frac{2\omega^2(z_2 - Z)^2 - w^2(\zeta - Z)^2(3x^2 - 1)}{(\omega + w)^2}, \quad (4.519)$$

$$\langle d\alpha|Q_0|+\alpha'\rangle = \theta_{d\alpha}\theta_{\alpha+} \frac{2\omega(z_2 - Z) [\nu(z_1 - Z) + wx(\zeta - Z)]}{(\omega + n)(\nu + w)}, \quad (4.520)$$

$$\langle d\alpha|Q_0|-\alpha'\rangle = \theta_{d\alpha}\theta_{\alpha-} \frac{2\omega(z_2 - Z) [\nu(z_1 - Z) - wx(\zeta - Z)]}{(\omega + n)(\nu + w)}, \quad (4.521)$$

$$\langle \alpha\alpha|Q_0|+\rangle = \theta_{\alpha+}\theta_{\alpha-} \frac{2\nu^2(z_1 - Z)^2 - w^2(\zeta - Z)^2(3x^2 - 1)}{(\nu + w)^2}, \quad (4.522)$$

$$\langle dd|Q_0|\alpha'\alpha'\rangle = \theta_{d\alpha}^2 \frac{2\omega^2(z_2 - Z)^2}{(\omega + n)^2}. \quad (4.523)$$

These terms are summed together using the normal overlaps for the interference term (eqs.(3.56)-(3.61) and eqs.(3.62)-(3.76) for the two-body term), and divided by the norm. This completes the discussion of the interference term of ${}^6\text{Li}$, and indeed the Gaussian approximation of ${}^6\text{He}$ and ${}^6\text{Li}$ as individual nuclei. We just have one final section on the beta decay of ${}^6\text{He}$, which incorporates the interplay of both nuclei and configurations.

4.9 Beta decay

Beta decay is how the ${}^6\text{He}$ nucleus transforms into the stable ${}^6\text{Li}$ nucleus. We will start with some background on the subject, then apply it directly to our system.

4.9.1 Background

The process of nuclear beta decay transforms a nucleus to a neighboring nucleus in its isobaric chain:



The form of beta decay illustrated above is the one relevant for the present work, called beta-minus or negatron decay. For completeness, the other types of beta decay are beta-plus or positron decay



and electron capture:



The theory of beta decay was first formulated by Fermi in 1934 [55]. Later, it was found out that nuclear beta decay is just part of a class of reactions described by the so-called weak interaction. The weak interaction is mediated by very massive particles (80-90 times the mass of a nucleon), so at normal nuclear energies, Fermi's contact formulation is essentially valid. One can infer the selection rules from looking at eqs.(4.524) and (4.525). In both of those equations, the right-hand side, in addition to the daughter nucleus, contains two other particles. These particles are electrons (or positrons) and neutrinos (or antineutrinos). These particles are spin one-half particles, and thus can be emitted with total spin zero or total spin one. Since transitions are much more probable if no orbital angular momentum is carried away by the particles, we have two kinds of "allowed" beta decay. The spin zero case is called Fermi beta

decay, and the spin one case Gamov-Teller [56]. These selection rules are summarized here:

Fermi	Gamov – Teller
$\Delta J = 0$	$\Delta J = 0, 1$ (but not $0 \rightarrow 0$)
$\pi_i \pi_f = +1$	$\pi_i \pi_f = +1$

ΔJ is the difference in total angular momentum of the initial and final states, $|\mathbf{J}_f - \mathbf{J}_i|$, and $\pi_i \pi_f$ is the product of the parities of the initial and final states. With these selection rules, we have the two kinds of allowed beta decay transitions, and can calculate transition probabilities.

In beta decay, experimenters often measure the half-life of the given state or nucleus. The half-life is

$$t_{1/2} = \frac{\ln 2}{T_{fi}}, \quad (4.527)$$

where T_{fi} is the transition rate between a specific set of initial and final states. Inserting the expression for T_{fi} , eq.(4.527) simplifies to

$$t_{1/2} = \frac{K_0}{f_0 (B_F + B_{GT})}, \quad (4.528)$$

where K_0 is a collection of fundamental constants:

$$K_0 = \frac{2\pi^3 \hbar^7 \ln 2}{m_e^5 c^4 G_F^2} = 6147\text{s}, \quad (4.529)$$

f_0 is a dimensionless phase-space integral involving the lepton kinematics in the Coulomb field of the daughter nucleus (known as the Fermi integral), and B_F and B_{GT} are the reduced transition probabilities, analogous to the $B(E2)$ of the electro-

magnetic transitions. They are:

$$B_F = \frac{g_V^2}{2J_i + 1} |\mathcal{M}_F|^2 \quad B_{GT} = \frac{g_A^2}{2J_i + 1} |\mathcal{M}_{GT}|^2, \quad (4.530)$$

where g_V and g_A are the vector and axial vector coupling constants, respectively, J_i is the total spin of the initial state, and \mathcal{M} is the matrix element that contains all the nuclear information. A simpler quantity to work with than the half-life is a quantity that removes the Fermi integral:

$$\log ft = \log f_0 t_{1/2}, \quad (4.531)$$

where the logarithm is used because ft is often a very large number.

The matrix elements in eq.(4.530) involve the Fermi and Gamov-Teller transition operators. For B_F , we have

$$|\mathcal{M}_F|^2 = |\langle f | T_{\pm} | i \rangle|^2, \quad (4.532)$$

where

$$T_{\pm} = \sum_k t_{\pm}, \quad (4.533)$$

where t_{\pm} is the isospin raising or lowering operator and is summed over all nucleons.

The Gamov-Teller operator is

$$\hat{O}_{GT} = \boldsymbol{\sigma} t_{\pm}, \quad (4.534)$$

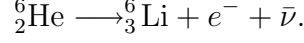
where $\boldsymbol{\sigma}$ is the spin vector, and t_{\pm} is the isospin raising or lowering operator as before.

This operator is also a one-body operator, and is summed over all nucleons.

We now have all the information we need in order to proceed to our specific problem, the decay of ${}^6\text{He}$.

4.9.2 Helium-6 beta decay

The beta decay of ${}^6\text{He}$ proceeds like in eq.(4.524):



Given that ${}^6\text{He}$ has a ground state of 0^+ , and the ground state of ${}^6\text{Li}$ is a 1^+ state, we have a pure Gamov-Teller decay. A decay to any of the excited states of lithium would be a forbidden decay, as $\Delta J > 1$. We then just need to concern ourselves with the Gamov-Teller transition from the previous section.

Our goal is to calculate B_{GT} , which for our specific case is:

$$B_{GT} = \sum_{\nu, m_f} \left| \langle {}^6\text{Li}(1m_f) | \sum_k \sigma_\nu^k t_+^k | {}^6\text{He}(00) \rangle \right|^2, \quad (4.535)$$

where the sums go over k , the neutrons in ${}^6\text{He}$, m_f , the magnetic sub-states of the final state in ${}^6\text{Li}$, and ν , which is the index of the Pauli spin matrices. We work with the following representation of the Pauli matrices:

$$\boldsymbol{\sigma} = \sigma_x \hat{\mathbf{x}} + \sigma_y \hat{\mathbf{y}} + \sigma_z \hat{\mathbf{z}} \quad (4.536)$$

$$= \frac{1}{2} (\sigma_+ + \sigma_-) \hat{\mathbf{x}} + \frac{1}{2i} (\sigma_+ - \sigma_-) \hat{\mathbf{y}} + \sigma_z \hat{\mathbf{z}}, \quad (4.537)$$

where

$$\sigma_+ = \begin{pmatrix} 0 & 2 \\ 0 & 0 \end{pmatrix} \quad \sigma_- = \begin{pmatrix} 0 & 0 \\ 2 & 0 \end{pmatrix}, \quad (4.538)$$

and σ_z is the normal z term of the Pauli matrices. We then have to calculate the overlap of ${}^6\text{Li}$ with a ${}^6\text{He}$ nucleus where a neutron has been changed into a proton. To guide our calculation, we will begin by verifying the Gamov-Teller sum rule for our system.

For Gamov-Teller decays, a sum rule exists that states:

$$\sum_f [B_{GT+}^{(i,f)} - B_{GT-}^{(i,f)}] = 3(N_i - Z_i), \quad (4.539)$$

where the sum is over the final states, and the sum rule itself is the difference in the B_{GT} value for a given initial state to either β^+ or β^- decay. The result depends on the proton and neutron numbers of the initial state. In the case of ${}^6\text{He}$, the sum rule is equal to six. To see if we can obtain this result, we first look back at our starting equation, eq.(4.535). In principle, because of the sum over spin projections and final m states, we would have nine terms in the sum. However, by re-writing the sigma operator in terms of the raising and lowering operators, we can reduce the number. Since the σ_{\pm} operators flip the spin of a particle, they can only connect ${}^6\text{He}$'s ground state with the ± 1 projections of the final state in ${}^6\text{Li}$, while the σ_z operator connects to the longitudinal projection of the final state. The sum in eq.(4.535) runs over all the neutrons in ${}^6\text{He}$, but if it acts on a neutron in the alpha particle, the matrix element vanishes. This is because it creates a third proton inside the alpha particle where there are already two s -wave protons, thus a proton cannot be created there without an excitation in orbital angular momentum, which is not permitted for an allowed Gamov-Teller transition, so we can simplify our calculation by considering the external neutrons only.

In calculating the sum rule, we begin with the term that corresponds to σ_x , which connects to the $m_f = \pm 1$ final state in ${}^6\text{Li}$:

$$\langle {}^6\text{Li}(1 \pm 1) | \sigma_x t_+ | {}^6\text{He}(00) \rangle = \frac{1}{2} \langle 1 \pm 1_{Li} | (\sigma_+ + \sigma_-) | 00_{\text{He}} \rangle. \quad (4.540)$$

Now we work with just the $m_f = 1$ final state. Only the σ_+ term contributes, and

consider only the external particles. We write in first quantization to be clear:

$$\frac{1}{4}\langle(n_+p_+ - p_+n_+)|\sigma_+t_+|(n_+n_- - n_-n_+)\rangle = \frac{1}{2}\langle(n_+p_+ - p_+n_+)|(n_+p_+ - p_+n_+)\rangle = 1. \quad (4.541)$$

This equals one only because we have assumed, in this ideal case, that all parameters are identical between the two nuclei, and then the overlap can be one. Now, for the $m_f = -1$ final state:

$$\frac{1}{4}\langle(n_-p_- - p_+n_+)|\sigma_-t_+|(n_+n_- - n_-n_+)\rangle = \frac{1}{2}\langle(n_-p_- - p_+n_+)|(p_-n_- - n_-p_-)\rangle = -1. \quad (4.542)$$

When summed together, the result for σ_x is zero. We now look at the σ_y terms. For σ_y , our starting point is

$$\frac{1}{2i}\langle 1 \pm 1_{\text{Li}} | (\sigma_+ - \sigma_-) | 00_{\text{He}} \rangle. \quad (4.543)$$

The action of the operators is the same as for σ_x , but there is an extra minus sign, which makes the result equal to $2i$. We then take the magnitude squared, which is four. We have two thirds of the expected sum, with one term left, the σ_z term.

The wave function of the longitudinal state of ${}^6\text{Li}$ looks like this in first quantization (again, referring only to the external particles):

$$|\psi({}^6\text{Li}); 10\rangle = \frac{1}{2}(|p_+n_- \rangle + |p_-n_+ \rangle - |n_+p_- \rangle - |n_-p_+ \rangle), \quad (4.544)$$

where p is a proton and n is a neutron, and the \pm refer to spin projections. One can see that the wave function is symmetric with regards to spin exchange, and antisymmetric with respect to the “flavor” exchange of proton and neutron (the state is an isosinglet). We now turn to the action of the σ_z operator which connects ${}^6\text{He}$ with with $m_f = 0$ state in ${}^6\text{Li}$. We begin with

$$\frac{1}{2\sqrt{2}}\langle p_+n_+ + p_-n_+ - n_+p_- - n_-p_+ | \sigma_z t_+ | n_+n_- - n_-n_+ \rangle. \quad (4.545)$$

After the operator acts, the result is

$$\frac{1}{2\sqrt{2}}\langle p_+n_+ + p_-n_+ - n_+p_- - n_-p_+ | p_+n_- - n_+p_- + p_-n_+ - n_-p_+ \rangle = \sqrt{2}. \quad (4.546)$$

We then square the result, we get two, which then completes the sum rule.

Now that we have verified the sum rule, we can look into the overlap of our lithium and helium wavefunctions. We must find the overlap of alpha-dineutron with alpha-deuteron, cigar with cigar, and the cross terms. Each overlap is of the form similar to that which was calculated in the interference term (eq.(3.49)), except it is an overlap of a configuration of ${}^6\text{Li}$ with a configuration of ${}^6\text{He}$ where one of the neutrons has been turned into a proton.

We will begin with the alpha-dineutron alpha-deuteron overlap. For clarity, we will call the alpha-two-particle cluster configurations c_1 , the first configuration, and the cigar configurations c_2 . We then want to calculate:

$$\langle \psi_1(\text{Li}) | \psi_1(\text{He}) \rangle = \frac{\theta_{\alpha\alpha}^2 (\theta_{\alpha\alpha}\theta_{dd} - \theta_{d\alpha}\theta_{\alpha d})^2}{\sqrt{\langle \psi_1(\text{Li}) | \psi_1(\text{Li}) \rangle \langle \psi_1(\text{He}) | \psi_1(\text{He}) \rangle}}. \quad (4.547)$$

The denominator in eq.(4.547) contains the usual normalizations of both systems. We now have some new overlaps to list, and we will need a new convention for the symbols of each configuration and nucleus. Greek letters will refer to parameters in lithium, and Latin letters will refer to parameters in helium. Parameters will also be labeled with subscripts. A subscript one will indicate the first configuration of the particular nucleus, and a subscript two will indicate the cigar configuration. With

that in mind, we list the overlaps used in eq.(4.547):

$$\theta_{\alpha\alpha} = \langle \alpha | \alpha' \rangle = \left(\frac{2\sqrt{\nu_1 n_1}}{\nu_1 + n_1} \right)^{3/2} \exp \left[-\frac{\nu_1 n_1 (\delta_1^2 + d_1^2 - 2d_1 \delta_1 x)}{18(\nu_1 + n_1)} \right], \quad (4.548)$$

$$\theta_{dd} = \langle d | d' \rangle = \left(\frac{2\sqrt{\omega_1 w_1}}{\omega_1 + w_1} \right)^{3/2} \exp \left[-\frac{2\omega_1 w_1 (\delta_1^2 + d_1^2 - 2d_1 \delta_1 x)}{9(\omega_1 + w_1)} \right], \quad (4.549)$$

$$\theta_{\alpha d} = \langle \alpha | d' \rangle = \left(\frac{2\sqrt{\nu_1 w_1}}{\nu_1 + w_1} \right)^{3/2} \exp \left[-\frac{\nu_1 w_1 (\delta_1^2 + 4d_1^2 + 4\delta_1 d_1 x)}{18(\nu_1 + w_1)} \right], \quad (4.550)$$

$$\theta_{d\alpha} = \langle d | \alpha' \rangle = \left(\frac{2\sqrt{\omega_1 n_1}}{\omega_1 + n_1} \right)^{3/2} \exp \left[-\frac{\omega_1 n_1 (4\delta_1^2 + d_1^2 + 4\delta_1 d_1 x)}{18(\omega_1 + n_1)} \right]. \quad (4.551)$$

These are the overlaps contained in eq.(4.547). We then look at the transition between the two cigar configurations:

$$\langle \psi_2(\text{Li}) | \psi_2(\text{He}) \rangle = \frac{\theta_{\alpha\alpha}^4 (\theta_{nn}^2 + \theta_{\pm}^2) + 2\theta_{\alpha\alpha}^2 \theta_{\alpha n}^2 \theta_{n\alpha}^2 - 2\theta_{\alpha\alpha}^3 \theta_{\alpha n} \theta_{n\alpha} (\theta_{nn} + \theta_{\pm})}{\sqrt{\langle \psi_2(\text{Li}) | \psi_2(\text{Li}) \rangle \langle \psi_2(\text{He}) | \psi_2(\text{He}) \rangle}}. \quad (4.552)$$

The overlap in the above equation are:

$$\theta_{\alpha\alpha} = \langle \alpha | \alpha' \rangle = \left(\frac{2\sqrt{\nu_2 n_2}}{\nu_2 + n_2} \right)^{3/2}, \quad (4.553)$$

$$\theta_{nn} = \langle \pm | \pm' \rangle = \left(\frac{2\sqrt{\omega_2 w_2}}{\omega_2 + w_2} \right)^{3/2} \exp \left[-\frac{\omega_2 w_2 (\delta_2^2 + d_2^2 - 2\delta_2 d_2 x)}{8(\omega_2 + w_2)} \right], \quad (4.554)$$

$$\theta_{\pm} = \langle \pm | \mp' \rangle = \left(\frac{2\sqrt{\omega_2 w_2}}{\omega_2 + w_2} \right)^{3/2} \exp \left[-\frac{\omega_2 w_2 (\delta_2^2 + d_2^2 + 2\delta_2 d_2 x)}{8(\omega_2 + w_2)} \right], \quad (4.555)$$

$$\theta_{\alpha n} = \langle \alpha | n' \rangle = \left(\frac{2\sqrt{\nu_2 w_2}}{\nu_2 + w_2} \right)^{3/2} \exp \left[-\frac{\nu_2 w_2 d_2^2}{8(\nu_2 + w_2)} \right], \quad (4.556)$$

$$\theta_{n\alpha} = \langle n | \alpha' \rangle = \left(\frac{2\sqrt{\omega_2 n_2}}{\omega_2 + n_2} \right)^{3/2} \exp \left[-\frac{\omega_2 n_2 \delta_2^2}{8(\omega_2 + n_2)} \right]. \quad (4.557)$$

The next transition is from the cigar configuration of ${}^6\text{He}$ to the alpha-deuteron configuration of ${}^6\text{Li}$. The form of the matrix element is:

$$\langle \psi_1(\text{Li}) | \psi_2(\text{He}) \rangle = -\frac{\sqrt{2}\theta_{\alpha\alpha}^2 [\theta_{\alpha\alpha}^2 \theta_{d+} \theta_{d-} + \theta_{d\alpha}^2 \theta_{\alpha+} \theta_{\alpha-} - \theta_{\alpha\alpha} \theta_{d\alpha} (\theta_{\alpha+} \theta_{d-} + \theta_{\alpha-} \theta_{d+})]}{\sqrt{\langle \psi_1(\text{Li}) | \psi_1(\text{Li}) \rangle \langle \psi_2(\text{He}) | \psi_2(\text{He}) \rangle}}. \quad (4.558)$$

The minus sign makes the overlap equal to positive one when all parameters are equal

and the distances are set to zero. The overlaps are:

$$\theta_{\alpha\alpha} = \langle \alpha | \alpha' \rangle = \left(\frac{2\sqrt{\nu_1 n_2}}{\nu_1 + n_2} \right)^{3/2} \exp \left[-\frac{\nu_1 n_2 \delta_1^2}{18(\nu_1 + n_2)} \right], \quad (4.559)$$

$$\theta_{d+} = \langle d | +' \rangle = \left(\frac{2\sqrt{\omega_1 w_2}}{\omega_1 + w_2} \right)^{3/2} \exp \left[-\frac{\omega_1 w_2 (16\delta_1^2 + 9d_2^2 - 24\delta_1 d_2 x)}{72(\omega_1 + w_2)} \right], \quad (4.560)$$

$$\theta_{d-} = \langle d | -' \rangle = \left(\frac{2\sqrt{\omega_1 w_2}}{\omega_1 + w_2} \right)^{3/2} \exp \left[-\frac{\omega_1 w_2 (16\delta_1^2 + 9d_2^2 + 24\delta_1 d_2 x)}{72(\omega_1 + w_2)} \right], \quad (4.561)$$

$$\theta_{\alpha+} = \langle \alpha | +' \rangle = \left(\frac{2\sqrt{\nu_1 w_2}}{\nu_1 + w_2} \right)^{3/2} \exp \left[-\frac{\nu_1 w_2 (4\delta_1^2 + 9d_2^2 + 12\delta_1 d_2 x)}{72(\nu_1 + w_2)} \right], \quad (4.562)$$

$$\theta_{\alpha-} = \langle \alpha | -' \rangle = \left(\frac{2\sqrt{\nu_1 w_2}}{\nu_1 + w_2} \right)^{3/2} \exp \left[-\frac{\nu_1 w_2 (4\delta_1^2 + 9d_2^2 - 12\delta_1 d_2 x)}{72(\nu_1 + w_2)} \right], \quad (4.563)$$

$$\theta_{d\alpha} = \langle d | \alpha' \rangle = \left(\frac{2\sqrt{\omega_1 n_2}}{\omega_1 + n_2} \right)^{3/2} \exp \left[-\frac{2\omega_1 n_2 \delta_1^2}{9(\omega_1 + n_2)} \right]. \quad (4.564)$$

Finally, we have the transition from the alpha-dineutron of ${}^6\text{He}$ to the cigar configuration of ${}^6\text{Li}$. The matrix element is:

$$\langle \psi_2(\text{Li}) | \psi_1(\text{He}) \rangle = -\frac{\sqrt{2}\theta_{\alpha\alpha} [\theta_{\alpha\alpha}^2 \theta_{+d} \theta_{-d} + \theta_{n\alpha}^2 \theta_{+\alpha} \theta_{-\alpha} - \theta_{\alpha\alpha} \theta_{n\alpha} (\theta_{+\alpha} \theta_{-d} + \theta_{-\alpha} \theta_{+d})]}{\sqrt{\langle \psi_2(\text{Li}) | \psi_2(\text{Li}) \rangle \langle \psi_1(\text{He}) | \psi_1(\text{He}) \rangle}}. \quad (4.565)$$

The overlaps are:

$$\theta_{\alpha\alpha} = \langle \alpha | \alpha' \rangle = \left(\frac{2\sqrt{\nu_2 n_1}}{\nu_2 + n_1} \right)^{3/2} \exp \left[-\frac{\nu_2 n_1 d_1^2}{18(\nu_2 + n_1)} \right], \quad (4.566)$$

$$\theta_{+d} = \langle + | d' \rangle = \left(\frac{2\sqrt{\omega_2 w_1}}{\omega_2 + w_1} \right)^{3/2} \exp \left[-\frac{\omega_2 w_1 (9\delta_2^2 + 16d_1^2 - 24\delta_2 d_1 x)}{72(\omega_2 + w_1)} \right], \quad (4.567)$$

$$\theta_{-d} = \langle - | d' \rangle = \left(\frac{2\sqrt{\omega_2 w_1}}{\omega_2 + w_1} \right)^{3/2} \exp \left[-\frac{\omega_2 w_1 (9\delta_2^2 + 16d_1^2 + 24\delta_2 d_1 x)}{72(\omega_2 + w_1)} \right], \quad (4.568)$$

$$\theta_{+\alpha} = \langle + | \alpha' \rangle = \left(\frac{2\sqrt{\omega_2 n_1}}{\omega_2 + n_1} \right)^{3/2} \exp \left[-\frac{\omega_2 n_1 (9\delta_2^2 + 4d_1^2 + 12\delta_2 d_1 x)}{72(\omega_2 + n_1)} \right], \quad (4.569)$$

$$\theta_{-\alpha} = \langle - | \alpha' \rangle = \left(\frac{2\sqrt{\omega_2 n_1}}{\omega_2 + n_1} \right)^{3/2} \exp \left[-\frac{\omega_2 n_1 (9\delta_2^2 + 4d_1^2 - 12\delta_2 d_1 x)}{72(\omega_2 + n_1)} \right], \quad (4.570)$$

$$\theta_{n\alpha} = \langle n | \alpha' \rangle = \left(\frac{2\sqrt{\omega_2 n_1}}{\omega_2 + n_1} \right)^{3/2} \exp \left[-\frac{2\omega_2 n_1 d_1^2}{9(\omega_2 + n_1)} \right]. \quad (4.571)$$

We now have all the overlaps of all the configurations. The total matrix element

depends on these overlaps as well as the coefficients of the individual coefficients in their wave functions:

$$\langle \Psi(\text{Li}) | \sigma t_+ | \Psi(\text{He}) \rangle = c_{1\text{Li}} c_{1\text{He}} \mathfrak{M}_{11} + c_{2\text{Li}} c_{2\text{He}} \mathfrak{M}_{22} + c_{1\text{Li}} c_{2\text{He}} \mathfrak{M}_{21} + c_{2\text{Li}} c_{1\text{He}} \mathfrak{M}_{12}, \quad (4.572)$$

where \mathfrak{M}_{if} is shorthand for the overlap matrix elements given above, and the first subscript is the initial configuration and the second subscript is the final configuration. The coefficients c_i are determined by the minimization of the expectation values of the Hamiltonians of the individual nuclei. Since the overlap does not depend on the magnetic sub-states of ${}^6\text{Li}$, the result of eq.(4.572) is squared, then multiplied by six to obtain the final result for B_{GT} . Thus, if the overlap was a perfect one, then we would obtain the sum-rule of six. The result is then plugged into the equation

$$\log ft = \log \left(\frac{6147s}{g_A^2 B_{GT}} \right), \quad (4.573)$$

where the axial-vector coupling constant g_A is equal to 1.2695 [57], which gives the $\log ft$ value for the beta decay of ${}^6\text{He}$.

This concludes the chapter which shows the results of the Gaussian approximation in the two systems of interest in this work. In the next chapter, we will show the numerical results of the calculations and compare them with experiment and other theories.

Chapter 5

Numerical Results

In this chapter, we show the numerical results of the calculations outlined in the previous two chapters. They are then discussed and compared with experimental findings and the results of other theories. The results will be presented in several tables. The first to be discussed will be ${}^6\text{He}$, beginning with the optimal variational parameters and relative weights of the configurations, then energies, and finally other observables. We will then follow with the same for ${}^6\text{Li}$.

5.1 Helium-6

5.1.1 Spatial parameters

We begin the discussion of the ${}^6\text{He}$ results with showing the optimal values of the variational parameters for the ground and excited states, which are displayed in Table 5.1. The variational parameters are the two oscillator strengths, ν and ω , and the alpha-external neutron distance d . They are shown in the table for three potentials: Volkov V1 (the column V1), Volkov V2 (column V2), and the Minnesota potential (column M).

The table shows that there is little difference in the minimization between the two sets of Volkov parameters, and indeed the Minnesota parameters are also similar,

Table 5.1: This table shows the optimized variational parameters of the two configurations of ${}^6\text{He}$ for the three different potentials considered: Volkov V1 (V1), Volkov V2 (V2), and Minnesota (M).

	ν (fm^{-2})			ω (fm^{-2})			d (fm)		
	V1	V2	M	V1	V2	M	V1	V2	M
α -2n	0.51	0.51	0.56	0.40	0.40	0.35	3.71	3.71	3.71
cigar	0.50	0.50	0.50	0.48	0.48	0.45	1.61	1.61	1.51
α -2n(2^+)	0.50	0.50	0.56	0.30	0.30	0.30	3.01	3.01	2.41
cigar(2^+)	0.50	0.50	0.51	0.40	0.40	0.42	1.01	1.01	0.91

even for the excited state. This is not too surprising, as was seen in the plots of the previous chapter, there was not a lot of qualitative difference between the potentials. There is an interesting contrast between the two configurations when it comes to the location of the minimum. In the alpha-dineutron, the alpha-neutron distance is rather large, and if one looks at the kinetic energy plot (Figure 4.5), one can see that the kinetic energy is still close to its asymptotic value, meaning the neutrons are still mostly all in s -waves. In the cigar configuration, however, if one looks at its kinetic energy (Figure 4.17), at the point where the minimum occurs, the kinetic energy is much higher than its asymptotic value, which means that two of the neutrons spend most of their time in the p -shell. The minimum is at a smaller value of d in the cigar configuration because the potential falls off faster in this configuration. This is due to the fact that as d increases, not only is the attraction between the external neutron and the alpha particle decreasing, but the attraction from the other neutron decreases even faster, which keeps the neutrons closer to the alpha particle in the cigar configuration.

5.1.2 Energy

The energy results and relative weights of the configurations are shown in Table 5.2. One can see when comparing the results obtained with the two Volkov potentials, that there is consistently about a 1.5 MeV difference in the energy calculations, and a 9.5 MeV difference between the alpha-dineutron configuration and the cigar con-

figuration. This in turn gives similar results for the relative contributions of each configuration in the overall wave function. In the Minnesota potential, the two configurations are much closer in energy. This is because ${}^6\text{He}$ is built up mostly of singlet pairs, which have a much weaker attraction in the Minnesota potential. It is then less favorable to have the two external neutrons close to each other than with the Volkov potentials. Thus, the alpha-dineutron configuration is less dominant in the system described by the Minnesota potentials. In the case of the weights of the configurations, the balance of the wave function (since the sum of the two c_i^2 's is not one) is carried by the interference term, which means there is a fairly large overlap between the two spatial configurations (around 32% in the case of the Volkov potentials and 39% in the case of the Minnesota potential). As for the energy of the 2^+ excited state, the origin of the large gap is the alpha-dineutron configuration, and specifically the kinetic energy. At the larger values of d , the Volkov potentials do not greatly distinguish between the two levels, but the kinetic energy does, which contributes the most to the large gap between the ground state and first excited state. In the case of the Minnesota potential, the source is in the interference term. Though the two individual configurations match up well with the observed gap, the interference term is still close to 40% of the wave function, and it has a much larger gap, which then creates the large overall gap seen in the table. For considering the excited state, one often needs a larger amount of input than to describe the ground state. For the excited state, the spin-triplet configuration of the external neutrons may become important. According to a few-body calculation [58], the spin-triplet configuration accounts for 32% of the wavefunction of the 2^+ excited state. Also, eventually, triton clustering would also become important, but we don't expect triton clustering to be important just 2 MeV above the ground state.

Other theoretical models have also done well in reproducing the binding energy of ${}^6\text{He}$. The Fermionic Molecular Dynamics (FMD) approach obtains a -29.1 MeV value when working with the realistic Argonne V18 potential [59]. A similar method, An-

Table 5.2: The total energy results for the individual configurations and the minimized results, plus the weights of the configurations in the wave function and the excitation energy of the 2^+ excited state. The calculated energies of the alpha particle and the alpha particle plus dineutron are provided for comparison.

	$\langle E \rangle$ (MeV)			c_i^2			$E(2^+)$ (MeV)		
	V1	V2	M	V1	V2	M	V1	V2	M
α -2n	-25.7	-27.2	-19.1	.598	.607	.441	+3.891	+3.770	+1.932
cigar	-16.3	-17.7	-14.3	.0864	.0824	.168	+1.665	+1.571	+1.002
overall	-27.2	-28.7	-22.1	N/A			+4.990	+4.912	+4.714
exp [31]	-29.3			N/A			+1.797		
α	-28.0	-28.9	-25.1	N/A			N/A		
α +2n	-26.1	-27.2	-19.7	N/A			N/A		

tisymmetrized Molecular Dynamics (AMD), obtains -28.6 MeV with the Volkov V2 interaction (modified with the addition of Bartlett and Heisenberg exchange terms), the Coulomb interaction and a spin-orbit interaction (which does not vanish in their formulation) [60]. AMD calculations also obtained excellent agreement for the excited state of ${}^6\text{He}$ with a result of +1.86 MeV relative to the ground state. Unsurprisingly, the *ab initio* models, Variational and Green's Function Monte Carlo (VMC and GFMC) [33, 61] and No-Core Shell Model (NCSM) [32] achieve almost perfect agreement with experiment with their energy results. These models have many more parameters, including some kind of three-body interaction in order to achieve agreement with experiment. Their results for two-body forces only are -23.8 MeV (Argonne V18) [61] and -26.7 (CD-Bonn 2000), respectively.

As for the relative contributions of the two configurations, FMD obtains two minima in their calculations, corresponding to our cigar and dineutron configurations. In their results, the cigar configuration only lies 1.1 MeV above the alpha-dineutron configuration. Thus, they agree that the dominant configuration would be the alpha-dineutron configuration, but not nearly as dominant as in our results. This could be a result of the interaction, as we have seen with a more realistic interaction (the Minnesota potential), the two configurations are much closer in energy compared to the Volkov potential results, so perhaps we would obtain a similar result with a more

complicated interaction.

Another point of view is expressed by Bertulani and Hussein [62]. From electromagnetic dissociation data, they have extracted a $B(E1)$ value, and from that determined the opening angle between the neutrons in ${}^6\text{He}$ to be 83° . This is an interesting result, as that angle is almost halfway between our two configurations. However, the opening angle of 83° also leads to a matter radius that is much larger than the experimental matter radius, so the question seems far from resolved. A mean field calculation studying dineutron correlations [63] found both cigar-like and dineutron correlations in ${}^6\text{He}$, both of which were dominated by spin singlets. They also found more particle density in the dineutron configuration than the cigar configuration, but their results were obtained with Hartree-Fock-Bogoliubov model with Quasi-particle Random Phase Approximation, which has questionable validity for a six-particle system.

Experiments have also been done in order to try and determine the dominant component of the ${}^6\text{He}$ wave function. An experiment that looked at ${}^6\text{He}$ break-up on a ${}^{209}\text{Bi}$ target found that the cross section for one neutron transfer was one-fourth that of the two-neutron transfer [64]. Another experiment looked explicitly for one and two-neutron transfer with a reaction on copper, and its preliminary results show the two-neutron cross section is greater by two orders of magnitude [29]. Most experiments use the dineutron model in their analysis to calculate things such as reaction cross sections [65], but this has more to do with the ease of the calculation than a completely accurate structural picture of ${}^6\text{He}$. In other words, the geometrical picture of ${}^6\text{He}$ is still an open question, but from the current results, the cluster picture appears more adequate.

5.1.3 Radii and other observables

Table 5.3 shows our results for the charge radius, matter radius, and $B(E2); 0^+ \rightarrow 2^+$ for ${}^6\text{He}$, and includes experimental results and the results of other theoretical models.

As before, for our results, we divide them into columns for each of the different potentials, and show results for each individual configuration. Configuration results for the $B(E2)$ are not really applicable since the transition links both configurations. Items in the table marked “N/A” in the rows for other theoretical results mean the author is unaware of results for that particular quantity.

When looking at our results for the charge radius, the result obtained in the alpha-dineutron configuration most closely matches the experimentally observed number. The cigar configuration is much smaller, since the charge resides at the center-of-mass in this configuration, and thus should just be the size of the alpha cluster. The alpha is enlarged in our model slightly, which gives the value shown in the table compared to the measured 1.67 fm for the alpha particle. This is not a problem, as the presence of the neutrons could certainly cause the alpha particle to swell when compared to an isolated alpha. An enlarged alpha could better overlap with the somewhat distant external neutrons. The cigar component is a small part of the wave function, but the interference term, which comprises 32% of the wave function in the case of the Volkov potentials contributes an even smaller value, which accounts for the slightly undersized charge radius. Since the interference and cigar configurations account for an even larger part of the wave function calculated with the Minnesota, both the charge and matter radii obtained with these wave functions are small. The matter radius calculated with the Volkov potentials is satisfactory, especially when one considers the wide dispersion of experimental values that have been reported. Values of 2.26 [66], 2.33 [67], and 2.52 [68] have also been published from experiments performed in the late 1980s and early 1990s. The other theories also do well for the radii, especially the *ab initio* models. It should be noted that the AMD calculations add constraints in order to fit matter radii, so it is no surprise that they can produce a large neutron radius.

Our result for the $B(E2)$ is comparable with other theories and experiment, but there is a large spread of results. The experiment is a difficult one because the 2^+ state

Table 5.3: Results for the charge radius (r_{ch}), matter radius (r_m), and $B(E2)$ calculated with the three different potentials discussed in this work. Experimental values and the values of other theoretical models are also shown. Experimental uncertainties are shown in parentheses after the quoted value.

	$\sqrt{r_{ch}^2}$ (fm)			$\sqrt{r_m^2}$ (fm)			$B(E2)0^+ \rightarrow 2^+$ ($e^2\text{fm}^4$)		
	V1	V2	M	V1	V2	M	V1	V2	M
α -2n	2.08	2.08	2.05	2.51	2.52	2.36	N/A	N/A	N/A
cigar	1.75	1.75	1.75	2.14	2.14	2.14	N/A	N/A	N/A
overall	1.99	1.98	1.91	2.40	2.40	2.26	2.891	2.932	2.305
exp	2.05(1) [70]			2.48(3) [71]			5.4(7) [64], 3.2(6) [69]		
AMD	N/A			2.37 [60]			N/A		
FMD	2.02 [59]			2.42 [59]			N/A		
GFMC	2.05 [72]			N/A			9.05 [73]		
NCSM	2.03 [74]			N/A			1.056 [32]		

is above the alpha- $n - n$ threshold, and the experiments report varying amounts of model dependence in their results (more so in the older experiment [69]). To add to the theoretical results, we quote a few-body calculation, which gives a $B(E2)$ of around $1.0 e^2 \text{ fm}^4$ at the resonance, then grows as more of the continuum is included [58]. As mentioned, this is a difficult experiment, and it seems more experiments should be done before any consensus will be formed on this process.

5.1.4 Asymptotics

Loosely-bound, few-body systems are unique in many ways, one of which is the asymptotic behavior of the wave function. Since the external particles, in this case neutrons, exist further away from the tightly bound core than the typical range of the nuclear force (1-2 fm), they are in the classically forbidden region. Particles in the classically forbidden region should have exponential asymptotic behavior. In our formulation so far, all particles have Gaussian asymptotics. We wanted to test to see what kind of impact these asymptotics might have.

We reasoned that these asymptotics are first most appropriate for the alpha-dineutron configuration. Our minimum in energy occurs at 3.7 fm, which is far into the classically forbidden region. The cigar configuration is more compact, and has a

minimum at 1.6 fm, which is a borderline case. We also decided to check the effect in the body-fixed frame. Adding the exponential tail destroys the analyticity of the calculations, and further including angular momentum projection is extremely taxing computationally, therefore we proceeded with calculations in the body-fixed frame. We did not change the alpha-particle wave functions, since it is a tightly bound system. The dineutron wave functions were changed to:

$$\phi_d(r) = \begin{cases} \left(\frac{\omega}{\pi}\right)^{3/4} \exp(-\omega r^2/2) & r < R \\ \left(\frac{\omega}{\pi}\right)^{3/4} \exp(\omega R^2/2) \exp(-\omega Rr) & r \geq R, \end{cases}$$

where R is the matching radius. The calculations were done in spherical coordinates, with the modified tails of the dineutron particles going away from the alpha particle. For our calculations, R was chosen to be 3 fm, which is the approximate point at which the Volkov interaction becomes negligible.

In Table 5.4, we show some results from the body-fixed frame with the alternate asymptotics (Exp Asym) and the reference Gaussian asymptotics (Ref Asym). We show them in this form because as a plot, the two curves would be on top of each other. As one can see from the values in the table, the difference is not tremendous. The new asymptotics create a minimum which is lower by about 180 keV, then it falls off slightly faster, becoming shallower by around 300 keV before converging to essentially the same asymptotic value. The matter radius was also calculated for the value of d which is the minimum in the projected ground state (3.71 fm), and the value was 2.342 fm with the new asymptotics and 2.341 with the old asymptotics.

In our calculations, the exponential asymptotics did not appear to make a great difference. They should, however, be perhaps investigated further. Perhaps a more realistic potential, or the addition of a long-ranged interaction such as the Coulomb interaction (not necessary for ${}^6\text{He}$, but would be desirable for ${}^6\text{Li}$). Also, upgraded computational techniques would make examining the effect of the asymptotics easier, as with the current methods some of the numerical integrals took 48 hours to com-

Table 5.4: A table of values at various values of d of the total energy calculated with exponential asymptotics(Exp Asym) and Gaussian asymptotics (Ref Asym) in the body-fixed frame of ${}^6\text{He}$. For the exponential asymptotics, the matching radius was set to 3 fm.

d	$\langle E \rangle$ (MeV)	
	Alt Asym	Ref Asym
2.1	-11.2654	-11.5031
2.6	-11.8268	-11.6410
3.1	-11.5632	-11.3159
3.6	-10.6260	-10.6390
5.1	-8.3442	-8.6718
7.1	-8.1492	-8.1432

plete, which makes progress on calculating matrix elements (of several integrals) very sluggish, and additionally projected wave functions could be examined.

This concludes the section on the numerical results for ${}^6\text{He}$. We have shown results with fair to good agreement with experimental data. It is important to note that our model is a simple model with six parameters in two configurations (two oscillator parameters and one distance per configuration). AMD calculations have three parameters per basis state, and approximately 150 basis states are used for a converged calculation. FMD calculations have $7A$ parameters (where A is the number of nucleons) per Slater determinant, and the best results are obtained with a superposition of many Slater determinants. They are able to generate very accurate results with these highly computational methods, but we are able to obtain comparable results with physically clear, and simple input.

5.2 Lithium-6

5.2.1 Spatial parameters

As with the section on helium, we begin by showing the minimized variational parameters for ${}^6\text{Li}$. These can be found in table 5.5. The results for the two Volkov potentials are nearly identical once again, though this time there are some very small

Table 5.5: The minimized variational parameters of the ground state ${}^6\text{Li}$ and two excited states. Results are shown for the three potentials discussed throughout this work.

	ν (fm^{-2})			ω (fm^{-2})			d (fm)		
	V1	V2	M	V1	V2	M	V1	V2	M
α -d	0.54	0.54	0.56	0.55	0.55	0.60	3.51	3.50	2.71
cigar	0.50	0.50	0.52	0.50	0.50	0.52	1.21	1.11	1.01
α -d(2^+)	0.53	0.54	0.56	0.52	0.50	0.58	3.51	3.40	2.71
cigar(2^+)	0.50	0.50	0.52	0.50	0.52	0.52	1.11	1.11	1.01
α -d(3^+)	0.53	0.53	0.56	0.52	0.52	0.58	3.40	3.40	2.61
cigar(3^+)	0.50	0.50	0.52	0.52	0.52	0.52	1.01	1.01	1.01

differences (and more for the excited states). The Minnesota results are fairly similar to the Volkov ones in the oscillator lengths, but are different in the minimum value of d , especially in the case of the alpha-deuteron configuration. The reason for this will be discussed in the section on energy. We also see that the cigar configurations are consistently more compact than the alpha-deuteron configurations, though their single-particle constituents are more diffuse (a lower oscillator parameter means a more spatially diffuse object). The alpha-deuteron configurations have much lower kinetic energies than the cigar configurations because of their large values of d . Even in the case of the Minnesota potential, the alpha-deuteron configuration is 20 MeV lower in kinetic energy. The more rapidly falling potential once again confines the cigar configuration into a smaller space.

5.2.2 Energy

In Table 5.6, the ground state energy and relative weights are shown for ${}^6\text{Li}$. When looking at the table, we see some similarities with the results for ${}^6\text{He}$. Once again, the Volkov potentials are much stronger in binding the alpha-deuteron configuration rather than the cigar configuration. The disparity is even greater in the case of ${}^6\text{Li}$, where the margin is almost 12 MeV where it was 9 in the case of ${}^6\text{He}$. The disparity is less when calculated with the Minnesota potentials. When compared with exper-

Table 5.6: The results for the ground state energies of ${}^6\text{Li}$ calculated with the Volkov V1, Volkov V2, and the Minnesota potential. The Volkov calculations were done with a tensor interaction, and all three were performed with a spin-orbit interaction. Results for the alpha particle plus deuteron are given as a guide (row “ $\alpha + d$ ”).

	$\langle E \rangle$ (MeV)			c_i^2		
	V1	V2	M	V1	V2	M
α -d	-35.6	-37.4	-27.6	.700	.722	.741
cigar	-24.2	-25.8	-21.3	.0493	.0445	.0279
overall	-36.5	-38.2	-27.9	N/A		
α +d	-33.2	-34.4	-24.9	N/A		
exp [31]	-32.0			N/A		

iment, the Volkov potentials over-bind substantially while the Minnesota potential seems to be underbound. The source of the over-binding the Volkov potentials can be traced to the tensor interaction. The Volkov potential was not designed with a tensor interaction, and thus using it as a radial form factor for a tensor interaction produces too much binding. This also, however, keeps the value of d large for ${}^6\text{Li}$ despite being over-bound. The tensor interaction in the free deuteron is stronger than when the deuteron is brought closer to the alpha particle, so the tensor interaction effectively pushes the deuteron further away from the alpha particle. In the case of the cigar configuration, asymptotically there is only a free proton and neutron, so there is no tensor interaction, and thus in the cigar configuration, the tensor pulls the two particles closer to the alpha particle. The spin-orbit interaction, which also does not follow any prescription of any particular potential model, appears to only have a small effect with its current set of parameters, affecting the binding energy by at most 500 keV and pulling the particles to slightly smaller values of the distance parameter.

Other than the *ab initio* models (which reproduce the binding energy of ${}^6\text{Li}$ very well), there are not many other theoretical models to compare with. The author is unaware of results for ${}^6\text{Li}$ in either AMD or FMD. There are mid-90s calculations of a Russian group using a method inspired by Resonating Group Method that they call Antisymmetrized Multicluster Dynamic Model with Pauli projection (AMDMP),

which uses cluster wave functions, nucleon-nucleon potentials, and an alpha-deuteron potential of their own devising [75]. They use a Pauli projection technique in order to exclude Pauli forbidden states, such as all particles sitting in s -waves, though we have seen under certain conditions this is not necessarily forbidden. Their best result for the binding energy of ${}^6\text{Li}$ is -31.5 MeV [76] with the Reid soft core potential and their own alpha-deuteron potential. We can also compare with the results of Wildermuth and Tang, who were mentioned in the introduction as earlier pioneers of cluster models. Their best result for the ${}^6\text{Li}$ binding energy is -29.9 MeV [24], calculated with an early version of the Minnesota potential.

Our results for the relative weights show that the alpha-deuteron configuration dominates for all three potentials, containing between 70-74% of the wave function. The weight of the cigar configuration is quite small, less than 5%, which means the interference term accounts for around 25% of the wave function. There is very little discussion of the cigar configuration of ${}^6\text{Li}$ in the literature. One mention was in a recent three-body calculation by Horiuchi and Suzuki [77]. They calculated two-particle correlation functions, and found that while the cigar-like peaks were of equal height in helium and lithium, the deuteron peak in ${}^6\text{Li}$ was twice the height of the dineutron peak in ${}^6\text{He}$. This is qualitatively similar to the results of our calculations.

In Table 5.7, we report our results for the excited states of ${}^6\text{Li}$. Here our results do not reflect what is observed in experiment. The excitations are far too low, and the levels occur in the wrong order. Only the Volkov V2 interaction in the cigar configuration yields the observed sequence of states. The other theoretical models correctly predict the order of states, and are able to calculate with fair agreement the excitation energy of the levels. The most likely cause is in the interactions, specifically the tensor and spin-orbit interactions. Our method is variational, but our results are lower than the experimental results. It would be interesting to see the results using a potential with a more realistic tensor and spin-orbit part.

Table 5.7: Results for the excited states of ${}^6\text{Li}$, calculated with the usual three potentials. We also show the results of the *ab initio* models and AMDMP. Experimental uncertainties are indicated in parentheses.

	$E(2^+)$ (keV)			$E(3^+)$ (keV)		
	V1	V2	M	V1	V2	M
α -d	684	687	132	1257	1267	1557
cigar	18	212	503	316	196	1020
overall	536	738	728	1273	1202	1513
exp [31]	4312(22)			2186(2)		
NCSM [32]	4610			2841		
GFMC [61]	4000			2800		
AMDMP [76]	4989			2660		

5.2.3 Charge radius and other observables

In Table 5.8, we show our results for the charge radius, quadrupole moment and magnetic moment. Our charge radius is smaller than the observed charge radius, and those obtained from other theories (except NCSM). From our minimum parameters, one can see why this occurs. First, the radii are smaller than the ${}^6\text{He}$ minimum values, as the push and pull between the tensor interaction and the spin-orbit and central potential slightly favors smaller radii. This is especially so in the case of the Minnesota potential where there is no tensor interaction, and thus the Minnesota results are very small. Also, the oscillator parameters are rather large for lithium, which focuses the particles more, causing the radius to be smaller. Our quadrupole moment results are large and positive. Cluster models seem to always achieve a positive value, as commented on by Wiringa in [33]. Horiuchi claims this is caused by using an alpha cluster with four *s*-wave particles and a tensor interaction [77]. Our large value comes from the dominance of the alpha-deuteron cluster which has the larger size (the quadrupole moment does scale with d , though not as quickly as r^2), and is also sensitive to the method of angular momentum projection. The three-body calculation of Horiuchi [77] also gives a positive result, $+0.164 e \text{ fm}^2$. The magnetic moment, as mentioned in section 4.7, is independent of configuration and geometry. Our value of $.69 \mu_N$ is above the pure Schmidt model [78] result of $0.62 \mu_N$, but below the

Table 5.8: Shown here are the charge radius, quadrupole moment, and magnetic moment calculated for ${}^6\text{Li}$, plus experimental values and values obtained by other theoretical models.

	$\sqrt{r_{ch}^2}$ (fm)			Q ($e \text{ fm}^2$)			μ (μ_N)		
	V1	V2	M	V1	V2	M	V1	V2	M
α -d	2.30	2.30	2.08	1.20	1.20	0.77	+ .690	+ .690	+ .690
cigar	2.03	2.02	1.95	0.53	0.50	0.46	+ .690	+ .690	+ .690
overall	2.26	2.27	2.09	1.02	1.04	0.70	+ .690	+ .690	+ .690
exp	2.52(3) [79], 2.55(4) [80]			-0.0818(17) [31]			+ .822 [31]		
NCSM [32]	2.31			-0.042			+ .847		
GFMC [72]	2.53			-0.32			+ .817		
AMDMP [76]	2.53			0.49			+ .829		

experimental value. A contribution that would depend on the configuration and the interaction is one proportional to the spin-orbit interaction, but in our estimates it was too small in our model to have a significant effect. Our model is too simple to incorporate things such as meson-exchange currents which also contribute to the magnetic moment. Perhaps a different spin-orbit interaction would allow us to achieve better agreement with experiment.

5.3 Beta decay

In Table 5.9 we show the results of the ${}^6\text{He} \rightarrow {}^6\text{Li}$ beta decay. Our result for the Volkov potentials agrees very well with experiment. The Minnesota result does not, and one might ask why the Volkov results are so much better than the Minnesota result. The Gamov-Teller decay is essentially an overlap of the two wavefunctions. Thus, what is essential are the relative similarity of the minimum variational parameters and the relative weights. For ${}^6\text{He}$, the Minnesota result shows that the wave function is only 44% alpha-dineutron, compared to almost 75% alpha-deuteron for ${}^6\text{Li}$, whereas the Volkov results are around 10% of each other. Also, the oscillator parameters and especially d values are closer together with the Volkov potentials. The energy results may seem at first glance to be also less than ideal, but within the potential model

Table 5.9: Shown here are the results of the beta decay calculation for the decay of ${}^6\text{He}$ to ${}^6\text{Li}$ along with the experimental results and other theoretical calculations.

	$\log ft$		
	V1	V2	M
This Work	2.90	2.90	3.81
exp [31]	2.91		
NCSM [32]	2.86		
GFMC [73]	2.92		
AMDMP [76]	2.90		

used, they are not that bad. The over-binding is not that big when compared with the alpha-deuteron threshold (experimentally 1.47 MeV [31]). Thus, the ground state wave functions are actually decent, and the beta decay result reflects this. This helps to also answer why the Volkov result is so close to experiment, despite other results for ${}^6\text{Li}$ that do not agree as well with the experimental results. The other theories also reproduce the experimental result with good agreement. As an example of a general principle, a mean field calculation carried out in [52] gives a $\log ft = 3.07$, which shows that for small nuclei, mean field/shell model type approaches do not give the best results.

This concludes the chapter listing the numerical results of the calculation. We proceed then to our conclusions and outlook for the future of these calculations.

Chapter 6

Conclusions and outlook

6.1 Summary

The purpose of this dissertation was to build a simple model that provides a reasonable description of light, loosely-bound nuclei. This was done by the calculation of many observables and comparing them to experimental data; the instrument of the calculations was the Brink Formalism in secondary quantization.

After a background of the history of nuclear theory in general and cluster models in particular in Chapter One, the formalism used throughout the dissertation was introduced. Simple examples were worked out which illustrated the use of non-orthogonal orbitals and how the formalism accounts for the Pauli principle. Examples were also performed to illustrate the calculation of one- and two-body operator expectation values. The final ingredient in the formalism was the method of projecting into good states of angular momenta, which was explained in the final section of Chapter Two.

In Chapter Three, we introduce the formalism to the six-body systems of interest. The calculation of expectation values is outlined in a completely general sense; no choice has been made yet about single-particle wave functions or nucleon-nucleon interaction. The two configurations, alpha-two particle cluster and cigar, are also introduced, and the calculation of one-body and two-body expectation values is out-

lined for both configurations. The interference term and minimization routine are also introduced. Lithium-6 calculations are then previewed, and are compared and contrasted with the calculations for ${}^6\text{He}$. Finally, the calculation of spin-dependent operators such as the tensor operator and spin-orbit operator are described.

Chapter Four delves into a particular choice of variational single-particle wave function, the Gaussian. The Gaussian wave functions are described, then used to calculate several things in both configurations. For ${}^6\text{He}$, the expectation value of the Hamiltonian as a function of alpha-external neutron distance is calculated, along with the charge and matter radii. The kinetic energy calculation in particular illustrates how the formalism handles the Pauli principle. Interactions are chosen and described, and plots are shown of several expectation values as a function of alpha-neutron distance. After the calculations are shown in the two configurations, electromagnetic transitions are introduced and the transition rate is calculated for the transition from the ground state of ${}^6\text{He}$ to its first excited state. Next, the calculations in the interference term are shown for all the previously mentioned operators. The next subject is ${}^6\text{Li}$, and operators that are different from those in ${}^6\text{He}$ are discussed. These include the tensor operator, spin-orbit operator, electric quadrupole moment and magnetic dipole moment. Finally, the topic of beta decay is introduced and the calculation of the beta decay of ${}^6\text{He}$ to ${}^6\text{Li}$ is discussed.

The penultimate chapter, Chapter Five, reports the numerical results obtained with our model. Starting with ${}^6\text{He}$, the optimized values of the variational parameters are reported, then the results for the ground and excited state energies results, weights of the configurations, charge and matter radii, and the quadrupole transition probabilities between the ground and first excited state. All results were reported for the three potentials used throughout this dissertation: the Volkov V1 and V2 interactions, and the Minnesota potential. Next, a calculation with different single-particle wave functions with different asymptotic properties was described and tables of results that compared the new asymptotics with the Gaussian asymptotics were shown.

All results were compared with experimental data and the results of other theoretical models. Then the results for ${}^6\text{Li}$ were reported for energies, excited state excitation energies, relative weights of the configurations, charge radius, electric quadrupole moment and magnetic dipole moment. Finally the results for the beta decay of ${}^6\text{He}$ were reported and discussed.

6.2 Conclusions

The goal of this study was to use transparent physical input which was at the same time quantum mechanically rigorous, and try and reproduce the main features of the nuclei of interest, ${}^6\text{He}$ and ${}^6\text{Li}$. In this case, the study can be considered to have met its goal. The input is simply the two extreme cases of an alpha plus two particles, with the Pauli principle exactly handled through non-orthogonal orbitals and secondary quantization. Helium-6 is fairly well described with our model, and ${}^6\text{Li}$ less so, but the description is still adequate. Improvements can be made, and ideas for improving the model will be discussed in the next section.

For ${}^6\text{He}$, we were able to reproduce its halo nature, which is seen in the large difference between its charge and matter radius. Our numerical results are slightly smaller than experimental results for each quantity, but the extended neutron structure is evident. We found that ${}^6\text{He}$ is loosely-bound, and mostly in the alpha-dineutron configuration. Most other theories have come to similar conclusions. The experimental charge radius supports correlated neutrons in ${}^6\text{He}$, as do preliminary transfer reaction data, but more is forth-coming from these experiments. A larger input is needed to be able to accurately describe excited states. Our results with the Minnesota potential were generally worse than with the Volkov potentials. The Minnesota potential produced smaller radii (although the extended neutron structure is still present), and either much less or too much binding, depending on one's perspective (the energy of ${}^6\text{He}$ against the alpha is much higher than with Volkov, but because of the very

strongly repulsive dineutron, the binding compared to the asymptotic state of an alpha particle and separated dineutron is much larger than with Volkov). We also saw that more realistic exponential asymptotic behavior had little effect on bound state properties.

Lithium-6 proved to be more of a challenge. With the Volkov potentials, our system is overbound, thanks to the Volkov form factor attached to the tensor interaction. The size is smaller than experiment, and we once again have problems with the excited states. The quadrupole moment is also quite a bit larger than experiment. The Minnesota results are similar in many respects, save the binding and the size is very small, but this is due to the lack of a tensor interaction. Both the Minnesota and Volkov potentials show a very dominant alpha-deuteron structure. From these results, it can be concluded that a better treatment of the spin-orbit and tensor interaction should be used to improve the results for ${}^6\text{Li}$. The wave functions themselves do not seem to be too bad, at least in the case of the Volkov potentials, as the beta decay of ${}^6\text{He}$ agrees extremely well with experiment.

6.3 Future work

Regarding the future, there are two main thrusts: how we can improve the model for ${}^6\text{He}$ and ${}^6\text{Li}$ without sacrificing its transparency and simplicity, and on which other systems would be interesting to use a similar approach. For improving the current model, one could think about starting to represent single particles as sums of Gaussians, although this starts to increase the complexity of the calculation and make the model more similar to other cluster models. For better treatment of excited states, including the contribution spin-triplet dineutron and cigar states in ${}^6\text{He}$ would probably achieve better results. We should also do a calculation of something that is more sensitive to asymptotic behavior to see then the difference exponential tails can make. Such a calculation could be of an asymptotic normalization coefficient, or a reaction

calculation such as charge exchange. Another improvement would be to introduce a continuous, smoothly changing $f(\beta)$, where β is the angle between the two external particles to describe the system instead of two extreme configurations. Finally, as mentioned in the previous paragraph, a potential that properly includes the spin-orbit and tensor interaction would be very interesting to apply to ${}^6\text{Li}$. One such potential is the Argonne V8'. One possible drawback is that most Argonne potentials require a three-body force in order to achieve good agreement with experiment. Finally, the Coulomb interaction should be included, especially for ${}^6\text{Li}$. It is small (820 keV at the distance of the minimum in energy in ${}^6\text{Li}$), but long range and repulsive, which could also be important for improving our description of ${}^6\text{Li}$.

As for new calculations, a reaction involving ${}^6\text{He}$ or ${}^6\text{He}$ and ${}^6\text{Li}$ would be very interesting application of our wave function. Our wave function treats Fermi statistics exactly, which is sometimes not the case in reaction calculations. It would be interesting to see the role of asymptotics versus Fermi statistics in such a calculation. For other systems, ${}^8\text{He}$ would be a topical system, as its charge radius has also recently been measured [81]. The preliminary result is that it is smaller than the charge radius of ${}^6\text{He}$. We would model ${}^8\text{He}$ as a mixture of a dineutron-alpha-dineutron chain and an alpha-tetraneutron, and see what kind of charge radius we obtain. Another system that could be modeled is ${}^7\text{Li}$ as a proton hole orbiting a two-alpha ${}^8\text{Be}$ system. This is more of a pure theoretical interest, though the Li isotope chain has been the subject of a few recent study [79]. Finally, the chain of Be isotopes has always been good for cluster studies, and applying our model to those isotopes would be natural.

In this dissertation, we have developed a simple but fully microscopic formalism for describing clusters in nuclei. It has been shown that though simple, the model can still capture essential physics. The formalism is extremely flexible, and it is sure to be applied to other light nuclear systems in the future.

Bibliography

- [1] J. Dalton. *A New System of Chemical Philosophy*. Peter Owen Limited, London, 1808.
- [2] J. J. Thomson. *Phil. Mag.*, **44**:293, 1897.
- [3] E. Rutherford. *Phil. Mag.*, **21**:669, 1911.
- [4] H. Becquerel. *Compt. Rend.*, **122**:420, 1896.
- [5] E. Rutherford and T. Royds. *Phil. Mag.*, **17**:281, 1909.
- [6] J. Chadwick. *Nature*, **129**:312, 1932.
- [7] W. Heisenberg. *Z. Physik*, **77**:1, 1932.
- [8] E. P. Wigner. *Phys. Rev.*, **51**:947, 1937.
- [9] N. Bohr and F. Kalckar. *Kgl. Danske Videnskab. Selskab, Mat-fys. Medd.*, **14**:10, 1937.
- [10] J. M. Blatt and V. F. Weisskopf. *Theoretical Nuclear Physics*. John Wiley & Sons, New York, 1952.
- [11] D. R. Tilley, H. R. Weller, and G. M. Hale. *Nucl. Phys.*, **A541**:1, 1992.
- [12] E. Borie and G. A. Rinker. *Phys. Rev. A*, **18**:324, 1978.
- [13] J. A. Wheeler. *Phys. Rev.*, **52**:1083, 1937.
- [14] W. Wefelmeier. *Z. Physik*, **107**:332, 1937.
- [15] C. F. von Weizsäcker. *Naturwiss.*, **26**:209,225, 1938.
- [16] U. Fano. *Naturwiss.*, **25**:602, 1937.
- [17] L. R. Hafstad and E. Teller. *Phys. Rev.*, **54**:681, 1938.
- [18] C. Kittel. *Phys. Rev.*, **62**:109, 1942.
- [19] H. A. Bethe. *Phys. Rev.*, **53**:842, 1938.
- [20] R. G. Sachs. *Phys. Rev.*, **55**:825, 1939.

- [21] D. R. Inglis. *Phys. Rev.*, **55**:329, 1939.
- [22] J. A. Wheeler. *Phys. Rev.*, **59**:16, 1941.
- [23] M. Born and J. R. Oppenheimer. *Ann. Physik*, **84**:457, 1927.
- [24] K. Wildermuth and Y. C. Tang. *A Unified Theory of the Nucleus*. Academic Press, New York, 1977.
- [25] R. Jastrow. *Phys. Rev.*, **79**:389, 1950.
- [26] H. Feldmeier and J. Schnack. *Rev. Mod. Phys.*, **72**:655, 2000.
- [27] Y. Kanada-En'yo, H. Horiuchi, and A. Ono. *Phys. Rev. C*, **52**:628, 1995.
- [28] T. Bjerge. *Nature*, **138**:400, 1936.
- [29] A. Navin, 2007. Private communication.
- [30] A. Galonsky and M. T. McEllistrem. *Phys. Rev.*, **98**:590, 1955.
- [31] D. R. Tilley, C. M. Cheves, J. L. Godwin, G. M. Hale, H. M. Hoffman, J. H. Kelley, C. G. Sheu, and H. R. Weller. *Nucl. Phys.*, **A708**:3, 2002.
- [32] P. Navrátil, J. P. Vary, W. E. Ormand, and B. R. Barrett. *Phys. Rev. Lett.*, **87**:172502, 2001.
- [33] B. Wiringa. *Nucl. Phys.*, **A631**:70, 1998.
- [34] D. M. Brink. *International School of Physics "Enrico Fermi"*, XXXVI:247, 1966.
- [35] P. Löwdin. *Phys. Rev.*, **97**:1475, 1955.
- [36] S. Rombouts and K. Heyde. *J. Phys. A*, **27**:3293, 1994.
- [37] J. M. Ziman. *Elements of Advanced Quantum Theory*. Cambridge University Press, Cambridge, 1969.
- [38] G. C. Wick. *Phys. Rev.*, **80**:268, 1950.
- [39] P. Ring and P. Schuck. *The Nuclear Many-Body Problem*. Springer-Verlag, New York, 1980.
- [40] D. M. Brink and G. R. Satchler. *Angular Momentum*. Oxford University Press, Oxford, third edition, 1993.
- [41] F. Hund. *Z. Physik*, **43**:805, 1927.
- [42] D. M. Dennison and G. E. Uhlenbeck. *Phys. Rev.*, **41**:313, 1932.
- [43] G. Herzberg. *Infra Red and Raman Spectra*. D. Van Nostrand Co., Inc., New York, 1945.

- [44] W. D. Ehmann and D. E. Vance. *Radiochemistry and Nuclear Methods of Analysis*. John Wiley & Sons, New York, 1991.
- [45] A. B. Volkov. *Nucl. Phys.*, **74**:33, 1965.
- [46] I. Reichstein and Y. C. Tang. *Nucl. Phys.*, **A128**:529, 1970.
- [47] D. R. Thompson, M. Lemere, and Y. C. Tang. *Nucl. Phys.*, **A286**:53, 1977.
- [48] D. Gogny, P. Pires, and R. De Tourreil. *Phys. Lett. B*, **32**:591, 1970.
- [49] H. Esbensen, K. Hagino, P. Mueller, and H. Sagawa. *Phys. Rev. C*, **76**:024302, 2007.
- [50] I. Sick. *Phys. Lett. B*, **576**:62, 2003.
- [51] S. Kopecky, J. A. Harvey, N. W. Hill, M. Krenn, M. Pernicka, and S. Steiner. *Phys. Rev. C*, **56**:2229, 1997.
- [52] J. Suhonen. *From Nucleons to Nucleus*. Springer-Verlag, New York, 2007.
- [53] E. P. Wigner. *Z. Physik*, **43**:624, 1927.
- [54] C. Eckart. *Rev. Mod. Phys.*, **2**:305, 1930.
- [55] E. Fermi. *Z. Physik*, **88**:161, 1934.
- [56] G. A. Gamov and E. Teller. *Phys. Rev.*, **49**:895, 1936.
- [57] W. M. Yao et al. *J. Phys. G*, **33**:1, 2006.
- [58] B. V. Danilin, I. J. Thomson, J. S. Vaagen, and M. V. Zhukov. *Nucl. Phys.*, **A632**:383, 1998.
- [59] T. Neff and H. Feldmeier. *Nucl. Phys.*, **A738**:357, 2004.
- [60] N. Itagaki, A. Kobayakawa, and S. Aoyama. *Phys. Rev. C*, **68**:054302, 2003.
- [61] S. C. Pieper, R. B. Wiringa, and J. Carlson. *Phys. Rev. C*, **70**:054325, 2004.
- [62] C. A. Bertulani and M. S. Hussein. *Phys. Rev. C*, **76**:051602, 2007.
- [63] K. Hagino and H. Sagawa. *Phys. Rev. C*, **72**:044321, 2005.
- [64] J. J. Kolata et al. *Phys. Rev. C*, **75**:031302, 2007.
- [65] E. A. Benjamim et al. *Phys. Lett. B*, **647**:30, 2007.
- [66] L. Chulkov et al. *Europhys. Lett.*, **8**:245, 1989.
- [67] I. Tanihata et al. *Phys. Lett. B*, **206**:592, 1988.
- [68] I. Tanihata, D. Hirata, T. Kobayashi, K. Sugimoto S. Shimoura, and H. Toki. *Phys. Lett. B*, **289**:261, 1992.

- [69] T. Aumann et al. *Phys. Rev. C*, **59**:1252, 1999.
- [70] L.-B. Wang et al. *Phys. Rev. Lett.*, **93**:142501, 2004.
- [71] A. Ozawa, T. Suzuki, and I. Tanihata. *Nucl. Phys.*, **A693**:32, 2001.
- [72] S. C. Pieper, V. R. Pandharipande, R. B. Wiringa, and J. Carlson. *Phys. Rev. C*, **64**:014001, 2001.
- [73] M. Pervin, S. C. Pieper, and R. B. Wiringa, 2007. arXiv:0710.1265v2.
- [74] E. Caurier and P. Navrátil. *Phys. Rev. C*, **73**:021302, 2006.
- [75] G. G. Ryzhikh, R. A. Eramzhyan, V. I. Kukulin, and Yu. M. Tchuvil'sky. *Nucl. Phys.*, **A563**:247, 1993.
- [76] V. I. Kukulin, V. N. Pomerantsev, Kh. D. Razikov, V. T. Voronchev, and G. G. Ryzhikh. *Nucl. Phys.*, **A586**:151, 1995.
- [77] W. Horiuchi and Y. Suzuki. *Phys. Rev. C*, **76**:024311, 2007.
- [78] T. Schmidt. *Z. Physik*, **106**:358, 1937.
- [79] R. Sánchez et al. *Phys. Rev. Lett.*, **96**:033002, 2006.
- [80] C. W. de Jager, H. de Vries, and C. de Vries. *At. Data and Nucl. Data Tables*, **14**:479, 1974.
- [81] Z.-T. Lu. *Bulletin of the American Physical Society*, **52.9**:71, 2007.